Pedro Jorge Araújo Alves da Silva

ISOLATION AND CHARACTERIZATION OF ENZYMES INVOLVED IN THE HYDROGEN METABOLISM FROM *PYROCOCCUS FURIOSUS*

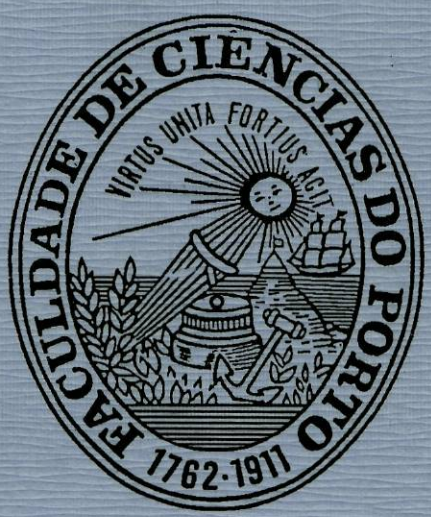

Departamento de Química

Faculdade de Ciências da Universidade do Porto

2000

Pedro Jorge Araújo Alves da Silva

ISOLATION AND CHARACTERIZATION OF ENZYMES INVOLVED IN THE HYDROGEN METABOLISM FROM *PYROCOCCUS FURIOSUS*

Dissertação submetida à Faculdade de Ciências da Universidade do Porto
para obtenção do grau de Doutor em Química

Departamento de Química
Faculdade de Ciências da Universidade do Porto
2000

AGRADECIMENTOS

Ao Departamento de Química da Faculdade de Ciências da Universidade do Porto por me ter aceite como aluno de Doutoramento.

À Fundação para a Ciência e Tecnologia a concessão de uma Bolsa de Doutoramento.

Ao Prof. Baltazar de Castro, meu orientador, que me propôs a realização de um Doutoramento no seu grupo de investigação.

To the Department of Biochemistry of the Wageningen Agricultural University (the Netherlands) and to the Department of Enzymology of the Technical University of Delft (the Netherlands) for accepting me as a visiting graduate student.

To Prof. Dr. Fred Hagen, my co-supervisor, for supporting my research, for the long and fruitful lab-talks, for the EPR lessons, for the Friday afternoon "evaluation meetings" (aka *borrels*) and for so much more....From Fred I have probably learned far more than I am aware of, and I am very glad I had the chance to work with him.

To Hans Wassink, for all the times he left his experiments to assist me in my research, the many activity measurements in cell extracts he performed for me, for the kind gifts of *P. furiosus* POR and ferredoxin, etc. But above all for his friendship and support.

To every one else in the Department of Biochemistry at the WAU, especially to my colleagues in lab 2, Peter-Leon, Eyke, Petra, Juul, Ilse, Marielle, Maria João and Bart for providing a wonderful working environment. A special "thank you" to Maria João Amorim and Peter-Leon Hagedoorn for the work they performed in the SuDH part of the project and to Eyke van den Ban for the continuous supply of inocula and for her assistance in the research described in the first sections of chapter 6.

To Huub Haaaker, for his interest and creative ideas, which formed the basis of the research described in the first sections of chapter 6.

To Alfons Stams, for allowing me to use his labs in the Department of Microbiology of the Wageningen Agricultural University when the Department of Biochemistry was closed due to asbestos contamination.

To Frank de Bok and Caroline Plugge, who were always available to help me during my short stay in the Department of Microbiology.

To Frank T. Robb, for checking the accuracy of the *P. furiosus* genome data.

Aos colegas de laboratório na Faculdade de Ciências da Universidade do Porto, pela amizade e pelo bom humor.

Ao Stéphane Besson, pela amizade e pela tradução do resumo para Francês.

Um obrigado muito especial aos meus pais, irmão, sogros e restante família, pelo apoio incondicional, pela amizade e pelo amor.

E principalmente à Dora, pelo incentivo constante, pelas boas ideias, por me obrigar a superar-me, e acima de tudo pelo Amor. A ela, e à nossa filha Sofia, dedico esta tese e todas as alegrias e dores da sua elaboração. Por vós tudo vale a pena!

Pedro Silva

RESUMO

Ma *et al.*(Ma *et al.* (1994) *FEMS Microbiol. Lett.* **122**: 245-250) sugeriram que no organismo hipertermofílico *Pyrococcus furiosus* a eliminação de equivalentes redutores através da produção de H_2 seguia a sequência:

fermentação → ferredoxina → FNOR(SuDH) → NADPH → sulfidrogenase → H^+ [1]

O presente trabalho descreve a investigação individual das enzimas envolvidas neste processo (SuDH e sulfidrogenase) e o estudo das actividades fisiológicas em extractos celulares. Os resultados obtidos fornecem uma nova visão do metabolismo do H_2 neste organismo.

A sulfidrogenase de *Pyrococcus furiosus* é um complexo heterotetramérico com actividades de hidrogenase e de redutase de enxofre. Além de um agregado dinuclear de NiFe, prevê-se que contenha uma molécula de FAD e seis agregados de ferro-enxofre. Ao contrário de relatos anteriores, parece cumprir principalmente um papel de absorção de H_2. Incubação a 80°C provoca uma auto-redução espontânea da sulfidrogenase. Este fenómeno permitiu pela primeira vez a observação por ressonância paramagnética electrónica do centro de NiFe de uma hidrogenase hipertermofílica. Esta atravessa um conjunto de estados, alguns dos quais são semelhantes a estados observados anteriormente em hidrogenases mesofílicas. A complexidade das transições observadas reflecte uma combinação de activação e potenciais redox dependentes da temperatura. Apenas três sinais de Fe/S são observados por RPE após redução por ditionito, NADPH ou pelo redutor interno após aquecimento. Provavelmente todos os outros agregados possuem potenciais de redução bastante inferiores ao do par H^+/H_2.

A desidrogenase do sulfureto (SuDH) é uma proteína heterodimérica que contém duas moléculas de FAD, um agregado $[3Fe\text{-}4S]^{(1+;0)}$, um agregado $[4Fe\text{-}4S]^{(2+;1+)}$ e um agregado $[2Fe\text{-}2S]^{(2+;1+)}$. Este exibe valores de g e potencial de redução semelhantes aos de agregados do tipo Rieske. No entanto, uma análise comparativa das sequências das subunidades revela que este agregado é coordenado por um novo motivo contendo um Asp e três Cys. O centro 3Fe possui um potencial de redução invulgarmente elevado e o centro 4Fe não pode ser reduzido com ditionito; pode no entanto ser reduzido facilmente pelo NADPH.

A comparação das actividades da hidrogenase solúvel e da desidrogenase do sulfureto com a actividade da glicólise em extractos celulares mostra que a via metabólica proposta [1] não é suficientemente activa para eliminar os equivalentes de redução produzidos pela fermentação. Descobriu-se porém que as membranas do *P. furiosus* podem produzir H_2 utilizando a ferredoxina [4Fe-4S] solúvel como dador de electrões. Esta actividade está também presente numa proteína membranar solubilizada e purificada em condições suaves. Esta hidrogenase membranar tem propriedades invulgares: é bastante resistente à inibição pelo monóxido de carbono e apresenta uma razão de produção de H_2/ oxidação de H_2 extremamente elevado em comparação com outras hidrogenases. A actividade da enzima é sensível à inibição pela dicicloexilcarbodiimida, um inibidor da desidrogenase I do NADH (presente em mitocôndrias) o que sugere que esta proteína está envolvida na translocação de protões. A descoberta desta hidrogenase membranar levou à elaboração de um novo model do metabolismo do H_2 em *P. furiosus*. Segundo este modelo, a ferredoxina reduzida produzida pelo catabolismo transfere os seus electrões à hidrogenase membranar, que reduz protões a H_2, provavelmente como parte de um processo de conservação de energia. A via metabólica proposta por Ma *et al.* poderá funcionar como uma "válvula de segurança" para eliminar o excesso de equivalentes de redução sob a forma de H_2; por outro lado, a sulfidrogenase pode utilizar o H_2 para reduzir $NADP^+$, fornecendo assim uma fonte suplementar de NADPH para os processos anabólicos.

O genoma também possui uma segunda (hipotética) hidrogenase membranar com um motivo de ligação ao centro Ni-Fe bastante invulgar. Estes dois tipos de hidrogenase membranar assemelham-se mais a proteínas envolvidas em processos respiratórios do que a outras hidrogenases. Uma análise cuidadosa das suas sequências de aminoácidos permitiu a descoberta de motivos conservados específicos que poderão ser usados para evitar erros de identificação em projectos de anotação automática de genomas. Uma análise semelhante efectuada em sulfidrogenases sugere que os potenciais de redução de alguns agregados Fe-S poderão ser dependentes do pH, o que poderia permitir uma melhor regulação da actividade da proteína, e poderia explicar a indetectabilidade de alguns destes centros por ressonância paramagnética electrónica.

ABSTRACT

The disposal of reducing equivalents through H_2 production in the hyperthermophile *Pyrococcus furiosus* has been proposed by Ma *et al.*(Ma *et al.* (1994) *FEMS Microbiol. Lett.* **122**: 245-250) to follow the sequence:

fermentation → ferredoxin → FNOR(SuDH) → NADPH → sulfhydrogenase → H^+ [1]

The present work describes the individual investigation of the enzymes involved in this pathway (SuDH and sulfhydrogenase), as well as of the physiological activities in cell extracts. The results obtained afford several new insights on the H_2 metabolism in this organism.

The sulfhydrogenase complex of *Pyrococcus furiosus* is a heterotetramer with both hydrogenase activity and sulfur reductase activity. Besides the dinuclear Ni-Fe cluster, it is predicted to carry one FAD and six [Fe-S] clusters. Contrary to previous reports, the sulfhydrogenase appears to fulfill primarily a H_2-uptake role. Upon incubation at 80°C sulfhydrogenase spontaneously self-reduces. This phenomenon allows for the first time the EPR-monitoring of the NiFe center in a hyperthermophilic hydrogenase, which passes through a number of states some of which are similar to states previously observed for mesophilic hydrogenases. The complexity of the observed transitions reflects a combination of temperature-dependent activation and reduction potentials. Only three Fe/S signals are observed in EPR-monitored reduction by dithionite, NADPH or internal substrate upon heating. All other clusters presumably have reduction potentials well below that of the H^+/H_2 couple.

Sulfide dehydrogenase, a heterodimeric protein, carries two FAD, a [3Fe-4S]$^{(1+;0)}$, a [4Fe-4S]$^{(2+;1+)}$ cluster and a [2Fe-2S]$^{(2+;1+)}$ prosthetic group. The latter exhibits EPR g-values and reduction potential similar to those of Rieske-type clusters, however, a comparative sequence analysis indicates that this cluster is coordinated by a novel motif of one Asp and three Cys ligands. The 3Fe cluster has an unusually high

reduction potential and the 4Fe cluster cannot be reduced with sodium dithionite; it is however readily reduced with NADPH.

Comparison of the activities of soluble hydrogenase and sulfide dehydrogenase with that of glycolysis in cell extracts shows that the proposed pathway [1] is not sufficiently active to dispose of the reducing equivalents produced during fermentation. However, *P. furiosus* membranes were found to be able to produce H_2 using the soluble [4Fe-4S] ferredoxin as electron donor. This activity is retained in an extracted membrane protein when solubilized and purified under mild conditions. The properties of this membrane-bound hydrogenase are unique: it is rather resistant to inhibition by carbon monoxide and it exhibits also an extremely high ratio of H_2 evolution to H_2 uptake activity when compared with other hydrogenases. The activity is sensitive to inhibition by dicyclohexylcarbodiimide, an inhibitor of mitochondrial NADH dehydrogenase I, suggesting a proton-translocating role for this protein. The discovery of this membrane-bound hydrogenase prompted the formulation of a new model of H_2 metabolism in *P. furiosus*. According to this model, reduced ferredoxin produced by the catabolism transfers its electrons to the membrane-bound hydrogenase, which reduces protons to H_2 presumably in an energy-conserving process. The pathway proposed by *Ma et al.* could function as a safety valve for the disposal of excess reducing equivalents as H_2. Besides, sulfhydrogenase can use H_2 to reduce $NADP^+$, thus providing an extra source of NADPH for anabolic processes.

The genome also includes a putative second membrane-bound hydrogenase with a highly unusual binding motif for the Ni-Fe-cluster in the large hydrogenase subunit. Both types of membrane-bound hydrogenases are more similar to proteins involved in respiratory processes than to other hydrogenases. Careful analysis of their aminoacid sequences allowed the discovery of specific conserved motifs that may be used to prevent misidentification in automatic genome annotation projects. Similar analysis, performed in sulfhydrogenases, suggests a pH-dependence of some cluster's redox potentials, which may provide better regulation of the protein activity, as well as explaining the undetectability of some Fe-S centers by electron paramagnetic resonance.

RÉSUMÉ

Ma *et al.*(Ma *et al.* (1994) *FEMS Microbiol. Lett.* **122**: 245-250) ont proposé que, chez l'hyperthermophile *Pyrococcus furiosus*, l'élimination des équivalents réducteurs par production de H_2 suit la séquence suivante:

fermentation → ferrédoxine → FNOR(SuDH) → NADPH → sulfhidrogénase → H^+ [1]

Ce travail décrit l'étude individuelle des enzymes impliquées dans cette voie métabolique (SuDH et sulfhidrogénase), et aussi l'étude des activités physiologiques dans des extraits cellulaires. Les résultats obtenus révèlent de nombreuses et nouvelles facettes du métabolisme de H_2 chez cet organisme.

Le complexe sulfhidrogénase de *Pyrococcus furiosus* est un hétérotétramère possédant à la fois une activité hidrogénase et soufre réductase. À part le centre binucléaire Ni-Fe, il est supposé contenir un FAD et six centres [Fe-S]. Contrairement à ce qui a été publié antérieurement, la sulfhidrogénase semble remplir principalement un rôle dans l'absortion de H_2. Au cours d'uine incubation à 80 °C, la sulfhidrogénase s'autoréduit spontanément. Ce phénomène permet pour la premiére fois l'observation par RPE du centre NiFe d'une hidrogénase hyperthermophile, qui passe par différent stades, certains étant similaires à des stades observés auparavant chez les hidrogénases mésophiles. La complexité des transitions observées reflet une combinaison de l'activation et de potentiels de réduction dépendantes de la température. Trois signaux Fe/S seulement sont observés par RPE au cours d'une reduction par le dithionite, par NADPH ou par le substrat interne pendat le chauffage. Touts les autres centres sont supposés avoir des potentiels de réduction trés en dessous du potentiel du couple H^+/H_2.

La Soufre déshidrogénase (SuDH), une protéine hétérodimérique, posséde deux FAD, un $[3Fe\text{-}4S]^{(1+;0)}$, un $[4Fe\text{-}4S]^{(2+;1+)}$ et un groupement prosthétique $[2Fe\text{-}2S]^{(2+;1+)}$. Ce dernier présente des valeurs de *g* de RPE et un potentiel de réduction similaires à ceux des centres de type Rieske; cependant, une analyse comparée des séquences indique que ce centre est coordoné par un nouveau motif avec un Asp et trois Cys comme ligands. Le centre 3Fe posséde un potential de réduction inhabituellement élevé et le centre 4Fe ne peut pas être réduit avec le dithionite; il est néamoins trés bien réduit par le NADPH.

La comparaison des activités de l'hidrogénase soluble et de la soufre deshidrogénase avec l'activité de la glicolyse dans des extraits cellulaires démontre que la voie métabolique proposée [1] n'est pas suffisament active pour éliminer les équivalents réducteurs produits au cours de la fermentation. Cependat, il a été découvert que les membranes de *P. furiosus* puvaient produire H_2 en utilisant la ferrédoxine [4Fe-4S] soluble comme donneur d'électrons. Cette activité est aussi présente dans une protéine membranaire extraite lorsqu'elle est solubilisée et purifiée selon méthodes douces. Les propriétés de cette hidrogénase membranaire sont uniques: elle est assez résistanteà l'inhibition par le monoxyde de carbone et présente un rapport H_2 produit/H_2 consommé extrêmement élevé par comparaison avec d'autres hidrogénases. L'activité est sensible à l'inhibition par le dicycloexylcarbodiimide, un inhibiteur de la NADH dehidrogénase I mitochondriale, ce qui suggère que cette proteíne joue un rôle dans la translation des protons. La découverte de cette hidrogénase membranaire entraîna la formulation d'un nouveau modèle de métabolisme du H_2 chez *P. furiosus*. D'aprés ce modèle, la ferrédoxine réduite produite par le catabolisme transfère ses électrons à l'hidrogénase membranaire, qui réduit des protons en H_2, probablement dans le cadre d'un processus conservateur d'énergie. La voie métabolique proposée par Ma *et al.* pourrait fonctionner comme valve de sécurité pour éliminer l'excès d'équivalents réducteurs sous la forme de H_2. Par ailleurs, la sulfidrogénase peut utiliser le H_2 pour réduire le $NADP^+$, fournissant ainsi une source supplémentaire de NADPH pour les processus anaboliques.

Le génome contient également une hypothétique seconde hidrogénase membranaire avec un motif de liaison de centre Ni-Fe trés inhabituel dans la grande sous-unité de l'hidrogénase. Ces deux types d'hidrogénase membranaire sont plus proches de protéines impliquées dans des processus reapiratoires que des autres hidrogénases. Une analyse méticuleuse de leurs séquences d'aminoacides a permis la découverte de motifs conservés spécifiques qui pourraient être utilisés pour éviter une mauvaise identification dans le cadre de projets d'annotation automatique de génome. Une analyse similaire, effectué sur des sulfhidrogénases, suggère la dépendance vis-à-vis du pH des potentiels rédox de certains centres [Fe-S], ce qui permettrait une meilleure régulation de l'activité de la protéine,et pourrait expliquer aussi le caractère indétectable de certains centres Fe-S par résonance paramagnétique électronique.

TABLE OF CONTENTS

INDEX OF FIGURES

INDEX OF TABLES

LIST OF ABBREVIATIONS

AegA - Expression product of *aegA*, an *a*naerobically *e*xpressed *g*ene of *Escherichia coli* with unknown function

ASR - Assimilatory sulfite reductase

ADP - Adenosine diphosphate

AMP - Adenosine monophosphate

ATP - Adenosine triphosphate

AsrB - β-subunit of assimilatory sulfite reductase

BV - Benzyl viologen

CAPS - (3[cyclohexylamino]-1-propanesulfonic acid)

CoASH - Coenzyme A

DCCD - *N, N'*-dicyclohexylcarbodiimide

DEAE - Diethylaminoethyl

DHOD - Dihydroorotate dehydrogenase

DOC - Sodium deoxycholate

DPD - Dihydropyrimidine dehydrogenase

EPPS - N-[2-hydroxyethyl]-piperazine-N'[3-propanesulfonic acid]

EPR - Electron paramagnetic resonance

$F_{420}H_2$ - (*N*-L-lactyl-γ-L-glutamyl)-L-glutamic acid phosphodiester of 7,8-didemethyl-8-hydroxy-5-deazariboflavin-5'-phosphate

FAD - Flavin adenine dinucleotide

Fd - Ferredoxin

Fd_{ox} - Oxidized form of *P. furiosus* ferredoxin

Fd_{red} - Reduced form of *P. furiosus* ferredoxin

FNOR - Ferredoxin:$NADP^+$ oxidoreductase

FTIR - Fourier transformed infrared spectroscopy

G - Gauss (0.1 mT)

GAPDH - Glyceraldehyde-3-P dehydrogenase

GAPOR - Glyceraldehyde-3-P:ferredoxin oxidoreductase

GltS - Glutamate synthase

GOGAT - Glutamine oxoglutarate aminotransferase (≡ glutamate synthase)

H_2ase - Hydrogenase

HydG - Hydrogenase γ-subunit

K_m - Michaelis constant

MV - Methyl viologen

MV_{SQ} - Methyl viologen semiquinone

NAD^+ - Nicotinamide adenine dinucleotide (oxidized form)

NADH - Nicotinamide adenine dinucleotide (reduced form)

$NADP^+$ - Nicotinamide adenine dinucleotide phosphate (oxidized form)

NADPH - Nicotinamide adenine dinucleotide phosphate (reduced form)

nuo - NADH:ubiquinone oxidoreductase

ORF - Open Reading Frame

pI - Isoelectric point

PMS - Phenazine methosulfate

POR - Pyruvate:ferredoxin oxidoreductase

PVDF - Polyvinylidenefluoride

RBS - Ribosome binding site

SH_2ase - Sulfhydrogenase

SHE - Standard Hydrogen Electrode

SudA - α-subunit of SuDH

SudB - β-subunit of SuDH

SuDH - Sulfide dehydrogenase

V_{max} - Rate of reaction at infinite concentration of substrate

OUTLINE OF THE THESIS

P. furiosus grows near 100°C by fermentation of carbohydrates (Fiala and Stetter, 1986) through a modified Embden-Meyerhoff pathway, producing acetate, alanine, CO_2 and H_2 (Kengen and Stams, 1994). Two H_2-producing enzymes were known in this organism: sulfhydrogenase I (Bryant and Adams, 1989) and sulfhydrogenase II (Ma *et al.*, 2000). During metabolism of carbohydrates and amino acids, reducing equivalents are transferred to an iron-sulfur protein, ferredoxin. The oxidized form of ferredoxin must be regenerated in order to sustain the continuing operation of these metabolic pathways. However, the sulfhydrogenases from *P. furiosus* cannot use reduced ferredoxin as an electron donor, which prevents them from directly disposing of the reducing equivalents produced by the metabolism of *P. furiosus*. Instead, they are able to oxidize NADPH to $NADP^+$ with concomitant production of H_2 (Ma *et al.*, 2000; Ma *et al.*, 1994). It was therefore suggested that these reducing equivalents may be transferred to $NADP^+$ (thus generating NADPH) by the sulfide dehydrogenase, which can also function as a ferredoxin:$NADP^+$ oxidoreductase (Ma *et al.*, 1994). The produced NADPH will be used to reduce hydrogenase. It has been shown that the reduction, catalyzed by enzymes, of protons to H_2 by pyridine nucleotides is possible only when the partial pressure of H_2 is kept below 0.1 kPa (Schink, 1997; Stams, 1994). *P. furiosus* is however able to grow under H_2 accumulating conditions ($pH_2 \approx 30$ kPa) (Fiala and Stetter, 1986).

In order to understand the pathway of electron disposal in *P. furiosus* each of the enzymes involved (sulfide dehydrogenase and sulfhydrogenase) was purified and characterized. The physiological activities of these proteins in cell extracts were also investigated. The results of this study are described in this thesis.

Chapter 1 introduces the organism studied, the archaeon *Pyrococcus furiosus*. Its primary metabolism is explained, and the pathways proposed for disposal of reducing equivalents are described.

Chapter 2 reviews the current knowledge on the physiological functions, structure, redox properties and spectroscopic characterization of hydrogenases. This class of proteins is proposed to play a major role in the maintenance of the redox equilibrium in *P. furiosus*.

Chapter 3 describes the methods used to study the enzymes involved in the pathway of hydrogen evolution in *P. furiosus*.

Chapter 4 presents the results of kinetic and spectroscopic characterization of the soluble sulfhydrogenase I of *P. furiosus*. The first [NiFe] EPR signals in a hyperthermophilic hydrogenase are described. The electronic environment of the active site cluster is shown to be significantly different from that of hydrogenases isolated from mesophilic organisms. The protein is also shown to be more active in the H_2-uptake than in the H_2 evolution reaction, in contrast to previous reports.

Chapter 5 describes the results of sequence analysis and redox characterization of sulfide dehydrogenase (SuDH). The protein contains three [Fe-S] clusters with uncommon redox behavior, one of which is a [2Fe-2S] cluster with novel $Asp(Cys)_3$ coordination.

In **Chapter 6** the physiological activities of SuDH and sulfhydrogenase are investigated. The partial purification of a membrane-bound hydrogenase and subsequent characterization are also described. The results obtained allow the formulation of a novel mechanism of H_2 evolution by *P. furiosus*.

In **Chapter 7** the sequences of several soluble and membrane-bound hydrogenases are compared. Specific motifs allowing their classification are presented. Some of these motifs suggest that the potentials from some of the Fe-S clusters may be pH-dependent.

1

THE METABOLISM OF *PYROCOCCUS FURIOSUS*

1.1 THE METABOLISM OF CARBOHYDRATES

Pyrococcus furiosus is a member of the Domain Archaea originally isolated anaerobically from geothermally heated marine sediments with temperatures between 90 °C and 100 °C collected at the beach of Porto Levante, Vulcano Island, Italy (Fiala and Stetter, 1986). It appears as mostly regular cocci of 0.8 μm to 1.5 μm diameter with monopolar polytrichous flagellation (Figure 1.1). It grows between 70 °C and 103 °C, with an optimum temperature of 100 °C, and between pH 5 and 9 (with an optimum at pH 7). It grows well on yeast extract, maltose, cellobiose, β-glucans, starch, and protein sources (tryptone, peptone, casein and meat extracts). Growth is very slow, or non-existent, on amino acids, organic acids, alcohols, and most carbohydrates (including glucose, fructose, lactose and galactose).

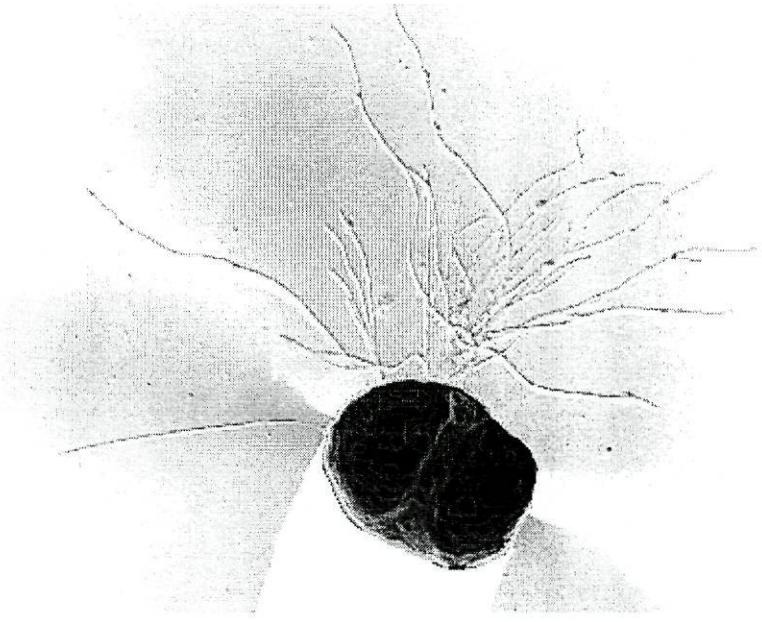

Figure 1.1 Electron micrograph of *Pyrococcus furiosus*, showing monopolar polytrichous flagellation. (taken from www.biologie.uni-regensburg.de/Microbio/Stetter/)

The ability to grow on polysaccharides (maltose, cellobiose, starch) but not on the monomeric sugars suggests that oligosaccharides with various degrees of polymerization may be imported into the cell, and only subsequently hydrolyzed to glucose.

The main fermentation products of maltose are acetate, CO_2, H_2 and alanine. As the H_2 partial pressure increases more pyruvate is transformed in alanine instead of being oxidized to acetate and producing ATP (Kengen *et al.*, 1994). At high partial pressures of H_2 no growth is observed (Fiala and Stetter, 1986). However if there is elemental sulfur in the medium growth is observed even at very high H_2 partial pressures and H_2S is formed instead of H_2 (Fiala and Stetter, 1986). This has been proposed to be either a means of removing the growth-inhibiting excess H_2 or an energy-conserving process (Schicho *et al.*, 1993).

The activity of several of the enzymes involved in the conventional glucose degradation pathways was found to be very low or non-existent in *P. furiosus*, which led to the suggestion that glucose originated from the hydrolysis of maltose is degraded to pyruvate via a modified non-phosphorylating Entner-Doudoroff pathway, "pyroglycolysis", without the intervention of nucleotide-dependent enzymes (Mukund and Adams, 1991; Schäffer and Schönheit, 1992) In this pathway a key role was fulfilled by a tungsten-dependent aldehyde oxidoreductase (Mukund and Adams, 1991). Additional studies (Kengen *et al.*, 1994; Schäffer *et al.*, 1994) showed that the actual pathway is a variation of the conventional Embden-Meyerhoff pathway. A major difference resides in the nucleotides used in the initial steps of the pathway: in *P. furiosus* glucose and fructose-6-phosphate are phosphorylated by ADP instead of ATP (Figure 1.2) (Kengen *et al.*, 1994). The free energy change in ADP hydrolysis is about the same as in ATP hydrolysis (Voet and Voet, 1990), but ADP is probably more stable than ATP at higher temperatures and therefore the ATP produced during catabolism

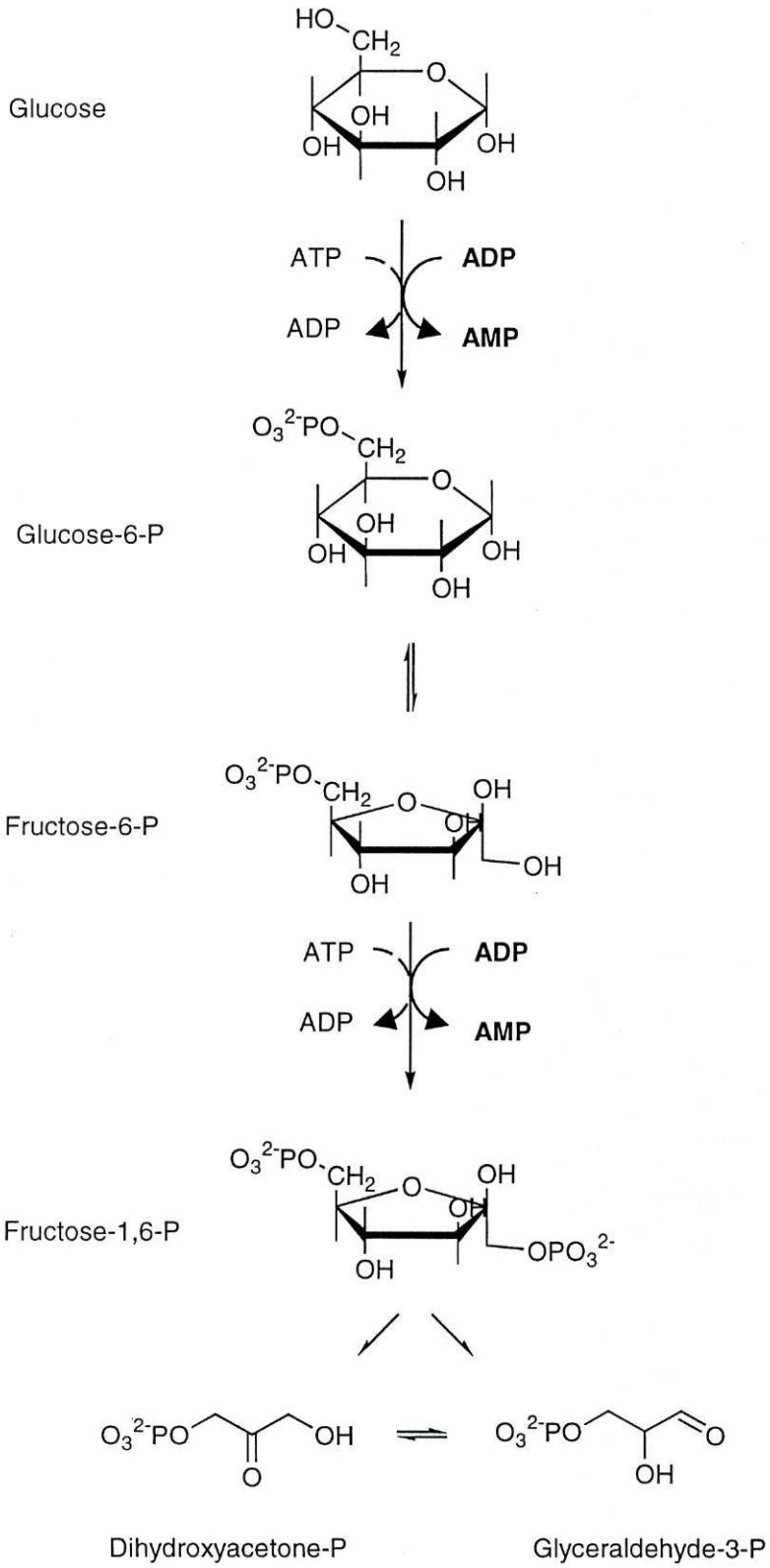

Figure 1.2 Glucose degradation to trioses in *P. furiosus*. Dashed arrows show the reactions where the conventional Embden-Meyerhoff pathway differs from the *P. furiosus* one.

may be deliberately converted to ADP by an adenylate kinase reaction (ATP +AMP⇌ADP +ADP). However, since ATP-dependent hexose-kinases are present in other hyperthermophiles (*Desulfurococcus*, *Thermoproteus* and *Thermotoga* (Selig *et al.*, 1997)), the optimal growth temperature of which is lower by only 5-15 °C, factors other than temperature might be responsible for this unusual nucleotide specificity [ibidem].

Another major difference in the *P. furiosus* pathway is the glyceraldehyde-3-phosphate:ferredoxin oxidoreductase (GAPOR) bypass (Figure 1.3). In the conventional Embden-Meyerhoff pathway glyceraldehyde-3-phosphate is oxidized to 3-phosphoglycerate in two steps. Glyceraldehyde-3-phosphate is first oxidized by glyceraldehyde-3-phosphate dehydrogenase to 1,3-bisphosphoglycerate. The high-energy phosphate in 1,3-bisphosphoglycerate is afterwards transferred to ADP by a phosphoglycerate kinase, yielding one ATP molecule and one 3-phosphoglycerate molecule as final products. However in *P. furiosus* both proteins involved in this process (glyceraldehyde-3-phosphate dehydrogenase and phosphoglycerate kinase) have been shown to have a low activity in the glycolytic direction under normal growth conditions (Kengen *et al.*, 1994; Schäffer and Schönheit, 1993), and to be induced up to 10-fold during growth on pyruvate, suggesting they function primarily in gluconeogenesis (Schäffer and Schönheit, 1993). Instead, *P. furiosus* contains a glyceraldehyde-3-phosphate:ferredoxin oxidoreductase (GAPOR) (Mukund and Adams, 1995). The final product of the oxidation of GAP by GAPOR has not been determined, but is believed to be 3-phosphoglycerate (and not 1,3-bisphosphoglycerate, as in the standard pathway).

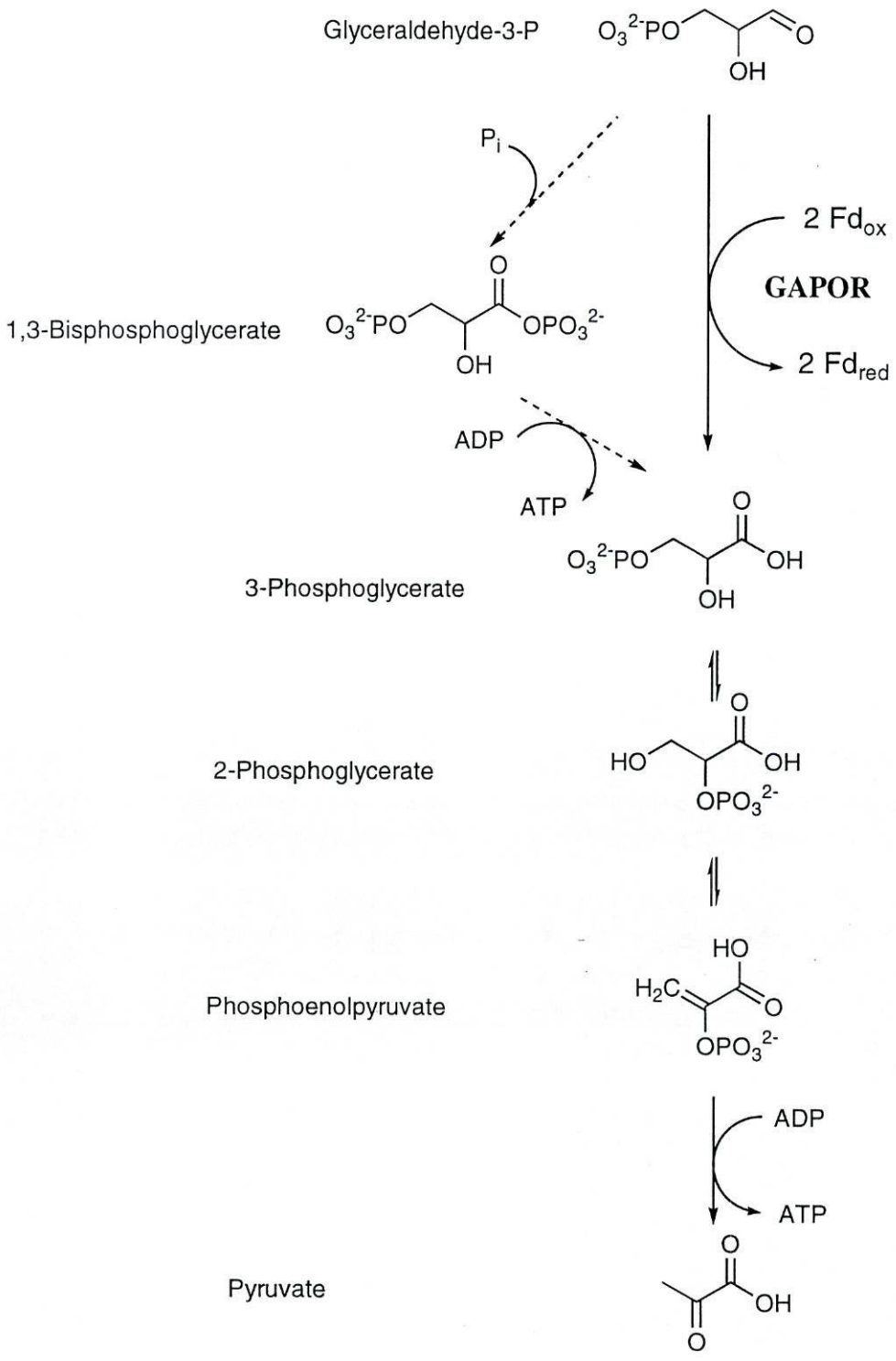

Figure 1.3 Degradation of trioses to pyruvate in *P. furiosus*. Dashed arrows show the reactions where the conventional Embden-Meyerhoff pathway differs from the *P. furiosus* one.

This pathway yields 2 ATP molecules and 4 reducing equivalents for each glucose molecule metabolized to pyruvate (assuming that ADP is readily available from anabolic processes). Additional energy and reducing equivalents may be produced from pyruvate, as depicted in Figure 1.4. Two enzymes are involved in this process: a pyruvate:ferredoxin oxidoreductase (POR) and a novel acetyl-CoA synthetase (ADP-forming) (Schäffer and Schönheit, 1991). Pyruvate:ferredoxin oxidoreductase has been purified to homogeneity and shown to be a thiamin pyrophosphate-containing iron-sulfur enzyme. (Blamey and Adams, 1993). In the absence of ferredoxin, however, POR decarboxylates pyruvate to acetaldehyde (Ma *et al.*, 1997), which can not be used to produce ATP.

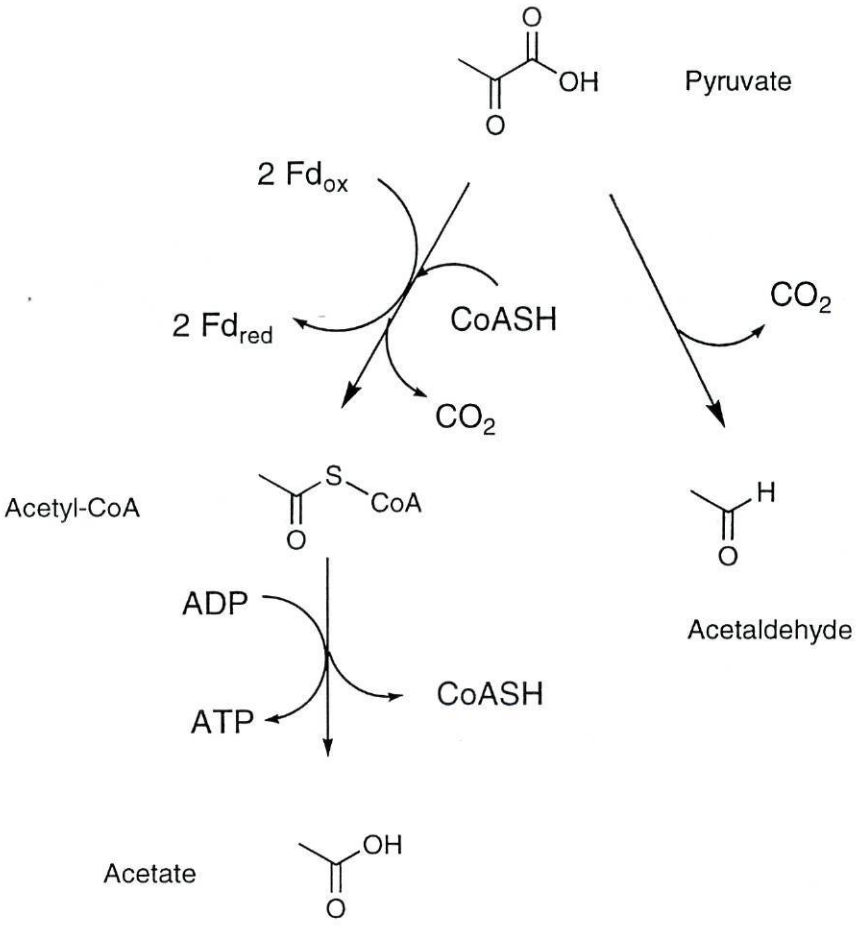

Figure 1.4 Metabolism of pyruvate in *P. furiosus*.

Acetyl-CoA synthetase (ADP-forming) catalyzes the one-step formation of acetate from acetyl-CoA and concomitant ATP synthesis. The oxidation of one molecule of glucose to two molecules of acetate and two molecules of CO2 in P. furiosus therefore yields 4 molecules of ATP and the reduction of 8 ferredoxin molecules. The concerted action of these two enzymes allows growth of P. furiosus on pyruvate as sole energy source (Schäffer and Schönheit, 1991).

Two distinct isoenzymes of Acetyl-CoA synthetase (ADP-forming) have been isolated from P. furiosus (Mai and Adams, 1996b). Both appear to be heterotetramers ($\alpha_2\beta_2$) of two different subunits of 45 (α) and 23 (β) kDa. One of them, termed acetyl-CoA synthetase I, uses acetyl-CoA and isobutyryl-CoA, but not indoleacetyl-CoA or phenylacetyl-CoA, while the other utilizes all four CoA derivatives. This allows generation of ATP from a wide range of 2-ketoacids (e.g. the 2-ketoacids produced by the transamination of amino acids).

1.2 THE FATE OF THE REDUCING EQUIVALENTS

Besides POR and GAPOR *P. furiosus* contains several other ferredoxin-linked oxidoreductases, and those oxidizing aldehydes (Mukund and Adams, 1991), formaldehyde (Mukund and Adams, 1993), and several 2-ketoacids (indolepyruvate (Mai and Adams, 1994), 2-ketoglutarate (Adams, 1993; Mai and Adams, 1996a) and 2-ketoisovalerate (Heider *et al.*, 1996)) have been purified and suggested to play a role in amino acid fermentation. Both glycolysis and peptide fermentation therefore generate reduced ferredoxin. However, the sustained operation of glycolysis requires an influx of oxidized ferredoxin. Regeneration of oxidized ferredoxin is assumed to be accomplished by three mechanisms: either by S^0 reduction to H_2S, by the formation of alanine, or by proton reduction to H_2.

1.2.1 Reduction of elemental sulfur

Biomass yield of *P. furiosus* is larger when the organism is grown in the presence of S^0. Under these conditions H_2S is produced rather than H_2. Since growth is inhibited under high H_2 partial pressures, S^0 reduction (with H_2 as electron donor) has been suggested to be a means of detoxification (Fiala and Stetter, 1986). However, it has been reported that the onset of growth inhibition by H_2 occurred at relatively high H_2 concentrations (0.40 atm), suggesting that in the conditions used growth was unaffected by moderate concentrations of H_2 even in the absence of elemental sulfur (Schicho *et al.*, 1993). The same authors also observed that growth yields in the presence of sulfur can be almost twice as large as the ones obtained with physical removal of H_2 in the absence of elemental sulfur, showing that the effect of S^0 is not due to a lowering of the H_2 concentration. These results suggest either that S^0 reduction is an energy-conserving process, or that S^0 facilitates a process that would otherwise require energy. Schicho *et al.* also reported that neither the sulfur reductase activity nor the hydrogenase activity (the enzyme responsible for disposing of excess reductant in the absence of S^0 – see below) appear to be induced by the addition of S^0.

Chemolithotrophic archaea, such as *Pyrodictium*, utilize the redox couples H^+/H_2 and S^0/H_2S in an energy yielding reaction. *Pyrodictium brockii*, an obligate sulfur-reducing species that grows at 105 °C, has been shown to possess a primitive membrane-bound electron transport chain for coupling H_2 oxidation and S^0 reduction (Pihl *et al.*, 1992). The chain contained a hydrogenase (Pihl and Maier, 1991), a cytochrome, and a novel quinone. The S^0-reducing entity was not purified. A sulfur-reducing complex proposed to contain the entire electron chain required for the reduction of S^0 to H_2S (including a hydrogenase, a sulfur reductase and electron-transferring components) has been successfully purified from the membranes of related species, *Pyrodictium abyssi* (Dirmeier *et al.*, 1998). The occurrence of these respiratory

proteins in the membranes of *Pyrodictium* species presumably allow the resulting pH gradient and membrane potential generated across the membrane to be used in ATP production by an ATP synthase, as in mitochondrial O_2 respiration (Voet and Voet, 1990). A similar mechanism may occur in the mesophilic bacterium *Wolinella succinogenes*, which grows on formate using S^0 as electron acceptor using a membrane-bound polysulfide reductase, a molybdoenzyme consisting of three subunits (Kraft *et al.*, 1992).

Several enzymes that catalyze the reduction of sulfur and polysulfides have since been isolated from cell extracts of *P. furiosus*:

- Sulfide dehydrogenase (SuDH) catalyses the reduction of polysulfides to H_2S using NADPH as electron donor (Ma and Adams, 1994). SuDH is also a ferredoxin:$NADP^+$ oxidoreductase (FNOR) (Ma and Adams, 1994; Ma *et al.*, 1994). The heterodimer (≈52+29 kDa) was found to contain approximately 11 iron atoms and approximately two flavins. The flavins are presumably FAD because 3.2 P per αβ-dimer were found in plasma emission analysis. EPR spectroscopic analysis was interpreted in terms of one [3Fe-4S] cluster and three additional Fe/S clusters with an S=1/2 signal in the reduced state i. e. 2Fe and/or 4Fe clusters. N-terminal amino-acid sequences were also determined for each subunit.
- Sulfhydrogenases I (Bryant and Adams, 1989) and II (Ma *et al.*, 2000) can reduce both S^0 and polysulfides to H_2S using H_2 as electron donor. Surprisingly, H_2 seems to supply only the electrons needed to reduce sulfur. The protons released in H_2S seem to originate from solvent water, rather than from H_2 (Kim *et al.*, 1999). Both sulfhydrogenases consist of four subunits and contain Ni and iron-sulfur clusters (Bryant and Adams, 1989; Ma *et al.*,

2000) and FAD (see chapter 4.2). These proteins are further described in section 1.2.3-Proton reduction to H_2 (pg. 13).

In contrast to *Pyrodictium* and *Wolinella succinogenes*, sulfur-reducing proteins in *P. furiosus* are cytoplasmic instead of membrane-bound, which does not allow a straightforward energy-conservation mechanism. It is thought that S^0 reduction may increase the ratio of oxidized to reduced electron carriers, thereby favoring the oxidative rather than the non-oxidative decarboxylation of the 2-ketoacids produced by glycolysis and amino acid transamination (Ma *et al.*, 1997).

1.2.2 Formation of alanine

The second alternative, formation of alanine, is found when *P. furiosus* is grown in the absence of S^0. In addition to acetate, a significant amount of alanine is excreted into the medium (Kengen and Stams, 1994; Schäffer *et al.*, 1994). The amount of alanine produced varies, with an increase in the H_2 partial pressure resulting in an increase in the amount of alanine produced. The transamination of pyruvate with glutamate (1) by the action of an alanine aminotransferase (AlaAT) has been detected in cell extracts of *P. furiosus* (Kengen and Stams, 1994).

pyruvate + glutamate $\leftrightharpoons$ α-ketoglutarate + alanine (1)

Glutamate must be replenished through the action of the NADP-dependent glutamate dehydrogenase (GDH) and this replenishment should accomplish the removal of electrons. Glutamate dehydrogenase from *P. furiosus* has been purified (Consalvi *et al.*, 1991; Robb *et al.*, 1992) and shown to be very abundant, especially in cells grown

on yeast extract (Consalvi *et al.*, 1991). The exact role of glutamate dehydrogenase in the metabolism of *P. furiosus* is disputed, since it may function both in catabolism and in anabolism, respectively through glutamate degradation to α-ketoglutarate (Robb *et al.*, 1992) or through ammonia assimilation by the reverse reaction (Consalvi *et al.*, 1991):

$$\text{glutamate} + NAD(P)^+ + H^+ \leftrightharpoons \alpha\text{-ketoglutarate} + NH_4^+ + NAD(P)H \qquad (2)$$

The necessary NADPH can be generated by the transfer of reducing equivalents from reduced ferredoxin to $NADP^+$ by the ferredoxin: $NADP^+$ oxidoreductase activity of the sulfide dehydrogenase (Ma *et al.*, 1994).

The alanine aminotransferase has recently been purified and characterized (Ward *et al.*, 2000). The k_{cat} / K_m values for alanine and pyruvate formation were 41 and 33 s^{-1} mM^{-1}, respectively, suggesting that the enzyme is not biased toward either the formation of pyruvate, or alanine. It can thus act in a dual role, generating either pyruvate from alanine during peptide fermentation or alanine from pyruvate when an additional electron sink is needed. Both the *aat* gene (encoding the alanine aminotransferase) and *gdh* (encoding the glutamate dehydrogenase) transcripts appear to be coregulated at the transcriptional level, which is in good agreement with these enzymes acting in a concerted manner to form an electron sink in *P. furiosus* (Ward *et al.*, 2000).

1.2.3 Proton reduction to H_2

As mentioned before, in the absence of elemental sulfur H_2 is produced by cultures of *P. furiosus*. Two soluble hydrogen-metabolizing enzymes (hydrogenases) have been purified from this organism (Bryant and Adams, 1989; Ma *et al.*, 2000) and

shown to possess also sulfur reductase activity (Ma *et al.*, 1993; Ma *et al.*, 2000). Both proteins are therefore also referred to as "sulfhydrogenases".

They consist of four subunits, but their arrangement seems to differ: sulfhydrogenase I (H-I) is a heterotetramer ($\alpha\beta\gamma\delta$), but sulfhydrogenase II (H-II) has been proposed to be a dimer of heterotetramers $(\alpha\beta\gamma\delta)_2$. The structural genes of each sulfhydrogenase are organized in a single transcription unit with reading direction $\beta\gamma\delta\alpha$. The δ and α subunits are homologous to the small and large subunits of mesophilic NiFe hydrogenases, and the β and γ subunits show similarity to the α and β subunits of the anaerobic, NADH-linked, $\alpha\beta\gamma$ sulfite reductase from *Salmonella typhimurium* (Ma *et al.*, 2000; Pedroni *et al.*, 1995).

Both proteins have a high iron-sulfur content (Arendsen *et al.*, 1995; Bryant and Adams, 1989). They also contain nickel. However, so far only three EPR signals were found in sulfhydrogenase I: a rhombic signal, attributed to a [4Fe-4S] cluster with a reduction potential $E_{m,\,7.5}$ = -90 mV, an axial signal arising from a [2Fe-2S] cluster with reduction potential $E_{m,\,7.5}$= -303 mV, and a broad signal, possibly caused by interaction of the cluster that gives rise to the rhombic signal and another (fast-relaxing) paramagnet that becomes detectable upon reduction with $E_{m,\,7.5}$ = - 310 mV (Arendsen *et al.*, 1995). The same signals (and no others) have also been found in sulfhydrogenase II (Ma *et al.*, 2000). No nickel signals have been found in redox studies at ambient temperature (Arendsen *et al.*, 1995; Bryant and Adams, 1989; Ma *et al.*, 2000) but an EPR signal reminiscent of the Ni-C signal was claimed in thus far unpublished work to be detectable after incubation of the sulfhydrogenase I at 80 °C and poising the redox potential at approximately -0.3 V (Adams, 1992).

The two hydrogenases of *P. furiosus* seem to differ primarily in their relative catalytic activities. H-II is approximately an order of magnitude less active than H-I in H_2-production, H_2-uptake and S^0-reduction assays (Ma *et al.*, 2000). Both proteins can use NADPH as an electron donor for the reduction of protons to H_2 and polysulfide to

H_2S. H-II can also use NADH to reduce polysulfides. They seem to have a preference for sulfide production (from polysulfide) rather than H_2 production: adding polysulfide to an assay vessel containing NADPH and hydrogenase increased the rate of NADPH oxidation and reduced H_2 production. The two enzymes are present in the cytoplasm at roughly similar concentrations, and the authors concluded that they may serve different functions. Since H-II has a higher affinity for both S^0 and polysulfides in the standard assays, the authors proposed that this enzyme becomes physiologically relevant at low S^0 concentrations. H-I would then function primarily in H_2 evolution from NADPH, a reaction in which it is about 60 times more efficient than H-II.

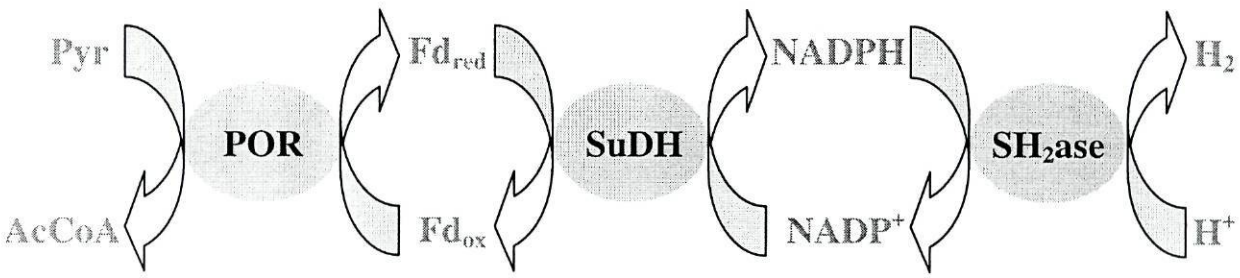

Figure 1.5 Proposed model for the transfer of electrons from ferredoxin to sulfhydrogenase.

The reducing equivalents from glycolysis are stored in the ferredoxin. The sulfhydrogenases, however, cannot use ferredoxin as an electron donor (Ma *et al.*, 2000; Ma *et al.*, 1994), contrary to what was initially believed (Bryant and Adams, 1989). Later this idea was rejected in favor of a concerted model in which the sulfide dehydrogenase (SuDH) (which also has ferredoxin: $NADP^+$ oxidoreductase activity) catalyzes the transfer of electrons from the reduced ferredoxin to $NADP^+$. Sulfhydrogenase would then use the NADPH generated in this reaction to reduce protons to H_2 (Ma *et al.*, 1994). The net result of this soluble electron-transfer chain is thus evolution of H_2 from ferredoxin, thus regenerating the oxidized form of the ferredoxin (Figure 1.5).

2

THE MOLECULAR BASIS OF HYDROGEN METABOLISM

2.1 ECOLOGICAL FLUXES OF H_2

Molecular hydrogen is an important intermediate in the degradation of organic matter by microorganisms in anaerobic environments such as freshwater and marine sediments, wet land soils, and the gastrointestinal tract of animals. Bacteria living in such anaerobic environment, using the fermentation of organic substrates for the supply of energy-rich reducing equivalents often dispose of their excess of electrons by reducing protons. In some habitats anaerobic protozoa, anaerobic fungi, anaerobically adapted algae, and/or anaerobic archaea are also involved. One major source of reducing equivalents for H_2 production is pyruvate. Some organisms convert it to acetyl-CoA and formate, whereupon the latter is decomposed into H_2 and CO_2 by the formate-hydrogen-lyase reaction, in which hydrogenase is involved. Pyruvate can also be oxidized by the enzyme pyruvate: ferredoxin oxidoreductase. Reduced ferredoxin then transfers its electrons to a hydrogenase.

The H_2 generated by these microorganisms is generally consumed by microorganisms living at the same site, the quantitatively most important H_2 consumers in anoxic habitats being methanogenic archaea, acetogenic bacteria, sulfate-reducing bacteria, and nitrate-reducing bacteria. In order to acquire energy-rich reducing equivalents, these bacteria have the capacity to oxidized H_2 to two protons and two electrons. The standard oxidation-reduction potential of the equilibrium

$$2\ H^+ + 2\ e^- \leftrightharpoons H_2 \qquad (1)$$

is quite low, by definition, –413 mV at pH 7.0, 25 °C and 101.325 kPa (1 atm) of H_2 pressure. The reducing equivalents obtained in this way enable bacteria to reduce a variety of substrates, notably CO_2, and to generate enough energy for ATP synthesis.

Estimates are that in anaerobic habitats more than 200 million tons of H_2 are globally formed and consumed per year. Despite this high rate the steady state

concentration of H_2 in most anoxic habitats is only very low (1-10 Pa), indicating that H_2 formation rather than H_2 consumption is the rate-limiting step in the overall process (Bélaich *et al.*, 1990).

H_2 is also generated in oxic habitats (e.g. oxic soils and fresh water) by aerobic and microaerophilic microorganisms as an inevitable side product of dinitrogen fixation (Burns and Bulen, 1965; Simpson and Burris, 1984). More than 10 million tons of H_2 are globally formed associated with this process. The diversion of reducing equivalents to the production of H_2 reduces the overall efficiency of nitrogen fixation. In most dinitrogen-fixing organisms a hydrogenase recaptures these energy-rich electrons, preventing larger energy losses. Other microorganisms consuming H_2 in oxic habitats are the "Knallgas" bacteria (bacteria capable of growing using the "knallgas" reaction – the reduction of O_2 by H_2 – as energy source).

2.2 TYPES OF HYDROGENASES

Hydrogenases are a diverse family of enzymes. A classification of hydrogenases in two major groups is commonly accepted: iron-only and nickel-iron hydrogenases. Fe-only hydrogenases contain no metals other than iron, and are usually monomeric enzymes that catalyze primarily H_2 evolution (Adams, 1990). Ni-Fe hydrogenases contain nickel, in addition to Fe-S clusters. They are considerably less active (0.1-0.8 mmol H_2 produced or oxidized/min/mg protein) than Fe-hydrogenases (5-10 mmol H_2 produced /min/mg protein; 10-50 mmol H_2 oxidized/min/mg protein) but have a much higher affinity for H_2 (Albracht, 1994). Enzymes such as nitrogenase (Burns and Bulen, 1965; Simpson and Burris, 1984) and carbon monoxide dehydrogenase (Menon and Ragsdale, 1996) catalyze the formation of H_2 as a side product, and are therefore referred to as having hydrogenase activity. These latter enzymes will not be considered in any detail in this introduction.

The Fe-only and the Ni-Fe hydrogenases have several catalytic properties in common which will be described first before summarizing what is known about the structure of these catalysts (Adams, 1990; Albracht, 1994).

2.2.1 Catalytic Properties in Common

Both, the Fe-only and the Ni-Fe hydrogenases catalyze the reversible conversion of H_2 to two protons and two electrons (reaction 1, pg. 19), the latter being acceptable by one-electron acceptors such as viologen dyes. Both enzymes catalyze an exchange between H_2 and protons of water indicative of a ping-pong catalytic mechanism. Single exchanges (reaction 2) and double exchanges (reaction 3) are simultaneously observed.

$$H_2 + D^+ \rightleftharpoons H^+ + HD \qquad (2)$$

$$H_2 + 2\,D^+ \rightleftharpoons 2\,H^+ + D_2 \qquad (3)$$

Both enzymes also catalyze the conversion of para-H_2 (H_2 with anti-parallel nuclear spins) and ortho-H_2 (H_2 with parallel nuclear spins) (reaction 4).

$$p\text{-}H_2\,(\uparrow\downarrow) \rightleftharpoons o\text{-}H_2\,(\uparrow\uparrow) \qquad (4)$$

This conversion will not occur in D_2O (Krasna and Rittenberg, 1954). Homolytic cleavage of the H_2 molecule would inevitably lead to the conversion of p-H_2 to o-H_2 regardless of the nature of the liquid phase, for recombination of atomic hydrogen must yield normal H_2, which is an equilibrium mixture of p-H_2 (25%) and o-H_2 (75%) (Farkas, 1936). It is therefore generally admitted that upon binding of H_2 to Fe-only or Ni-Fe hydrogenases the hydrogen molecule undergoes a reversible heterolytic cleavage resulting in a hydride bound to the metal center in the active site. A base nearby the active site may bind the proton during the catalytic process.

The activity of both enzymes is competitively inhibited by carbon monoxide (Albracht, 1994; Thauer *et al.*, 1974). Inhibition by carbon monoxide is relieved during illumination with near UV/visible light (Albracht, 1994). Competitive inhibition indicates that binding of carbon monoxide and H_2 to the enzyme is mutually exclusive and light reactivation showed that the binding site is a metal center. Both enzymes contain at least one [4Fe-4S] cluster to which the electrons are transferred from H_2 and from which the electrons can be picked up by one-electron accepting dyes.

2.3 Hydrogenases Containing only Iron-Sulfur Clusters

Fe-only hydrogenases, in which no other metal than Fe can be detected, have been purified from *Acetobacterium woodii*, *Clostridium pasteurianum*, *Desulfovibrio desulfuricans*, *Desulfovibrio vulgaris*, *Megasphaera elsdenii*, *Thermotoga maritima*, and *Trichomonas vaginalis*. Fe-only hydrogenases contain large amounts of iron, organized in two kinds of clusters. Most of the iron is found in the form of ferredoxin-type [4Fe-4S] clusters (the "F" clusters). The remaining Fe comprises a novel type of Fe-S cluster, termed the "hydrogenase" or "H" cluster (Adams, 1990).

The X-ray structures of two Fe-only hydrogenases have been recently determined (Nicolet *et al.*, 1999; Peters *et al.*, 1998). It was found that the active site of Fe-only hydrogenases is composed of a novel cluster that exists as a single [4Fe–4S] subcluster (which presumably functions in electron transfer) bridged through a cysteine S to a unique two-Fe subcluster where the reversible oxidation of hydrogen is supposed to occur (Figure 2.1 and Figure 2.2). Each of the Fe atoms of this binuclear subcluster is coordinated by several small diatomic ligands. These have been variously assigned as CO and CN, based in part on the presence of these ligands in the NiFe hydrogenase

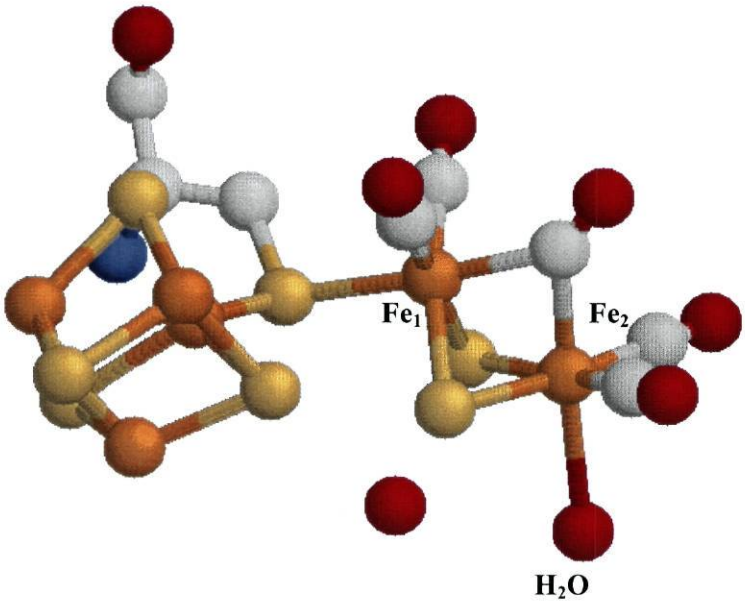

Figure 2.1 X-Ray crystal structure (at 1.8 Å resolution) of the (probably oxidized or "resting") Fe-only hydrogenase I (CpI) from *C. pasteurianum* (Peters *et al.*, 1998). Iron: orange; Sulfur: yellow; Carbon: grey; Oxygen: red; Nitrogen: blue.

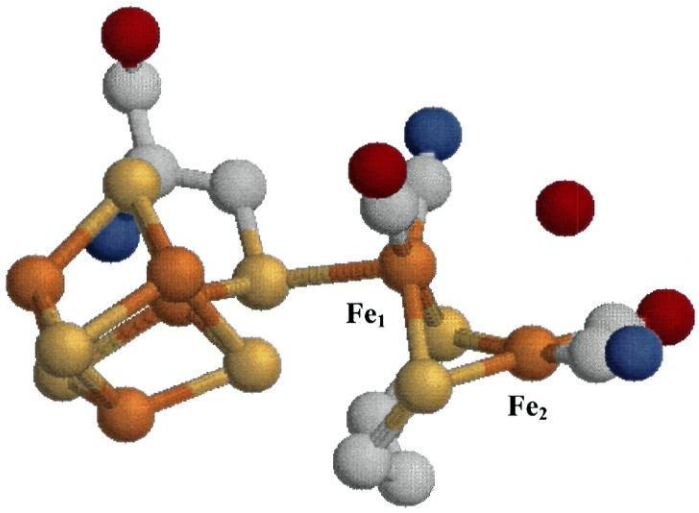

Figure 2.2 X-Ray crystal structure (at 1.6 Å resolution) of the (probably reduced or "turnover") Fe-only hydrogenase (DdH) from *D. desulfuricans* (Nicolet *et al.*, 1999). Iron: orange; Sulfur: yellow; Carbon: grey; Oxygen: red; Nitrogen: blue.

from *D. gigas* (Volbeda *et al.*, 1996) and on the results of FTIR studies that indicate that these ligands are also present in the Fe-only hydrogenases (van der Spek *et al.*, 1996). The most recent FTIR studies concerning the composition of the diatomic ligands suggested that both terminal CO and terminal CN^- ligands are bound to Fe and that a bridging carbon monoxide is present in an oxidized state in anaerobically purified Fe-only hydrogenase from *Desulfovibrio vulgaris* prior to reductive activation (Pierik *et al.*, 1998).

Although the structures of the H clusters of CpI and DdH are very similar, there are some interesting differences. The bridging moiety in the H cluster of DdH has been tentatively assigned as a propane linkage between the S atoms (Nicolet *et al.*, 1999); the resolution of the X-ray diffraction data used in the CpI structure determination would not allow this moiety to be assigned (Peters *et al.*, 1998) but are consistent with such an assignment (Peters, 1999). A significant difference between the DdH and CpI H clusters is the nature of the third bridging ligand of the two Fe atoms. In CpI, this ligand clearly refines as a single diatomic ligand (tentatively assigned as CO), whereas in DdH, this ligand has been assigned as an asymmetrically coordinated water molecule. Another notable difference between the H cluster structures is the presence of a terminally coordinated water molecule in CpI that is absent in DdH. The manner in which the crystals of CpI and DdH were obtained is most consistent with the structure of CpI representing an oxidized state and that of DdH representing a reduced state. This would be consistent with a proposed mechanism of reversible hydrogen oxidation involving displacement of the terminally bound water molecule (Figure 2.1) and a change in the binding mode of the bridging carbon monoxide molecule from bridging (in the oxidized state) to terminally-bound to Fe_2 in the active state. The recent observation that exogenous CO (which strongly inhibits the enzyme activity) binds to the reduced hydrogenase at Fe_2 at the site of the terminally bound water (Peters and Lemon, 1999) further argues in favor of the proposed mechanism.

2.4 NICKEL-CONTAINING HYDROGENASES

Most hydrogenases contain nickel, as first established by Graf and Thauer in 1981 for the enzyme from *Methanobacterium thermoautotrophicum*. The purified enzyme from this methanogenic archaeon was found to harbor one nickel per mole (Graf and Thauer, 1981) and displays a simple rhombic EPR signal (Albracht *et al.*, 1982) which could be ascribed to nickel by using ^{61}Ni (a stable isotope with a nuclear spin of 3/2). Moreover, the signal disappeared upon contact of the enzyme with H_2, indicating that the nickel in the enzyme was redox active.

Nickel hydrogenases have been characterized from various organisms. Besides one nickel they all appeared to contain several iron atoms, most of the iron being organized in iron-sulfur clusters, at least one having cubane structure. Some Ni-containing hydrogenases contain selenium in the form of selenocysteine (He *et al.*, 1989; Sorgenfrei *et al.*, 1993) and are often called [NiFeSe] hydrogenases. [NiFeSe] are considerably more active than normal [NiFe]enzymes. The selenocysteine residue in these hydrogenases replaces the terminal cysteine residue corresponding to Cys 530 of the *D. gigas* enzyme in the first coordination sphere of nickel (Fauque *et al.*, 1988). The H_2/HD ratio measured in the D_2-H^+ exchange reaction also appears to be very different in the two kinds of enzymes (Teixeira *et al.*, 1987), and has been interpreted as evidence of proton binding to this (seleno)cysteine residue upon heterolytic cleavage of H_2.

Spectroscopic methods (most notably Mössbauer spectroscopy (Surerus *et al.*, 1994) and ENDOR (Huyett *et al.*, 1997)) detect the presence of one low-spin diamagnetic Fe (II) in close vicinity to the nickel, and in some enzymes its redox state shuttles between low-spin paramagnetic Fe (III) and low-spin diamagnetic Fe (II) (Surerus *et al.*, 1994) at an E_m of approximately +150 mV in the enzyme from *Chromatium vinosum* at pH 8.0 (Coremans *et al.*, 1992) and +105 mV in the hydrogenase from *Thiocapsa roseopersicina* (Cammack *et al.*, 1989).

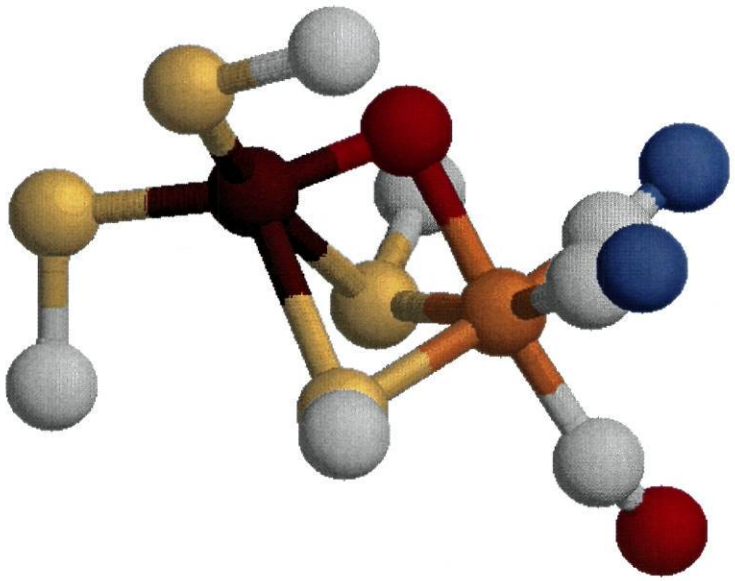

Figure 2.3 X-Ray crystal structure (at 2.45 Å resolution) of the oxidized periplasmic NiFe hydrogenase from *D. gigas* (Volbeda *et al.*, 1996). Nickel: brown; Iron: orange; Sulfur: yellow; Carbon: grey; Oxygen: red; Nitrogen: blue.

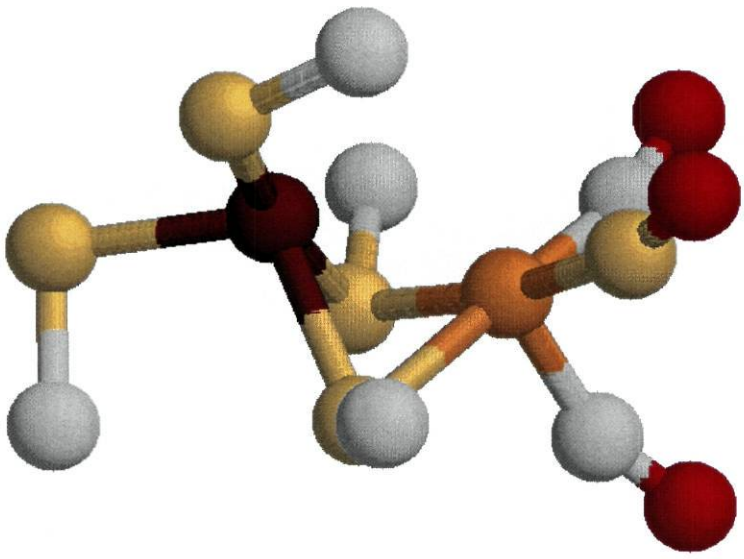

Figure 2.4 X-Ray crystal structure (at 1.8 Å resolution) of the reduced NiFe hydrogenase from *D. vulgaris* Miyazaki F (Higuchi *et al.*, 1999b). Nickel: brown; Iron: orange; Sulfur: yellow; Carbon: grey; Oxygen: red.

All Ni-hydrogenases contain at least a small (around 30 kDa) subunit, which harbors a variable number of Fe-S clusters, and a larger (around 60 kDa subunit) subunit where the active site, a cysteine-bridged dinuclear Ni-Fe cluster (Volbeda *et al.*, 1995), is located. Other subunits may also be present, allowing the hydrogenase to interact with dedicated electron carriers (NAD^+, F_{420}, cytochrome b) (Albracht, 1994).

D. gigas hydrogenase, as seen by X-ray crystallography, is a roughly globular protein with the two subunits interacting extensively. The hydrogen-activating site is deeply buried inside the protein at about 30 Å from the surface. The protein contains one [3Fe-4S] and two [4Fe-4S] clusters distributed in the small subunit along an almost straight line, resembling a "conducting wire" between the active site and the protein surface (Volbeda *et al.*, 1995).

The original *D. gigas* NiFe hydrogenase structure showed that the active site contained besides nickel a second metal bound to three unidentified ligands (Volbeda *et al.*, 1995). These ligands were tentatively assigned as water molecules. The nickel atom is bridged to the second metal by a pair of cysteine thiolates (Cys 68 and Cys 533) and a third unidentified atom (X) with a low atomic number. As a consequence of the short Ni-X distance (1.7 Å), it was postulated that X represents a Ni-oxo group that bridges to the second metal. The remaining ligands involved in the Ni site are two terminally bound cysteine thiolates (Cys 65 and Cys 530) (Figure 2.3). The second metal was soon proved to be an iron atom (Volbeda *et al.*, 1996) and the three ligands were shown to be small diatomic molecules. In the closely related hydrogenase from *D. vulgaris* Miyazaki F these ligands were assigned as one SO, one CO and one CN (see Figure 2.4), based on a X-ray structure obtained with a higher (1.8 Å) resolution (Higuchi *et al.*, 1997).

X-ray structures of [NiFe] hydrogenases in the reduced, active state have also been published (Garcin *et al.*, 1999; Higuchi *et al.*, 1999b) (Figure 2.4). These show small, but suggestive, differences compared to the structures of the oxidized, inactive enzyme. The original bridging ligand (proposed to be an oxygen (Volbeda *et al.*, 1995)

or a sulfur (Higuchi *et al.*, 1999a; Higuchi *et al.*, 1997) species) is absent in the reduced state, consistent with the proposed change of coordination of the active site upon activation (de Lacey *et al.*, 1997; Gu *et al.*, 1996). The Ni-Fe distance shortens appreciably upon reduction (from 2.9 Å to 2.5-2.6 Å), which is consistent with the presence of a hydride in a bridging position between both metals. In the [NiFeSe] hydrogenase from *Desulfomicrobium baculatum* Garcin *et al.* also observed higher-than-average temperature factors for both the active site nickel-selenocysteine ligand and the neighboring Glu18 residue, suggesting that both these moieties are involved in proton transfer between the active site and the molecular surface (Garcin *et al.*, 1999). The 2.54 Å resolution structure of Ni-Fe hydrogenase has revealed the existence of hydrophobic channels connecting the molecular surface to the active site. A crystallographic analysis of hydrogenase crystals incubated in a xenon atmosphere together with molecular dynamics simulations of xenon and H_2 diffusion in the enzyme interior suggests that these channels may serve as pathways for gas access to the active site (Montet *et al.*, 1997).

2.4.1 EPR Spectroscopy

Most [NiFe] hydrogenases exhibit a number of redox-dependent EPR signals that exhibit ^{61}Ni hyperfine splittings when the enzyme is isotopically enriched (Albracht, 1994). The as-isolated oxidized and catalytically inactive enzyme can show two similar signals, which differ mainly in the position of the g_y line: forms A ($g \approx 2.31$, 2.23, 2.02) and B ($g \approx 2.34$, 2.16, 2.01). Enzyme preparations showing a Ni-B signal can be activated by hydrogen within a few minutes. Enzyme molecules showing a Ni-A signal can only be fully activated after incubation under hydrogen for several hours (Fernandez *et al.*, 1985). Ni-B and Ni-A forms are therefore also called "ready" (proposed to be enzyme in the "right" conformation and the "wrong" redox state) and

"unready" (proposed to be enzyme in the "wrong" conformation and the "wrong" redox state), respectively. Consistent with the above proposal is the observation by ENDOR spectroscopy that, contrary to Ni-B, in the Ni-A form the active site is inaccessible to solvent protons (Fan *et al.*, 1991).

Reductive activation of the enzyme by H_2 or by low-potential reductants results in the loss of the EPR signals associated with forms A and B and the appearance of the EPR signal of form C ($g \approx 2.19, 2.16, 2.02$) (Teixeira *et al.*, 1986; Teixeira *et al.*, 1983; Teixeira *et al.*, 1985). In redox titrations performed at room temperature forms A and B are in equilibrium with EPR-silent (Ni-SI) one-electron reduction products (Teixeira *et al.*, 1985). However, if the titration is performed at 2 °C, the reductions of both forms A and B are seen to from spectroscopically distinct EPR-silent forms (de Lacey *et al.*, 1997), SI_u and SI_r, respectively, that do not interconvert at low temperature (Coremans *et al.*, 1992). The SI_u state cannot be further reduced at 2 °C, whereas the SI_r is reduced very slowly to form C, *via* a third EPR-silent form, SI_a (Coremans *et al.*, 1992). The redox potential of this transition is strongly pH-dependent: it decreases 120 mV/pH unit, corresponding to an increase of the protonation of the active site of two protons by each electron taken up by the enzyme (Cammack *et al.*, 1987). Under a H_2 atmosphere, form C is further reduced to R, the fully reduced EPR-silent state of the enzyme (Teixeira *et al.*, 1985). The reduction Ni-C to Ni-R is accompanied by the uptake of one proton (Cammack *et al.*, 1987).

Ni-C is photochemically labile and can be converted to yet another EPR-active state, Ni-L, by exposure to light at 77 K (Van der Zwaan *et al.*, 1985). Form C can be regained by incubating the sample in the dark at 200 K. Since the photoconversion is 6 times slower when performed in D_2O, the authors suggested that light causes the dissociation of a hydrogen species (H^-, H^+ or H_2) from the active site (Van der Zwaan *et al.*, 1985). At the low temperatures used (typically 77 K) the rigidity of the protein matrix will not allow this hydrogen species to again bind to the active site but would

also prevent it from diffusing away. However, upon increasing the temperature the increased flexibility of the protein would allow the regeneration of the bond.

The presence of hydrogen species close to the active site is expected to cause splitting or broadening of the signals, due to the hydrogen nucleus spin (I = ½). However, when NiFe hydrogenases are prepared in D_2O only a small (0.5 mT) sharpening of the Ni-C signals is observed (Van der Zwaan *et al.*, 1985). ENDOR spectroscopy reveals weak (10-20 MHz) coupling of two sets of solvent-exchangeable proton(s) to the electron spin at the active site in Ni-C, one of which is lost upon conversion to the Ni-L form (Whitehead *et al.*, 1993). These data argue against the presence of an axially bound hydride, since such a hydride causes very large proton hyperfine couplings (≈ 460 MHz (15.0 mT) in the model compound $[Hi(CN)_4]^{2-}$ (Symons *et al.*, 1979)). It has also been reported that the orientations of the magnetic axes of Ni-C and of the Ni-L species are only slightly different from each other (Dole *et al.*, 1996). This suggests that the photochemical event does not correspond to a photolysis of a Ni-(H) bond, since in this case the removal of the (H) ligand would strongly change the coordination symmetry of the Ni ion and would induce large rotations of its magnetic axes. Dole *et al.* suggested that the photolyzable H species could be bound either to one of the terminal sulfur ligands, or to the iron atom of the Ni-Fe cluster.

A few members of the [NiFe] hydrogenase family do not display the full complement of these EPR signals, or may be normally isolated in a state that exhibits no EPR in the g =2 – 2.3 region of the spectrum that are due to the active site, e.g. the NADH-linked soluble hydrogenase (Erkens *et al.*, 1996; Hornhardt *et al.*, 1986) from *Ralstonia eutropha* (previously called *Alcaligenes eutrophus*).

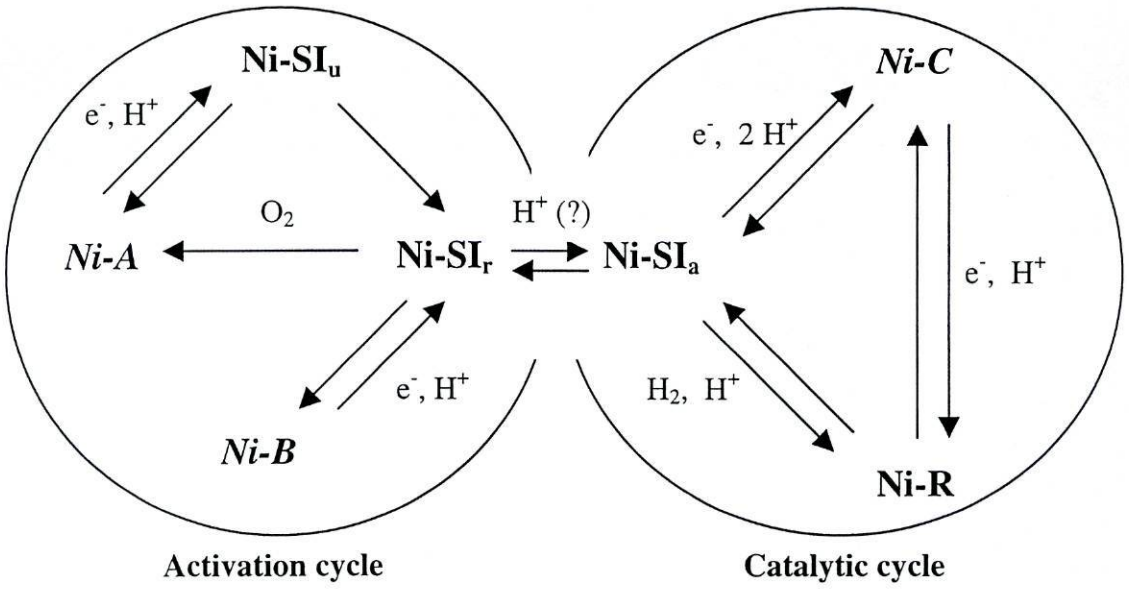

Figure 2.5 Functional relationships between the different states of [NiFe] hydrogenases. EPR active states are shown in italic. Based on (Cammack *et al.*, 1987; de Lacey *et al.*, 1997).

2.4.2 *X-ray absorption spectroscopy*

The appearance and disappearance of different Ni signals upon activation of the enzyme suggested that the formal Ni oxidation state may change from Ni^{3+} to Ni^{1+} or even Ni^0 (Albracht, 1994). This proposal was questioned when it was observed that the X-ray absorption edge of the nickel ion in *Thiocapsa roseopersicina* hydrogenase did not change significantly when the enzyme was poised in the different redox states of the nickel (Bagyinka *et al.*, 1993; Whitehead *et al.*, 1993). Analyses of several other [NiFe] hydrogenases reveal only a 0.8 – 1.5 eV shift of the Ni edge to lower energies among any of the characterized redox states (A, B, SI, C and R) indicating at most a one-electron change in the Ni redox state and strongly challenging the concept that solely Ni-centered redox chemistry is involved in hydrogenase activation (Gu *et al.*, 1996). For most hydrogenases studied, the shift to lower energies occurs mainly upon reduction to the SI state (~ 0.8 eV) and the edge position changes little upon further reduction to the C and R states, suggesting that the redox states responsible for Ni-SI → Ni-C→ Ni-R

interconversions do not involve significant electron density changes at the nickel. Upon conversion to Ni-SI, the Ni coordination number was observed to change in all hydrogenases studied (*D. gigas*, *D. desulfuricans*, *C. vinosum* and *R. eutropha*), except in that from *T. roseopersicina*. The nickel site of the latter enzyme also appears to have a higher proportion of N,O-ligands than S-ligands (Bagyinka *et al.*, 1993; Gu *et al.*, 1996) compared to the other enzymes, which is unexpected due to its high sequence similarity to them.

More recent XAS studies of the *C. vinosum* hydrogenase have allowed a more refined description of the multiple states of the active site (Davidson *et al.*, 2000). A short Ni-O bond is present in the oxidized enzyme (Ni-A and Ni-B) and also in the unready EPR-silent intermediate (Ni-SI_u) but is lost upon conversion to NI-SI_r, confirming that this change is a feature of the reductive activation of the enzyme. Ni-A, Ni-B and Ni-SI_u are five-coordinated, Ni-SI_r and Ni-R seem to be four-coordinated and Ni-C appears to be a six-coordinated species. The formal redox state of the Ni center appears to oscillate between Ni (III) in all of the EPR-active states and Ni (II) in all of the EPR-silent states. The change in the Ni K-edge energy associated with the Ni-B $\rightarrow$ Ni-SI_r is large enough to account for a one-electron redox state change in a Ni ligand in a covalent ligand environment. The K-edge energy increases with Ni-SI_r $\rightarrow$ Ni-C reduction, showing that the Ni center loses electron density in the process, but the magnitude of the change is not enough to be a simple reoxidation of the Ni center. However, Ni-SI_r $\rightarrow$ Ni-C reduction seems to be accompanied by a change in coordination of the active site, and if the effects of geometry/coordination number change accompanying these conversions are factored in, both the changes in edge energy of the Ni-SI_r $\rightarrow$ Ni-C transition and of the subsequent Ni-C $\rightarrow$ Ni-R reduction are of sufficient magnitude to account for one-electron redox state changes in the Ni center.

2.4.3 Fourier Transform Infra Red Spectroscopy

Infrared spectroscopy can provide information on protein species that are otherwise spectroscopically silent and is particularly useful when applied in conjunction with π-acid ligands (CO, RCN, etc.) which have infrared absorbances near 2000 cm^{-1} where few intrinsic protein vibrations occur. Fourier Transform Infra Red (FTIR) studies of the [NiFe] hydrogenase from *C. vinosum* revealed the presence of three absorption bands in the 2100-1900 cm^{-1} spectral region (Bagley *et al.*, 1995; Bagley *et al.*, 1994). The positions of each of these three infrared absorption bands correspond in a consistent way to changes in the formal redox state of the active site (from Ni-A/B → Ni-SI → Ni-C → Ni-R) and to the photodissociation of hydrogen bound to nickel (Bagley *et al.*, 1995). Sets of three bands of similar frequencies were also observed for the different redox states of *D. gigas* hydrogenase (Volbeda *et al.*, 1996).

FTIR studies of *C. vinosum* hydrogenase enriched separately with ^{13}C and ^{15}N have allowed the unambiguous identification of the three diatomic Fe ligands found in *D. gigas* hydrogenase as two CN molecules and one CO molecule (Pierik *et al.*, 1999). FTIR spectra of the hydrogenase from *D. vulgaris* Miyazaki F (which was proposed to contain one SO, one CO and one CN as ligands to the Fe) are very similar to those observed with the *C. vinosum* and *D.gigas* enzymes (Higuchi *et al.*, 1997).

FTIR-monitored titrations have shown the existence of two forms of Ni-SI_r, which differ by one proton, suggested to bind to a cysteine ligand (de Lacey *et al.*, 1997). EPR-monitored titrations (which follow changes at the Ni site) and FTIR-monitored titrations (which follow the ligands bound to the Fe site) have a very similar behavior (de Lacey *et al.*, 1997), showing that the redox changes on the Ni site affect the electron density at the Fe site, even though the Fe atom remains diamagnetic in all states studied (Huyett *et al.*, 1997).

2.5 CATALYTIC MECHANISM OF [NIFE] HYDROGENASES

Despite the detailed spectroscopic and structural information available, the catalytic mechanism of [NiFe] hydrogenases is not yet well understood. The catalytic cycle involves necessarily several steps of different nature, such as the diffusion and the heterolytic cleavage of H_2, proton and electron transfers and interactions with redox partners, and this complicates any analysis.

2.5.1 Electron transfer

A recent study carried out with the enzyme from *Chromatium vinosum* has shown that the H_2 uptake activity measured by electrochemical techniques is much higher than that measured using dyes as electron acceptors (Pershad *et al.*, 1999). Analysis of the kinetic data obtained with the *Thiocapsa roseopersicina* enzyme (Zorin *et al.*, 1996) also showed that at pH 7.2 neither diffusion nor heterolytic cleavage of H_2 are rate-limiting in H_2 uptake or H_2 evolution (Bertrand *et al.*, 2000). Those data suggest that proton uptake and electron transfer are the rate-limiting steps in the H_2 evolution and the H_2 uptake, respectively.

The location of the high potential [3Fe-4S] cluster between the two low potential [4Fe-4S] clusters has further complicated analysis by casting doubts on the efficiency of the electron transfer system in hydrogenase (Volbeda *et al.*, 1995). However, recent experiments carried out on *Desulfovibrio fructosovorans* hydrogenase have shown that converting the central high-potential [3Fe-4S] cluster (E_m=65 mV) into a [4Fe-4S] (Em=-250 mV) causes only moderate changes in both H_2 uptake and H_2 evolution activities (Rousset *et al.*, 1998). Thermodynamic analysis of these data shows that despite the apparently unfavorable ΔG values deduced from potentiometric experiments, the electron transfer between the high-potential central [3Fe-4S] cluster and the low-

potential [4Fe-4S] clusters in *D. fructosovorans* hydrogenase may be fast enough to be non-limiting in both H_2 uptake and H_2 evolution reactions (Bertrand *et al.*, 2000).

The protein environment may, however, greatly influence the effect of the high potential of the [3Fe-4S] cluster in the efficiency of electron transfer. For example, *Methanococcus voltae* possesses a F_{420}-reducing hydrogenase which carries three [4Fe-4S] clusters in its small subunit, instead of two [4Fe-4S] clusters and one [3Fe-4S]. One probable cause of this adaptation has recently been uncovered by site-directed mutagenesis experiments, which have shown that converting the central [4Fe-4S] cluster into a [3Fe-4S] cluster increases the redox potential of the central cluster by about 400 mV and causes a tenfold decrease of H_2 uptake activity with the natural electron acceptor F_{420} (Bingemann and Klein, 2000) turning electron-transfer into a rate-limiting step.

2.5.2 *Hydrogen activation*

Uncertainty remains about the nature of the various steps that take place at the active site itself. Before the determination of the X-ray structure (and concomitant discovery of the binuclear nature of the active site) several mechanisms involving a mononuclear site composed of a nickel atom of unknown coordination were proposed, often differing in important details, such as the formal Ni redox states or the nature of the hydrogen species bound to Ni (Cammack *et al.*, 1987; Roberts and Lindahl, 1994; Teixeira *et al.*, 1989; Van der Zwaan *et al.*, 1985). A model proposing a complex cluster involving nickel and a putative iron atom was also proposed, based on the detection of an unknown paramagnet that interacted with the Ni site in *C. vinosum* hydrogenase (Albracht, 1994). However, in contrast to some of these hypotheses, which call for up to four different redox states available for nickel, synthetic compounds are known to display widely separated Ni (III)/Ni (II) and Ni (II)/Ni (I) redox couples. A great deal of

effort has gone into designing model compounds able to accommodate both redox transitions within the rather narrow redox potential range (- 100 mV to –450 mV) found in hydrogenases (reviewed in (Fontecilla-Camps, 1996)).

The unexpected binuclear nature of the active site implies that a great number of the results obtained from model chemistry, which were mostly based on mononuclear nickel compounds cannot be applied to [NiFe] hydrogenases in a straightforward manner. However, these studies have provided valuable information that can still be used to evaluate the plausibility of proposed mechanisms. For example, they have shown that a thiolate-rich environment (like the one seen around the active site) favors stabilization of the Ni (III) species, that H^- binding seems to occur in the equatorial position and to require S (or Se) ligands in the first coordination sphere of Ni (to act as bases able to accommodate the proton released in the heterolytic cleavage of H_2), and that EPR spectra similar to Ni-C can originate from either Ni(III) or Ni(I) species (Fontecilla-Camps, 1996).

The resolution of the X-ray structure of [NiFe] hydrogenases has sparked a new round of creative thinking regarding the possible reaction mechanism. Fontecilla-Camps proposed a catalytic cycle where Fe alternates between Fe (II) and Fe (I) and Ni remains Ni (I) throughout (Fontecilla-Camps, 1996). Although the Fe atom was soon established to be redox inactive (Dole *et al.*, 1997; Huyett *et al.*, 1997), it was proposed to play a role in the activation of hydrogen. Pavlov *et al.* have used density functional theory to calculate plausible intermediates of the catalytic cycle, and consistently found that under the assumptions used (among others, that all species have the same overall charge) H_2 initially binds to Fe (Pavlov *et al.*, 1999; Pavlov *et al.*, 1998). A proton is quickly transferred to one of the bridging Cys residues and the formed hydride then occupies a bridging position between Fe and Ni. Additional calculations that did not assume identity of overall charge during the catalytic cycle (Niu *et al.*, 1999) have also suggested that the Fe center is the initial site of H_2 activation. Like in Pavlov's

description the hydride would assume a bridging position between the two metals, but the proton would be taken up by a terminal Cys, rather than by a bridging cysteine. Niu's model predicts the existence of additional EPR-active states, for which there is still no experimental evidence.

Dole *et al.* have reformulated a previous mechanism (Roberts and Lindahl, 1994) and proposed a delocalized model for the spin density in the paramagnetic states (Dole *et al.*, 1997). The Ni-SI state is assumed to be the active species that interacts with H_2, yielding Ni-R. In Ni-R a hydride is present, bridging both metal centers. Both terminal cysteines become protonated in this state: one of them by the proton produced by the heterolytical cleavage of H_2 and the other by a solvent proton (see Figure 2.5 for the proton and electron stoichiometries). One-electron oxidation and loss of one of the protons yields Ni-C. The paramagnet in Ni-C will be delocalized onto a terminal cysteine ligand (Ni (III)–S– $\leftrightarrow$ Ni (II)–$S^{\bullet+}$–), therefore explaining the small hydrogen splittings observed in EPR and ENDOR measurements of this species. Loss of the second electron and rearrangement of the spin density would turn the hydride into a proton, and the last protonated cysteine would deprotonate, yielding Ni-SI. Quantum chemical calculations performed on the possible intermediates predicted by this model show that in the paramagnetic species the spin density is mainly localized on the nickel atom and its sulfur ligands, and that in Ni-C a sizable spin density is found on one of the terminal sulfur ligands (De Gioia *et al.*, 1999a). They also show that despite valence changes of the nickel ion the electronic density on this metal is very similar in all forms, which agrees with the XAS results.

Additional calculations by the same group on the catalytic intermediates of [NiFeSe] hydrogenases suggest that the activity differences between [NiFe] and [NiFeSe] hydrogenases cannot be attributed to the substitution of S by Se alone (De Gioia *et al.*, 1999b), since the structural and electronic parameters calculated in the [NiFeSe] active site are very similar to the ones found in the regular [NiFe] center.

2.6 POTENTIAL APPLICATIONS OF HYDROGENASE

The combustion of hydrogen is a highly exergonic reaction which, in principle, does not produce toxic products (see equation 5).

$$2\ H_2 + O_2 \leftrightharpoons 2\ H_2O \quad \Delta G^0 = -474\ kJ\ mol^{-1} \qquad (5)$$

Hydrogenases have therefore enjoyed considerable attention due to their potential application to produce H_2. One of the underlying ideas was that hydrogenase, in combination with the capacity of photosystem II to oxidize water into O_2 and low-potential electrons, might be employed to construct a reactor for the biophotolysis of water to H_2 and O_2, driven by solar energy. The products thus formed can be used to

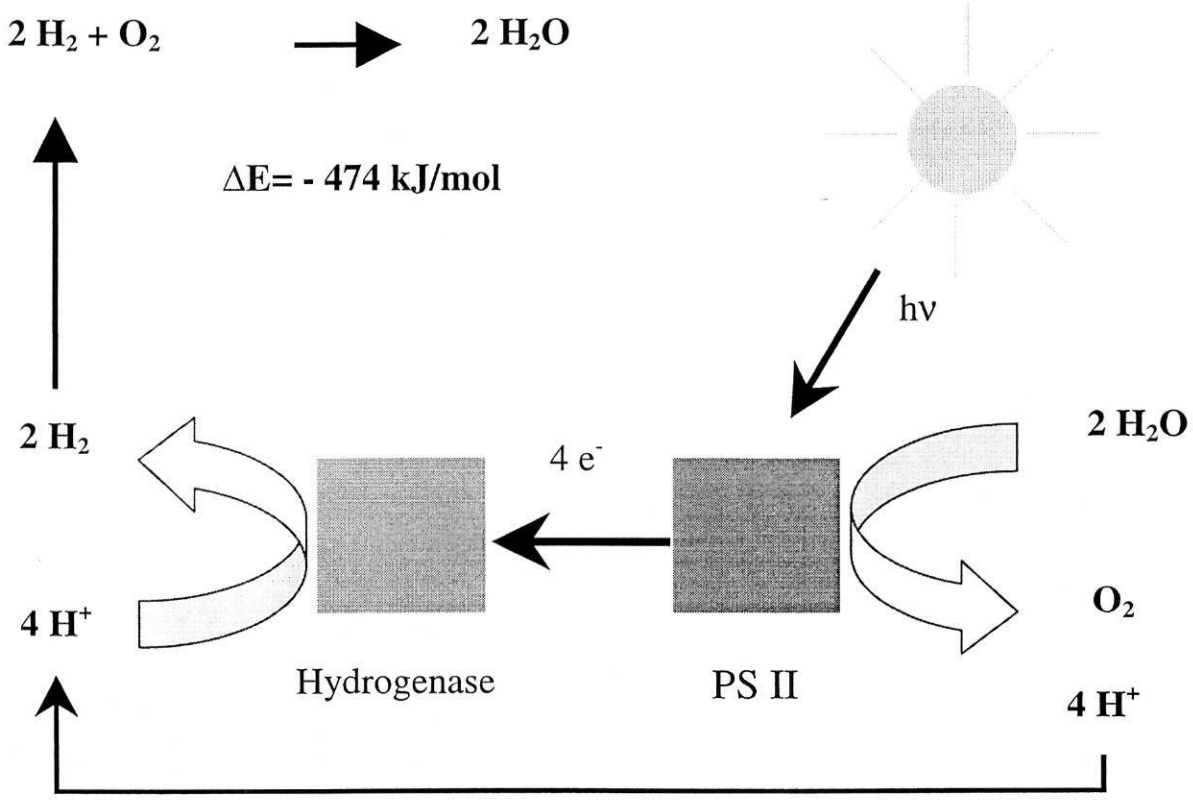

Figure 2.6 Photobiological production of Hydrogen

regain the stored energy by just burning the H_2 to H_2O again. In the initial phases of research the photobiological system (algae, cyanobacteria and photosynthetic bacteria) had short lifetimes (hours, or even minutes) and had very low efficiencies (much lower than 1%), in part due to instability of the biological components. Nowadays it is possible to produce H_2 photobiologically for months at a time, with efficiencies above 1 % (Benemann, 1996). The study of thermophilic hydrogenases may assist the engineering of more resistant hydrogenases for potential biotechnological applications.

3

Materials and Methods

3.1 GROWTH OF ORGANISM

Pyrococcus furiosus (DSM 3638) was grown as in (Arendsen *et al.*, 1995) in a medium described in (Kengen *et al.*, 1994). A 200 L fermentor (lp300, Bioengineering, Wald, Switzerland) was filled with growth medium (except vitamins), potato starch (5 g /L growth medium) and yeast extract (1.25 g/L growth medium) at room temperature. The temperature was then raised to 90 °C and the medium was continually flushed with a stream of N_2 gas. When the pO_2 in the medium was low enough (which usually took from 4 to 6 hours), cysteine (0.5 g / L growth medium) was added in order to eliminate all O_2 and to provide a reducing environment. *Pyrococcus furiosus* innoculum (ca. 5 L) and vitamins were then added to the medium. During growth the medium was continually flushed with N_2, in order to remove evolved H_2 gas, which has an inhibitory effect above a certain level (Fiala and Stetter, 1986). As the fermentation progressed, the pH dropped. The pH was kept at 7.0 by automatic addition of appropriate amounts of a 5 M NaOH solution. Cells were harvested in a Sharples centrifuge after 20 h growth, frozen and kept at –80 °C until use.

3.2 CELL LYSIS

Frozen cells (typically around 150 g) of *P. furiosus* were broken by osmotic shock by a 2 h incubation at 30°C in 3 l of degassed 20 mM Tris buffer, pH=8.0 in the presence of DNAse, RNAse and 1 mM $MgCl_2$. Cell debris and membranes were separated by centrifuging at 9,000 × g for 120 min. The supernatant, henceforth referred to as cell free-extract (CFE), was dark brown and slightly turbid (due to the presence of small amounts of membranes).

NaCl (as table salt)	30 g/L	Mg SO_4	3.4 g/L	$MgCl_2$	2.7 g/L
$NaHCO_3$	1 g/L	KCl	0.33 g/L	NH_4Cl	0.25 g/L
KH_2PO_4	0.14 g/L	$CaCl_2.2H_2O$	0.14 g/L	$NaWO_4$	3.3 mg/L
Trace elements	1 ml/L	Vitamins	1 ml/L		

Table 3.1 Growth medium composition.

$CuSO_4$	36 mg/L	$NaSeO_3$	450 mg/L	H_3BO_3	50 mg/L
$ZnCl_2$	50 mg/L	$MnCl_2$	50 mg/L	$CoSO_4$	50 mg/L
$FeCl_2$	2 g/L	$NiCl_2$	92 mg/L	Na_2MoO_4	73 mg/L
EDTA	0.5 g/L	HCl	1 ml/L		

Table 3.2 Trace elements solution composition.

Biotin	2 mg/L	Nicotinamide	5 mg/L
Folic acid	2 mg/L	Riboflavin	5 mg/L
Thiamin HCl	5 mg/L	Pyridoxine HCl	10 mg/L
Lipoic acid	5 mg/L	Pantothenic acid	5 mg/L
p-aminobenzoic acid	5 mg/L	Cyanocobalamine	5 mg/L

Table 3.3 Vitamins solution composition.

3.3 ISOLATION OF MEMBRANES

Cytoplasmic membranes were isolated from the pellet obtained after centrifugation of the osmotically lysed cells for 1-h at 20,000 × g. The pellet was suspended in 50 mM N-[2-hydroxyethyl]-piperazine-N'[3-propanesulfonic acid] (Epps), pH 8.0, and passed three times through a French press pressure cell at 70 MPa at room temperature. Cell debris was removed by centrifugation at 8, 000 × g for 10 min, and membranes were precipitated by centrifugation for 90 min at 200, 000 × g. The last traces of soluble proteins were removed by suspending the membranes in buffer and repeating the centrifugation procedure.

3.4 PREPARATION OF CELL EXTRACTS

The cell extract used to measure whole-cell activities was prepared from cells (5 g wet cells suspended in 30-ml Epps buffer, pH 8.0) broken by passing through a French pressure cell three times. The cell debris was removed by centrifugation at 8,000 × g for 10 min.

3.5 PROTEIN PURIFICATION

3.5.1 The soluble sulfhydrogenase I

Two different methods were used to purify the soluble sulfhydrogenase I. The first method was a modification of that used by Arendsen *et al.* (Arendsen *et al.*, 1995). The supernatant was first precipitated with 60% $(NH_4)_2SO_4$. Hydrogenase activity was found in the pellet, which was then resuspended in standard buffer (20 mM Tris HCl pH=8.0 with 2 mM dithionite), dialyzed twice against standard buffer and anaerobically purified by sequentially loading onto a DEAE-Sepharose, a Phenyl-Sepharose and a

hydroxyapatite column. All buffers contained 2 mM dithionite as a reducing agent and oxygen scavenger.

The second method did not involve a $(NH_4)_2SO_4$ precipitation step. The cell extract was chromatographed on a Source-Q ion-exchange column. Hydrogenase containing fractions were pooled and dialyzed twice against anaerobic 20 mM Tris HCl pH=8.0 buffer containing 2 mM dithiothreitol in order to eliminate dithionite, and loaded on a Blue Sepharose column. A 0-2000 mM NaCl gradient in 20 mM Tris HCl pH=8.0 2 mM dithiothreitol was applied to the column. Hydrogenase activity eluted around 600 mM NaCl. These fractions were then loaded on a Phenyl-Sepharose column, and eluted with a reverse gradient 450-0 mM NaCl. Hydrogenase eluted when 0 mM NaCl were applied to the column.

Purified sulfhydrogenase was concentrated in an Amicon concentration cell fitted with a YM 30 filter and frozen in liquid N_2.

3.5.2 Sulfide dehydrogenase

Cell-free extract was precipitated with 60% ammonium sulfate. The SuDH activity was purified under anaerobic conditions from the 60% pellet after dialysis. The precipitated pellet (50 ml) was resuspended in 100 ml growth medium, dialyzed twice against deaerated buffer A (50 mM Tris pH 8.0 with 10% glycerol, 1 mM dithionite and 1 mM dithiothreitol) and sequentially loaded onto a Source-Q ion-exchange column, a Blue Sepharose affinity column and Superdex 200 molecular sieve column, as in (Ma and Adams, 1994). The buffer used in the Blue Sepharose column included no dithionite, which irreversibly affects the Blue Sepharose resin.

Purified SuDH was concentrated in an Amicon concentration cell fitted with a YM 30 filter and frozen in liquid N_2.

3.5.3 Partial purification of the membrane-bound hydrogenase.

The membrane-bound hydrogenase was solubilized by mixing freshly-prepared membranes (diluted to a final protein concentration of 10 mg/ml) with 2 % sodium deoxycholate, incubating at room temperature for 30 minutes, and centrifuging at 14, 000 × g for 15 minutes. Protein was precipitated with ammonium sulfate (to 25% saturation) and resuspended in buffer A (10 mM Tris HCl, pH 8.0, 0.1% (w/v) Triton X-100). Ammonium sulfate was eliminated by repeatedly concentrating the sample and exchanging the buffer with buffer A in an Amicon concentration cell with a 30 kDa filter. The sample was then loaded onto a 300 ml Q-Sepharose column and eluted with a 1250-ml gradient from 0 to 500 mM NaCl, followed by a steeper gradient of 100 ml from 500 to 1000 mM NaCl, and a column wash with 1000 m NaCl. Hydrogenase-containing fractions (eluting between 440-480 mM NaCl) were pooled and concentrated to 4 ml, dialyzed against 1 liter buffer A, and loaded onto a 20-ml hydroxyapatite column equilibrated with 10 mM Tris pH 8.0. In these conditions, the membrane-bound hydrogenase flows though the column without binding. Samples with hydrogenase activity were pooled, concentrated and frozen in liquid N_2.

3.5.4 Ferredoxin

Ferredoxin was purified anaerobically as described in (Hagedoorn *et al.*, 1998). The cell-free extract was loaded onto a Source Q column and eluted with a 0-500 mM NaCl gradient. Ferredoxin eluted as the last, very well-resolved, brown peak. It was then loaded onto a Phenyl-Sepharose column, to which ferredoxin does not bind. As a final polishing step, ferredoxin was chromatographed on a Superdex 200 molecular sieve.

3.5.5 *Pyruvate: ferredoxin oxidoreductase*

Pyruvate: ferredoxin oxidoreductase (POR) was anaerobically purified as described in (Blamey and Adams, 1993) using ion-exchange chromatography, gel filtration and affinity chromatography with hydroxyapatite.

3.6 ASSAYS.

3.6.1 *Hydrogen production*

Hydrogen production activity was routinely measured at 80 °C over a period of 15 minutes in 100 mM Epps buffer, pH 8.0 in the presence of 1 mM methyl viologen. The reaction was started by adding buffered dithionite (final concentration 20 mM) and the evolved H_2 was analyzed on a Varian 3400 gas chromatograph equipped with a TCD detector. Argon was used as carrier gas. H_2 was measured on a molesieve 5A 45/50 column (1.5 m x 1/4" SS, Chrompack, Bergen op Zoom, The Netherlands). One unit of hydrogenase catalyzes the production of 1 μmol H_2 min^{-1}. For measurements at different pH, and in order to minimize changes in pH brought about by the change in temperature, buffers with a low $\Delta pK/\Delta T$ (Ches, Mops, Epps or Mes, all at 100 mM) were used.

3.6.1.1 *Sensitivity to inhibitors*

CO-inhibition assays were performed by adding CO to the headspace of the assay vials to yield from 0 to 100% CO in the headspace and measuring the H_2-evolution activity as described above.

N, N'-dicyclohexylcarbodiimide (DCCD) inhibition was assayed by incubating 10 μl of a 50 mg/ml solution of DCCD in 100 % ethanol and 20 μl *P. furiosus*

membranes in 1.9 ml assay buffer for variable periods of time at room temperature and at 80 °C and measuring the H_2-evolution activity as described above.

3.6.1.2 H_2 production from pyruvate

Unless otherwise noted, the pyruvate oxidation driven, ferredoxin mediated, H_2-formation assay mixture contained: 100 mM Epps pH 8.0, 0.1 mM $MgCl_2$, 0.1 mM thiamin pyrophosphate, 10 mM pyruvate, 1.5 mM CoASH, 15 mM dithiothreitol, 13 µM *P. furiosus* ferredoxin, 75 µg POR, 10 µg sulfhydrogenase (activated). The assays were performed in a warmed bath at 80°C in a butyl rubber stoppered bottle (8-ml) with a reaction volume of 1 ml. H_2 production was followed in time with gas chromatography. The sulfhydrogenase was previously activated by an incubation of 20 min at 80 °C under a hydrogen atmosphere.

With $NADP^+$/NADPH as oxidant/reductor for the sulfhydrogenase the POR reaction mixture (minus ferredoxin) was supplemented with 1 mM $NADP^+$ and 100% H_2 in the gas phase or with 1.5 mM NADPH. When SuDH was used as NADPH regenerating system, the POR system was supplemented with 0.3 mM $NADP^+$ and 30 µg SuDH.

3.6.2 Hydrogen uptake

Hydrogen uptake was measured by following the H_2-dependent reduction of methyl viologen or benzyl viologen (1 mM) by the hydrogenase in H_2-saturated 50 mM EPPS pH 8.0 buffer containing 1 mM methyl (or benzyl) viologen. When necessary, hydrogenase was activated in the vial by addition of a small amount of dithionite solution. Reduction of methyl viologen was followed at 604 nm (ε=13.6 mM^{-1} cm^{-1}) and that of benzyl viologen at 540 nm (ε=13.05 mM^{-1} cm^{-1}) (van Dijk *et al.*, 1979).

3.6.3 *Sulfide dehydrogenase*

The kinetic parameters of SuDH were measured as described in (Ma and Adams, 1994). The NADH-dependent reduction of benzyl viologen catalyzed by SuDH was regularly measured at 60 °C. The reaction was carried out in anaerobic vials containing 50 mM CAPS pH 10.3 buffer, 0.3 mM NADH and 1 mM benzyl viologen. The polysulfide-dependent oxidation of NADPH was followed at 340 nm (ε=6.2 mM^{-1} cm^{-1}). The assay mixture contained 100 mM EPPS pH 8.0, 0.3 mM NADPH and 1.5 mM polysulfide. Reaction was started by addition of enzyme. NADPH-dependent glutamate synthase activity was determined as in (Vanoni *et al.*, 1991). When dithionite was omitted from the assays, and in view of the O_2 sensitivity of SuDH and the sulfhydrogenase during their activity measurements, the last traces of O_2 in the assay bottles or cuvettes were removed prior to the start of the reaction by reducing the viologen to "slightly blue" with deazaflavin and light (10 μM deazaflavin and 50 mM N-[Tris(hydroxymethyl)methyl]glycine as electron donor). When no viologens were involved in the reaction, the last traces of O_2 were removed during the temperature equilibration by POR. When no standard deviation is given, the values have a standard deviation of 15% or less.

3.7 PROTEIN DETERMINATION

Protein concentration was determined according to the microbiuret method with TCA-DOC precipitation (Bensadoun and Weinstein, 1976).

Reagents:

- Sodium deoxycholate (DOC) 0.15% w/v
- Trichloroacetic acid (TCA) 70% w/v (VERY CORROSIVE. **CAUTION !**)

- Sodium hydroxide solution 3% w/v
- Microbiuret reagent

  Dissolve 173 g trisodium citrate dihydrate and 100 g Na_2CO_3 in distilled water to a final volume of 600 ml (solution 1). Dissolve 17.3 g $CuSO_4.5H_2O$ are in 300 ml of warm distilled water. Slowly add this solution, with stirring, to solution 1. Make up the volume to 1000 ml. This dark blue solution is stable for several months when kept in the dark.
- Bovine Serum Albumin

  Prepare a 10.00 mg/ml solution. Due to the hygroscopic nature of lyophilized proteins gravimetric preparation of protein standards is difficult. Usually the concentration is determined spectrophotometrically. A 1 mg/ml solution of BSA has an absorbance of 0.667 at 279 nm.

Procedure

Add three samples of unknown concentration (20, 50 and 200 µl), two blanks and six samples of bovine serum albumin standards (5, 10, 20 30, 40 and 50 µl ≡ 0.05-0.5 mg of protein) to separate Eppendorf reaction vessels. Adjust volume to 1.0 ml with distilled water and mix.

Add 100 µl 0.15% DOC, mix and allow to stand for 5 minutes (at room temperature).

Add 100 µl 70% TCA, mix and centrifuge for 10 minutes at 9,000 × g (Eppendorf centrifuge). Mark the orientation of the vessels in the centrifuge. Precipitated protein can be observed as a pale shade on the side of the vessel. Carefully remove the supernatant (to be discarded) by aspiration with a Pasteur pipette. Avoid touching the inner surface of the Eppendorf vessels with the pipette tip.

Add 1 ml of 3% NaOH to each reaction vessel.

Mix thoroughly by vortex until full solubilization is achieved.

Add 50 µl microbiuret reagent, and mix thoroughly for 10 seconds.

Allow color development at room temperature in the dark for at least 10 minutes, and measure the absorbance of the solutions at 545 nm against water.

3.8 IRON DETERMINATION WITH FERENE

Iron was measured as the ferene complex as described in (Smith *et al.*, 1984).

Reagents:

- Dilute hydrochloric acid, 1% w/v
- Ammonium acetate solution, 15%
- Sodium dodecyl sulfate (SDS), 2.5% w/v
- Ascorbic acid, 4% (w/v) (freshly prepared)
- Iron chelator: 3-(2-pyridyl)-5,6-bis(5-sulfo-2-furyl)-1,2,4-triazine, disodium salt trihydrate (Ferene), 1.5% w/v
- Iron standard: 0.2 mM $(NH_4)_2Fe(SO_4)_2.6H_2O$ (Mohr's salt, 0.008% w/v) (freshly prepared)

Procedure

Dilute three protein samples (10,20 and 40 µl), two blanks and five samples of iron standard (10,25,50,74 and 100 µl ≡ 2-20 nmol Fe) to 100 µl with demineralized water in Eppendorf reaction vessels. Subsequently add 100 µl 1% HCl. Gently mix the samples.

Close the reaction vessels and incubate at 80 °C for 10 minutes.

Allow the vessels to cool down after the 80 °C treatment (keep closed).

Add sequentially, with vortexing after each addition:

- 500 µl ammonium acetate
- 100 µl 4% ascorbic acid
- 100 µl 2.5% sodium dodecyl sulphate
- 100 µl iron chelator

Centrifuge for at least 5 minutes at 9,000 × g.

Measure the absorbance of the solutions at 593 nm against water.

3.9 FLAVIN EXTRACTION AND CHARACTERIZATION

The flavin moieties in sulfhydrogenase I and sulfide dehydrogenase were analyzed after quantitative extraction of the cofactor by unfolding and precipitation of the protein.

10 µl of 70 % (w/v) trichloroacetic acid solution were added to 100 µl of protein. Samples were thoroughly mixed and allowed to stand. Water was added to 1000 µl, and excess acid was neutralized by the addition of 200 µl of a 100 mg/ml $NaHCO_3$ solution. The final pH of the samples was around 8. The absorbance of the solution was measured at 450 nm against water. For the calibration curve determination, 5 µl of either FAD or FMN (10 mM stock solutions) were diluted to 1000 µl (solution F). To 50, 100, 150, 300 and 400 µl of solution F were added 50 µl Tris HCl pH=8.0 and 10 µl TCA 70%. Volumes were adjusted to 1000 µl with Nanopure water. Samples and standards were kept wrapped in aluminum foil to protect the flavins from light-induced damage.

For identification of the isolated cofactor the fluorescence emission of the sample between 400 nm and 600 nm (excitation wavelength = 360 nm) was measured

before and after addition of 5 µl of a 1.7 mg/ml snake-venom phosphodiesterase (*Naja naja* venom) solution.

3.10 ANAEROBIC OXIDATION OF SULFHYDROGENASE

A small (around 15 ml) 6-PG desalting column was poured and extensively equilibrated under an Ar flow with a thoroughly deaerated 50 mM Tris HCl pH=8.0 solution (evacuated and flushed with Ar for more than 2 hours). 500 µl of a freshly-prepared anaerobic solution of phenazine methosulfate (6 mg/ml) were then placed on the column, immediately followed by up to 500 µl of concentrated sulfhydrogenase. Sulfhydrogenase elutes much faster than phenazine methosulfate (PMS), allowing full separation of the oxidized protein (red-brown) from the reduced phenazine methosulfate (green). Both the PMS solution and the 6-PG desalting column were kept wrapped in aluminum foil to prevent light-induced degradation of PMS.

3.11 PREPARATION OF SAMPLES FOR EPR.

PMS-oxidized hydrogenase samples (~ 80 µl) were introduced anaerobically in EPR tubes, heated to 80 °C in a water bath for different time periods and rapidly frozen in liquid nitrogen. Photoreduction of hydrogenase was performed using deazaflavin was as in (Massey and Hemmerich, 1978).under a H_2 atmosphere by stepwise illumination using a tungsten lamp fitted with a fiber optics cable to prevent undesired sample heating. The sample contained 50 mM Tris, pH 8.0, 2 mM EDTA and 25 µM 5-deaza-riboflavin and was first illuminated at 80 °C for 25 minutes and then at 0 °C for 70 minutes. NADPH-reduced samples were prepared at room temperature by anaerobic addition of fresh NADPH solution to PMS-oxidized hydrogenase to a final concentration of 0.7 mM.

3.12 MEDIATED REDOX TITRATIONS.

Anaerobic redox titration of the different proteins was carried out as follows. An enzyme solution in 50 mM Tris/HCl buffer, pH 8.0, was poised at different redox potentials in the presence of redox mediators (40 μM). The mediators and their respective potentials were: tetramethyl-phenylene diamine (260 mV), 2, 6-dichloro-4-[4-(hydroxyphenyl)imino] (271 mV), N-methylphenazonium methosulfate (80 mV), thionine (56 mV), methylene blue (11 mV), indigo tetrasulfonate (-46 mV), indigo disulfonate (-125 mV), 2-hydroxy-1, 4-naphtoquinone (-152 mV), antraquinone-2-sulfonate (-225 mV), phenosafranin (-252 mV), safranin O (-280 mV), neutral red (-329 mV), benzyl viologen (-359 mV) and methyl viologen (-449 mV). The reductive redox titration was performed by adding small aliquots of dithionite solutions of appropriate concentration (0.2, 2, and 20 mM). Oxidative titrations were performed by adding aliquots of potassium ferricyanide, $K_3Fe(CN)_6$. After a suitable equilibration time samples were transferred to anaerobic EPR tubes and immediately frozen in liquid N_2. When the titration was performed at 80 °C, the samples were frozen in cold isopenthane (-180 °C).

3.13 EPR SPECTROSCOPY

X-band EPR spectra were acquired on a Bruker EPR 200 D spectrometer. The microwave frequency was measured with a Systron Donner frequency counter, model 1292A. The direct-current magnetic field was measured with an AEG Kernresonanz Magnetfeldmesser, type GA-EPR 11/2102. The spectrometer was interfaced with a DASH-16 card to a PC with software written in ASYST for 1024-point data acquisition, correction for background signals (with frequency alignment), double integration procedures, and *g*-value determinations. as in (Pierik and Hagen, 1991). The modulation

frequency was 100 kHz and the modulation amplitude was 0.5 mT, unless otherwise noted. The spectra were simulated using 100 x 100 orientations and assuming (a superposition of) S=1/2 species subject only to electronic Zeeman interaction plus co-linear g-strain broadening. This means that each species is defined by maximally three g-values, g_i, and three linewidth parameters, Δ_i, in g-value units. The theory and procedure has been detailed in (Hagen, 1989) and Refs. quoted therein. The assumption of g-strain is not crucial because broadening by unresolved superhyperfine interactions (or by a combination with g-strain) would result in virtually identical spectra (cf. (Hagen, 1989)).

3.14 SEQUENCE ANALYSIS

The published (Pedroni *et al.*, 1995) amino-acid sequences of the four sulfhydrogenase subunits were searched for highly conserved regions by comparison with the closest described homologous sequences found using BLAST 2.0.3 (Altschul *et al.*, 1997) (available at http://www.ncbi.nlm.nih.gov/BLAST/) with the non-redundant protein databases of the National Center for Biotechnology Information (Bethesda, MD, USA) and aligned with CLUSTALX (Thompson *et al.*, 1997), with subsequent manual inspection.

Phylogenetic trees were built using the CLUSTALX and plotted with NJplot (Perriere and Gouy, 1996) and TreeView (Page, 1996). Confidence values for groupings in a tree were derived by bootstrapping (Felsenstein, 1985). Bootstrapping involves making N random samples of sites from the alignment (N should be large, e.g. 500 - 1000); drawing N trees (1 from each sample) and counting how many times each grouping from the original tree occurs in the sample trees. N was set to 1000. The number of times each grouping from the original tree occurs in the sample trees is shown at the relevant node in the tree.

Data of the genome of *P. furiosus* (Borges *et al.*, 1996) are available on www.genome.utah.edu or http://combdna.umbi.umd.edu/bags.htm. The *P. furiosus* genomic sequence database was screened for Ni-Fe hydrogenase-coding regions using the amino acid sequence of the large subunit of hydrogenase-2 from *E. coli*. Open reading frames in the relevant genome regions (with a minimum size around 80 amino acids, to eliminate statistical artifacts) were evaluated according to codon usage. Codon usage was compared to the average codon usage in genes coding for known *P. furiosus* proteins. The codon usage data were obtained from the Codon Usage Database at http://www.kazusa.or.jp/codon/.

Membrane spanning helices were predicted according to (Tusnády and Simon, 1998) using the interface at http://www.enzim.hu/hmmtop/index.html.

Ribosome-binding sites were identified by comparing the gene sequences to the 3'-terminal of the 16S rRNA small subunit rRNA (Achenbach, LA (1995) *Pyrococcus furiosus* 16S small subunit rRNA sequence, accession number U20163).

3.15 PROTEIN ANALYSIS.

SDS-PAGE was performed as described in (Laemmli, 1970).

Reagents

- Running buffer (1.5 M Tris pH 8.8): dissolve 18.17 g Tris in a final volume of 100 mL using Nanopure water, and adjust to pH 8.8 with HCl. Keep in the dark at 4 °C.
- Stacking buffer (0.5 M Tris pH 6.8): dissolve 6.06 g Tris in a final volume of 100 mL using Nanopure water, and adjust to pH 6.8 with HCl. Keep in the dark at 4 °C.

- Acrylamide (30%)/ bisacrylamide (0.8%): dissolve 30 g de acrylamide e 0.8 g de bisacrylamide in a final volume of 100 mL using Nanopure water. Filter through a 0.45 μm membrane and keep in the dark at 4 °C. **CAUTION**: Acrylamide and bisacrylamide monomers are neurotoxic. Always wear gloves and induce polymerization before disposal.
- Sodium dodecyl sulfate stock solution (SDS) 10%. Keep at room temperature.
- Ammonium persulfate solution (APS) 10%. Freshly prepared.
- N,N,N',N'-tetramethyletilenediamine (TEMED)
- Tris-Glycine electrophoresis buffer (10×): dissolve 30.3 g Tris, 144.1 g glycine and 10 g SDS in a final volume of 1 L. Adjust pH to 8.3. Dilute 10 times before using.
- Sample buffer (2×) : add 2.4 mL de 0.5 M Tris pH 6.8 (stacking buffer), 4 mL SDS 10%, 2 mL glycerol, 1 mL β-mercaptoethanol e 0.5 mL of a 1% solution of bromophenol blue in water. Adjust volume to 10 ml. Divide in aliquots, and keep at -20 °C in Eppendorf. Dilute twice before use.

Procedure

Assemble the gel apparatus. Check that no leaks are present. Prepare a convenient amount of running gel solution (5 mL for a mini-gel, 30 mL for a long gel) using Table 3.4, below. Polymerization starts upon addition of TEMED. Carefully pour the gel in the apparatus. Overlay the running gel with a small amount of n-butanol.

After the running gel has polymerized, decant the overlay, prepare the stacking gel solution according to Table 3.5, add the TEMED, and pour. Insert the comb and allow to polymerize completely before running.

Dilute sample twice in sample buffer. Use ≈5 μg protein on a mini-gel and ≈30 μg on a long-gel). *P. furiosus* proteins are remarkably thermostable. Boil samples for at least 5 minutes, centrifuge and load the gel.

Run the gel at constant current, 25-50 mA, depending on gel size.

Stock solution	% acrylamide			
	7.5	**10**	**12.5**	**15**
1.5 M Tris pH 8.8	1.25 mL	1.25 mL	1.25 mL	1.25 mL
Acrylamide 30%	1.25 mL	1.67 mL	2.08 mL	2.5 mL
SDS 10%	50 μL	50 μL	50 μL	50 μL
H_2O	2.42 mL	2.00 mL	1.60 mL	1.18 mL
degass				
APS 10%	25 μL	25 μL	25 μL	25 μL
TEMED	2.5 μL	2.5 μL	2.5 μL	2.5 μL

Table 3.4 Running gel composition. Volumes are shown for a 5 mL mini-gel.

Stock solution	**% acrylamide**
	4
0.5 M Tris pH 6.8	0.5 mL
Acrylamide 30%	0.27 mL
SDS 10%	20 μL
H_2O	1.20 mL
degass	
APS 10%	10 μL
TEMED	2 μL

Table 3.5 Stacking gel composition. Volumes are shown for a 5 mL mini-gel.

3.16 GEL BLOTTING

a. After running, incubate the gel for 30 minutes in 10 mM CAPS buffer in 10 % methanol (pH=11.0)
b. Wet a PVDF membrane in 100% methanol.
c. Blot during 2-3 h at 200 mA in CAPS buffer in 10% methanol
d. Wash the membrane with Nanopure water for 5 minutes.
e. Color the membrane with 0.1% Coomassie Brilliant Blue R-250 in 50 % methanol for 5 minutes.
f. Decolor the membrane for 10 minutes in 50% methanol 10% acetic acid solution.
g. Wash with Nanopure water.
h. Dry the gel and cut the relevant bands.

The N-terminals were sequenced by Edman degradation in the gas phase sequenator at the Sylvius Laboratories, Department of Medical Biochemistry, State University of Leiden.

4

THE SOLUBLE SULFHYDROGENASE I

4.1 REPORTED PROPERTIES OF *PYROCOCCUS FURIOSUS* SULFHYDROGENASE

The sulfhydrogenase from *Pyrococcus furiosus* is the only NiFe hydrogenase from hyperthermophilic organisms that has been studied in some detail (Arendsen *et al.*, 1995; Bryant and Adams, 1989; Ma *et al.*, 1993; Ma *et al.*, 1994). The protein is an $\alpha\beta\gamma\delta$ heterotetramer of 48.7 + 41.8 + 33.2 + 29.6 kDa. The δ and α subunits are homologous to the small and large subunits of mesophilic NiFe hydrogenases, and the β and γ subunits show similarity to the α and β subunits of the anaerobic, NADH-linked, $\alpha\beta\gamma$ sulfite reductase from *Salmonella typhimurium* (Pedroni *et al.*, 1995).

Unlike all other hydrogenases the *P. furiosus* enzyme has been reported to preferably catalyze H_2 production (Bryant and Adams, 1989). It contains close to one Ni and 17-31 Fe per heterotetramer (Arendsen *et al.*, 1995; Bryant and Adams, 1989). Based on the sequence homology and on the metal content one would expect to find at least half a dozen different EPR signals. So far, only three EPR signals were found: a rhombic signal, attributed to a [4Fe-4S] cluster, an axial signal arising from a [2Fe-2S] cluster and a broad signal, possibly caused by interaction of the cluster that gives rise to the rhombic signal and another (fast-relaxing) paramagnet that becomes detectable upon reduction (Arendsen *et al.*, 1995). Nothing is known regarding the redox-states of the NiFe moiety: no nickel-EPR has been reported yet. An EPR signal reminiscent of the Ni-C signal was claimed in thus far unpublished work to be detectable after incubation of the protein at 80 °C and poising the redox potential at approximately -0.3 V (Adams, 1992). In order to investigate the physiological significance of these data we have performed a series of experiments with sulfhydrogenase at physiological temperature (80 °C) with subsequent monitoring by low-temperature EPR to find conditions which would allow the identification and characterization of physiologically relevant states of the NiFe cluster.

4.2 DERIVATION OF PROSTHETIC GROUP STRUCTURES FROM SEQUENCE ANALYSIS

The nucleotide sequence of the *HydBGDA* transcription unit encoding the heterotetrameric *P. furiosus* sulfhydrogenase has been determined by Pedroni *et al.* (Pedroni *et al.*, 1995), and they have also analyzed the primary structures of the four proteins encoded by the transcription unit through comparison versus protein sequence databases and using the X-ray structure of the *Desulfovibrio gigas* NiFe-hydrogenase (Volbeda *et al.*, 1995). Two classical, [4Fe-4S] ferredoxin-like ligands, CxxCxxCxxxCP, were identified in the sequence of the β-subunit, however, no deductions were made regarding the specific structures of the iron-sulfur clusters in the γ- and δ-subunit. As a prelude to our redox-EPR analysis we have re-inspected the primary sequence of the enzyme with comparison to newly available sequence data from other proteins, and we have found evidence for a total of five [4Fe-4S] cubanes, no [3Fe-4S] clusters, and one [2Fe-2S] cluster.

Pedroni *et al.* found a strong homology between the γ-subunit of *P. furiosus* hydrogenase and AsrB, the β-subunit of anaerobic sulfite reductase from *S. typhimurium*, with four Cys residues conserved. In Figure 4.1A a second look is taken at this putative binding sequence with inclusion not only of novel sequence information from archaeal genomes, but also of the classical sequence for a [2Fe-2S] ferredoxin here taken from *Spirullina platensis* (and 49 other sequences available). The consensus sequence consists of two motifs, CxxGxCxxC and CxxxP, and we conclude that all proteins presented in Figure 4.1A carry a [2Fe-2S] cluster of the 'plant ferredoxin' type. This is the only iron-sulfur cluster present in the γ-subunit.

A) [2Fe-2S] cluster on γ-subunit

```
HydG Pfur  251  M K C G I G K C G H C (11x) C K D G P V
HydG Phor  264  M K C G I G I C G S C ( 7x) C R D G P V
HydG Mjan  206  M K C G I G I C G Q C ( 9x) C K D G P V
AsrB Ecol  238  M A C S V G K C G H C ( 7x) C T D G P I
Fd   Splat 39   Y S C R A G A C S T C (29x) C V A Y P T
```

B) Proximal [4Fe-4S] cubane:

```
HydD Pfur  14   C x G C (66x) G x C x x x G (44x) G C P P
HynB Dgig  17   C x G C (89x) G x C x x x G (30x) G C P P
```

C) Distal [4Fe-4S] cubane:

```
HydD Pfur  163  V C x x C ( 6x) C (8x) C x G P x T
HynB Dgig  184  V H x x C (24x) C (5x) C x G P x T
```

D) Intermediate [3Fe-4S] or [4Fe-4S]:

```
HydD Mjan  224  C x A x C P ( 5x) C x G C
HydD Pfur  192  C x A x C P ( 5x) C x G C
HynB Dgig  228          C P (16x) C x x C
```

Figure 4.1 Analysis of cluster-coordinating segments of *P. furiosus* hydrogenase subunits. HydG is the γ-subunit of tetrameric hydrogenases, AsrB is the β-subunit of anaerobic NADH-dependent trimeric sulfite reductases, Fd is ferredoxin, HynB is the β-subunit of dimeric hydrogenases and HydD is the δ-subunit of tetrameric hydrogenases. Pfur is *P. furiosus*, Phor is *P. horikoshii,* Splat is *Spirulina platensis* and Dgig is *D. gigas*.

The δ-subunit sequence has been compared to sequences of the small subunit from 25 other hydrogenases. For reason of readability in Figure 4.1 the comparison is limited to the sequence from the *D. gigas* enzyme for which an X-ray structure is available. In *D. gigas* NiFe-hydrogenase the binding motifs are consecutive (i. e. not intertwined as for 8Fe ferredoxins) and we assume this to hold for all hydrogenase small subunits. The first binding sequence is for the [4Fe-4S] cubane that is proximal to the NiFe active center in the *D. gigas* enzyme. The three motifs, CxGC and GxCxxxG and GCPP, are fully conserved in 24 out of 25 hydrogenases: the proximal cubane is also present in *P. furiosus* sulfhydrogenase.

The F_{420}-dependent hydrogenases differ considerably in the subsequent iron-sulfur binding motifs from the other hydrogenases, therefore the comparison is continued with the remaining 17 sequences. The second binding sequence is for the [4Fe-4S] cubane that is distal to the NiFe site in *D. gigas* hydrogenase. The sequence is unusual in that it is the first example of a [4Fe-4S] clusters with histidine as one of the coordinating ligands. The consensus sequence, HxxC and C and CxGPxT, is fully conserved, except that the His is replaced with Cys in the archaeal proteins. Thus, the distal cubane is present in *P. furiosus* sulfhydrogenase as an all-Cys cluster.

The third binding motif in the *D. gigas* sequence is for the [3Fe-4S] cluster that is spatially in between the two cubanes. There is no convincing sequence homology in this region between the *D. gigas* and the *P. furiosus* proteins; however, all the archaeal sequences carry the motif CxAxCPxxxxxCxGC (cf. Figure 4.1D). Therefore, it appears that the [3Fe-4S] cluster is replaced in these proteins with a [4Fe-4S] cubane and with a different polypeptide ligand. In summary, the δ-subunit of *P. furiosus* sulfhydrogenase should grossly have the same 3D structure as the small subunit of the *D. gigas* hydrogenase, but the former contains three cubanes.

The α-subunit was previously shown to be homologous to the large subunit of NiFe-hydrogenases, including the *D. gigas* enzyme, with the binding motif for the

binuclear NiFe cluster fully conserved. Therefore, in *P. furiosus* sulfhydrogenase residues Cys-68 and Cys-421 are identified as the bridging ligands between the Ni and the Fe, and Cys-65 and Cys-418 coordinate only the Ni.

The β-subunit was previously shown to be homologous to AsrA, the α-subunit of *S. typhimurium* anaerobic sulfite reductase (Pedroni *et al.*, 1995). The comparison identified not only the two classical CxxCxxCxxxCP motifs for [4Fe-4S] cubanes but also other seven Cys were found to be conserved between the two subunits. However not enough homologous sequences are available to decide whether these cysteine residues might be involved in cluster coordination.

The sequence analysis in terms of ligands for prosthetic groups is summarized schematically in Figure 4.2. The four subunits are presented as squares with relative magnitudes that approximately reflect their molecular masses. The approximate topology of the four cubanes and the NiFe cluster in the αδ-subdimer are by analogy to the *D. gigas* enzyme. In the γ-subunit Pedroni *et al.* found binding sequences for flavin and nucleotide (Pedroni *et al.*, 1995). The flavin is identified as FAD, below. The overall topology of all redox groups is suggestive of a specific electron-transfer route from NADPH to H^+. Reduction of the Fe-S clusters of hydrogenase with NADPH is documented below.

Not indicated in Figure 4.2 are the seven conserved Cys residues in the β-subunit (in addition to the eight Cys for the two regular cubanes) because it is presently not known if they are involved in ligation of yet another Fe/S cluster.

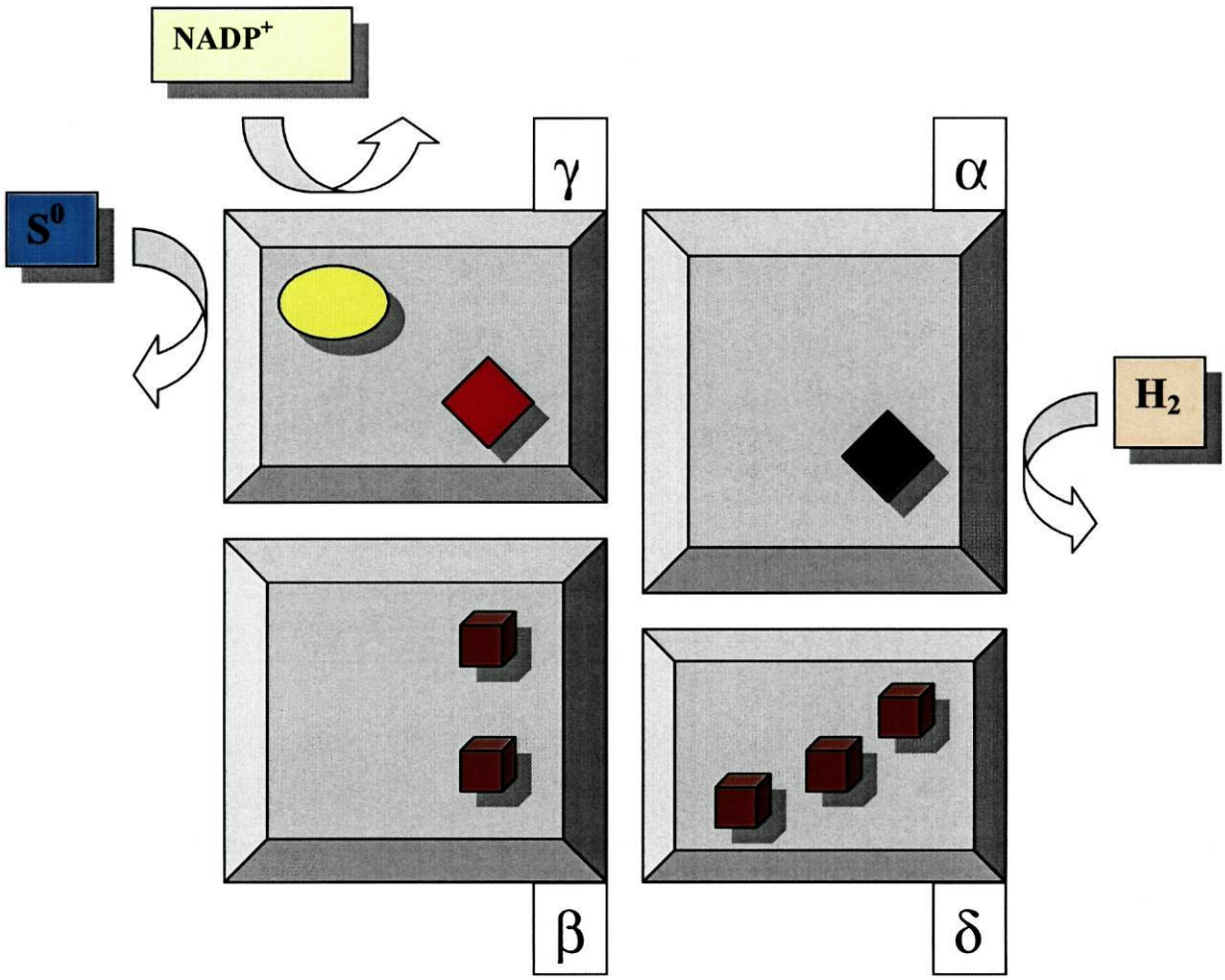

Figure 4.2 Proposed arrangement of the redox centers in the four subunits of the sulfhydrogenase from *P. furiosus*. Cubes stand for [4Fe-4S] clusters, the oval for FAD, the green diamond for the NiFe cluster and the red diamond for the [2Fe-2S] cluster.

4.3 CATALYTIC PROPERTIES

Sulfhydrogenase was originally proposed to be primarily a H_2-evolving enzyme (H_2 evolution 11 times larger than H_2 uptake) that used reduced ferredoxin as electron donor (Bryant and Adams, 1989). A subsequent report showed that H_2 evolution from dithionite-reduced ferredoxin was an experimental artifact, and that instead NADPH (but not NADH) can be used as electron donor for H_2 evolution (Ma *et al.*, 1994). Some kinetic data in the latter report seem to contradict the previously reported ratios of H_2 to H_2 uptake (Table 1 in (Ma *et al.*, 1994)), and suggest instead that in physiological conditions the enzyme might function primarily in H_2 oxidation.

Some catalytic properties of sulfhydrogenase were therefore reexamined. The study of the temperature dependence of H_2 uptake activity (using 1 mM methyl viologen as electron acceptor) shows a fourteen-fold increase in activity from 45 °C to 96 °C (Figure 4.3).

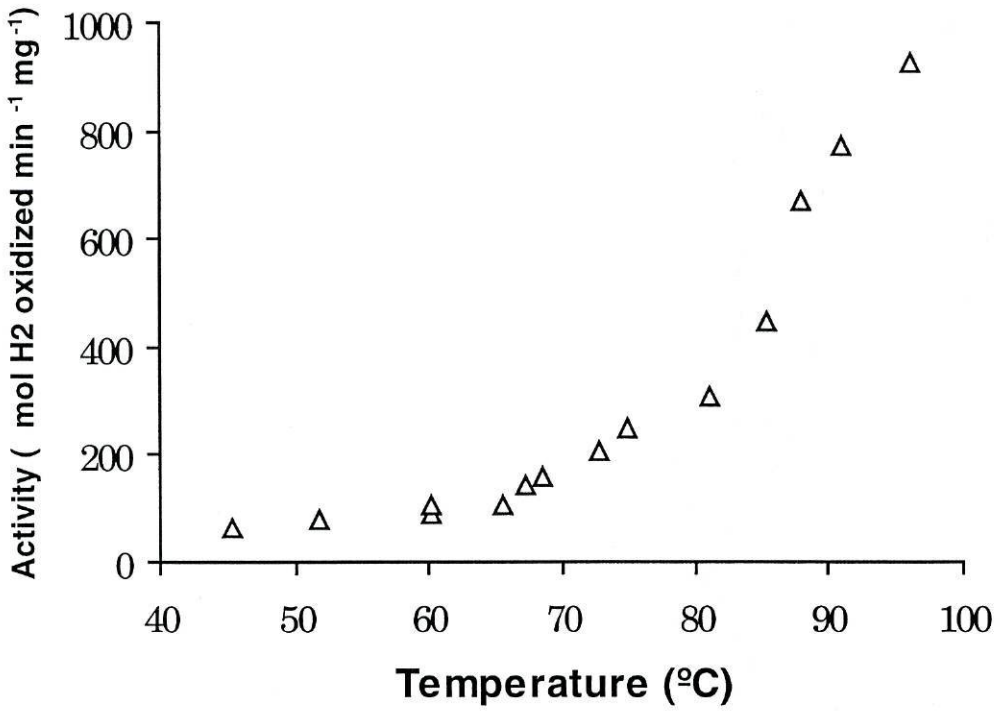

Figure 4.3 Temperature dependence of the H_2 uptake activity of *P. furiosus* sulfhydrogenase.

These data can be analyzed according to the Arrhenius equation:

$$k_1 = AT\, e^{-Ea/RT}$$

where k_1 is the reaction rate, A is a parameter slightly dependent on temperature, and Ea is the activation energy. If we identify the energy of activation as $\Delta G\ddagger$, the Gibbs free energy of activation (Glasstone *et al.*, 1941), we get:

$$k_1 = BT\, e^{-\Delta H\ddagger/RT}\, e^{-\Delta S\ddagger/R}$$

where B is a proportionality factor, $\Delta S\ddagger$ is the entropy of activation and $\Delta H\ddagger$ is the enthalpy of activation. Dividing by T and taking logarithms:

$$\ln (k_1/T) = \ln B + \Delta S\ddagger/R - \Delta H\ddagger/RT$$

Under the conditions used (pH 8.0, 100 kPa H_2), the H_2-uptake reaction can be considered irreversible, so k_{obs}, the observed reaction rate, is identical to k_1. Therefore, a plot of $\ln (k_{obs}/T)$ *vs.* 1/T (a so-called Eyring plot) allows the calculation of $\Delta H\ddagger$ and $\Delta S\ddagger$. The Eyring plot for the H_2 uptake reaction catalyzed by sulfhydrogenase under 1 atm H_2, pH 8.0 using 1 mM methyl viologen as an electron donor is presented in Figure 4.4.

The Eyring plot reveals a breakpoint at 64 °C. Below 64 °C the apparent $\Delta H\ddagger$ is 19.3 $kJmol^{-1}$, which changes to 68 $kJmol^{-1}$ above that temperature. The apparent $\Delta S\ddagger$ is 146 $JK^{-1}mol^{-1}$ higher above 64 °C. It is known that the redox behavior of methyl viologen (and hence its ability to accept electrons from the protein) does not change drastically with temperatures up to 90 °C (Hagedoorn *et al.*, 1998). Therefore, the

observed changes are most likely due to a conformational change in the protein, *e. g.*, a temperature-induced activation.

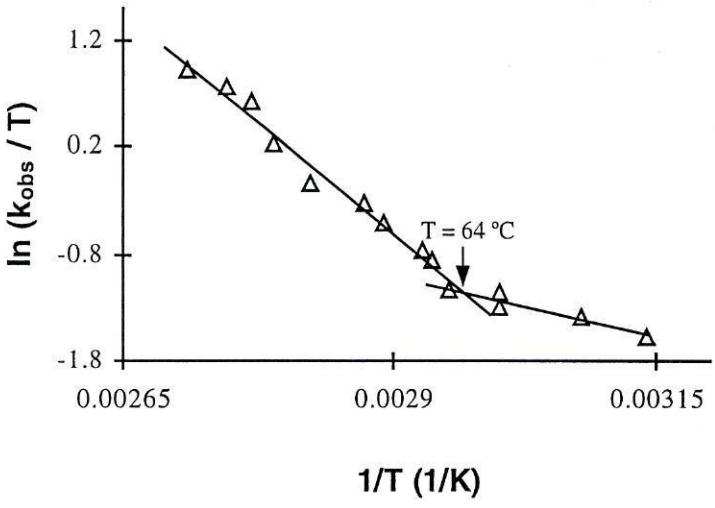

Figure 4.4 Eyring plot of the H_2-uptake reaction catalyzed by sulfhydrogenase.

A temperature-induced activation, though probably of a different nature, is also apparent when measuring the H_2-uptake activity of sulfhydrogenase after anaerobic oxidation with PMS. The specific activity increases markedly upon incubation at 80 °C under a H_2 atmosphere. The increase is much faster if methyl viologen is present in the incubation buffer. These data are consistent with the activation model common to other hydrogenases. Oxidized hydrogenase has a very low activity, but incubation under H_2 quickly reduces the hydrogenase molecules that are present in the "ready" state. The presence of methyl viologen (or other efficient electron carriers) greatly increases the rate of transfer of the reducing equivalents to "unready" molecules, thereby accelerating their activation. For unknown reasons, probably connected to the precise redox state of the sample, the magnitude of the activity increase varies from sample to sample, from around two-fold up to ten-fold.

The relative ratios of H_2-uptake to H_2 evolution activities were also measured after activation of anaerobically oxidized sulfhydrogenase. Surprisingly, the data show that even at 60 °C, the H_2-uptake activity is greater than the H_2 evolution at 80 °C (see

Figure 4.5). The estimated H_2-uptake/H_2-evolution ratio at 80 °C will therefore be lower than unity (*ca.* 0.25). Although this ratio is still greater than usual for [NiFe] hydrogenases, it can be concluded that the H_2-evolving role of this hydrogenase will probably be more modest than proposed by (Ma *et al.*, 1994).

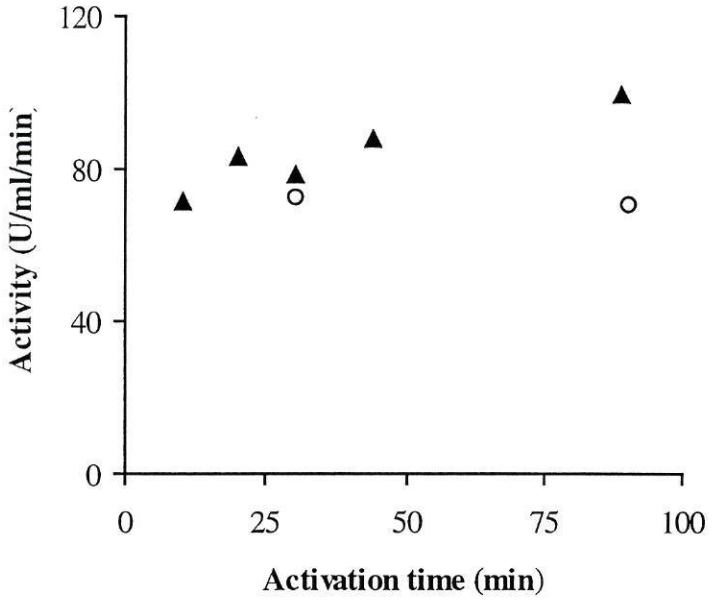

Figure 4.5 Effects of activation on the activities of sulfhydrogenase. (▲) H_2-uptake (measured at 60 °C). (o) H_2 evolution (measured at 80 °C).

4.4 EPR MEASUREMENTS

The EPR spectrum of PMS-oxidized enzyme shows a signal at g=2.007 and width=17 Gauss, consistent with a flavin-based radical (Figure 4.6). We measured the flavin content of the hydrogenase and found 0.52 mol flavin per mole of protein. This flavin was identified as FAD by the increase in fluorescence observed upon addition of *Naja naja* venom (Wassink and Mayhew, 1975).

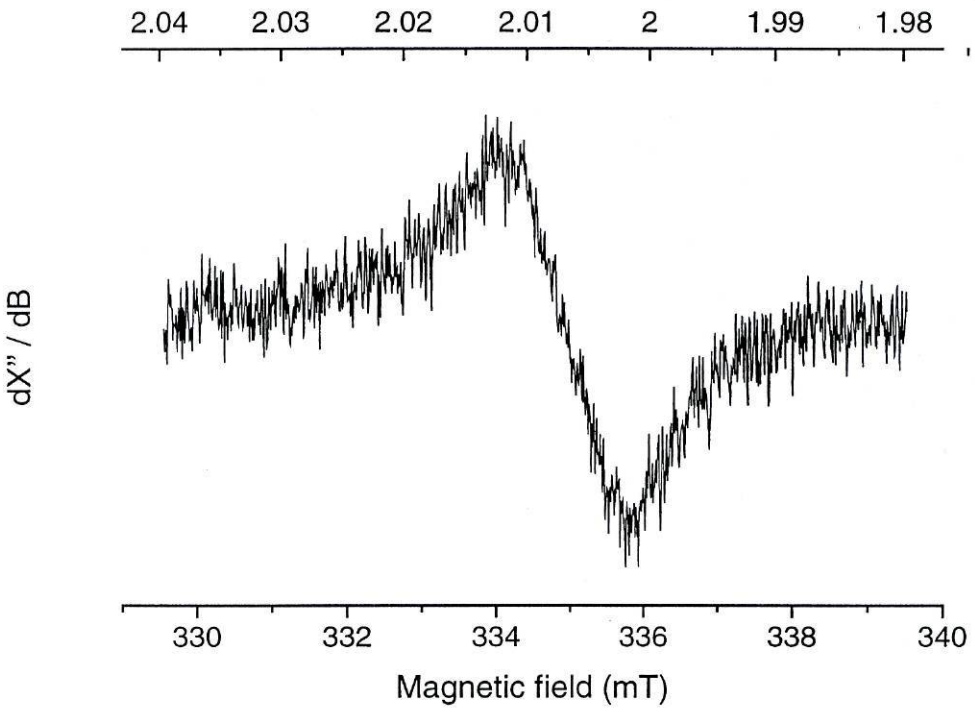

Figure 4.6 EPR spectrum of the flavin radical present in sulfhydrogenase. EPR conditions: microwave frequency, 9.4078 GHz; microwave power, 0.2 μW ; temperature, 16.5 K.

Previous redox titrations of *P. furiosus* hydrogenase performed at room temperature have yielded conflicting results regarding the redox potentials of the observed Fe-S clusters (see (Arendsen *et al.*, 1995) for a discussion). Only three Fe-S clusters have been found in these experiments, so that knowledge about half of the Fe-S clusters predicted in the protein is still missing. It is possible that these undetected Fe-S clusters may only be redox active under physiological temperatures. However, equilibrium in redox titrations performed at 80 °C is expected to be hampered by enzyme turnover since substrate (H^+) is always present in solution. Therefore we have examined the behavior of the sulfhydrogenase at 80 °C in the absence of electron donors as a first step towards the elucidation of its redox properties under physiological conditions. High temperature was found to induce a slow reduction of the sulfhydrogenase, which could be reverted by a temperature back-jump to room

temperature and this has been used as a convenient way to generate and identify novel nickel signals and to search for missing Fe-S signals.

Upon a short warming to 80 °C under anaerobic conditions the radical signal was replaced by the well-known [4Fe-4S] rhombic signal (Arendsen *et al.*, 1995). Upon further incubation of the sample at 80 °C the intensity of this signal decreased, and the [2Fe-2S] axial signal appeared (Figure 4.7 and Figure 4.8). At the same time the previously described (Arendsen *et al.*, 1995; Bryant and Adams, 1989) 'broad signal' also evolved. No significant signals from other Fe-S clusters were found, suggesting that their reduction potentials are probably too low to be observed under these conditions. After anaerobic incubation at room temperature all Fe-S clusters detected become oxidized.

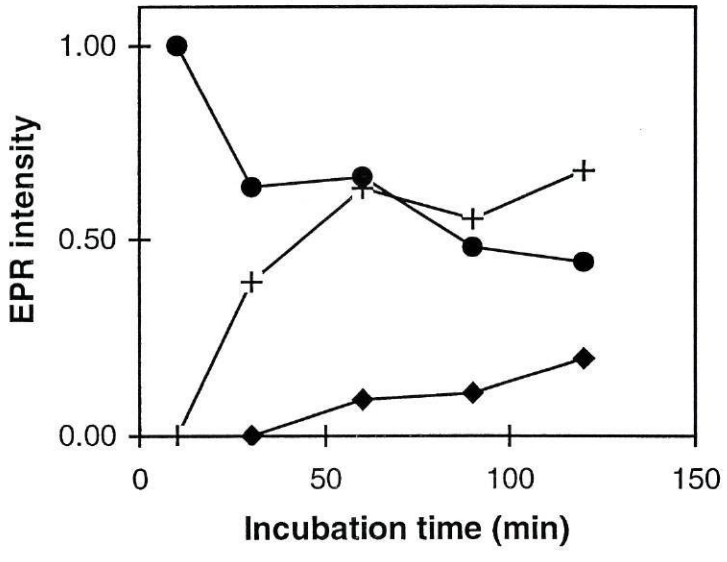

Figure 4.7 Time course of the evolution of the redox states of the sulfhydrogenase upon warming to 80 °C. (●) : [4Fe-4S]; (+) : [2Fe-2S]; (◆) Ni-C. The EPR intensities are shown normalized to the intensity of the 4Fe-4S signal obtained upon a 10 minute incubation of the hydrogenase at 80°C.

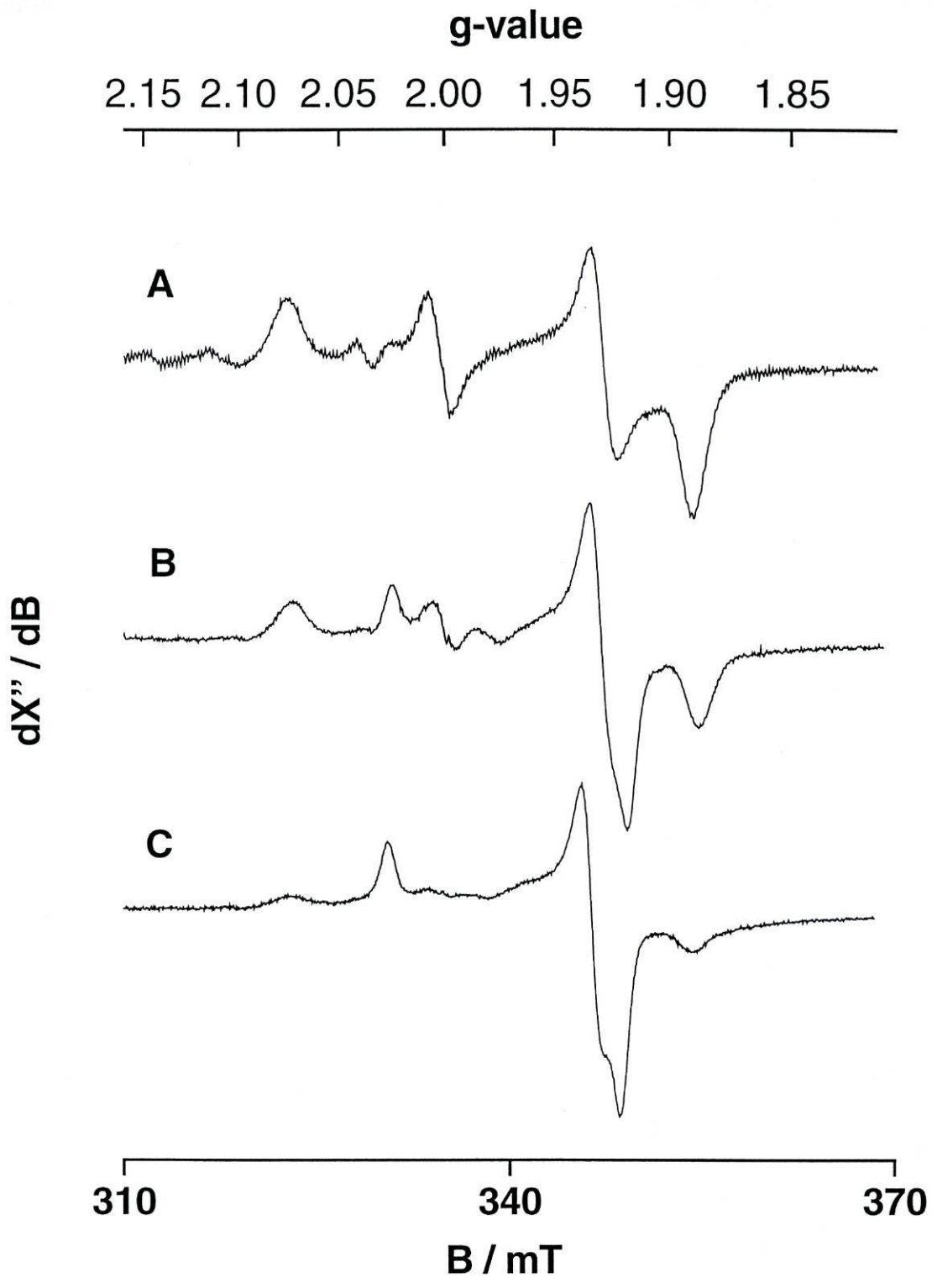

Figure 4.8 Evolution of the Fe-S redox states of the sulfhydrogenase upon warming to 80 °C. EPR spectra of sulfhydrogenase after warming to 80 °C for 10 minutes (trace A), 30 minutes (trace B), and 120 minutes (trace C). EPR conditions: microwave frequency, 9.41 GHz; microwave power, 1.3 mW (trace A) and 0.8 mW (traces B and C); temperature, 16 K.

Photo-reduction of hydrogenase at 80 °C under conditions where enzymatic turnover is prevented (under H_2 atmosphere and without electron acceptors) failed to reveal additional clusters. In order to confirm that this result was not due to loss of reducing equivalents through production of H_2 the experiment was repeated at 0 °C (no detectable hydrogenase activity), yielding the same result.

In the PMS-oxidized sample two other (weak) signals were also observed in the magnetic-field region where signals from the NiFe cluster are expected to be found (g = 2.0 - 2.4). We call these signals Ni-Ox^{resting} (Figure 4.9, upper trace, and Table 4.1). Upon a short warming to 80 °C under anaerobic conditions the intensity of these Ni-signals increased. As the incubation proceeded these Ni-signals changed into another set of two rhombic signals (which we call Ni-Ox$^{high\ T}$, Figure 4.9, second trace), then became undetectable and finally changed into the familiar Ni-C signal already found in most other Ni-hydrogenases but still not described in hyperthermophilic hydrogenases (Figure 4.9, third trace). This signal proved to saturate very easily at 25 K, and optimal results were obtained at liquid nitrogen temperatures. Visible light irradiation at 110 K causes this signal to disappear. Incubation of the sample at 200 K in the dark for 10 minutes restores the Ni-C signal, as observed for the NiFe hydrogenases from mesophilic organisms (Van der Zwaan *et al.*, 1985). However in contrast to the mesophilic hydrogenases no clear Ni-signals were found in the irradiated sample.

The behavior of the NiFe upon anaerobic incubation at room temperature after an incubation at high temperature depends on its redox state: samples where the NiFe cluster was still in the Ni-silent state reverted to the Ni-Ox$^{high\ T}$ state but samples containing NiFe cluster in the Ni-C state developed yet another new set of signals (which we called Ni-Ox$^{low\ T}$, Figure 4.9, lower trace).

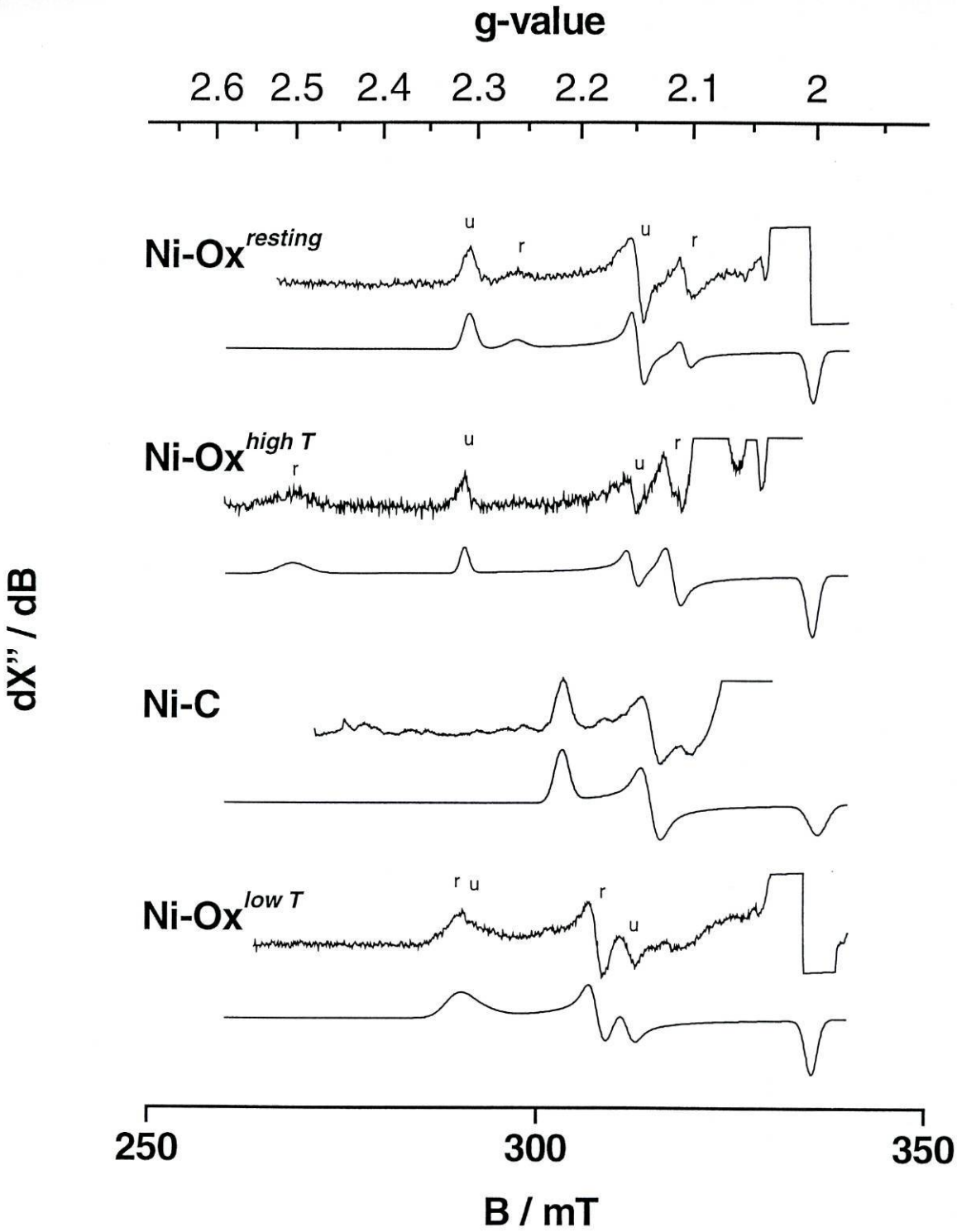

Figure 4.9 EPR spectra of sulfhydrogenase after warming to 80 °C for 1 minute (Ni-Ox^{resting}), 10 minutes (Ni-Ox$^{high\ T}$), 90 minutes (Ni-C) and 120 minutes followed by a 1.5 minutes incubation at room temperature (Ni-Ox$^{low\ T}$) and their simulations. NiFe-EPR features of unready and ready forms of hydrogenase (see text for details) are labeled *u* and *r*, respectively. EPR conditions: microwave frequency, 9.41 GHz, microwave power, 0.08 mW, temperature, 16 K (Ni-Ox^{resting} and Ni-Ox$^{high\ T}$); microwave power, 200 mW; temperature, 109 K; modulation amplitude, 1 mT (Ni-C); microwave power, 1.3 mW; temperature, 18.5 K (Ni-Ox$^{low\ T}$).

In order to assess the reversibility of this cycle Ni-Ox$^{low\ T}$ samples were again incubated at 80 °C. However only mild reduction occurred, which suggests the exhaustion of the electron supply (Figure 4.10). The Ni center could only be taken to the Ni-Ox$^{high\ T}$ state, and only the [4Fe-4S] cluster could be (partially) reduced. Reduction of this mildly reduced hydrogenase by H_2 at 80 °C yields hydrogenase with a fully reduced [2Fe-2S] cluster and the NiFe moiety in an EPR-silent state (most likely equivalent to the fully reduced Ni-R form found in mesophilic hydrogenases). Anaerobic oxidation of the hydrogenase in this state by PMS does not restore the ability to perform the whole cycle again. Enzyme cycled to the Ni-C state and back to Ni-Ox$^{high\ T}$ loses the ability to perform the cycle. This ability cannot be restored by dihydrogen incubation followed by anaerobic oxidation of the hydrogenase by PMS, suggesting that H_2 that might eventually be trapped close to the active site is not the internal reductant responsible for this cycle. The full temperature-induced reduction/oxidation cycle is reproducible on separate "as-isolated" samples from the same batch and from different batches of cells.

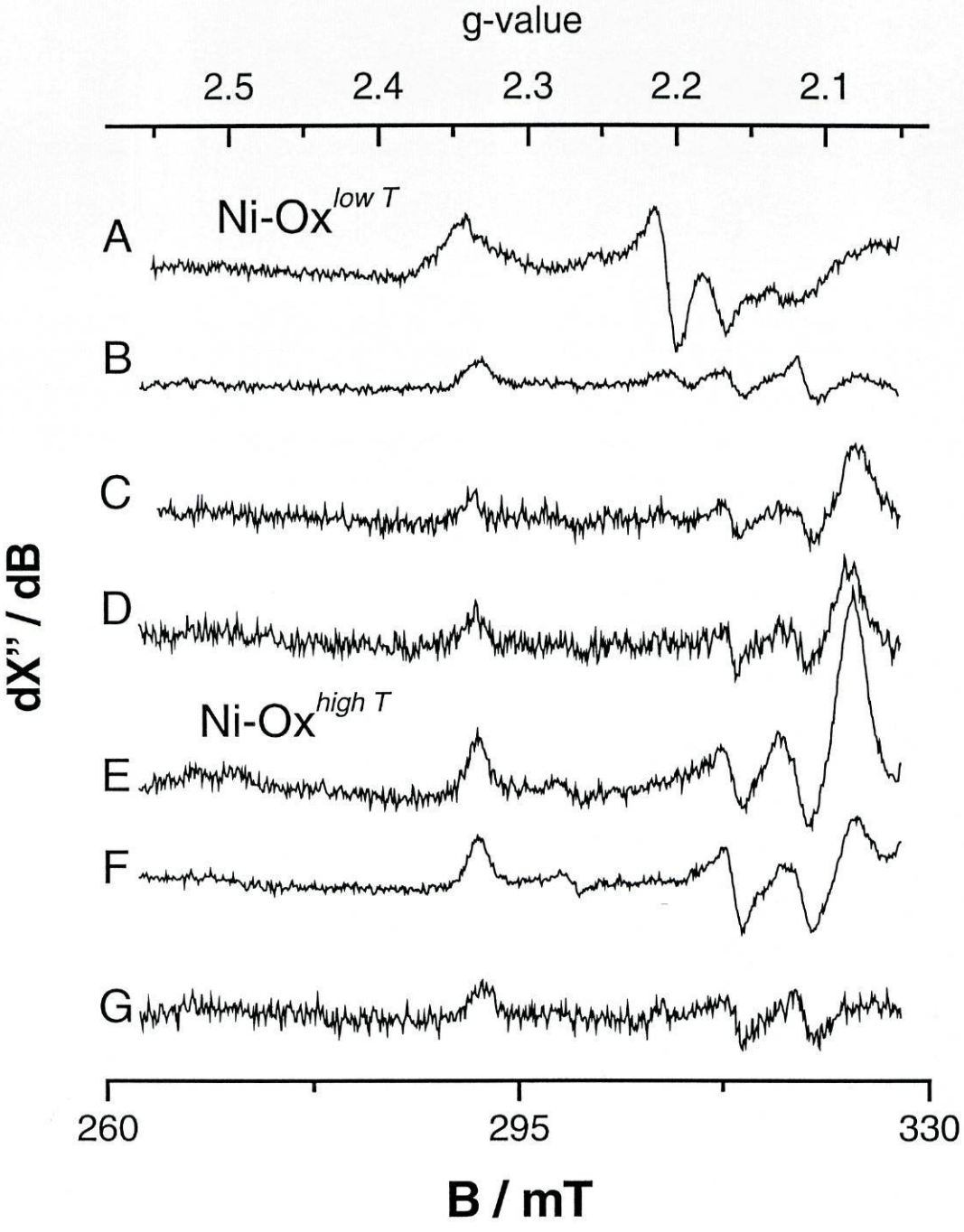

Figure 4.10 EPR spectra of sulfhydrogenase taken to the Ni-Ox$^{low\ T}$ state and subsequently incubated anaerobically at 80 °C for variable lengths of time. A) Ni-Ox$^{low\ T}$; B) 2 minutes incubation at 80 °C; C) 4 minutes incubation; D) 8 minutes incubation; E) 15 minutes incubation; F) 30 minutes incubation; G) 8 minutes incubation at 80 °C followed by 40 minutes at room temperature. EPR conditions: microwave frequency, 9.39 GHz, microwave power, 1.3 mW, temperature, 19 K. Spectra have been normalized to account for different gain settings.

4.5 REDUCTION WITH NADPH

Upon incubation of oxidized hydrogenase in the presence of NADPH at room temperature for 10 minutes the Fe-S clusters proved to be reduced to an extent comparable to that observed upon a 120 minutes incubation at 80 °C. However, the Ni-C signal observed in this 80°C incubated sample was not observed in the NADPH-reduced hydrogenase: instead a new set of signals appeared reminiscent of those observed during the initial stages of the 80 °C incubation (Figure 4.11).

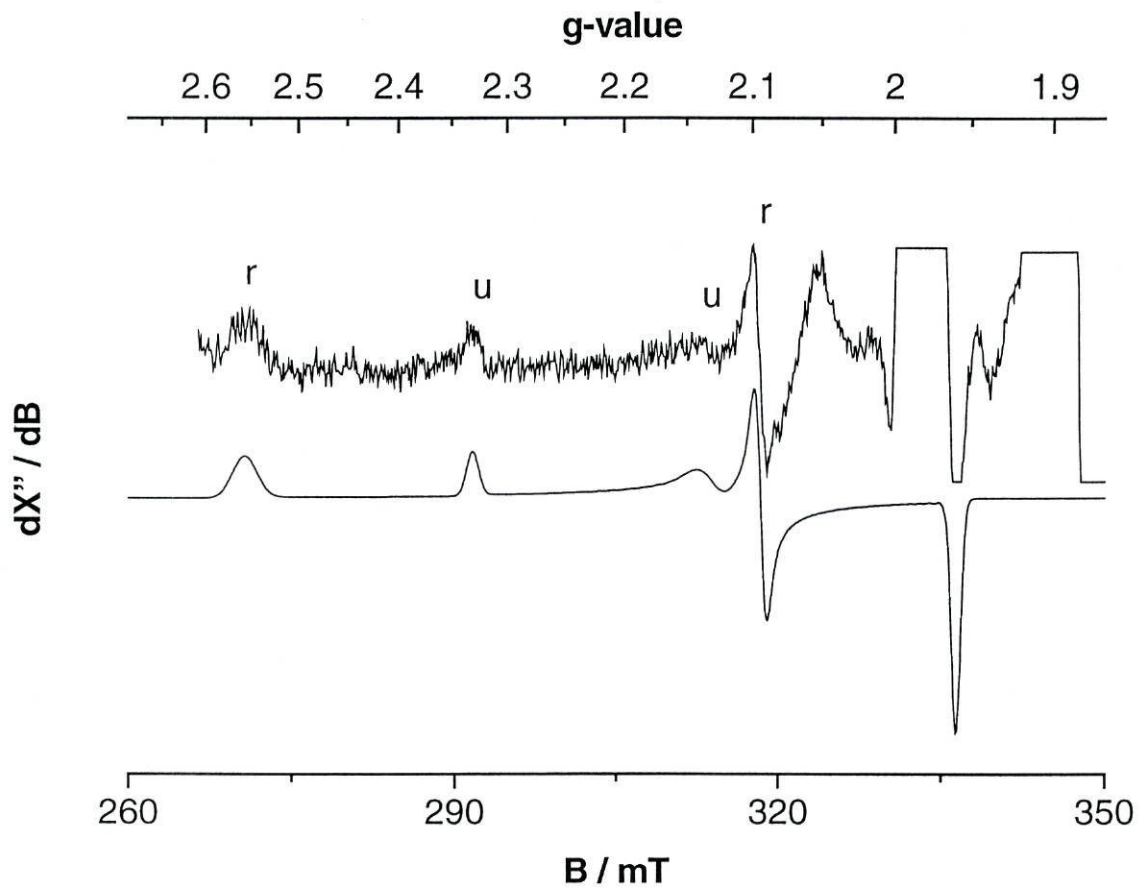

Figure 4.11 EPR spectrum and simulation (200 x 200 orientations) of sulfhydrogenase after incubation with NADPH (0.7 mM) at room temperature. EPR conditions: microwave frequency, 9.4164 GHz, microwave power, 0.13 mW, temperature, 16 K.

This indicates that upon warming the redox potential of the Ni-SI / Ni-C couple changes in a different way than the Fe-S clusters' potentials. Since NADPH was shown (Ma *et al.*, 1994) to be an electron donor to the hydrogenase this observation may be related to the catalytic inactivity of the enzyme at room temperature. Indeed, upon warming to 80 °C, NADPH is able to induce the appearance of a Ni-C signal in the sample.

4.6 REDOX TITRATION AT PHYSIOLOGICAL TEMPERATURES.

A redox titration of sulfhydrogenase was performed at 80 °C. After anaerobic incubation of an oxidized sample at 80 °C (to try to deplete the internal reductant) and poising the potential at –38 mV vs. SHE, only two small signals, attributable to Ni-$Ox^{high\ T}$ were found. These signals did not change appreciably, nor did any new signals become visible, upon reduction to –290 mV. Stable potentials then became very hard to attain, due to the H_2 evolution by the enzyme. During turnover both the [2Fe-2S] and the [4Fe-4S] clusters were found in the reduced state. Upon oxidation with ferricyanide, the [2Fe-2S] cluster oxidized immediately. However, the [4Fe-4S] cluster remained reduced, and oxidized at a potential close to –140 mV. This is a surprising behavior, since no reduced [4Fe-4S] cluster was observed when reducing the protein from –40 to –290 mV. It is possible that this cluster cannot be reduced by dithionite (or dyes) before activation of the enzyme. Upon activation at suitably low potentials, H_2 evolution is observed. The [NiFe] cluster might then become a suitable electron-relaying site, able to act as a connecting wire between the isolated [4Fe-4S] cluster and the mediators in solution, which would allow the equilibration of the cluster with the outside potential during the oxidation with ferricyanide.

	g_x	g_y	g_z	Δ_x	Δ_y	Δ_z
Ni-Ox^{resting}						
u	2.305	2.145	2.0	0.007	0.005	0.005
r	2.259	2.104	2.0	0.010	0.0045	0.005
D. gigas Ni-A	2.32	2.23	2.01	n.d.	n.d.	n.d.
D. gigas Ni-B	2.34	2.16	2.01	n.d.	n.d.	n.d.
Ni-Ox$^{high\ T}$						
u	2.309	2.149	2.0	0.005	0.005	0.005
r	2.499	2.1135	2.0	0.020	0.006	0.005
Ni-Ox$^{low\ T}$						
u	2.295	2.153	2.0	0.020	0.007	0.005
r	2.315	2.180	2.0	0.016	0.0075	0.006
Ni-Ox^{NADPH}						
u	2.307	2.143	2.0	0.005	0.010	0.003
r	2.486	2.113	2.0	0.012	0.0035	0.003
Ni-C	2.2185	2.137	2.0	0.008	0.008	0.008
D. gigas Ni-C	2.19	2.15	2.01	n.d.	n.d.	n.d.
Ni-L	n.o.	n.o.	n.o.	n.o.	n.o.	n.o.
D. gigas Ni-L	2.30	2.13	2.15	n.d.	n.d.	n.d.

Table 4.1 Simulation parameters of Ni-EPR signals from *P. furiosus* sulfhydrogenase. The Δ_i are the components, in *g*-value units, of a linewidth matrix co-linear with the *g*-matrix (cf. (Hagen, 1989)). The g_z-component is estimated: in all experimental spectra it is blanked by more intense Fe-S and/or radical signals. The *g*-values of the different Ni-states of the mesophilic hydrogenase from *D. gigas* (Cammack *et al.*, 1987; Teixeira *et al.*, 1986) are shown for comparison. N.d. = not determined; n.o. = not observed.

4.7 T-JUMP EXPERIMENTS

Incubation of oxidized hydrogenase at 80 °C proved to be a very convenient way to generate and identify several states of the NiFe cluster. In each of these states (except for Ni-C) two forms are clearly distinguishable (See Figure 4.9 and Table 4.1). One of these forms (which we have labeled form "u", from *unready,* see below) changes only slightly throughout the whole temperature-jump sequence, while the other form changes much more dramatically. The relative contributions of each form to the joint spectrum change drastically after the initial minutes of the temperature-jump and then remain fairly constant throughout the process. This suggests a two-stage process, whereby the initial temperature-jump induces a change in the equilibrium between "ready" and "unready" forms of hydrogenase, and subsequent incubation at high temperature induces the activation of the "ready" form of hydrogenase. We therefore propose that form "u" is due to "unready" hydrogenase, and the changes observed in form "r" reflect a temperature-induced activation of "ready" hydrogenase. Between Ni-Ox$^{high\ T}$ and Ni-C the NiFe cluster becomes EPR-silent (Ni-SI). Ni-C-containing samples do not show any contribution from "unready" hydrogenase although in Ni-Ox$^{low\ T}$ (which is obtained through anaerobic incubation of Ni-C samples at room temperature) the "unready" form is clearly visible. This observation suggests that only the "ready" form of the enzyme is reduced to the Ni-C state and therefore Ni-SI is also a heterogeneous state of the enzyme. The relationships between each of the NiFe cluster states in mesophilic hydrogenases and in the hyperthermophilic enzyme are compared in Figure 4.12 and Figure 4.13.

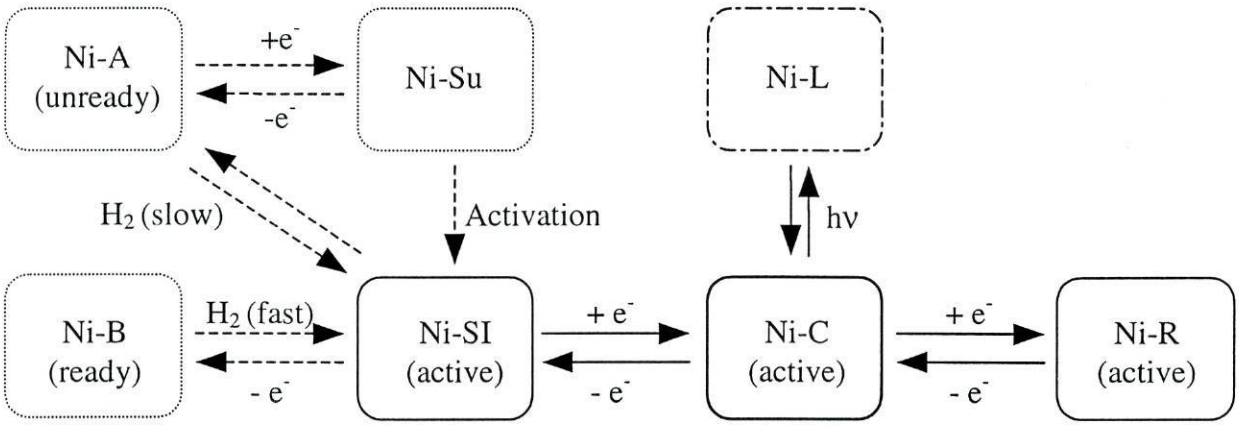

Figure 4.12 The NiFe cycle in mesophilic hydrogenase (adapted from (de Lacey *et al.*, 1997). H_2 (slow) and H_2 (fast): long (over 6 hours) or short (some minutes) incubation under H_2 atmosphere, respectively.

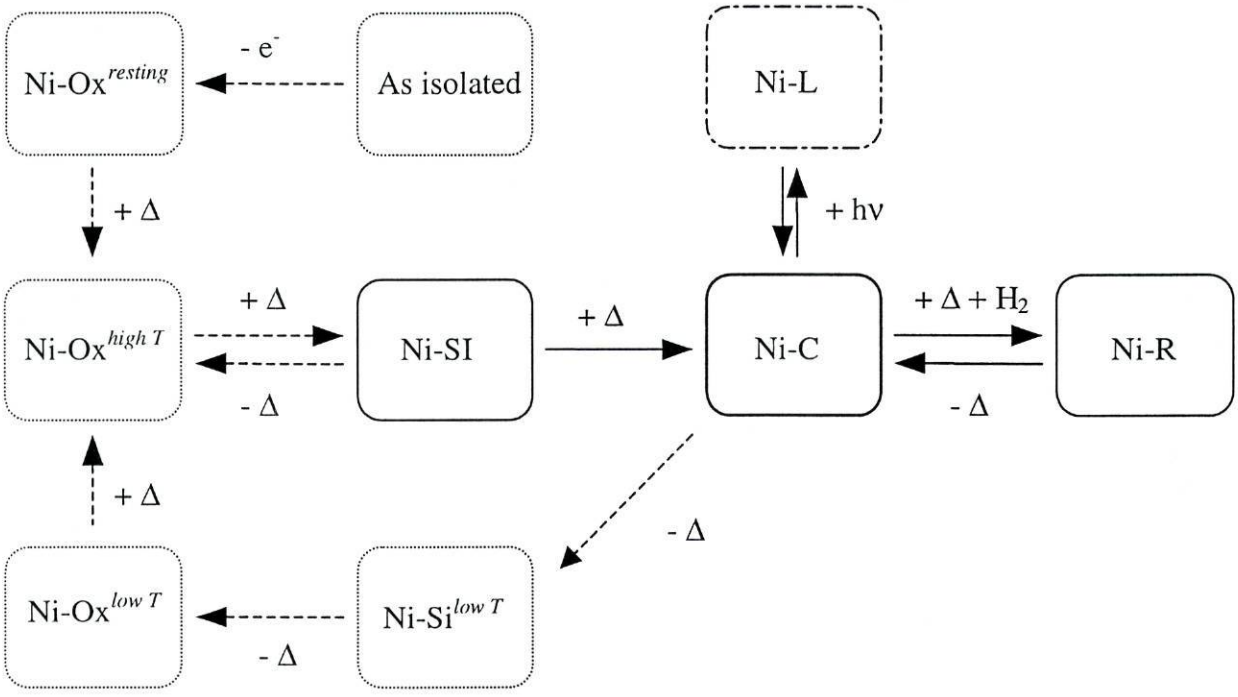

Figure 4.13 The NiFe cycle in *P. furiosus* hydrogenase. (+Δ) : anaerobic incubation at 80 °C; (-Δ) : anaerobic incubation at room temperature. In both schemes, dashed boxes represent the (in)activation cycle and whole boxes represent the active states.

The comparison suggests that the hyperthermophilic and the mesophilic forms of Ni-C/L are equivalent. However, our failure to detect a Ni-L EPR signal, and our observation of ready relaxation of the Ni-C signal indicate a possible structurally different surrounding of these Ni-states in *P. furiosus* enzyme.

The absence of EPR-signals from some of the predicted Fe-S clusters is surprising. This may be due to cluster breakdown, very low reduction potentials or undetectability of high spins. [4Fe-4S] clusters in hydrogenases are usually difficult to detect by EPR, showing extremely broad signals (Teixeira *et al.*, 1989), or else requiring coupling to Ni-C (Teixeira *et al.*, 1985) or very low temperatures (Teixeira *et al.*, 1986) to be detectable.

The origin of the reducing equivalents involved in the temperature-induced redox process is intriguing. The formation of disulfide bridges upon warming or a purification-induced conformational change that would trap H_2 in a state where it might transfer electrons to the protein are possible explanations to the observed temperature-induced self-reduction of the protein. The ability to perform the cycle appears to be sensitive to the purification conditions: if dithiothreitol is used as an O_2-scavenging system instead of dithionite the temperature-induced changes are much slower. Since dithiothreitol is a Cys-protecting compound this argues in favor of disulfide bridges formation as the source of internal reductant.

5

THE SULFIDE DEHYDROGENASE

5.1 BACKGROUND

Pyrococcus furiosus reduces elemental sulfur, S^0, (or polysulfides, S_nS^-) to hydrogen sulfide (Blumentals *et al.*, 1990; Fiala and Stetter, 1986). The reduction is non-obligate but growth by fermentation of peptides is greatly stimulated by the addition of sulfur (Schicho *et al.*, 1993). The physiological role of sulfur reduction is not clear; sulfur is thought to serve as an additional electron sink (Hedderich *et al.*, 1999). Two sulfur reductases have been identified: sulfide dehydrogenase (Ma and Adams, 1994) and sulfhydrogenase (Ma *et al.*, 1993). However, a completely different activity has also been established for each of these enzymes. Sulfide dehydrogenase (SuDH) is also a ferredoxin: $NADP^+$ oxidoreductase (FNOR) (Ma and Adams, 1994; Ma *et al.*, 1994), and sulfhydrogenase is also an NADPH-dependent hydrogenase (Bryant and Adams, 1989; Ma *et al.*, 1993). In fact, a major route of reducing equivalents in mainstream metabolism has been proposed to be(Ma *et al.*, 1994):

fermentation → ferredoxin → FNOR(SuDH) → NADPH → sulfhydrogenase → H^+

In this putative scheme the reduction of sulfur by SuDH and/or by sulfhydrogenase could be optional branches. The bioenergetic significance of the H_2-generating route and of its sulfide-generating branches is not clear.

EPR spectroscopic analysis has been interpreted in terms of one [3Fe-4S] cluster and three additional Fe/S clusters with an S=1/2 signal in the reduced state i. e. 2Fe and/or 4Fe clusters. We have extended the EPR analysis on the purified enzyme. The combined results now provide a consistent picture of all prosthetic groups of SuDH including a [2Fe-2S] cluster with a novel $Asp(Cys)_3$ binding pattern.

5.2 THE PRIMARY STRUCTURE OF SUDH TRANSLATED FROM THE GENOME

Ma and Adams have reported N-terminal sequences for the two subunits of SuDH. A search of the *P. furiosus* genome for correspondence with these sequences gives one positive for each, namely two subsequent open-reading frames, which can be identified as the structural genes for SuDH. Their complete translated sequence is given in Figure 5.1.

We propose to name the two open reading frames *sudB* and *sudA*; their identification with SuDH is based on the following. The reported N-termini for the α and β-subunit are RLIKDRVPTPERXVGY and LRKERLAPGINLFEIESPRI, respectively. These correspond fully with the translated sequences from the genome except that the protein sequences start at position 3 and 5, respectively. Each of the translated gene sequences start with methionine; post-translational modification may have deleted this initial residue. Without the initial M (and also without prosthetic groups) the translated proteins SudA and SudB have molecular masses of 52598 and 30686 Da, where the masses for the α and β-subunit of purified SuDH, estimated from SDS-PAGE, are 52.0 and 29.0 kDa, respectively (Ma and Adams, 1994). The calculated (Bjellqvist *et al.*, 1993) pI's of the α and β-subunit are 7.3 and 7.2. The optical spectrum and the phosphor elemental analysis of SuDH indicated the presence of two FAD (Ma and Adams, 1994); SudA and SudB each contain putative binding sites for one flavin and for one NADPH (see below). Preliminary EPR-spectroscopic analysis indicated the presence of 3-4 Fe/S clusters (Ma and Adams, 1994); SudA and SudB contain three putative binding motifs for Fe/S clusters (see below). SudB is strongly homologous to HydG, the γ-subunit of *P. furiosus* sulfhydrogenase, another sulfide dehydrogenase.

```
SudA
0       MPRLIKDRVP TPERSVGERV RDFGEVNLGY SWELALREAE RCLQCPVEYA
50      PCIKGCPVHI NIPGFIKALR ENRDNPSKAV REALRIIWRD NTLPAITGRV
100     CPQEEQCEGA CVVGKVGDPI NIGKLERFVA DYAREHGIDD ELLLEEIKGI
150     KRNGKKVAII GAGPAGLTCA ADLAKMGYEV TIYEALHQPG GVLIYGIPEF
200     RLPKEIVKKE LENLRRLGVK IETNVLVGKT ITFEELREEY DAIFIGTGAG
250     TPRIYPWPGV NLNGIYSANE FLTRINLMKA YKFPEYDTPI KVGKRVAVIG
300     GGNTAMDAAR SALRLGAEVW ILYRRTRKEM TAREEEIKHA EEEGVKFMFL
350     VTPKRFIGDE NGNLKAIELE KMKLGEPDES GRRRPIPTGE TFIMEFDTAI
400     IAIGQTPNKT FLETVPGLKV DEWGRIVVDE NLMTSIPGVF AGGDAIRGEA
450     TVILAMGDGR KAAKAIHQYL SKEK

SudB
0       MFKILRKERL APGINLFEIE SPRIAKHAKP GQFVMIRLHE KGERIPLTIA
50      DVDISKGSIT IVAQEVGKTT RELGTYEAGD YILDVLGPLG KPSHIDYFGT
100     VVMIGGGVGV AEIYPVAKAM KEKGNYVISI LGFRTKDLVF WEDKLRSVSD
150     EVIVTTNDGS YGMKGFTTHA LQKLIEEGRK IDLVHAVGPA IMMKAVAELT
200     KPYGIKTVAS LNPIMVDGTG MCGACRVTVG GEVKFACVDG PEFDAHLVDW
250     DQLMNRLAYY RDLEKISLEK WERERRMV
```

Figure 5.1 Primary sequence of SudB and SudA, the β- and α-subunits of sulfide dehydrogenase as translated from two contiguous open reading frames in the genome of *P. furiosus*. Previously determined (Ma and Adams, 1994) N-terminal protein sequences are in underlined italic. Putative iron-sulfur cluster binding motifs are in underlined bold with the coordinating Cys and Asp marked in dark gray and black, respectively. Putative binding regions for FAD are boxed and in light gray. Putative binding regions for NADPH are boxed and in white.

5.3 CHARACTERIZATION OF PROSTHETIC GROUPS THROUGH SEQUENCE COMPARISONS

Sequence comparison using the BLAST protocol and CLUSTAL-X alignment, complemented by direct inspection and judicious re-alignment, revealed each subunit to consist of a flavin-binding part, a cofactor binding domain, and an Fe/S binding part. In Figure 5.2A a Cys-rich sequence near the C-terminus of the β-subunit is compared to homologous sequences. The SudB sub-sequence is also found in the genomes of hyperthermophilic archaea *Pyrococcus horikoshii* and *Pyrococcus abyssi* and of the hyperthermophilic bacteria *Thermotoga maritima* and *Aquifex aeolicus*. Remarkably, the SudB sub-sequence is also highly similar to a sub-sequence in an unidentified open reading frame from the genome of mesophilic *Treponema pallidum*, the causative organism of syphilis. Both sequences are only slightly less similar to a second group of sub-sequences that contain, amongst others, the β-subunit of *Salmonella typhimurium* assimilatory sulfite reductase (Huang and Barrett, 1991) and the γ-subunit of *P. furiosus* sulfhydrogenase. The latter enzyme does not only have sulfide dehydrogenase activity, but it is also known, from EPR spectroscopy and sequence analysis, to contain a [2Fe-2S] cluster (see chapter 4). Both groups are homologous to a third group (50 sequences in the Swiss Prot data base): the 'plant-type' [2Fe-2S] ferredoxins from plants and algae. The latter homology is much weaker; it is limited to the consensus CxxGxCxxC and CxxxP, and it is not readily discerned in computer sequence analysis. We conclude that all the strict anaerobes and facultative anaerobes in Figure 5.2A have a protein that carries a [2Fe-2S] cluster, which is a variant of the well known 'plant type' ferredoxin [2Fe-2S]. Furthermore, it appears that *P. furiosus sudB* and similar (see below) genes in other hyperthermophiles, and the *T. pallidum* orf putative protein encode a novel variant in which the cluster is coordinated by three Cys and one Asp. The consensus for the two groups is Mx(C/D)xxGxCxxC and Cx(D/E)GPxF.

A) Cluster-I: [2Fe-2S]

SudB *P. furiosus*	220	N P I M V D G T G M C G A C	(10X)	A C V D G P E F
HydG *T. pallidum*	213	N T I M I D G T G M C G G C	(10X)	V C V D G P E F
HydG *P. furiosus*	248	E R R M K C G I G K C G H C	(10X)	I C K D G P V F
AsrB *S. typhimurium*	235	E R R M A C S V G K C G H C	(6X)	V C T D G P I F
Fd *S. platensis*	36	D L P Y S C R A G A C S T C	(28X)	T C V A Y P T G
Fd Spinach	34	D L P Y S C R A G S C S S C	(28x)	T C A A Y P V S

B) Cluster-II: [4Fe-4S]

SudA	*P. furiosus*	35	A L R E A E R C L Q C P V E Y A P C - - - I K G C P
GOGAT	*P. kodakaraensis*	37	A V K E A E R C L Q C P Y E Y A P C - - - I K G C P
DPD	pig liver	72	A L R E A M R C L K C - A D - A P C - - - Q K S C P
GltS	*A. brasilense*	41	A N E Q A N R C S Q C G V P F - - C - - - Q V H C P
GltS	*M. sativa*	1716	L L K Q S A R C M D C G T P F - - C H Q E N S G C P
AegA	*E. coli*	220	A Q R E A S R C L K C G - E H S V C - - - E W T C P

C) Cluster-III: [3Fe-4S]

SudA	*P. furiosus*	90	D N T L P A I T G R V C P Q E E Q C E G A C V
GOGAT	*P. kodakaraensis*	92	C N S L P A T T G R V C P Q E D Q C E M N C V
DPD	pig liver	119	D N P L G L T C G M V C P T S D L C V G G C N
GltS	*A. brasilense*	89	T N N F P E I C G R I C P Q D R L C E G N C V
GltS	*M. sativa*	1767	T N N F P E F T G R V C P A P - - C E G S C V
AegA	*E. coli*	268	T N T L P E I T G R V C P Q D R L C E G A C T

Figure 5.2 Sequence comparisons of iron-sulfur cluster binding motifs in *P. furiosus* sulfide dehydrogenase. In part A the putative [2Fe-2S] cluster Asp(Cys)$_3$-containing motif of *P. furiosus* SudB and of an unidentified protein in *T. pallidum* are compared to a similar (Cys)$_4$-containing motif in *P. furiosus* sulfhydrogenase and in *S. typhimurium* assimilatory sulfite reductase, and to the somewhat less similar 'classical' [2Fe-2S] cluster binding motifs in algae and plants. In parts B and C the [4Fe-4S] and [3Fe-4S] cluster binding motifs in *P. furiosus* SudA are compared to similar ones in proteins of the glutamate synthase class.

In Figure 5.2B and Figure 5.2C we compare two Cys-rich patterns near the N-terminus of the SuDH α-subunit with homologous sequences. The figure is an extension of a recent analysis of cubane-binding patterns in a small class of iron-sulfur flavoproteins consisting of dihydropyrimidine dehydrogenase, DPD, and glutamate synthase, GltS or GOGAT (Rosenbaum *et al.*, 1998; Vanoni and Curti, 1999), an uncharacterized regulatory protein AegA from *Escherichia coli* (Cavicchioli *et al.*, 1996), and here extended with sulfide dehydrogenase. The two Cys patterns appear to define a novel binding motif for two low-potential cubanes. In DPD the two cubanes are not reduced, not even by the light-excited deazaflavin/EDTA system (Hagen *et al.*, unpublished). In *Azospirillum brasilense* GltS one of the two putative cubanes is not quantitatively reducible with dithionite, although it is reducible with NADPH (Vanoni *et al.*, 1992). A similar behavior is found with SudA (see below). Interestingly, the first Cys of the second pattern is replaced by threonine in several sequences. This C/T modification occurs also within the GltS enzyme group. Unfortunately, none of the proteins with Thr in this position has been studied in purified form, except for *P. furiosus* SuDH. The initial EPR study by Ma and Adams strongly suggests that SuDH carries one [3Fe-4S] cluster (Ma and Adams, 1994). Since Thr is not known to be a ligand for Fe/S clusters, we propose that the two sequences in Figure 5.2B and Figure 5.2C bind one [4Fe-4S] cluster and one [3Fe-4S] cluster in SuDH and in some GltS's. It is not known whether the two binding motifs are consecutive in the primary sequence or intertwined (e. g. as in 8Fe ferredoxins).

Putative non-covalent binding regions for FAD and NADPH have previously been defined in GltS and DPD through sequence comparison. Homologous regions are readily found in SudA (Figure 5.1) using the GltS/DPD consensus pattern of Vanoni and Curti (Vanoni and Curti, 1999).

A different approach proved to be necessary for identifying binding regions in SudB. A BLAST search for sequence similarity between SudB and well-characterized

flavoproteins yielded scores on the borderline of significance. High similarity scores were, however, obtained with flavoprotein sequences not yet characterized at the protein level and with the product of *hydG*, the gamma subunit of *P. furiosus*'s own heterotetrameric hydrogenase (Pedroni et al., 1995). Therefore, binding domains were searched for by alignment of SudB, HydG, and other HydG-like proteins. Putative binding domains in SudB have been indicated in Figure 5.1. The analysis shows that there are a total of five HydG-like proteins in *P. furiosus* (including SudB and HydG); the HydG motif is also present five and four times, respectively, in the closely related genomes of *P. abyssi* and *P. horikoshii.*

The region around the putative (Cys/Asp)$(Cys)_3$ binding motif for the [2Fe-2S] cluster is of course highly conserved. Furthermore, several Gly/Pro rich stretches show significant mutual similarity including a few fully conserved amino acids. The boxed stretches in Figure 5.1 (SudB) have been defined by computer alignment, visual inspection, and comparison with conserved binding motifs for FAD and NADPH in well-characterized flavoenzymes. The first yellow box is similar to the RLYSIASS FAD-binding pattern in, e. g., ferredoxin: $NADP^+$ oxidoreductase, FNR (Karplus and Bruns, 1994), nitric oxide synthase, cytochrome P-450 reductase (Bredt *et al.*, 1991). The first part of the second yellow box is similar to the LCVKRL FAD-binding motif in FNR (Karplus and Bruns, 1994), and, following a fully conserved Gly, we find the fully conserved TX_8GD motif previously identified in rubredoxin reductase and other flavoprotein oxidoreductases to be involved in hydrophobic interaction and hydrogen bonding with FAD (Eggink *et al.*, 1990). The third yellow box is similar to the GPVGK motif proposed as part of a possible ferredoxin binding domain in FNR (Karplus and Bruns, 1994). The green fourth and fifth box, respectively, are similar to the GTGIAP and YMCGLKGM fingerprints for binding of the ribose and adenine part of NADPH by FNR (Bruns and Karplus, 1995; Karplus and Bruns, 1994; Serre *et al.*, 1996).

In summary, the sequence analysis of the translated *sudB* and *sudA* genes indicates *P. furiosus* SuDH to carry one unusual [2Fe-2S] cluster with Asp as a ligand, one [3Fe-4S] cluster, one low-potential [4Fe-4S] cluster, two FADs, and two putative binding sites for NADPH.

5.4 ISOENZYMES OF SULFIDE DEHYDROGENASE AND SULFHYDROGENASE

There are five HydG-like sequences in the *P. furiosus* genome. One corresponds to the β-subunit of sulfide dehydrogenase, SudB. One corresponds to the γ-subunit of sulfhydrogenase, HydG. The other three have not been characterized yet at the protein level. Inspection of flanking genes in the *P. furiosus* genome provides a putative operon context (Figure 5.3), which, in turn suggests biological functions. SudY is a homologue of SudB and defines the β-subunit of a second sulfide dehydrogenase. We have labeled the structural genes *sudX* and *sudY*. They encode a putative αβ-dimer of 52 plus 33 kDa. HydR is a homologue of HydG and defines the γ-subunit of a second sulfhydrogenase. We have labeled the structural genes *hydP*, *hydQ*, *hydR*, and *hydS*. They code for a putative αβγδ-tetramer of 46 plus 31 plus 33 plus 26 kDa. Hydrogenase activity is carried by the HydA subunit containing the dinuclear Ni-Fe active site (Pedroni et al., 1995). For completeness we note that the *P. furiosus* genome carries one more homologue of the HydA encoding gene. However, the gene for this third putative α-subunit appears to be part of a large operon, possibly consisting of 16 orfs, and apparently encoding a membrane-bound complex with some homology to subunits of mitochondrial NADH dehydrogenase. It does not contain a HydG-like subunit (not shown).

Orf3 is clearly not part of a sulfide dehydrogenase nor of a hydrogenase; *orf3* may be part of a four-orf operon possibly encoding a pyruvate-formate lyase activating system.

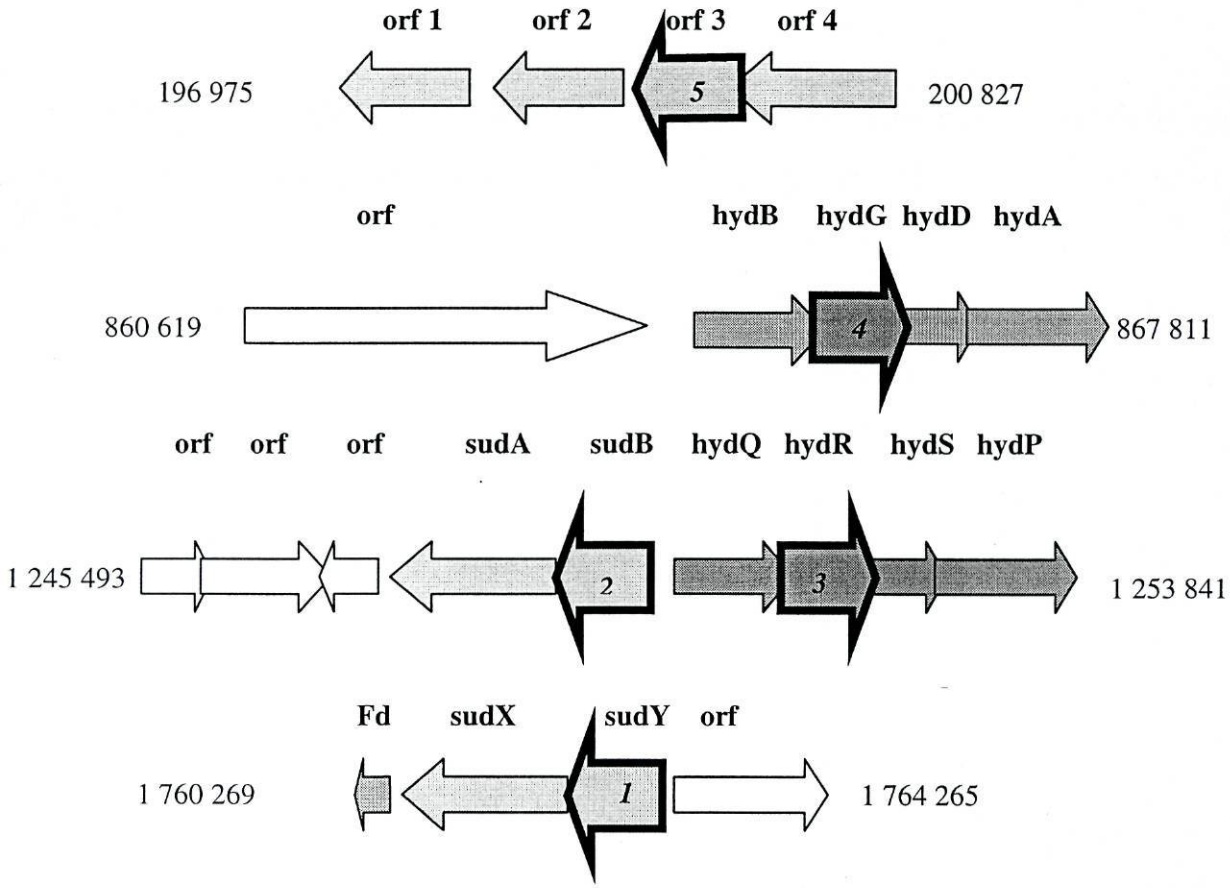

Figure 5.3 Putative operon context for five Hyd-G like proteins in *P. furiosus*. The context analysis indicates that SudB and SudY are β-subunits of two αβ sulfide dehydrogenase enzymes, HydG and HydR are γ-subunits of two αβγδ sulfhydrogenase enzymes, and Orf3 may be part of a radical enzyme activating system. The numbers give the left-hand and right-hand genomic addresses for the stretches shown.

5.5 CHEMICAL ANALYSIS AND ACTIVITY OF SUDH

The slightly modified purification procedure, as described in the methods section, resulted in a 182-fold purification and a specific NADH: benzyl viologen oxidoreductase activity of 137 U when measured at 60 °C, which compares favorably with the originally reported value of 160 U at 80 °C (Ma and Adams, 1994).

Elemental analysis gave 8 ± 1 Fe and 6 ± 1 S^{2-} per αβ-dimer; earlier reported values are 11 Fe and 6 S (Ma and Adams, 1994). Analytical chromatography of the enzyme on a small Superdex 200 column, with A_{436} and A_{280} monitoring, indicated an approximate 10% contamination by a single, colorless protein (i. e. with no absorbance at 436 nm), and this indicates that the Fe/S numbers of pure SuDH are slightly higher: approximately 9 Fe and 7 S, where 9 Fe and 10 S are predicted on the basis of the sequence analysis.

Flavin was determined from the fluorescence spectrum of liberated cofactor and from the increase in fluorescence upon incubation with *Naja naja* snake venom. This method afforded 2.2 FAD per αβ-dimer.

The purified SuDH was checked for NADPH-dependent glutamate synthase activity, and this was found to be zero both at ambient temperature and at 60 °C.

5.6 EPR MONITORED REDOX TITRATION OF THE FE/S CLUSTERS

The enzyme as isolated is in an intermediate state of reduction: its EPR spectrum changes both upon oxidation and reduction. In Figure 5.4 the middle trace, B, is the spectrum of the as isolated enzyme. The signal has g-values 1.786, 1.908, 2.035, and is reminiscent of that of the Rieske-type of [2Fe-2S] cluster in the reduced, mixed valence state. Rieske clusters have protein ligation through two cysteines and two histidines. The two His residues coordinate the iron ion that takes up the excess reducing electron. Rieske clusters have relatively high reduction potentials, $E_m \approx$ -150 to +300 mV (Link, 1999), compared to the 'regular', four Cys coordinated ferredoxin-type [2Fe-2S] clusters which may have $E_m \approx$ -650 to 0 mV (Cammack, 1992) with typical values in the -0.4 to -0.3 V range. The SuDH sequence does not have a binding motif for a Rieske cluster, but it does have a putative $Asp(Cys)_3$ motif for an unusual [2Fe-2S] cluster. The EPR signal amplitude titrates with an E_m in the range for Rieske clusters (see below). We propose that the Rieske-like EPR signal of SuDH is from reduced cluster-I (cf. Figure 5.2), a $[2Fe\text{-}2S]^{1+}$ cluster with the excess electron localized on the iron coordinated by Asp-216.

Upon oxidation with excess sodium ferricyanide ($E_{m,7}$ = +360 mV) the [2Fe-2S] cluster signal disappears, and a different signal appears which is characteristic for oxidized [3Fe-4S] clusters (Johnson *et al.*, 1999). Following the original proposal by Ma and Adams (Ma and Adams, 1994) we assign this signal (Figure 5.4, upper trace A) to oxidized cluster-III, a $[3Fe\text{-}4S]^{1+}$ cluster with the regular binding motif $(Cys)_3$ (cf. Figure 5.2).

Upon reduction of the as-isolated enzyme with visible light plus deazaflavin plus EDTA ($E_m << -0.5$ V (Massey and Hemmerich, 1978)) the $[2Fe\text{-}2S]^{+}$ signal is not affected (or only slightly so; see below). On top of the signal we find a complex pattern of lines,

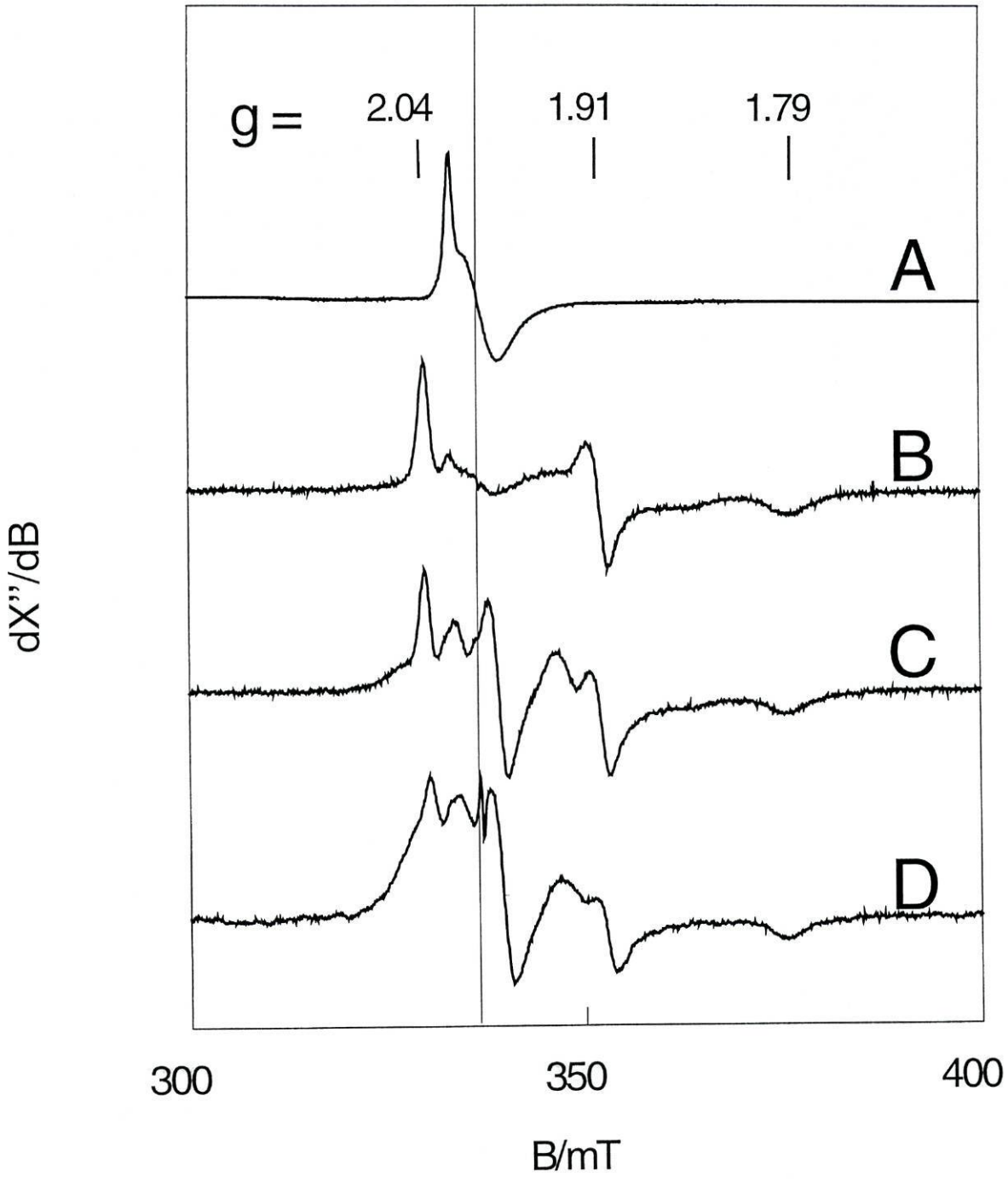

Figure 5.4 EPR spectroscopy of iron-sulfur clusters in *P. furiosus* sulfide dehydrogenase. The first three traces give an overview of redox states; the last trace illustrates temperature dependent changes. The vertical line is at the free electron g-value, g_e = 2.002 (335 mT). A: ferricyanide-oxidized protein. B: enzyme as isolated in an intermediate redox state; C: light-reduced protein. D: equivalent to trace C but taken at a higher temperature, showing that both the [2Fe-2S] signal and the [4Fe-4S] signal are lifetime-broadened but still readily detectable at 50 K. EPR conditions: microwave frequency, 9395 ±1 MHz; microwave power, 3.2 mW (trace D: 80 mW); modulation frequency, 100 kHz; modulation amplitude, 6.3 mT (trace A: 4 mT); temperature, 12, 17, 17, 50 K, respectively.

which, by exclusion, is assigned to the reduced cluster-II, a $[4Fe\text{-}4S]^{1+}$ cluster with a four-cysteine binding motif. The two sequences GxxCPxxxxCxxxC and $RCxxCx_6CxxxCP$ (cf. Figure 5.2) provide the ligands to the 3Fe and the 4Fe cluster. They can be either sequential or intertwined. The translated sequence of the α-subunit (cf. Figure 5.1) indicates that the 3Fe and the 4Fe clusters are in the same subunit and probably close in space, therefore, the unusual shape of the EPR spectrum is likely to be the result of dipolar interaction between the S=1/2 and S=2 spins of the $[4Fe\text{-}4S]^{1+}$ and the $[3Fe\text{-}4S]^{0}$ cluster, respectively. Such interaction spectra are well known for 7Fe ferredoxins (Hagen *et al.*, 1985).

The results of a redox titration in the presence of a mixture of redox dyes is presented in Figure 5.5. The experiment affords several remarkable findings. The signal of the $[3Fe\text{-}4S]^{1+}$ cluster titrates with a reduction potential, $E_{m,\,8}$ = +230 mV. This is quite an unusually high value for a 3Fe cluster (reported E_m values: -460 to + 90 mV (Hägerhäll, 1997). The [2Fe-2S] cluster titrates with $E_{m,\,8} \approx$ +80 mV an unusually high value for a non-Rieske cluster, although comparable values have been measured for the [2Fe-2S] cluster in succinate dehydrogenase or fumarate reductase (Hägerhäll, 1997). The integrated signal intensity of the fully oxidized $[3Fe\text{-}4S]^{1+}$ cluster is approximately equal to that of the fully reduced $[2Fe\text{-}2S]^{1+}$ cluster and corresponds to approximately 0.7-0.9 S=1/2 spins per heterodimer. The two high E_m-values explain why, in previous work, oxidation with excess thionine ($E_m \approx$ +60 mV) did not lead to complete disappearance of the 2Fe signal nor to the complete development of the 3Fe signal (Ma and Adams, 1994).

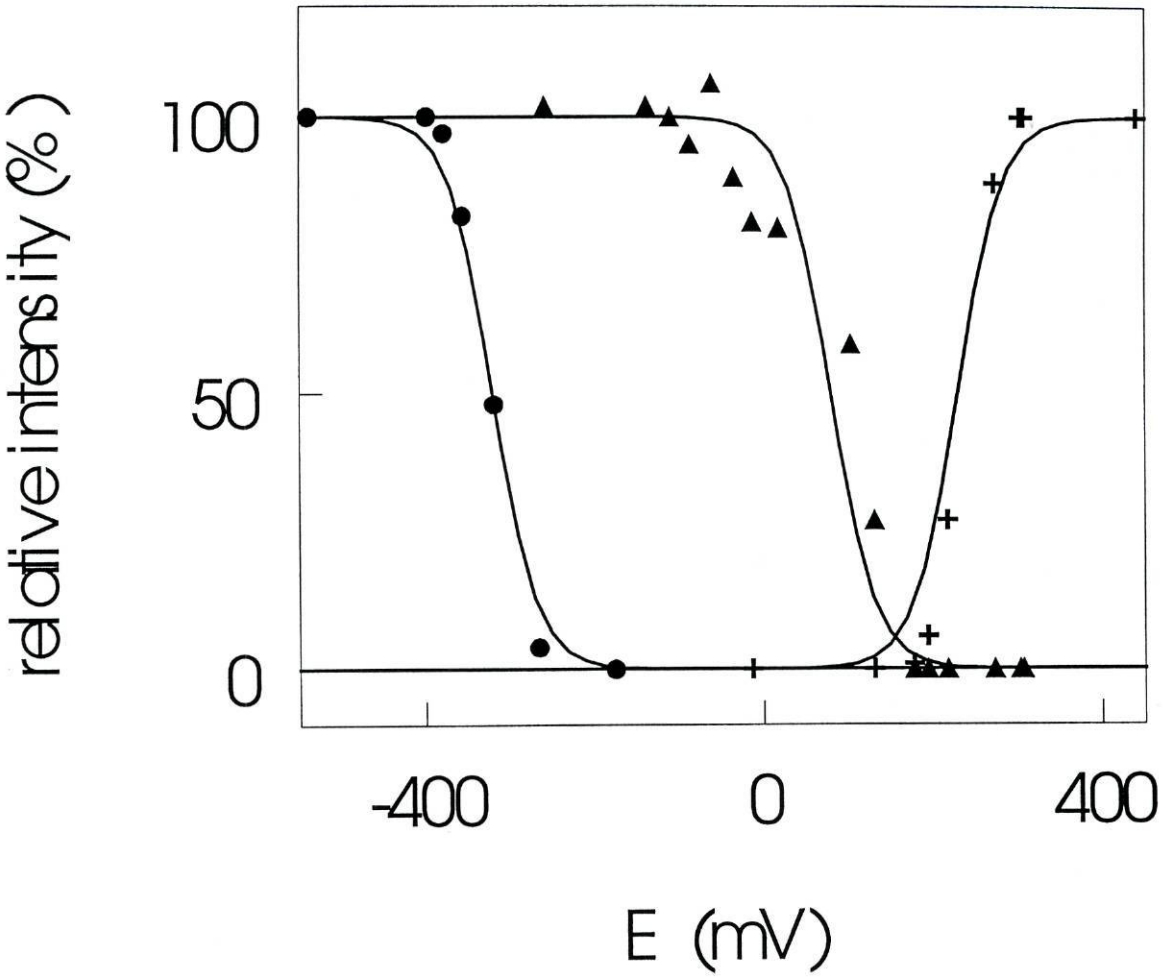

Figure 5.5 EPR-monitored redox titrations of iron-sulfur clusters in *P. furiosus* sulfide dehydrogenase. The [3Fe-4S] cluster was monitored at g_z = 2.0165 (✚) and the [2Fe-2S] cluster at g_y = 1.908 (▲). A change in the [2Fe-2S] spectrum at low potentials was followed at the satellite line with g^{eff} = 1.93 (●); its appearance is presumably related to reduction of FAD. The [4Fe-4S] cluster is not reducible with sodium dithionite.

The third signal monitored in Figure 5.5 is *not* from the third, [4Fe-4S] cluster. Upon lowering the potential the g_y line of the [2Fe-2S] signal changes value slightly from 1.908 to 1.906, and a satellite line appears at g = 1.93 (348 mT). It is the amplitude of this satellite line that is plotted in Figure 5.5. The two lines have exactly the same saturation behavior when measured at several temperatures in the range 10- 50 K (not shown). The total integrated intensity of the EPR spectrum does not change during this

redox transition. This means that we are monitoring an EPR-undetectable redox process through its effect upon the [2Fe-2S] signal shape. Since reduction of the [4Fe-4S] cluster should have lead to a doubling of the total integrated EPR intensity, we propose that we monitor here the two-electron reduction of one or both of the FAD groups. The [4Fe-4S] cluster is not reducible with dithionite, however, it is reducible with the deazaflavin/light system (cf. Figure 5.4, third trace). The total integrated intensity of this spectrum is approximately twice that of the reduced [2Fe-2S] cluster. Exactly the same spectrum is obtained when the enzyme is incubated with excess NADPH.

The temperature dependence of both the putative [2Fe-2S] signal and the putative [4Fe-4S] signal are unusual; this is illustrated in Figure 5.4, trace D. At 50 K the [2Fe-2S] signal starts to broaden. Usually, signals from [2Fe-2S] cluster, be it of the Rieske type or of the ferredoxin type, start to broaden at approximately 90 K, and they are still readily detected at 105 K. The [4Fe-4S] signal also shows some broadening at 50 K. Usually, [4Fe-4S] signals start to broaden at approximately 25 K, and they become undetectable above 45-50 K. In summary, the spin-lattice relaxation rate at elevated temperatures is unusually high for the [2Fe-2S] cluster, and it is unusually low for the [4Fe-4S] cluster.

5.7 DISCUSSION

A decade of structural studies on metalloproteins purified from archaeal hyperthermophiles has shown that their prosthetic groups do not grossly differ from those found in bacterial or eukaryal counterparts. In some details, however, bioinorganic chemistry has been enriched with novelties from the archaeal world. Examples are the di-dithioleno pterin dimer of tungsten in *P. furiosus* aldehyde oxidoreductase (Chan *et al.*, 1995) and the $[4Fe\text{-}4S]^{(2+;1+)}$ cubane with $(Cys)_3Asp$ coordination in *P. furiosus* 4Fe ferredoxin (Conover *et al.*, 1990; Hu *et al.*, 1998). The present work on *P. furiosus*

sulfide dehydrogenase adds to this list the first putative example of a [2Fe-2S] cluster with $Asp(Cys)_3$ coordination and with the combination of physico-chemical properties hitherto exclusively ascribed to Rieske-type clusters. Another new item is an apparently regular [3Fe-4S] cluster with an unusually high reduction potential. Also, the [4Fe-4S] cluster of SuDH has an unusual EPR signal and has unusual reduction properties.

However, a similar EPR signal has previously been found for a [4Fe-4S] cluster in bacterial glutamate synthase (Vanoni *et al.*, 1992), and similar unusual redox properties have been found for [4Fe-4S] clusters in mammalian dihydropyrimidine dehydrogenase (Hagen *et al.*, 2000). Since the SuDH exhibits significant sequence homology to these enzymes, it may be worthwhile to use these sequence comparisons as a starting point for the formulation of hypotheses on structural, functional and evolutionary relationships between these proteins. With reference to the comparison made in Figure 5.6 we propose that *P. furiosus* SuDH forms an archetypal iron-sulfur flavoprotein, whose subunits each are a paradigm for a separate class of these proteins. The SudB subunit carries the basic pattern found in a large class whose best known example is probably the ferredoxin plus reductase system from plants and algae. The SudA subunit carries the basic pattern found in a small class of iron-sulfur flavoproteins with iron-sulfur clusters of unusual properties, and for which crystallographic data are not yet available.

For the *P. furiosus* SudA sequence the highest homology score was found with glutamate synthase from *Pyrococcus kodakaraensis* KOD1. The structural gene for this protein was identified by Jongsareejit *et al.* using primers designed on the basis of conserved motifs in non-archaeal glutamate synthases (Jongsareejit *et al.*, 1997). Only a single gene was identified, overexpressed in *E. coli*, and purified. The resulting protein is a homotetramer from a single 53.3 kDa subunit. This complex has been identified as

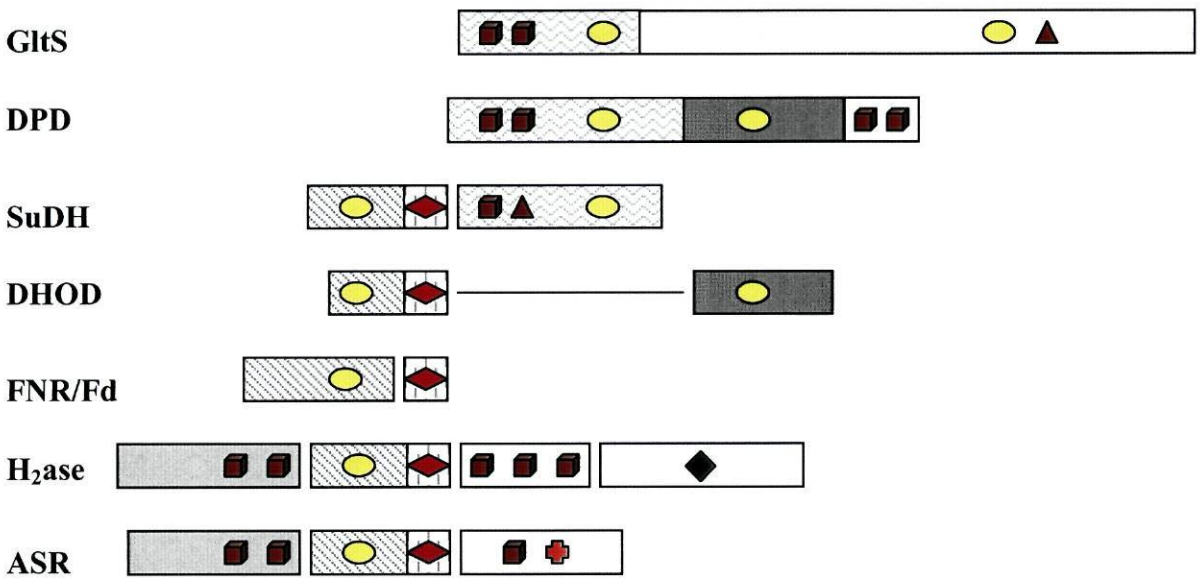

Figure 5.6 A graphical comparison of prosthetic-group binding motifs suggestively identifies *P. furiosus* sulfide dehydrogenase, SuDH, as a member of two different flavo-iron-sulfur protein 'superfamilies'. SudA is a paradigm for the GltS small subunit-like proteins (in wavy pattern), and SudB is a paradigm for the 'plant-type' reductase + ferredoxin like proteins (in diagonal stripes + vertical dash). Prosthetic groups are presented by symbols: brown cubes for [4Fe-4S], brown triangles for [3Fe-4S], red diamonds for [2Fe-2S], yellow ellipses for FAD/FMN, a dark green diamond for the Ni-Fe dimer in hydrogenase, and an orange cross for the siroheme in sulfite reductase. GltS, glutamate synthase (*Azospirillum brasilense*); DPD, dihydropyrimidine dehydrogenase (porcine liver); SuDH, sulfide dehydrogenase (*P. furiosus*); DHOD, dihydroorotate dehydrogenase (*Lactococcus lactis*); FNR, ferredoxin: $NADP^+$ oxidoreductase (Spinach); Fd, ferredoxin (Spinach); H_2ase, sulfhydrogenase (*P. furiosus*); ASR, assimilatory sulfite reductase (*Salmonella typhimurium*).

the first hyperthermophilic NADPH-dependent glutamate synthase, and it has been named KOD1-GOGAT or KOD1-GltA (Jongsareejit *et al.*, 1997). Therefore, we have tested purified *P. furiosus* SuDH for glutamate synthase activity. We have not been able to detect any such activity. This is a puzzling result, but, if anything, it indicates that assignment of function on the basis of primary structural homology only is a risky matter.

The E_m's of two of the iron-sulfur clusters of SuDH have relatively high values *per se*; it is also not clear at all how these numbers relate to any of the biological activities of the enzyme. The [4Fe-4S] cluster is not reducible with dithionite, however, this appears to be a kinetic effect because reduction is readily afforded with NADPH. Also, the putative reduction of FAD, monitored on the satellite line of the [2Fe-2S] EPR spectrum has an E_m= -320 mV, which would be in the ballpark for zero-valent sulfur reduction ($E_{m,\,7}$ = -272 mV (Hemmingsen, 1992)). The E_m's of all prosthetic groups taken together would not appear to define a particularly efficient link in a H_2-producing chain. They could, on the other hand, be compatible with catalysis of reduction of $NADP^+$ by *P. furiosus* ferredoxin (E_m = -350 mV). This is consistent with our recent conclusion, on the basis of kinetic analysis, that the physiological role of SuDH as part of a H_2-producing chain is, at best, marginal (see chapter 6.3).

All this is said realizing that working mechanisms for the different biological activities of SuDH have not been formulated yet, and that it is not clear in how far separate functions can be identified with separate subunits. Even intra-protein electron transfer pathways are not readily obvious, and the temperature-dependencies of the reduction potentials (cf. (Hagedoorn *et al.*, 1999; Hagedoorn *et al.*, 1998)) are still to be established for this intriguing enzyme complex. However, we speculate that the protein will prove to be a critical component of the novel sulfur metabolism system of *Pyrococcus furiosus* and related hyperthermophilic archaea.

6

THE MEMBRANE-BOUND HYDROGENASE

6.1 THE CURRENT MODEL OF HYDROGEN PRODUCTION BY *P. FURIOSUS*

It is known that the sulfhydrogenases from *P. furiosus* cannot use reduced ferredoxin as an electron donor, but are able to oxidize NADPH to $NADP^+$ with concomitant production of H_2 (Ma *et al.*, 2000; Ma *et al.*, 1994). The reducing equivalents produced during glycolysis and peptide fermentation are however stored in ferredoxin. It was therefore suggested that these reducing equivalents may be transferred to $NADP^+$ (thus generating NADPH) by the sulfide dehydrogenase, which can also function as a ferredoxin: $NADP^+$ oxidoreductase (Ma *et al.*, 1994). The produced NADPH is then thought to reduce hydrogenase.

However, it has been shown that the reduction, catalyzed by enzymes, of protons to H_2 by pyridine nucleotides is possible only when the partial pressure of H_2 is kept below 0.1 kPa (Schink, 1997; Stams, 1994). *P. furiosus* is however able to grow under H_2 accumulating conditions ($pH_2 \approx 30$ kPa) (Fiala and Stetter, 1986). This apparent inconsistency prompted this study on electron flow in pathways of H_2-metabolism.

The study shows the presence of a membrane-bound hydrogenase, which has been partially purified and characterized. This novel membrane-bound hydrogenase complex is able to produce large amounts of H_2 using ferredoxin as an electron donor. The results allow the formulation of a novel model of the hydrogen metabolism in *P. furiosus*.

Sapra *et al.* have recently described the solubilization and purification of a membrane-bound complex with hydrogenase activity from *P. furiosus* (Sapra *et al.*, 2000). In order to prevent contamination by cytoplasmic proteins and aggregation of the solubilized membrane proteins rather harsh extraction and purification procedures (washing the membranes extensively with a 4 M NaCl solution and addition of 2 M urea to every chromatographic buffer) were used by these authors. Solubilization and

purification apparently resulted in a heterodimeric protein with H_2 production activity from reduced artificial dyes. The authors found no H_2 production activity from reduced ferredoxin. The protein was reported to contain 4.4 Fe and to exhibit Fe/S-cluster EPR, although the sequence of the two subunits does not contain any putative iron-sulfur cluster binding motif. The results presented in this chapter argue that the subunit analysis of the membrane-bound complex isolated by Sapra *et al.* is probably not correct, and that the harsh conditions used by these authors prevented the isolation of a physiologically relevant complex.

6.2 KINETICS OF SOLUBLE SULFHYDROGENASE I AND OF SULFIDE DEHYDROGENASE I

In Table 6.1 the kinetic parameters of SuDH and the sulfhydrogenase are presented. The apparent K_m and V_{max} values of SuDH for the benzyl viologen reduction by NAD(P)H have been determined. The data are of the same order of magnitude as those published by Ma and Adams (Ma and Adams, 1994), but the K_m values for NADH and NADPH are significantly different. The V_{max} of the $NADP^+$ reduction by reduced *P. furiosus* ferredoxin is lower compared with the value reported by Ma and Adams (Ma and Adams, 1994). The sulfhydrogenase catalyzes the H_2-oxidation by $NADP^+$ about 10 times faster than the reverse reaction: the H^+-reduction by NADPH (Table 6.1). The proposed pathway from POR-reduced ferredoxin, via SuDH, $NADP^+$, sulfhydrogenase, to H_2 was also reconstituted with purified enzymes. 75 µg reduced POR (cf. Materials and Methods), 14 µM Fd, 30 µg SuDH, 0.3 mM $NADP^+$ and 10 µg sulfhydrogenase were incubated in a total volume of 1 ml. After 5 min a linear H_2 production of 58 nmol min^{-1} was observed. This is an activity of 5. 8 µmol H_2 produced min^{-1} (mg sulfhydrogenase)$^{-1}$, which indicates that the maximal specific activity of the sulfhydrogenase with NADPH as electron donor can be obtained using SuDH as a NADPH regenerating system.

Enzyme	Electron donor (mM)	Electron acceptor (mM)	Apparent V_{max}[a] (U/mg)	Apparent K_m (μM)
Sulfide dehydrogenase	Fd_{RED} (0 - 0.02)	$NADP^+$ (0.3)	3.9 ± 0.3 {8}[b]	1.8 ± 0.5 {0.7}
	Fd_{RED} (0.014)	NAD^+ (0.3)	0.7	
	NADPH (0 - 0.25)	BV (1)	355 ± 24 {263}	77 ± 13 {11}
	NADH (0 - 0.25)	BV (1)	85 ± 9 {182}	23 ± 8 {71}
	NADH (0.3)	BV (1)	16	
	NADPH (0.3)	BV (1)	144	
Sulfhydrogenase	Fd_{RED} (0 - 0.05)	H^+ (10^{-5})	0	
	NADPH (1.5)	H^+ (10^{-5})	6	
	dithionite (10)	MV (1), H^+ (10^{-5})	96	
	H_2[c]	MV (1)	420	
	H_2[c]	$NADP^+$ (1)	59	
	NADH (0.3)	BV (1)	3	
	NADPH (0.3)	BV (1)	81	

Table 6.1 Reactivity of purified sulfide dehydrogenase and sulfhydrogenase with different electron donors and acceptors. All enzyme activities were measured at pH 8.0, except in the experiments used to determine the kinetic parameters of the NAD(P)H reduction of BV catalyzed by SuDH. These experiments were performed with 50 mM CAPS buffer at pH 10.3. [a] When the electron donor concentration was varied the value is an apparent V_{max}, otherwise it is the activity at the indicated substrate concentration. Units (μmol) are the transfer of the equivalent of two electrons from the donor to the acceptor per min. [b] Data in braces were taken from (Ma and Adams, 1994) for comparison. [c] Pure H_2 was used at a pressure of 120 kPa.

6.3 WHOLE CELL ACETATE FERMENTATION AND ACTIVITIES IN H_2 METABOLISM

The activities of SuDH and sulfhydrogenase must be high enough to account for the flux of reductant observed in *P. furiosus* cells during starch fermentation. In the absence of elemental sulfur the major fermentation products in growing *P. furiosus* cells are acetate, CO_2, H_2 and alanine (Fiala and Stetter, 1986; Kengen and Stams, 1994). The maximal alanine production at a pH_2 of 60 kPa was 40% of the acetate formation (data not shown), but the formation of alanine from pyruvate (derived from starch) is neutral with respect of reductant usage/production (Kengen and Stams, 1994). Inspection of the glucose fermentation pathway shows that, for each molecule of acetate produced, four molecules of ferredoxin are reduced (Kengen *et al.*, 1996). It is therefore possible to determine the flux of reductant towards H^+ in whole cells from the rate of acetate formation during growth.

In growing *P. furiosus* cells the effect was studied of the pH_2 in the gas stream (0.17 l min^{-1} l^{-1}) on the rate of ferredoxin oxidation by H^+ reduction by measuring the acetate production. *P. furiosus* was grown at 90 °C in a 2-liter fermentor without elemental sulfur in the medium. The maximum acetate production at a pH_2 of 0, 12, 24, and 60 kPa was 0.71 ± 0.14, 0.58 ± 0.13, 0.54 ± 0.16, and 0.14 ± 0.04 µmol acetate formed min^{-1} (mg protein)$^{-1}$, respectively. These data indicate that *P. furiosus* can metabolize starch under H_2 and they confirm the observation of Fiala and Stetter (Fiala and Stetter, 1986) that *P. furiosus* is capable of growing under H_2 accumulating conditions.

The rate of acetate production at 80 °C, the standard temperature of the enzymatic assays, was 0.19 µmol min^{-1} (mg protein)$^{-1}$ (Table 6.2). The cells were grown with 100% N_2 in the gas stream. These cells were used to prepare cell-free extracts. Based on the acetate production, the activity of the enzymes involved in the disposal of

substrate(s) or reductant	activity (product formed min^{-1} mg $protein^{-1}$)	Enzymes involved
starch	0.19 ± 0.04 µmol acetate	whole cells
pyruvate, CoASH	4.0 ± 0.3 µmol MV_{SQ}	Cell extract: POR
NADPH	0.02 ± 0.003 µmol H_2	Cell extract: sulfhydrogenase
H_2 (120 kPa)	0.12 ± 0.02 µmol NADPH	Cell extract: sulfhydrogenase
Fd_{RED}	0.62 ± 0.08 µmol H_2	Cell extract: hydrogenase
Fd_{RED}	0.14 ± 0.01 µmol NADPH	Cell extract: hydrogenase, SuDH, sulfhydrogenase

Table 6.2 Comparison of whole cell acetate formation with cell-free extract activities of enzymes involved in the H_2-metabolism at 80 °C. The enzyme activities were measured at 80 °C and are the average of at least three experiments. Starch catabolism is a whole cell activity. In cell extracts the substrates and/or cofactors necessary to detect the indicated enzyme activity were present in the assay mixture.

catabolically generated reductant as H_2 must be at least 0.38 µmol electron-pairs min^{-1} (mg cell protein)$^{-1}$ (Table 6.2). The maximal activity of POR, a key enzyme of the glucose fermentation pathway, was found to be high enough. The rate of NADPH formation with reduced ferredoxin, an activity catalyzed by SuDH, is about the same as the observed disposal rate. However, the activity of the second enzyme in the proposed pathway, the sulfhydrogenase catalyzing the H_2 production with NADPH as electron donor, is only 5% of the disposal rate (0.02 versus 0.38 µmol H_2 min^{-1} mg $protein^{-1}$). The activity of the sulfhydrogenase in this reaction in cells is clearly too low to support acetate formation. Surprisingly, the overall reaction from reduced ferredoxin to H_2 is

catalyzed at a rate of 0.62 units mg protein^{-1}. This rate even exceeds the estimated rate of catabolically generated reductant. Since the soluble sulfhydrogenase shows no activity with ferredoxin, another hydrogenase system must be active in the cells.

6.4 MEMBRANE-BOUND HYDROGENASE ACTIVITY.

Fractionation of the cell extract demonstrated that the ferredoxin-dependent hydrogenase activity was associated with the cytoplasmic membranes. The apparent K_m for ferredoxin is 36 ± 7 μM. Surprisingly, the membranes showed a very low H_2-oxidation activity with 1 mM methyl viologen or 20 μM oxidized *P. furiosus* ferredoxin as acceptor. When combined with the soluble sulfhydrogenase I an effective NADPH producing system can be reconstituted (Figure 6.1 and Figure 6.2). Both hydrogenases

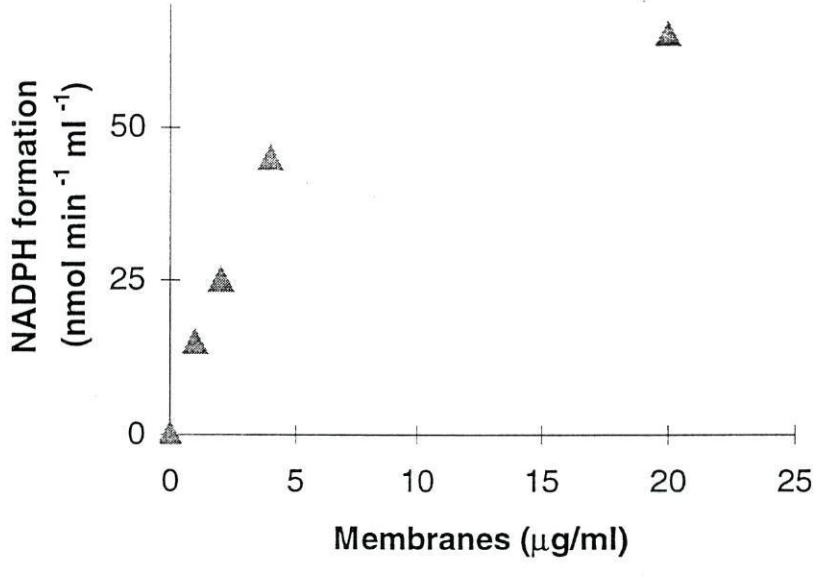

Figure 6.1 Reduction of $NADP^+$ by the joint activities of sulfhydrogenase I and the membrane-bound hydrogenase. The membrane-bound hydrogenase was reduced by *P. furiosus* ferredoxin (14 μM) was generated with POR (75 μg ml^{-1}). The sulfhydrogenase was activated in 20 min at 80°C under an H_2 atmosphere. Sulfhydrogenase concentration is constant and equal to 1 μg/ml.

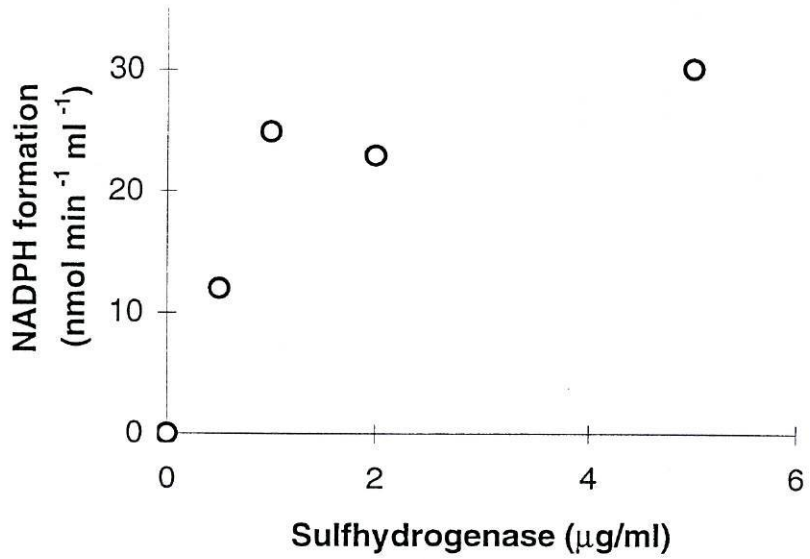

Figure 6.2 NADPH production by the joint activities of sulfhydrogenase I and the membrane-bound hydrogenase. Membrane protein concentration is constant, and equal to 2 μg membrane protein /ml.

are necessary for the reduction of $NADP^+$ by reduced ferredoxin. In both cases, the maximal activity of each hydrogenase was obtained when the other hydrogenase was present in excess. It is therefore possible that the soluble hydrogenase might function primarily as an energy-saving device, by recovering the high-energy electrons eliminated as H_2. The ability to reduce $NADP^+$ with H_2 thus allows the organism to have an additional source of electrons for regeneration of NADPH when other pathways are not functional.

6.5 PURIFICATION

After cell lysis a significant amount of H_2-production activity is found in the membrane fraction of *P. furiosus*. This activity remains even after extensive washing (2 times 60 min at 200, 000 × g) indicating that the enzyme responsible is firmly associated with the membrane. The activity remains largely associated with the membrane after treatment with Triton X-100, but it can be solubilized by incubating the membranes with 2 % sodium deoxycholate. Long exposure to deoxycholate however, leads to loss of activity. Therefore the protein was immediately precipitated with 25 % ammonium sulfate, which is enough to precipitate >90% of the solubilized membrane proteins and leads to minimum precipitation of soluble proteins still remaining in the sample. The pellet was resuspended in 0.1% Triton X-100 containing buffer and dialyzed in order to remove sodium deoxycholate and ammonium sulfate. The results of a typical purification are shown in Table 6.3.

Step	Protein (mg)	Activity (U)	Sp. act. (U/mg)	Purification (fold)	Recovery (%)
Membrane extract	1936	880	0.45	1.0	100
DOC extraction	1128	730	0.65	1.4	83
Q-Sepharose	157	280	1.78	3.9	32
Hydroxyapatite	32	135	4.18	9.2	15

Table 6.3 Purification of the membrane-bound hydrogenase from *P. furiosus*. The core complex was purified from 100 g cells (wet mass).

We have consistently found membrane-associated hydrogenase activities one order-of-magnitude less than those reported by Sapra *et al.* (Sapra *et al.*, 2000). These values are not due to lower amounts of hydrogenase in our membrane preparations: the purified core complex also has an activity (4.18 U mg^{-1}) one order-of-magnitude less

than that reported by Sapra *et al.* (30 U mg^{-1}), although the protein recoveries and purification factors are very similar (cf. Table 6.3 with Table 2 in (Sapra *et al.*, 2000)). Also the H_2 evolution rate by sulfhydrogenase I and the H_2 evolution / H_2 uptake ratio reported by these authors are about ten times greater than the values determined by us (see below). It has been previously argued (Pierik *et al.*, 1992) that the hydrogen-production assay is very sensitive to changes in pH, electron donor concentration, buffer composition, manometric vs. gas chromatography detection, etc. It is therefore possible that these differences arise from unreported differences in the method used.

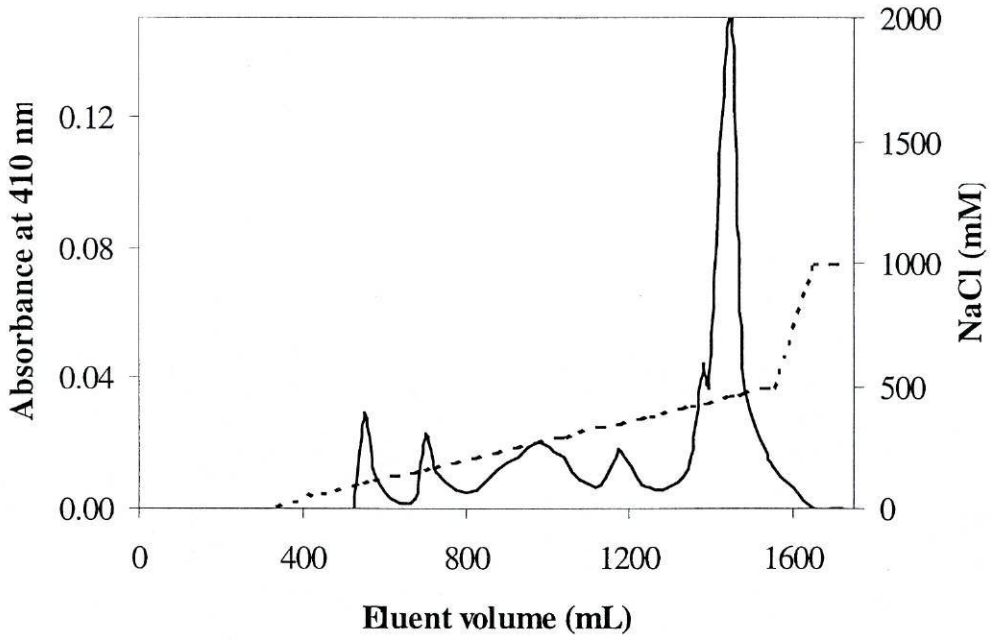

Figure 6.3 Ion-exchange chromatography of solubilized membrane proteins on a Source Q column (volume=300 mL). Membrane-bound hydrogenase is the last protein to elute.

6.6 SEQUENCE ANALYSES

A TBlastN search with the large subunit of *E. coli* hydrogenase-2 revealed three open reading frames in the *P. furiosus* genome with a high similarity score. One of these three sets of genes belongs to the gene cluster encoding the soluble sulfhydrogenase (Pedroni *et al.*, 1995) and the other to soluble sulfhydrogenase II (Ma *et al.*, 2000). The third detected open reading frame encodes a protein very similar to the large subunits of some membrane-bound hydrogenase. Using a combination of codon usage analysis and ORF searches, a total of 14 contiguous genes were detected in this putative operon (Figure 6.4 and Table 6.4). The operon has been recently identified by Sapra *et al.* to encode the membrane-bound hydrogenase of *P. furiosus*; it has been named *mbh* (Sapra *et al.*, 2000).

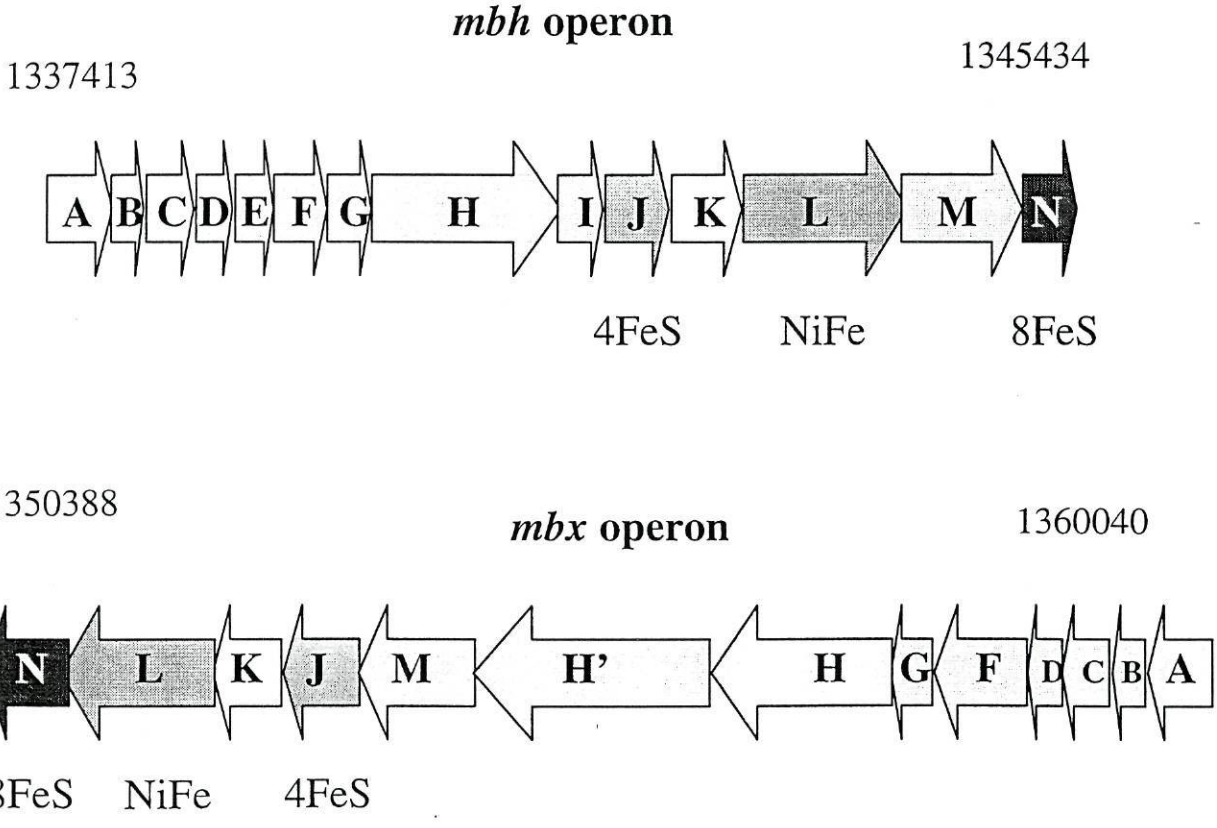

Figure 6.4 Organization of the putative operons in the genome of *P. furiosus* containing the genes that encode the membrane-bound hydrogenase and its "mirror" complex. The single-letter names of the open reading frames in the *mbx* operon indicate their high similarity with orfs in the *mbh* operon.

Gene (ortholog in *E. coli* complex I)	Translation product: Size (aa)	Translation product: Size (Da)	Predicted pI	Membrane-spanning helices
mbhA	167	18736	6.6	3
mbhB	84	9060	5.9	3
mbhC	124	13504	9.6	3
mbhD	96	10413	8.1	3
mbhE	99	11140	4.8	2
mbhF	148	15518	9.9	4
mbhG	117	12773	9.4	3
mbhH (nuoL)	510	54980	8.9	14
mbhI	115	13043	6.7	2
mbhJ (nuoB)	167	18284	6.0	0
mbhK (nuoC)	173	20184	5.0	0
mbhL (nuoD)	427	47934	6.6	0
mbhM (nuoH)	321	35388	9.5	8
mbhN (nuoI)	139	15686	8.7	0

Table 6.4 Predicted properties of the subunits of the membrane-bound hydrogenase from *P. furiosus*.

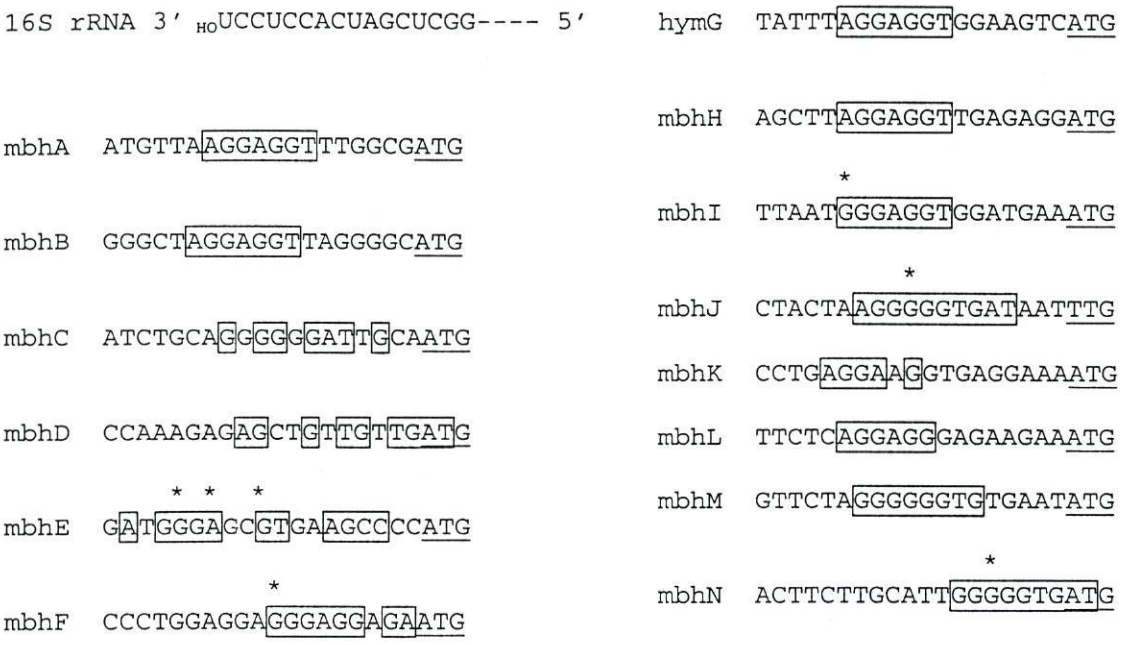

Figure 6.5 Ribosome-binding regions preceding the open-reading frames in the *mbh* operon. In each case, the initiation codon is underlined. Boxed regions are the ribosome-binding sites, complementary to the 3´end of 16S rRNA from *P. furiosus*. Nucleotides marked with * participate in G: U base pairing.

All of these genes are preceded by ribosome-binding regions, as shown in Figure 6.5. Several subunits show high similarity to subunits from the CO-induced hydrogenase from *R. rubrum* (Fox *et al.*, 1996b), hydrogenase-3 (Böhm *et al.*, 1990) and –4 (Andrews *et al.*, 1997) from *E. coli*, the Ech hydrogenase from *Methanosarcina barkeri* (Künkel *et al.*, 1998; Meuer *et al.*, 1999), and two putative membrane-bound hydrogenases from *Methanobacterium thermoautotrophicum* (Tersteegen and Hedderich, 1999). Striking homology is also observed with subunits of proton-translocating NADH: quinone oxidoreductase (complex I) from many sources. Below, comparison with complex I subunits is made with reference to the *nuo* operon (NADH: ubiquinone oxidoreductase) of E. coli (Leif *et al.*, 1995; Weidner *et al.*, 1993).

A very similar operon (13 contiguous genes) is present ca. 6 kbp downstream of *mbh*. As with the membrane-bound hydrogenase operon, all of these genes are preceded by ribosome-binding regions, as shown in Figure 6.6, suggesting that this putative operon is also transcribed. We have named this operon *mbx* (Figure 6.4, and see below).

Figure 6.6 Ribosome-binding regions preceding the open-reading frames in the *mbx* operon. In each case, the initiation codon is underlined. Boxed regions are the ribosome-binding sites, complementary to the 3′end of 16S rRNA from *P. furiosus*. Nucleotides marked with * participate in G:U base pairing.

6.7 DESCRIPTION OF THE MBH GENE PRODUCTS.

MbhA-G and MbhI. These putative gene products present no relevant similarities to any purified proteins, however the usage of "preferred codons" in these ORFs is close to the average in identified *P. furiosus* proteins. Furthermore, the prediction of membrane-spanning helices in all of these ORFs would be unlikely if they were mere statistical artifacts. Very close homologues exist in the genomes of *Pyrococcus horikoshii* (*mbhACEFGI*), *Pyrococcus abyssi* (*mbhABCEFGI*) and *Thermotoga maritima* (*mbhABG*). These subunits may have a role in anchoring the complex to the membrane.

MbhH. This subunit shows 28% identity and 44% similarity to the CooM subunit of the CO-induced hydrogenase from *R. rubrum*. A similar level of homology is found with the B subunit of hydrogenase-4 from *E. coli*. The function of these subunits is unknown. MbhH is also homologous to NADH dehydrogenase NuoL (*E. coli* labeling (Leif *et al.*, 1995; Weidner *et al.*, 1993)) chains from many organisms.

MbhJ. The translated protein sequences of *mbhJ-N* are given in Figure 6.8. Unlike the other ORFs (which use ATG as the start codon) *mbhJ* is predicted to start with TTG (cf. Figure 6.5). The gene encodes a protein with high similarity to the small subunits of the CO-induced hydrogenase from *R. rubrum*, hydrogenases-3 and –4 from *E. coli* and to the Ech hydrogenase from *M. barkeri* (Künkel *et al.*, 1998). It is considerably shorter than most small subunits from Ni-Fe hydrogenases, but it contains the four conserved cysteine residues predicted to bind the "proximal" Fe-S cluster (Albracht, 1994) (Figure 6.7).

MbhK. MbhK shows moderate homology to the N-terminal of HyfG (large subunit of hydrogenase-4 from *E. coli*) and to NADH dehydrogenase NuoC chains. The level of homology is much lower than that observed for MbhH.

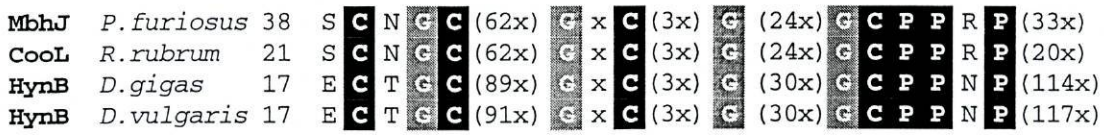

Figure 6.7 Sequence comparisons of iron-sulfur cluster binding motifs in *P. furiosus* membrane-bound hydrogenase "small" subunit. The putative [4Fe-4S] cluster motif of *P. furiosus* MbhJ and of *R. rubrum* CooL (Fox *et al.*, 1996b) are compared to a similar $(Cys)_4$-containing motif in typical Ni-Fe hydrogenase small subunits *viz.* from *Desulfovibrio vulgaris* Miyazaki F (Deckers *et al.*, 1990) and from *D. gigas* (Voordouw *et al.*, 1989).

MbhL. Analysis of the deduced MbhL protein sequence indicates moderate similarity to the large subunit of some Ni-Fe hydrogenases. The closest identified protein sequence is EchE, the large subunit of the Ech hydrogenase from *M. barkeri*. Alignment of the two sequences shows 41 % identity and 59 % similarity. The protein is more closely related to NuoD subunits of complex I of various organisms than to subunits of other Ni-Fe hydrogenases, however all four cysteines involved in the coordination of the active site Ni-Fe cluster are present.

MbhM. MbhM shows high homology to CooK from the CO-induced hydrogenase from *R. rubrum*, HycD and HyfC from *E. coli* hydrogenase-3 and –4, respectively, and to the NADH dehydrogenase NuoH subunit from several organisms, which have been proposed to be the site of proton translocation and energy coupling (Yagi, 1987; Yagi and Hatefi, 1988). The high number of strictly conserved charged residues present in these proteins (cf. Figure 6.8) argues in favor of such a role.

MbhN. This subunit is similar to CooX from the CO-induced hydrogenase from *R. rubrum* and to the complex I NuoI subunit from several organisms. The sequence comparisons show two conserved, canonical, ferredoxin-like CxxCxxCxxxCP motifs

MbhJ

```
0     LTNNSERKRL EKRIAQLCKF IGRSPWVFHV NSGSCNGCDI EIIAALTPRY
50    DAERFGVKLV GSPRHADILL VTGPVTNQSL ERVKLVYEQT PDPKIVIAIG
100   ACPTGGSVFY ESPFTNAPLD RIIPVDVFVP GCPPRPEAIL HGVVLALEKL
150   AKMIKGEVPP EEGEENE
```

MbhK

```
0     MSKAEMVANK IKERFPNAEV VVKTNKWGRE RVWVRISREE YKELMKFIRE
50    LDPEAHYSIG IEQDWGDELG FLNHILLFYD EPPGVSLLID VHAPKDNPVL
100   PDTSDIFPIS LQFEREGMEM VGLDFEGAPD KRRLFLPDDF PEGIYPLRTD
150   EKGVPEEMVK NAGHPYLLRR EKK
```

MbhL

```
0     MKKVEYWVKI PFGPIHPGLE EPEKFIITLD GERIVNVDVK LGYNLRGVQW
50    IGMRRNYVQI MYLAERMCGI CSFSHNHTYV RAVEEMAGIE VPERAEYIRV
100   IVGELERIHS HLLNLGVVGH DIGYDTVLHL TWLARERVMD VLEAVSGNRV
150   NYSMVTIGGV RRDIGEKQKR LILDMIKYYR EVLPQIEDVF LHDSTIEARL
200   RDVAVVPKKL AIEMGAVGPT ARGSGIKEDS RWSEQLGVYP DLGIKPVTPE
250   DVTGEKARGD VYDRMAVRIG ELWMSLDLLE HALDQMPEGK IKTFPKDNIL
300   VAKLKLLGDG EGIGRYEAPR GELVHYVRGQ KGRDGPVRWK PREPTFPNLF
350   TIAKALEGNE LADLVVAIAS IDPCLSCTDR VAIVKEGKKV VLTEKDLLKL
400   SIEKTKEINP NVKGDPTPTG IGCSRGV
```

MbhM

```
0     MKIVYGVIGL ILIYIYVSVV SLLFSGIDRK LVARMQRRIG PPILQPFYDF
50    LKLMSKETII PKTANFMFKA APILMLATVI ALLAYTPLGF PPIFGTKGDI
100   IVFIYLLTLA DFFLVVGVMS SGSPYGRIGA ARGIALLVSR EPAMMLGVFA
150   VMWAISKLGV EKPFSLSSLY EHTIWDFGPV AWVAGVVLIY VFMAWLASEI
200   EVGFFNIPEA EQEIAEGTLV EYSGRYLGII KLAESIKEFI AASLVVAVLF
250   PWQLNIPGVQ GYLINLLLHT LKVFIVLLVS KTIFRTITGR LKISQAVNLL
300   WTRVFTASVI GALLLALGVM L
```

MbhN

```
0     MIRLPLLPTV IKNLFKKPAT NPFPKTEPVP VPEDFRGKLV YNVDKCVGCR
50    MCVTVCPAGV FVYLPEIRKV TLWIGRCVMC KQCVDVCPTA ALQMSDEFLL
100   ASYDKYDAKL IYLTPEEAED IKKKLEEANK AKAEKQASK
```

Figure 6.8 Amino acid sequences of the Mbh JKLMN subunits. N-termini identified by Edman degradation in MbhK and MbhL are underlined; predicted membrane-spanning helices in MbhM are boxed; charged residues in MbhM that are conserved in other membrane-bound hydrogenases and complex I proteins are shown in bold (italic denotes conservation only within hydrogenases); metal-coordinating cysteine residues are shaded; the highly conserved [4Fe-4S] cluster binding-motifs in MbhN are underlined.

strongly suggesting the presence of two regular [4Fe-4S] cubane clusters in this subunit. A T-rich region (possibly a transcription termination signal) is present 6 bp downstream from the stop codon of this subunit.

An additional lone open-reading frame is present 121 bp downstream from the stop codon of *mbhN*. The C-terminal of this ORF shows 43% similarity (22% identity) to 3-phosphoadenosine-5-phosphosulfate (PAPS) sulfotransferase from *Synechocystis* sp.. The key KXECG(I/L)H conserved amino-acid cluster involved in the catalysis (Berendt *et al.*, 1995) is however absent. It is unlikely that this ORF belongs to the membrane-bound hydrogenase gene since all other subunits are consecutive or even overlapping. The absence of a ribosome-binding site in the sequence just upstream of the starting codon and the possible transcription termination signal after *mbhN* give credence to this hypothesis.

Assuming 1:1 stoichiometry of all 14 subunits, the assembled complex is expected to have a molecular mass of 297 kDa and to contain three [4Fe-4S] clusters and one dinuclear [NiFe] cluster.

6.8 N-TERMINAL SEQUENCING.

The N-terminal sequences of two subunits of the partially purified membrane-bound hydrogenase were determined after they were separated by SDS-polyacrylamide electrophoresis. These are as follows (where X is an unknown residue) : M K K V E Y W V K I P F G P I H P G L E E P E K F I I T L D- and K A E M V A N K I X E R F P N A E V V V G D N . The first sequence corresponds exactly to the N-terminal of the MbhL subunit, the Ni-Fe-cluster containing "large" subunit. The second sequence is almost identical (two misidentified amino-acids) to the N-terminus of MbhK (cf. Figure 6.8). Several other subunits were apparent in the gel. Some of those were too close to be excised without contamination from neighboring bands. The N-terminal sequencing of four of these proteins showed sequences that are not present in the proposed membrane-bound hydrogenase operon. A search of the available genome using these N-terminal as probes, allowed confirmation of their origin as contaminating *P. furiosus* proteins. One is a putative leucine-responsive element, and the other three have no homology with any protein with an established function.

6.9 ENZYMOLOGY.

6.9.1 General properties

Hydrogen formation was assayed with dithionite-reduced methyl-viologen as an electron donor. This activity was found to be insensitive to a three-hour O_2-exposure of the sample and to have a pH optimum around 6.8. The characteristics of the membrane-bound hydrogenase have proven to be quite interesting. Even though the enzyme appears to be an Ni-Fe hydrogenase based on its large-subunit sequence, its properties differ significantly from those of most other Ni-Fe hydrogenases. The ratio of H_2 evolution activity to H_2 uptake activity in crude extracts, as well as in the partially purified enzyme, is very large compared to that of other enzymes. Most Ni-Fe hydrogenases favor H_2 uptake over evolution and exhibit an H_2 evolution/H_2 uptake ratio of much less than unity. The 250:1 ratio of evolution to uptake for the *P. furiosus* enzyme (measured at pH 7.4) is one order of magnitude larger than the one observed for the membrane-bound hydrogenase from *Hydrogenovibrio marinus*, the most extreme ratio observed so far (Nishihara *et al.*, 1997). H_2-uptake activity does not show a significant increase at physiological pH when using benzyl viologen instead of methyl viologen as electron acceptor.

The isolated core complex was able to evolve H_2 from reduced *P. furiosus* ferredoxin (Figure 6.9). H_2 evolution did not occur if POR, ferredoxin or purified hydrogenase were absent. Under the conditions used the activity increased linearly with the amount of ferredoxin.

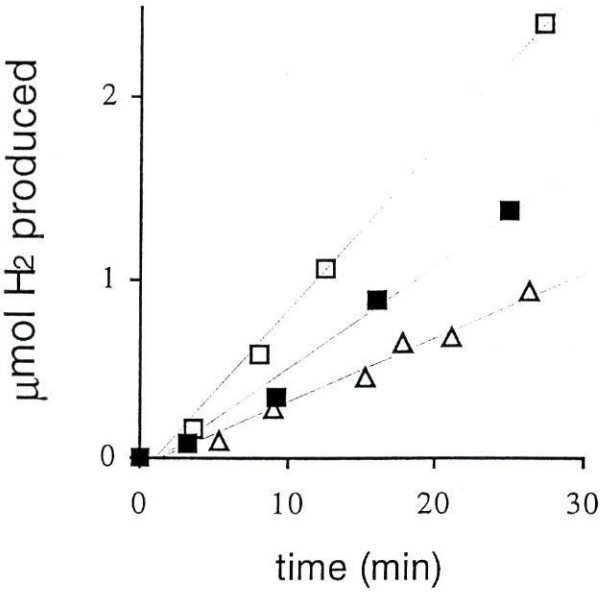

Figure 6.9 H_2 evolution from ferredoxin-reduced Mbh-core complex. (Δ) 7 nmol Fd; (■) 10 nmol FD; (□) 20 nmol Fd. Ferredoxin was reduced *in situ* by the POR system (10 mM pyruvate, 1 mM $MgCl_2$, 0.9 mM CoASH, 0.9 mM dithiothreitol, 60 µg POR), and H_2 evolution was measured by gas chromatography. The purified hydrogenase complex was 170 µg protein/ml.

6.9.2 CO inhibition.

Most hydrogenases are extremely sensitive to inhibition by CO. H_2-evolution by the Mbh hydrogenase is however only slightly inhibited by CO. The inhibition curve shows approximately 40 % inhibition at 100 % CO (≈ 860 µM), whereas, *e. g.* , the *D. gigas* enzyme is 50 % inhibited with only 35 µM CO. This membrane-bound hydrogenase thus joins the soluble sulfhydrogenase from *P. furiosus* (Bryant and Adams, 1989), the CO-induced hydrogenase from *R. rubrum* (Fox *et al.*, 1996a) and the soluble hydrogenase from *Ralstonia eutropha* (Schneider *et al.*, 1979) in the restricted group of CO-tolerant hydrogenases. A possible physiological relevance of this is not evident, since no reports on the metabolism of *P. furiosus* mention a role of CO. On the other hand, since H_2 and CO are predicted to bind at the same site, it is possible that the

low affinity for CO is simply a reflection of the low affinity of the membrane-bound hydrogenase for H_2.

6.10 INHIBITION BY DCCD.

N, N'-dicyclohexylcarbodiimide, DCCD, is a covalently carboxyl-modifying reagent that attacks specifically acidic amino-acids in hydrophobic domains (Solioz, 1984). It has been shown to inhibit the methyl-viologen-dependent H_2-evolution by the CO-induced hydrogenase from *R. rubrum* (Fox *et al.*, 1996a). The similarity of this hydrogenase to the membrane-bound hydrogenase from *P. furiosus* suggested that the latter might also be inhibited by DCCD. Indeed, upon pre-incubation of the protein at room temperature in the presence of DCCD a significant decrease of the activity was

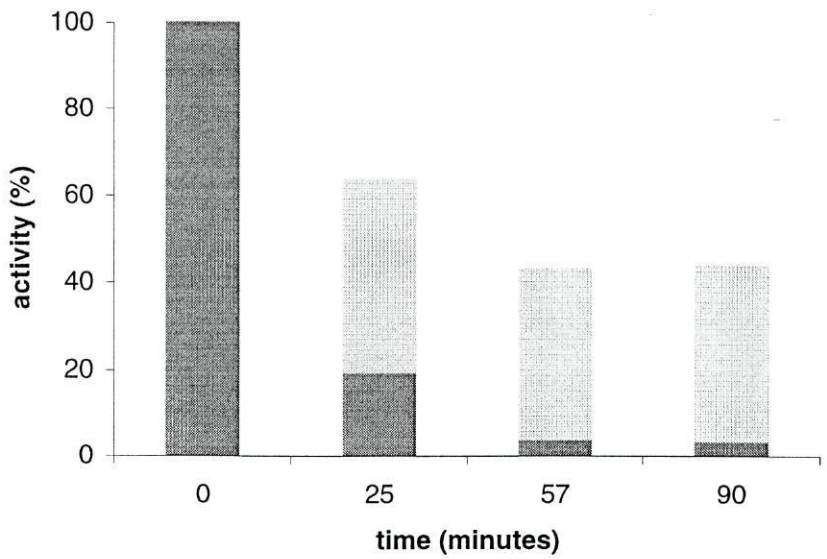

Figure 6.10 Effect of DCCD on the H_2-evolution activity in *P. furiosus* membranes. Dark gray: membranes incubated with 1.25 mM DCCD (10 µl of a 50 mg/ml solution in ethanol) at 80 °C; Light gray: membranes incubated with ethanol (10 µl) at 80 °C.

observed. Moreover, incubation of the protein in the presence of DCCD at 80 °C leads to a much faster and more drastic inactivation (Figure 6.10), possibly due to increased accessibility of the relevant amino acids as a result of increased backbone flexibility.

The likely target for inhibition by DCCD is MbhM, which is similar to the *R. rubrum* CooK and to the subunit 1 family of NADH dehydrogenase (complex I). Proteins of this family are probably involved in proton translocation and energy coupling (Yagi, 1987; Yagi and Hatefi, 1988), and have been shown to be inhibited by DCCD. It is likely that MbhM is also involved in similar processes. The membrane-bound complex is quite thermostable (with a half-life at 80 °C of approximately 3 hours) which rules out the possibility that the faster decrease in activity upon incubation with DCCD at 80 °C is due to protein denaturation. The isolated core complex is significantly less thermostable, with a half life at 80 °C of only 35 minutes, which suggests that some of the subunits lost during the purification may have a role in protecting the protein against denaturation. The isolated core complex is also susceptible to inhibition by DCCD.

6.11 EPR SPECTROSCOPY.

From +200 mV to –250 mV (vs. SHE) no signals were detected in the Mbh hydrogenase by EPR spectroscopy. Upon reduction of the protein to potentials below –300 mV (vs. SHE) redox equilibrium proved impossible to attain. This is probably due to H^+ reduction by the hydrogenase, as observed with other hydrogenases (Pierik *et al.*, 1992). At these potentials, a weak signal characteristic for two interacting [4Fe-4S] clusters (Mathews *et al.*, 1974) was observed. Reduction of the hydrogenase with excess dithionite at room temperature in the absence of redox mediators allowed the observation of this signal with a significantly higher intensity (Figure 6.11).

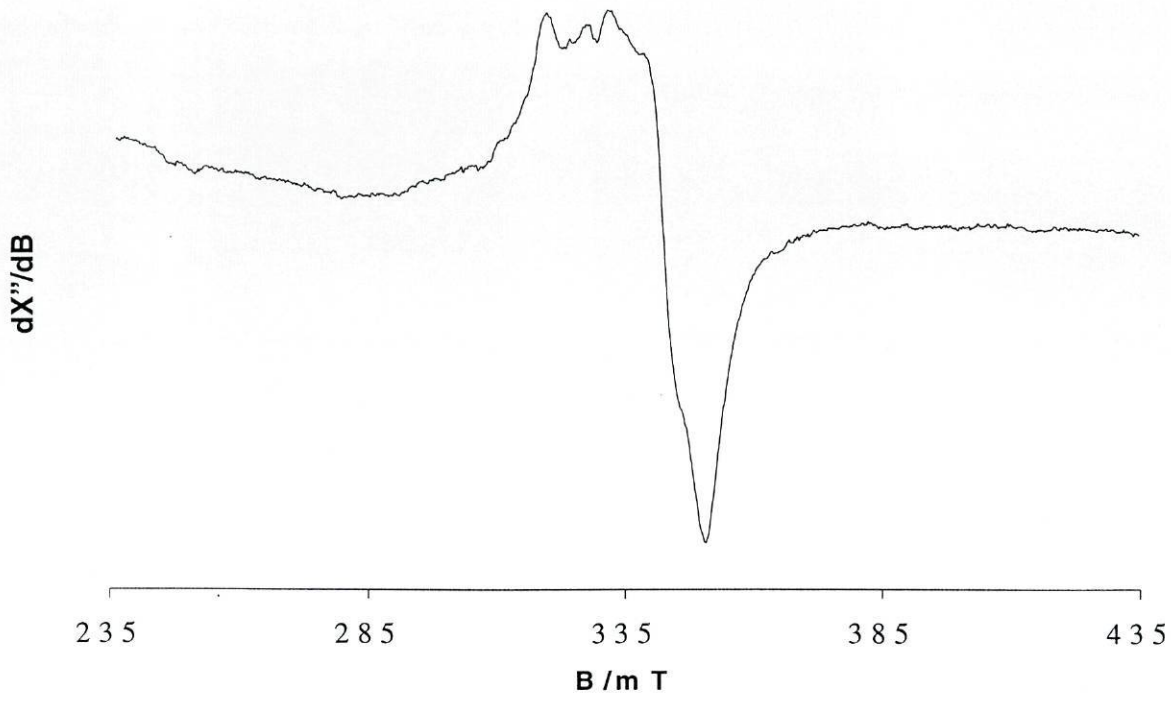

Figure 6.11 EPR spectrum of dithionite-reduced Mbh hydrogenase core complex from *P. furiosus*. The sample contained 34 mg/ml hydrogenase in 20 mM Tris/HCl, pH 8.0. The conditions of the measurement were: microwave power: 50 mW; microwave frequency, 9.22 GHz; temperature, 19 K.

The higher stability of the signal under these conditions is probably due to the low H_2-production activity from dithionite in the absence of redox mediators. No additional signals were detected upon reduction of the protein with deazaflavin and light. The signal disappeared upon anaerobic incubation of the protein at 60 °C, which is consistent with the clusters putative role in relaying electrons to the active site in order to reduce protons to H_2. In spite of the inability to obtain a fully reduced sample in the redox titration, comparison of the results obtained with a dithionite-reduced sample allowed the estimation of a potential of approximately –0.33 V for the reduction of the two interacting clusters, i. e. within the usual potential range for these centers.

6.12 A PUTATIVE FOURTH HYDROGENASE IN *P. FURIOSUS*

Using the MbhL amino-acid sequence as a probe, a fourth hydrogenase-containing operon was found in the genome of *P. furiosus* about 6 kbp downstream from the *mbhABCDEFGHIJKLMN* operon (see Figure 6.4). Like the membrane-bound hydrogenase, this complex is expected to coordinate three [4Fe-4S] clusters. Almost every subunit in this operon is more similar to the corresponding subunit in the *mbh* operon than to any other known protein (except homologs in other *Pyrococcus* species).

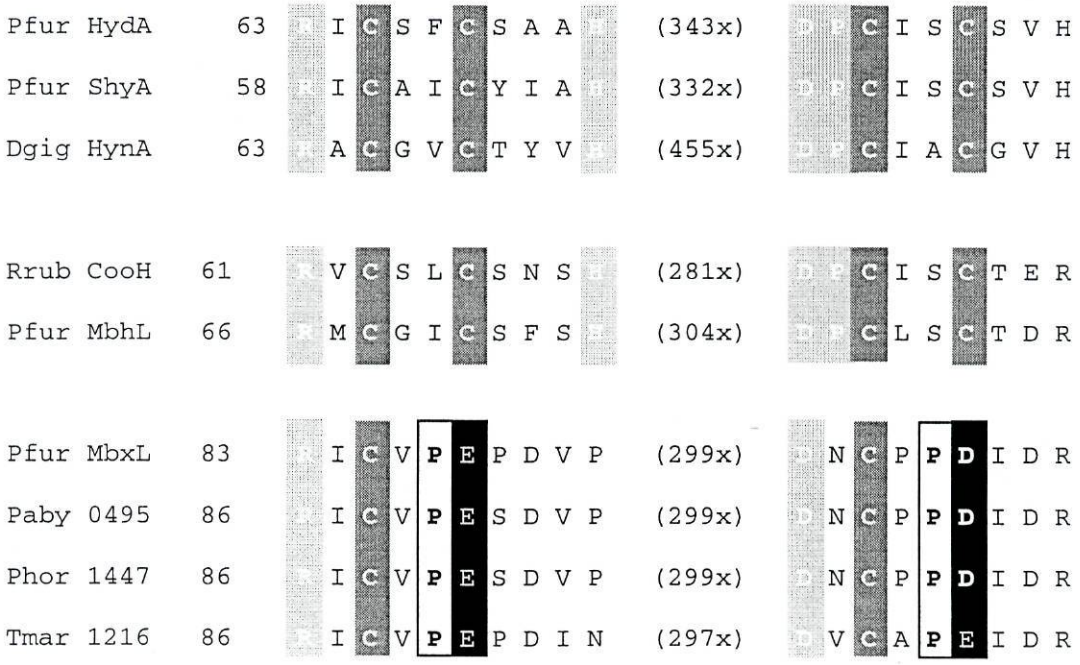

Figure 6.12 Sequence comparisons of the Ni-Fe cluster binding motifs in *P. furiosus* membrane-bound hydrogenase "large" subunit MbhL and in MbxL with the well-characterized Ni-Fe binding motifs in Ni-Fe hydrogenase "large" subunits from *R. rubrum* (Fox *et al.*, 1996a), *Desulfovibrio gigas,* (Deckers *et al.*, 1990; Volbeda *et al.*, 1995) and *P. furiosus* sulfhydrogenases I (Pedroni et al., 1995) and II (Ma *et al.*, 2000), and with genes in *P. abyssi* (PAB0495), *P. horikoshii* (PH1447), and *T. maritima* (TM1216).

However, in MbxL (the homologue to the hydrogenase large subunit) the Ni-Fe binding motif deviates from the commonly observed consensus (see Figure 6.12): in

each of the two Ni-Fe coordinating CxxC motifs the second cysteine (which normally provides the ligands bridging between the nickel and the iron ions) is replaced by an acidic residue. Additional proline residues are also present in the motifs. These residues may have a role in distorting the polypeptide chain in order to allow metal coordination by the carboxylato residues. The putative carboxylato-bridged NiFe cluster is not unique to *P. furiosus*. Genes coding for similar binding motifs are also present in the genomes of *P. abyssi, P. horikoshii,* and *T. maritima* (Figure 6.12).

6.13 DISCUSSION

The genome of the archaeal *P. furiosus* has four different and separate open reading frames with significant homology to the large subunit of well characterized bacterial Ni-Fe-hydrogenases: *hydA* (Pedroni *et al.*, 1995), *hydP/shyA* (Ma *et al.*, 2000), (see also 5.4), *mbhL*, and *mbxL*. The first two each encode a Ni-Fe-cluster carrying α-subunit of an αβγδ-heterotetrameric soluble sulfhydrogenase, i. e. a complex iron-sulfur flavoprotein with both sulfur reductase and hydrogenase activity (Ma *et al.*, 2000; Pedroni *et al.*, 1995). The expression product of the third orf, *mbhL*, is presumably part of a very different complex, namely a large, multisubunit transmembrane system, which we hypothesize to act as an energy transducing system coupled to proton-based respiration. This hypothesis is presently based on the following still limited information: the essentially unidirectional nature of the hydrogenase as a 'hydrogen synthase', the inhibition of this activity by DCCD, the predicted extensive membrane spanning of the product of the *mbhA-N* operon, and the homology of individual subunits, in particular MbhM, to subunits of the proton-translocating NADH: Q oxidoreductase complex. Several multi-subunit membrane-bound hydrogenases with high similarity to NADH: quinone oxidoreductase have been proposed previously to be involved in energy transduction under certain growth conditions. Proton translocation has been

suggested to occur through the CO-oxidizing, H_2 producing complex of *R. rubrum* when grown CO-dependent in the dark (Fox *et al.*, 1996a). The H_2-evolution activity was also shown to be inhibited by DCCD (Fox *et al.*, 1996b). Similarly, the Ech hydrogenase of *M. barkeri* has been proposed to function as a proton pump when producing H_2 during acetate-dependent growth (Meuer *et al.*, 1999). Two gene groups in the genome of *M. thermoautotrophicum* each encoding a putative multisubunit membrane-bound hydrogenase have been suggestively named *eha* and *ehb* for energy converting hydrogenase A and B (Tersteegen and Hedderich, 1999). Energy converting hydrogenase B subunits show homology to mbx subunits ABDFGHJLMN and to MbhAEFGJL. Eha homology is however limited to the JL subunits of both hydrogenases, and to mbxN (which encodes a 2 [4Fe-4S] ferredoxin).

The product of the fourth orf, *mbxL*, has not been characterized yet beyond the level of genomic inspection. Orf *mbxL* is part of a putative large operon *mbxABCDFGHH'MJKLN*, which is a 'mirror' of the *mbhA-N* operon, therefore it putatively codes for another energy transducing membrane complex.

The MbhL-containing complex was isolated from the membranes and partially purified under mild conditions in an attempt to maintain integrity a. o. with a view to future studies on its bioenergetics. The exact subunit composition and stoichiometry of the complex is not known, however, it presumably contains at least the MbhJKLMN core: the N-terminal sequence of MbhK and MbhL were identified on extracted subunits after SDS-PAGE; the two [4Fe-4S] cubanes of MbhN were putatively identified in EPR spectroscopy; the MbhJ subunit with the 'proximal' iron sulfur cluster for electron transfer to the Ni-Fe-cluster should be present because the complex catalyses H_2 production; at least one membrane-spanning subunit is expected to be present because detergent is required to keep the complex in solution; the MbhM subunit is a reasonable candidate because it would – by analogy with NADH dehydrogenase - confer DCCD sensitivity to the complex.

Isolation of a different core complex of membrane-bound *P. furiosus* hydrogenase has recently been described by Sapra *et al.* (Sapra *et al.*, 2000). Extraction from the membrane after repeated washing with up to 4 M NaCl and chromatography in the presence of 2 M urea resulted in a complex that has lost the ability to evolve H_2 using reduced ferredoxin as electron donor. The purified isolate was claimed to be a stoichiometric complex of MbhK and the Ni-Fe-cluster binding MbhL. However, this appears to be incompatible with the observation by the same authors of an EPR signal characteristic for iron-sulfur cluster(s). Thus, the composition and functionality of this complex is not clear. A soluble electron-transfer chain in *P. furiosus* has been proposed by Adams and collaborators (Ma *et al.*, 1994) for the generation of molecular hydrogen from reducing equivalents derived from fermentation: pyruvate oxidoreductase, POR, reduces ferredoxin, Fd, which reduces sulfide dehydrogenase, SuDH, which reduces $NADP^+$, which diffuses to sulfhydrogenase I to produce H_2. The kinetic data presented in the present paper argue against this hypothesis: the overall activity of the soluble chain is too low to sustain fermentation of glucose to acetate. As an alternative hypothesis we propose proton respiration coupled to energy transduction in a transmembrane 'hydrogen synthase' complex as outlined in Figure 6.13. The originally proposed route through SuDH and hydrogenase I could then function as a safety valve for the disposal of excess reducing equivalents as H_2, an option that would not be available via the tightly coupled energy transduction system. Furthermore, the SuDH branch can produce NADPH for biosynthetic purposes. Additionally, the soluble hydrogenase can save energy by also producing NADPH from the 'waste' product of respiration, H_2.

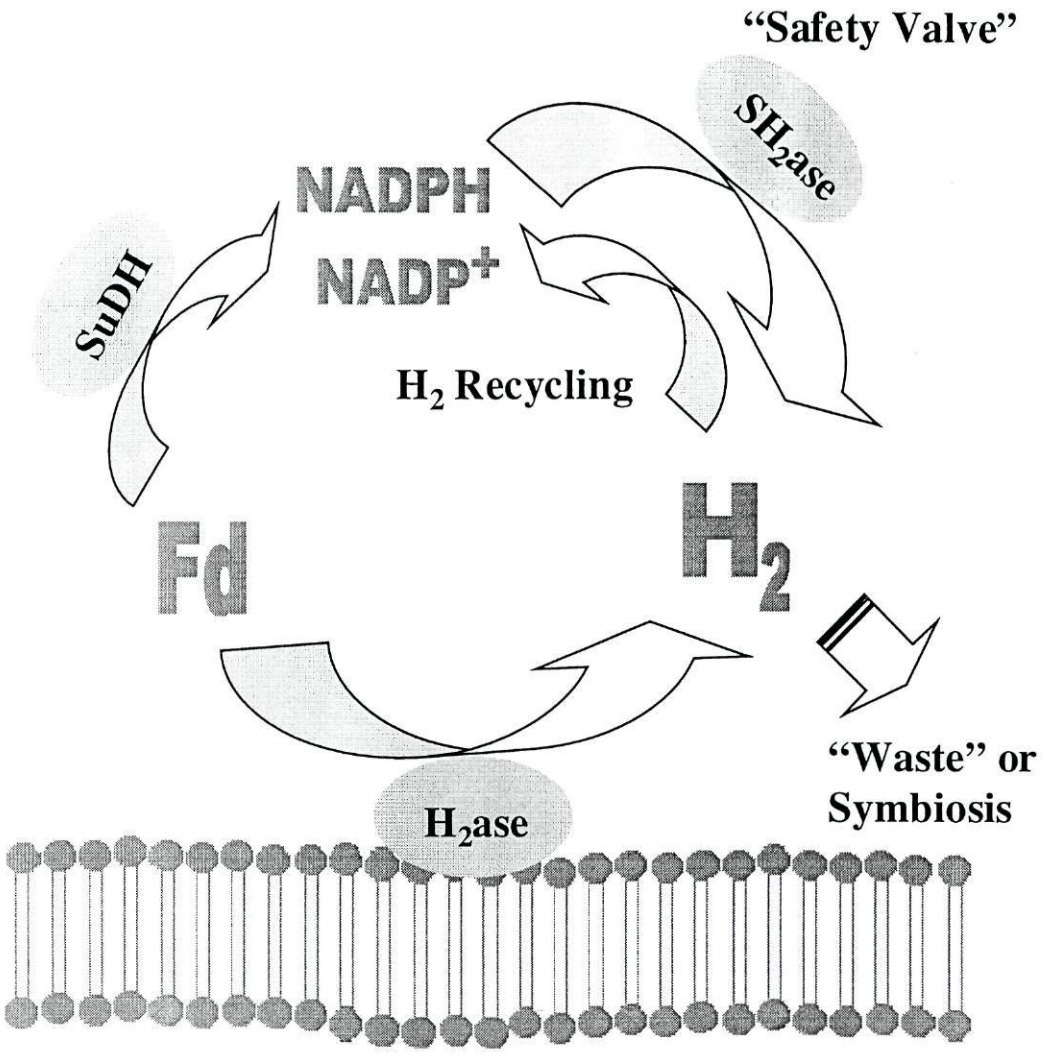

Figure 6.13 A working hypothesis of H_2-metabolism in *P. furiosus*.

7

THE MOLECULAR DIVERSITY OF HYDROGENASES

7.1 THE RELEVANCE OF SEQUENCE COMPARISONS

Comparative analysis of amino acid sequences of hydrogenase subunits has afforded remarkable insights concerning their evolutionary relationships, cofactor composition and active site ligands (Przybyla *et al.*, 1992; Voordouw, 1992; Wu and Mandrand, 1993). In 1992, Przybyla et al. correctly predicted (Przybyla *et al.*, 1992), based on sequence comparisons, that the nickel-containing active site was borne by the large subunit, and that the small subunit harbored the iron-sulfur clusters. Although the different genes for the large subunits may possess only superficial amino acid homology, the presence of two conserved motifs (postulated to bind the active site nickel) enables their unambiguous identification as hydrogenases. The cysteine residues in these two motifs (RXCXXC and DPCXXC) were later confirmed as the ligands to the [NiFe] active site in hydrogenases. In each motif, the first Cys residue binds the Ni atom only, and the second Cys bridges Ni and Fe (Volbeda *et al.*, 1995).

Wu and Mandrand (Wu and Mandrand, 1993) analyzed all hydrogenase sequences available to date, and classified them into six classes according to sequence homologies, metal content and physiological function. The first class contains the H_2-uptake membrane-bound NiFe-hydrogenases; the second comprises four periplasmic and two membrane-bound H_2-uptake NiFe(Se)-hydrogenases from sulphate-reducing bacteria; the third consists of four periplasmic Fe-hydrogenases from strict anaerobic bacteria; the fourth class contains methyl-viologen-(MV), factor F_{420}- (F420) or NAD-reducing soluble hydrogenases; the fifth is the H_2-producing labile hydrogenase isoenzyme 3 of Escherichia coli; the sixth class contains two soluble tritium-exchange hydrogenases of cyanobacteria. Specific signatures of the six classes of hydrogenases as well as of some subclasses were also detected by these authors. F_{420}-reducing, F_{420}-non-reducing and NAD-linked hydrogenases were recognized as very closely related, though sufficiently different to allow their classification into subclasses. Although signatures allowing the distinction of F_{420}-reducing from non-F_{420}-reducing hydrogenases were

found, no signatures for NAD-linked hydrogenases could be found, since at the time only one sequence of each of these kinds of hydrogenase were known. The same happened regarding the complex membrane-bound hydrogenases.

Since these studies many new hydrogenase sequences have become known, including sulfhydrogenases, NAD-linked hydrogenases, and complex membrane-bound hydrogenases. Complex membrane-bound hydrogenases have very often been mislabeled as NADH: ubiquinone oxidoreductases in several genome sequencing projects, including that of *P. furiosus*, due to its very low similarity to common hydrogenases.

Several of these sequences have therefore been studied in order to identify features that might assist in recognition of related proteins. Signatures allowing the reliable distinction between closely related subclasses (F_{420}-reducing, F_{420}-non-reducing, NAD-linked and sulfhydrogenases) and between membrane-bound hydrogenases and complex I proteins have been found. Besides their obvious utility in assisting and speeding up automatic genome annotation projects, several of these signatures seem to suggest possible explanations for the absence of EPR signals due to Fe-S clusters in some of these proteins.

7.2 PHYLOGENETIC RELATIONSHIPS BETWEEN THE SELECTED HYDROGENASES

In order to be able to test the consensus motifs found in the hydrogenases only some of the most recently available hydrogenase sequences of each of the disputed (sub)classes were selected for comparison. The sequences not included in the comparison thus form a testbench to evaluate the universality of the consensus motifs discovered. The degree of confidence on the use of a motif will be as high as its ability

to correctly identify every available sequence of a given class, even those not included in the original set.

The selected hydrogenase were: the "energy-conserving" hydrogenases of *Methanobacterium autotrophicum* (Tersteegen and Hedderich, 1999), the CO-induced hydrogenase from *Rhodospirillum rubrum* (Fox *et al.*, 1996b), the Ech hydrogenase from *Methanosarcina barkeri* (Künkel *et al.*, 1998), the membrane-bound hydrogenase, sulfhydrogenases (Ma *et al.*, 2000; Pedroni *et al.*, 1995) and mbx hydrogenase from *P. furiosus* (see section 6.7) and homologs from *Thermotoga maritima* (Nelson *et al.*, 1999), *P. horikoshii* (Kawarabayasi *et al.*, 1998) and *P. abyssi* (Genoscope, 2000), the sulfhydrogenase from *Thermococcus litoralis* (Rákhely *et al.*, 1999), hydrogenase-3 (Böhm *et al.*, 1990) and –4 (Andrews *et al.*, 1997) from *E. coli,* the hydrogenase from *Acetomicrobium flavidum* (Mura *et al.*, 1996), the bi-directional hydrogenases from *Anabaena variabilis* (Schmitz *et al.*, 1995) and *Synechocystis* sp. (Appel and Schulz, 1996), the NAD-reducing hydrogenase from *Ralstonia eutropha* (Tran-Betcke *et al.*, 1990), and the F_{420}-reducing and F_{420}-non-reducing hydrogenases from *Methanococcus voltae* (Halboth and Klein, 1992), *Methanococcus jannaschii* (Bult *et al.*, 1996), *Methanobacterium thermoautotrophicum* strain ΔH (Reeve *et al.*, 1989; Alex *et al.*, 1990) and *Methanothermus fervidus* (Steigerwald *et al.*, 1990).

The selected sequences of the small and large subunits were initially aligned to each other using ClustalX (Thompson *et al.*, 1997) and Gonnet´s scoring matrices (Gonnet *et al.*, 1992). Phylogenetic trees were built to show intimate relationships between the different hydrogenases. Further analysis was carried out separately with the hydrogenases from each of the major divisions revealed by the phylogenetic trees. These divisions very closely correspond to the functional distinctions between these hydrogenases revealed from biochemical characterization.

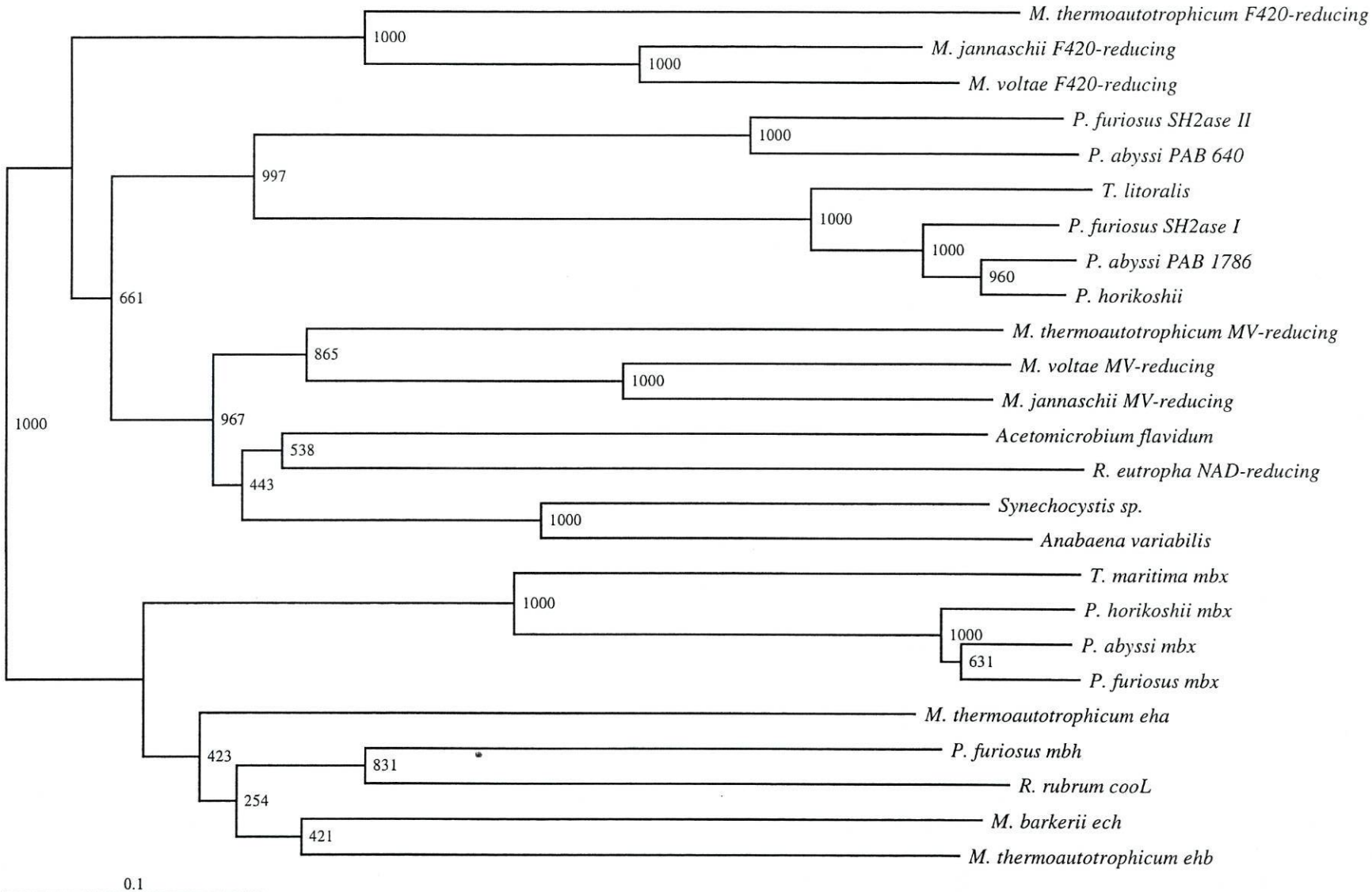

Figure 7.1 Phylogenetic tree of the sequences of the small subunits of the hydrogenases studied in this work.

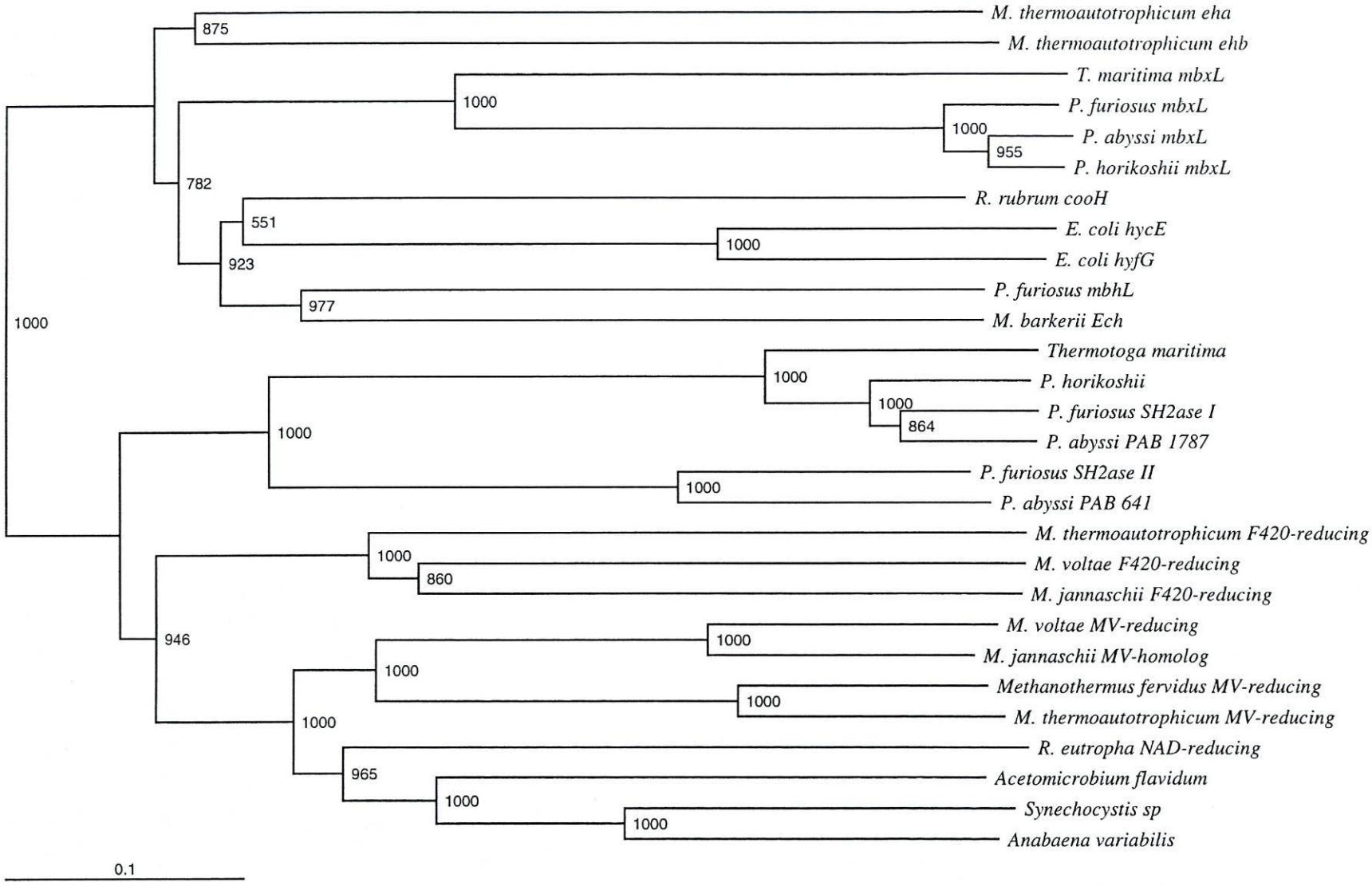

Figure 7.2 Phylogenetic tree of the sequences of the large subunits of the hydrogenases studied in this work

7.3 NAD-LINKED HYDROGENASES

NAD^+-linked hydrogenases are usually tetrameric enzymes composed of two heterodimers, one of which has hydrogenase activity and another with NAD(P)H: acceptor oxidoreductase (diaphorase) activity. The hydrogenase from *Acetomicrobium fervidum* has been included in this group due to its high similarity to the hydrogenase from *R: eutropha*, even though the purified hydrogenase only contains two subunits and no data are available regarding a possible diaphorase activity (Mura *et al.*, 1996). The operon of this hydrogenase has been only partially characterized, and genes encoding the extra subunits may be present in the uncharacterized region. It is therefore possible that more subunits may be present in the native protein, but lost during the purification.

The function of NAD-linked hydrogenases is dependent on the organism studied. For example, in *R. eutropha*, the NAD-linked hydrogenase provides low-potential reducing equivalents for autotrophic growth (Schneider *et al.*, 1979). In cyanobacteria, bi-directional NAD^+-linked hydrogenases have been suggested to function as a valve for low-potential electrons generated during the light reaction of photosynthesis, thus preventing a slowing down of electron transport (Appel *et al.*, 2000).

The small subunits of NAD-linked hydrogenases are much shorter than the small subunits of the other classes and subclasses of hydrogenases (excepting the complex membrane-bound hydrogenases — see below). There are four conserved Cys, (numbered Cys 41, 44, 114 and 179 in the *R. eutropha* sequence) arranged in a way very similar to the Cys that bind the proximal [4Fe-4S] cluster in *D. gigas* hydrogenase (Volbeda *et al.*, 1995). It can be concluded that all of these hydrogenases contain only one Fe-S cluster.

In the following motif analysis, strictly conserved amino acids are written in uppercase and amino acids conserved in most related sequences are written in lowercase.

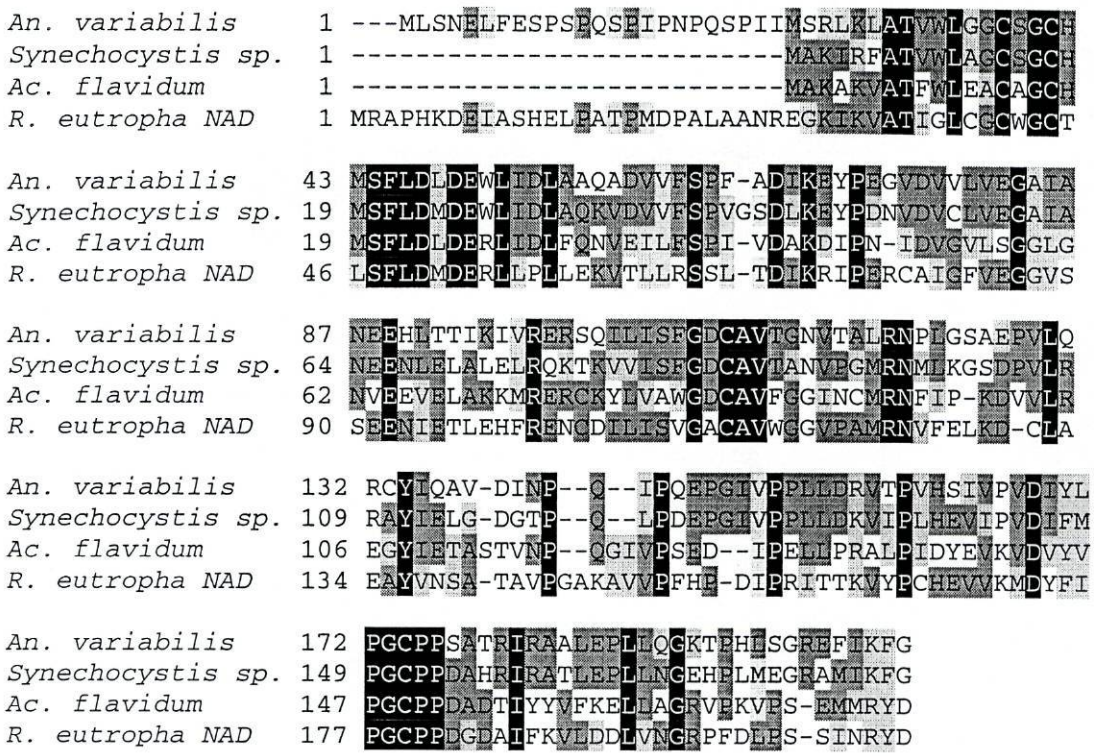

Figure 7.3 Multiple alignment of small subunits of NAD-linked hydrogenases. Strictly conserved amino acids are shaded black; amino acids conserved in most sequences are shaded dark grey; similar amino acids are shaded light grey.

The motif SFLDlDExLidL, present close to the N-terminus, is very conserved and was found to be strictly specific for this subclass of hydrogenases. No other proteins present in the relevant databases show this motif, that can thus be considered a signature of the small subunits of NAD-linked hydrogenases.

The large subunits of NAD-linked hydrogenases show several strictly conserved regions (Figure 7.4). Among these regions are the motifs containing the Ni-coordinating Cys residues (R I **C** G I **C** p V S H and D P **C** L S **C** x T H A). In spite of the wealth of conserved regions present in the large subunits of these hydrogenases, most of them are totally or partially conserved also among e.g. non-F_{420}-reducing hydrogenases, which does not allow their use as subclass-specific signatures.

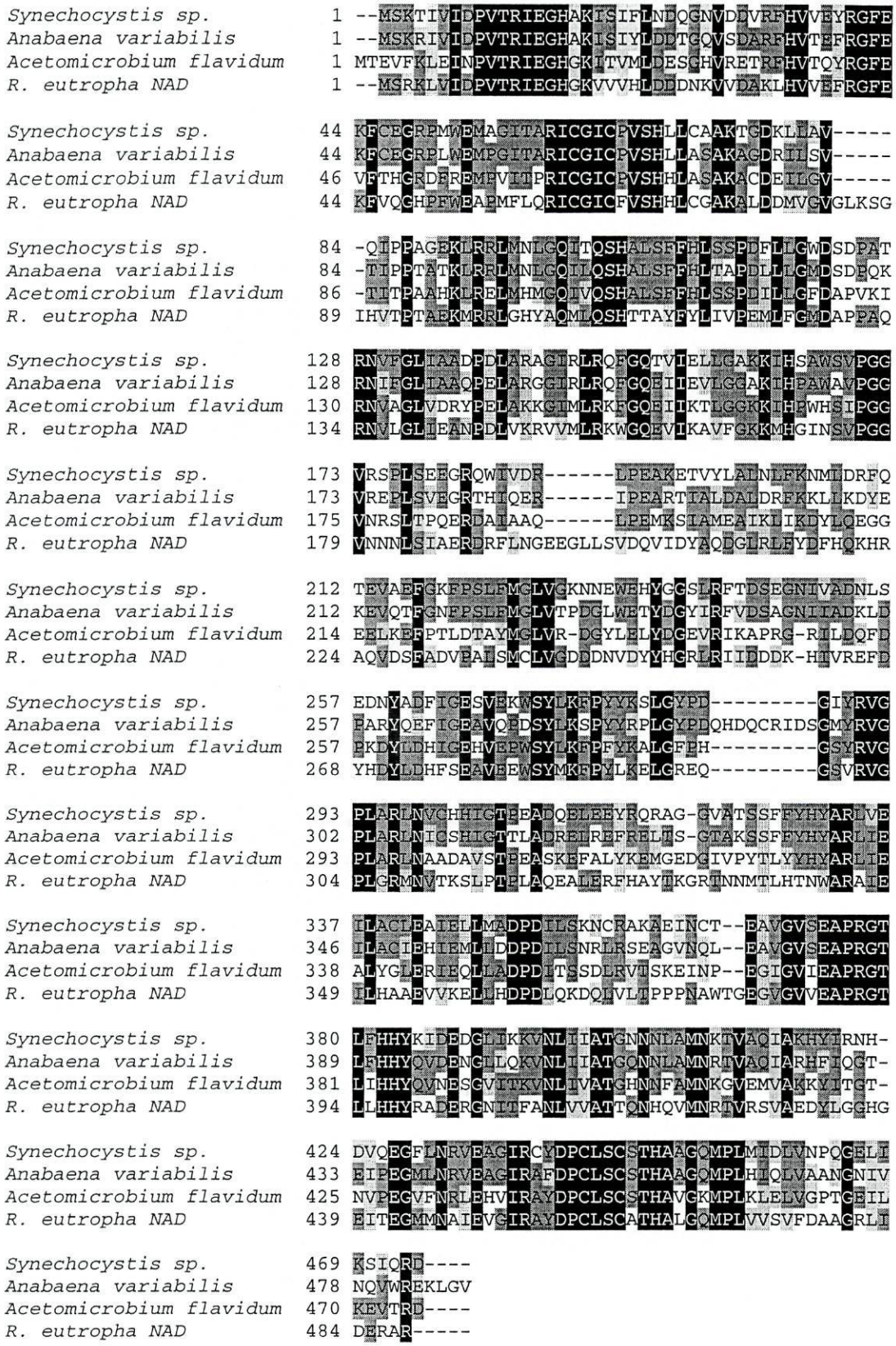

Figure 7.4 Multiple alignment of large subunits of NAD-linked hydrogenases. Strictly conserved amino acids are shaded black; amino acids conserved in most sequences are shaded dark grey; similar amino acids are shaded light grey.

However, the less well-conserved motif R N x_2 G L x_4 P (D/E) L x (R/K) (starting on position 307 in the *R. eutropha* sequence)has been found to selectively retrieve all large subunits of these class.

7.4 SULFHYDROGENASES

The two sulfhydrogenases isolated from *P. furiosus* are heterotetrameric proteins (Ma *et al.*, 2000; Pedroni *et al.*, 1995) able to reduce protons to H_2 and S^0 to H_2S (Ma *et al.*, 1993; Ma *et al.*, 2000). Very close homologs have been found in the genomes of other *Pyrococcus* species and purified from *Thermococcus litoralis* (Rákhely *et al.*, 1999).

As described in chapter 3, alignment of multiple sequences allowed the identification of the cluster coordinating ligands in the small subunit of *P. furiosus* sulfhydrogenase I. The availability of more sulfhydrogenase sequences confirms the high conservation of those Cys (Figure 7.5). It also shows that in all sulfhydrogenases known to date three [4Fe-4S] clusters are present in the small subunit, and allows a more precise definition of the cluster's environment in these proteins. In the following discussion the numbering of *P. furiosus* sulfhydrogenase I is used.

The proximal cluster is coordinated by the Cys residues (shown in bold) present in the motifs LTS**C**YG**C**QL (at position 11), Ga**C**AxqG (at position 84) and G**C**Py(D/E)K (at position 140). The distal cluster is coordinated by four Cys and not three Cys and one His as in D. gigas hydrogenase (Volbeda *et al.*, 1995). These Cys residues are carried by the motifs DYPV**C**LE**C**(R/K)L (at position 160), **C***L (at position 174), P**C**LGP*T (at position 182). The first of these motifs contains several charged residues that will probably be close to the active site in the three-dimensional structure. It is well known that when a protonation residue is present at or near a redox-active group the reduction potentials become pH-dependent, because the relative

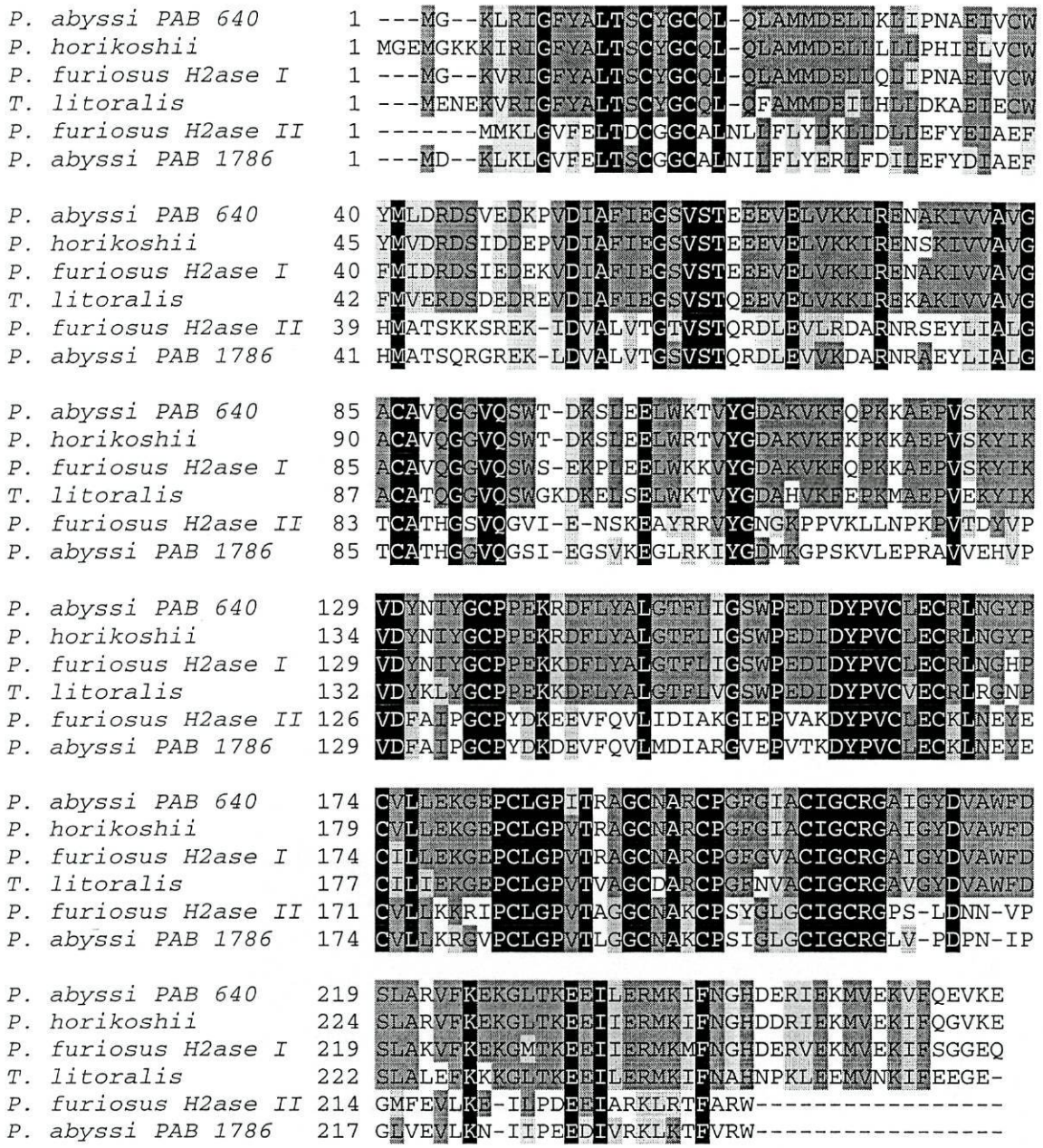

Figure 7.5 Multiple alignment of "small" subunits of sulfhydrogenases. Strictly conserved amino acids are shaded black; amino acids conserved in most sequences are shaded dark grey; similar amino acids are shaded light grey.

energies of the oxidized and reduced states is influenced by the positive charge of the proton or the negative charge of the deprotonated acid. In turn, the pKa of the group will be modified by the charge of the electron(s), resulting in a lower pK for the oxidized form and a higher pK for the reduced form (Clark, 1960). When the difference between

two successive pK´s is large enough the slope of the reduction potential *vs.* pH at 80 °C becomes (m_2 -m_1) 70/n mV for the overall half-reaction

$$Ox + m_1\ H^+ + n\ e^- \leftrightharpoons Red + m_2\ H^+$$

at $pK_i < pH < pK_j$.

The presence of both acidic (pKa ≈ 4) and basic (pKa ≈ 11 or 12) residues immediately adjacent to the cluster suggests that if these residues are correctly orientated with regard to the cluster its redox potential may be extremely sensitive to pH in the physiological range. This might allow the cluster to couple proton movement to the electron transfer, thus directly affecting the efficiency of the system. Additionally, this may explain the difficulty in finding EPR signals from some of the clusters of *P. furiosus* sulfhydrogenases (Arendsen *et al.*, 1995; Ma *et al.*, 2000), since according to theory, the potential of this cluster at pH 8.0 and 80 °C might be more than a hundred mV lower than what would be expected if those residues were replaced by unprotonable residues as in other iron-sulfur proteins.

The intermediate cluster is most probably a [4Fe-4S] cluster, coordinated by the Cys in motifs G**C**nA(R/K)**C**P (at position 191) and **C**IG**C**RG (at position 199). The first of these was the only (mildly) successful candidate for a specific signature for the small subunits of sulfhydrogenases.

The analysis of the sequences of the large subunits of sulfhydrogenases shows that, as with the small subunits, two subclasses seem to exist, one of which has high similarity to sulfhydrogenase I from *P. furiosus* (Pedroni *et al.*, 1995) and the other to sulfhydrogenase II (Ma *et al.*, 2000).

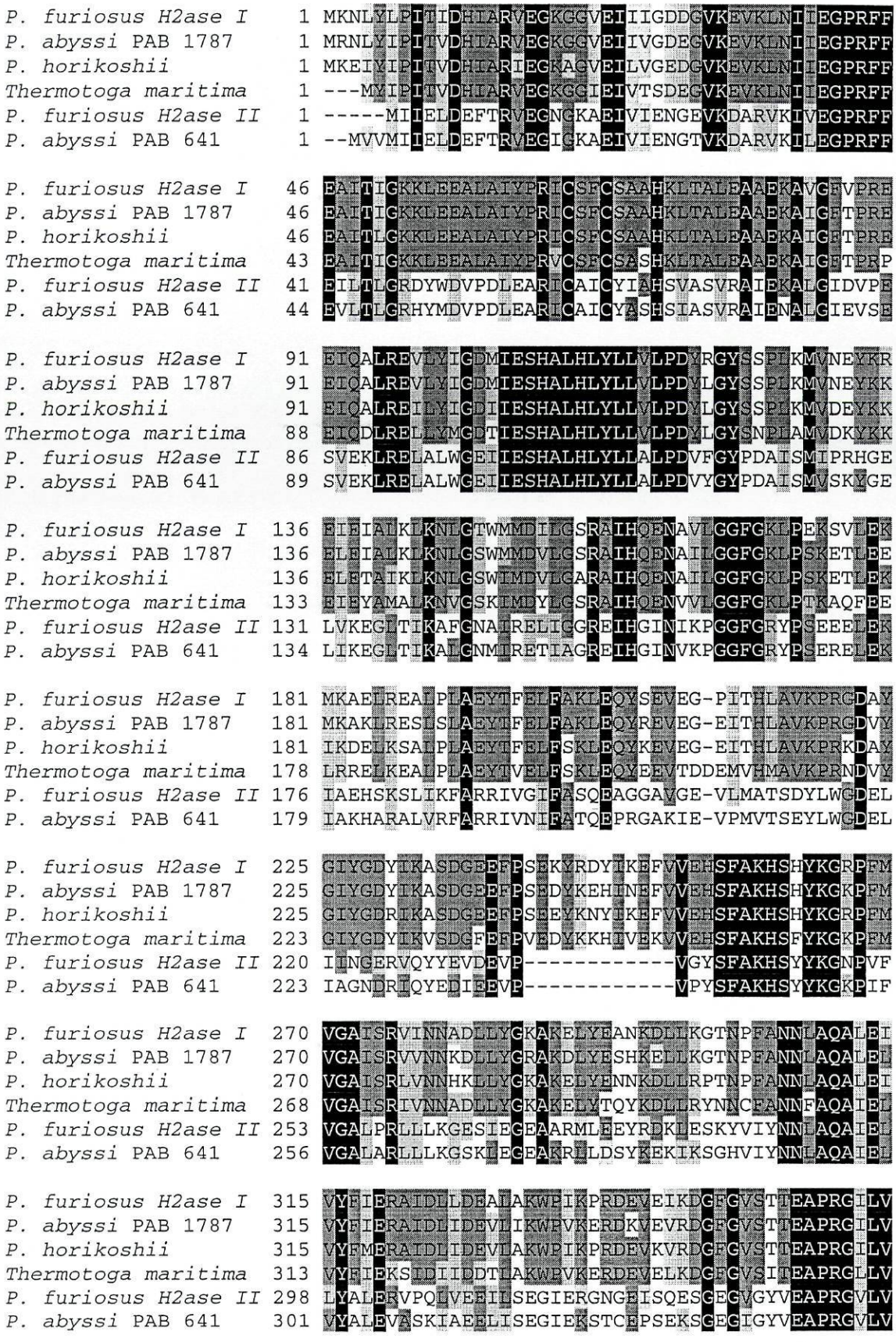
P. furiosus H2ase I 1 MKNLYLPITIDHIARVEGKGGVEIIIGDDGVKEVKLNIIEGPRFF
P. abyssi PAB 1787 1 MRNLYIPITVDHIARVEGKGGVEIIVGDEGVKEVKLNIIEGPRFF
P. horikoshii 1 MKEIYIPITVDHIARIEGKAGVEILVGEDGVKEVKLNIIEGPRFF
Thermotoga maritima 1 ---MYIPITVDHIARVEGKGGIEIVTSDEGVKEVKLNIIEGPRFF
P. furiosus H2ase II 1 -----MIIELDEFTRVEGNGKAEIVIENGEVKDARVKIVEGPRFF
P. abyssi PAB 641 1 --MVVMIIELDEFTRVEGIGKAEIVIENGTVKDARVKILEGPRFF
P. furiosus H2ase I 46 EAITIGKKLEEALAIYPRICSFCSAAHKLTALEAAEKAVGFVPRE
P. abyssi PAB 1787 46 EAITIGKKLEEALAIYPRICSFCSAAHKLTALEAAEKAIGFTPRE
P. horikoshii 46 EAITLGKKLEEALAIYPRICSFCSAAHKLTALEAAEKAIGFTPRE
Thermotoga maritima 43 EAITIGKKLEEALAIYPRVCSFCSASHKLTALEAAEKAIGFTPRP
P. furiosus H2ase II 41 EILTLGRDYWDVPDLEARICAICYIAHSVASVRAIEKALGIDVPE
P. abyssi PAB 641 44 EVLTLGRHYMDVPDLEARICAICYASHSIASVRAIENALGIEVSE
P. furiosus H2ase I 91 EIQALREVLYIGDMIESHALHLYLLVLPDYRGYSSPLKMVNEYKR
P. abyssi PAB 1787 91 EIQALREVLYIGDMIESHALHLYLLVLPDYLGYSSPLKMVNEYKK
P. horikoshii 91 EIQALREILYIGDIIESHALHLYLLVLPDYLGYSSPLKMVDEYKK
Thermotoga maritima 88 EIQDLRELLYMGDTIESHALHLYLLVLPDYLGYSNPLAMVDKYKK
P. furiosus H2ase II 86 SVEKLRELALWGEIIESHALHLYLLALPDVFGYPDAISMIPRHGE
P. abyssi PAB 641 89 SVEKLRELALWGEIIESHALHLYLLALPDVYGYPDAISMVSKYGE
P. furiosus H2ase I 136 EIEIALKLKNLGTWMMDILGSRAIHQENAVLGGFGKLPEKSVLEK
P. abyssi PAB 1787 136 ELEIALKLKNLGSWMMDVLGSRAIHQENAILGGFGKLPSKETLEE
P. horikoshii 136 ELETAIKLKNLGSWIMDVLGARAIHQENAILGGFGKLPSKETLEK
Thermotoga maritima 133 EIEYAMALKNVGSKIMDYLGSRAIHQENVVLGGFGKLPTKAQFEE
P. furiosus H2ase II 131 LVKEGLTIKAFGNAIRELIGGREIHGINIKPGGFGRYPSEEELEK
P. abyssi PAB 641 134 LIKEGLTIKALGNMIRETIAGREIHGINVKPGGFGRYPSERELEK
P. furiosus H2ase I 181 MKAELREALPLAEYTFELFAKLEQYSEVEG-PITHLAVKPRGDAY
P. abyssi PAB 1787 181 MKAKLRESLSLAEYTFELFAKLEQYREVEG-EITHLAVKPRGDVY
P. horikoshii 181 IKDELKSALPLAEYTFELFSKLEQYKEVEG-EITHLAVKPRKDAY
Thermotoga maritima 178 LRRELKEALPLAEYTVELFSKLEQYEEVTDDEMVHMAVKPRNDVY
P. furiosus H2ase II 176 IAEHSKSLIKFARRIVGIFASQEAGGAVGE-VLMATSDYLWGDEL
P. abyssi PAB 641 179 IAKHARALVRFARRIVNIFATQEPRGAKIE-VPMVTSEYLWGDEL
P. furiosus H2ase I 225 GIYGDYIKASDGEEFPSEKYRDYIKEFVVEHSFAKHSHYKGRPFM
P. abyssi PAB 1787 225 GIYGDYIKASDGEEFPSEDYKEHINEFVVEHSFAKHSHYKGKPFM
P. horikoshii 225 GIYGDRIKASDGEEFPSEEYKNYIKEFVVEHSFAKHSHYKGRPFM
Thermotoga maritima 223 GIYGDYIKVSDGFEFPVEDYKKHIVEKVVEHSFAKHSFYKGKPFM
P. furiosus H2ase II 220 IINGERVQYYEVDEVP----------VGYSFAKHSYYKGNPVF
P. abyssi PAB 641 223 IAGNDRIQYEDIEEVP----------VPYSFAKHSYYKGKPIF
P. furiosus H2ase I 270 VGAISRVINNADLLYGKAKELYEANKDLLKGTNPFANNLAQALEI
P. abyssi PAB 1787 270 VGAISRVVNNKDLLYGRAKDLYESHKELLKGTNPFANNLAQALEL
P. horikoshii 270 VGAISRLVNNHKLLYGKAKELYENNKDLLRPTNPFANNLAQALEI
Thermotoga maritima 268 VGAISRIVNNADLLYGKAKELYTQYKDLLRYNNCFANNFAQAIEL
P. furiosus H2ase II 253 VGALPRLLLKGESIEGEAARMLEEYRDKLESKYVIYNNLAQAIEL
P. abyssi PAB 641 256 VGALARLLLKGSKLEGEAKRLLDSYKEKIKSGHVIYNNLAQAIEL
P. furiosus H2ase I 315 VYFIERAIDLLDEALAKWPIKPRDEVEIKDGFGVSTIEAPRGILV
P. abyssi PAB 1787 315 VYFIERAIDLIDEVLIKWPVKERDKVEVRDGFGVSTIEAPRGILV
P. horikoshii 315 VYFMERAIDLIDEVLAKWPIKPRDEVKVRDGFGVSTIEAPRGILV
Thermotoga maritima 313 VYFIEKSIDIIDDTLAKWPVKERDEVELKDGFGVSITEAPRGLLV
P. furiosus H2ase II 298 LYALERVPQLVEEILSEGIERGNGEISQESGEGVGYVEAPRGVLV
P. abyssi PAB 641 301 VYALEVASKIAEELISEGIEKSTCEPSEKSGEGIGYVEAPRGVLV

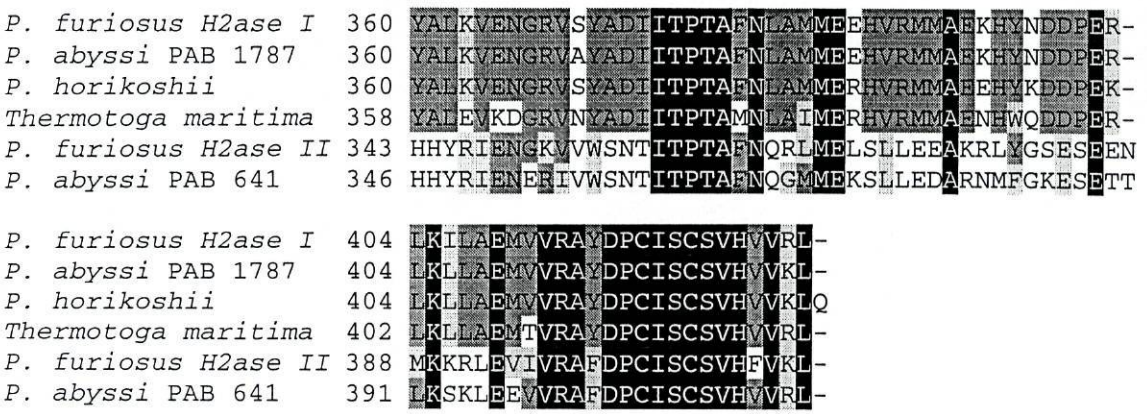

Figure 7.6 Multiple alignment of "large" subunits of sulfhydrogenases. Strictly conserved amino acids are shaded black; amino acids conserved in most sequences are shaded dark grey; similar amino acids are shaded light grey.

Several conserved regions that may be used as specific signatures for these large subunits have been found. These are I*EGPRFFE**T*G, IESHALHLYLL, SFAKHSxYKGrP, NN*AQA*E**Y**E and ITPTAfNxxxME. No hints as to the physiological significance of these regions are available, because of the very low similarity of these proteins to the hydrogenases of which the three-dimensional structure is known.

7.5 F_{420}-NON-REDUCING HYDROGENASES

Methanogens posses two different kinds of hydrogenases, which can be readily distinguished from each other by their ability to use F_{420} as electron acceptor. F_{420}-non-reducing hydrogenases from obligate hydrogenotrophic methanogens are very similar to each other, as already remarked by (Wu and Mandrand, 1993). In *Methanobacterium thermoautotrophicum* F_{420}-non-reducing hydrogenase was shown to be part of a membrane-associated complex which also contains heterodisulfide reductase and several other proteins with unknown functions (Setzke *et al.*, 1994).

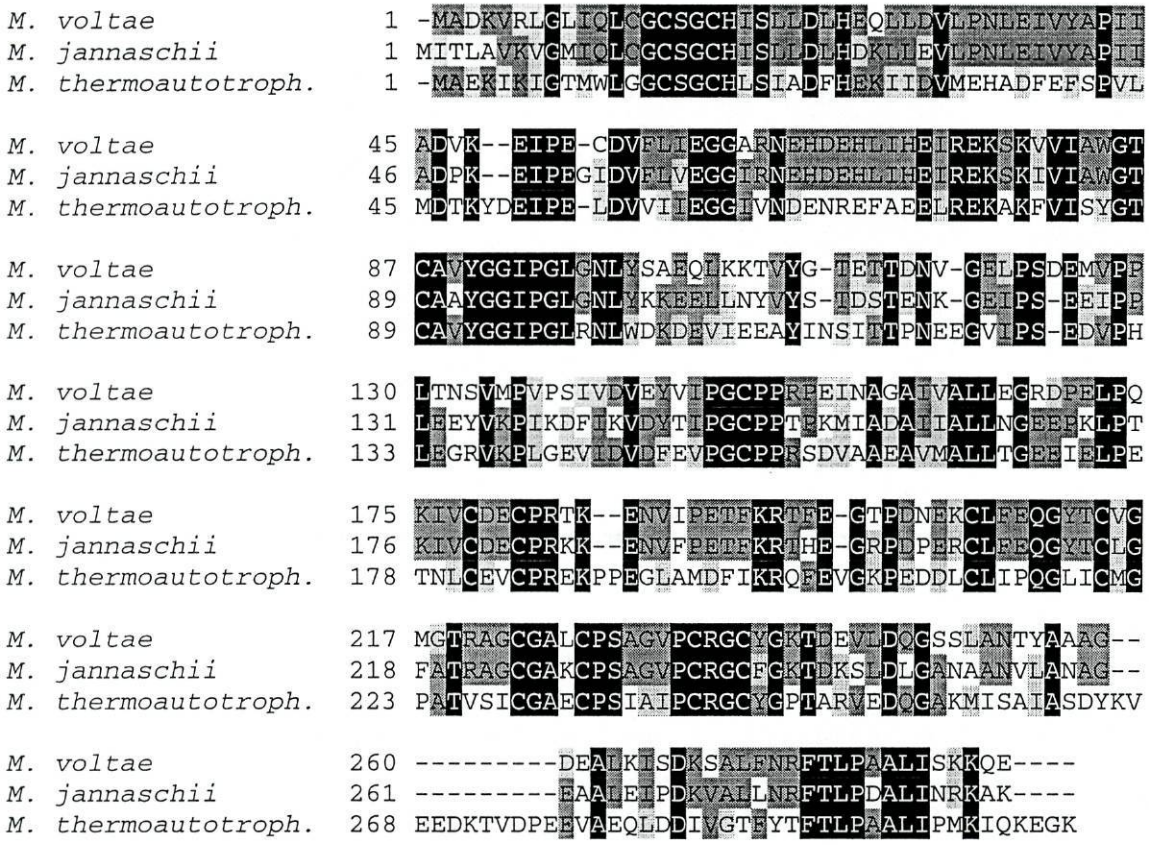

Figure 7.7 Multiple alignment of small subunits of F_{420}-non-reducing hydrogenases. Strictly conserved amino acids are shaded black; amino acids conserved in most sequences are shaded dark grey; similar amino acids are shaded light grey.

The proximal cluster is bound by four Cys arrayed in the common hydrogenase pattern — two close Cys (G**C**SG**C**HxS at position 13 in the *M. voltae* sequence) and two "scattered" Cys (GTCA at position 85 and PGCPP at position 148). The distal cluster is ligated by the motifs **C**(D/E)x**C**PRxK (at position 178) **C**LxxQGxx**C**xG (at position 206). As with sulfhydrogenases, the presence of charged residues adjacent to the Cys in the first of these motifs suggests a pH-dependent potential of this cluster. As in sulfhydrogenases, the intermediate cluster is a [4Fe-4S] center. The binding motif for

Figure 7.8 Multiple alignment of large subunits of F_{420}-non-reducing hydrogenases. Strictly conserved amino acids are shaded black; amino acids conserved in most sequences are shaded dark grey; similar amino acids are shaded light grey.

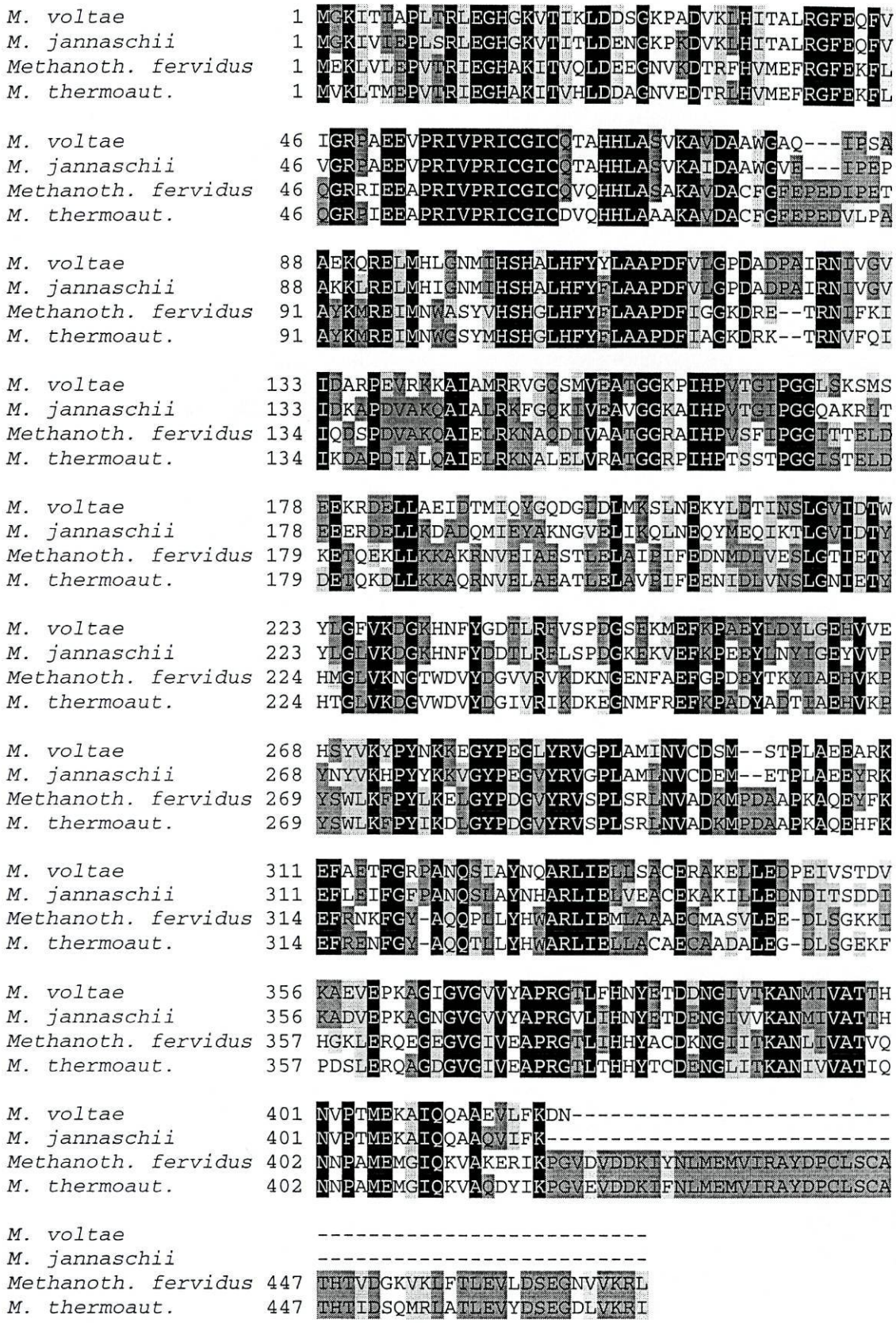
M. voltae 1 MGKITIAPLTRLEGHGKVTIKLDDSGKPADVKLHITALRGFEQFV
M. jannaschii 1 MGKIVIEPLSRLEGHGKVTITLDENGKPKDVKLHITALRGFEQFV
Methanoth. fervidus 1 MEKLVLEPVTRIEGHAKITVQLDEEGNVKDTRFHVMEFRGFEKFL
M. thermoaut. 1 MVKLTMEPVTRIEGHAKITVHLDDAGNVEDTRLHVMEFRGFEKFL
M. voltae 46 IGRPAEEVPRIVPRICGICQTAHHLASVKAVDAAWGAQ---IPSA
M. jannaschii 46 VGRPAEEVPRIVPRICGICQTAHHLASVKAIDAAWGVE---IPEP
Methanoth. fervidus 46 QGRRIEEAPRIVPRICGICQVQHHLASAKAVDACFGFEPEDIPET
M. thermoaut. 46 QGRPIEEAPRIVPRICGICDVQHHLAAAKAVDACFGFEPEDVLPA
M. voltae 88 AEKQRELMHLGNMIHSHALHFYYLAAPDFVLGPDADPAIRNIVGV
M. jannaschii 88 AKKLRELMHIGNMIHSHALHFYFLAAPDFVLGPDADPAIRNIVGV
Methanoth. fervidus 91 AYKMREIMNWASYVHSHGLHFYFLAAPDFIGGKDRE--TRNIFKI
M. thermoaut. 91 AYKMREIMNWGSYMHSHGLHFYFLAAPDFIAGKDRK--TRNVFQI
M. voltae 133 IDARPEVRKKAIAMRRVGQSMVEATGGKPIHPVTGIPGGLSKSMS
M. jannaschii 133 IDKAPDVAKQAIALRKFGQKIVEAVGGKAIHPVTGIPGGQAKRLT
Methanoth. fervidus 134 IQDSPDVAKQAIELRKNAQDIVAATGGRAIHPVSFIPGGITTELD
M. thermoaut. 134 IKDAPDIALQAIELRKNALELVRATGGRPIHPTSSTPGGISTELD
M. voltae 178 EEKRDELLAEIDTMIQYGQDGLDLMKSLNEKYLDTINSLGVIDTW
M. jannaschii 178 EEERDELLKDADQMIEYAKNGVELIKQLNEQYMEQIKTLGVIDTY
Methanoth. fervidus 179 KETQEKLLKKAKRNVEIAESTLELAIPIFEDNMDLVESLGTIETY
M. thermoaut. 179 DETQKDLLKKAQRNVELAEATLELAVPIFEENIDLVNSLGNIETY
M. voltae 223 YLGFVKDGKHNFYGDTLRFVSPDGSEKMEFKPAEYLDYLGEHVVE
M. jannaschii 223 YLGLVKDGKHNFYDDTLRFLSPDGKEKVEFKPEEYLNYIGEYVVP
Methanoth. fervidus 224 HMGLVKNGTWDVYDGVVRVKDKNGENFAEFGPDEYTKYIAEHVKP
M. thermoaut. 224 HTGLVKDGVWDVYDGIVRIKDKEGNMFREFKPADYADTIAEHVKP
M. voltae 268 HSYVKYPYNKKEGYPEGLYRVGPLAMINVCDSM--STPLAEEARK
M. jannaschii 268 YNYVKHPYYKKVGYPEGVYRVGPLAMLNVCDEM--ETPLAEEYRK
Methanoth. fervidus 269 YSWLKFPYLKELGYPDGVYRVSPLSRLNVADKMPDAAPKAQEYFK
M. thermoaut. 269 YSWLKFPYIKDLGYPDGVYRVSPLSRLNVADKMPDAAPKAQEHFK
M. voltae 311 EFAETFGRPANQSIAYNQARLIELLSACERAKELLEDPEIVSTDV
M. jannaschii 311 EFLEIFGFPANQSLAYNHARLIELVEACEKAKILLEDNDITSDDI
Methanoth. fervidus 314 EFRNKFGY-AQQPLLYHWARLIEMLAAAECMASVLEE-DLSGKKI
M. thermoaut. 314 EFRENFGY-AQQTLLYHWARLIELLACAECAADALEG-DLSGEKF
M. voltae 356 KAEVEPKAGIGVGVVYAPRGTLFHNYETDDNGIVTKANMIVATTH
M. jannaschii 356 KADVEPKAGNGVGVVYAPRGVLIHNYETDENGIVVKANMIVATTH
Methanoth. fervidus 357 HGKLERQEGEGVGIVEAPRGTLIHHYACDKNGIITKANLIVATVQ
M. thermoaut. 357 PDSLERQAGDGVGIVEAPRGTLTHHYTCDENGLITKANIVVATIQ
M. voltae 401 NVPTMEKAIQQAAEVLFKDN----------
M. jannaschii 401 NVPTMEKAIQQAAQVIFK----------
Methanoth. fervidus 402 NNPAMEMGIQKVAKERIKPGVDVDDKIYNLMEMVIRAYDPCLSCA
M. thermoaut. 402 NNPAMEMGIQKVAQDYIKPGVEVDDKIFNLMEMVIRAYDPCLSCA
M. voltae ----------
M. jannaschii ----------
Methanoth. fervidus 447 THTVDGKVKLFTLEVLDSEGNVVKRL
M. thermoaut. 447 THTIDSQMRLATLEVYDSEGDLVKRI

this cluster — **C**GAx**C**PSxP**C**RG**C**xGxT (at position 223) — can be used as a specific signature for this subclass of hydrogenases. Another specific signature (EIPE**DV***EGG) is found at position 49 in the *M. voltae* sequence.

Some F_{420}-non-reducing hydrogenases contain a truncated large subunit which misses the last two [NiFe]-binding Cys residues (Figure 7.8). In the operons that code those hydrogenases there is an additional ORF that codes a small polypeptide that carries the second [NiFe] binding motif absent from the large subunits (Sorgenfrei *et al.*, 1993). In spite of this variability, the large subunits of these hydrogenases contain two specific signatures: IHP****PGG (at position 152 in the *M. voltae* sequence) and HHLAxxKAxDAxxG (at position 68 in the *M. voltae* sequence). The last signature is especially selective.

7.6 F_{420}-REDUCING HYDROGENASES

Methanogens use cofactor F_{420} as electron donor to several key reactions in methanogenesis, like the stepwise reduction of formyl-tetrahydromethanopterin to methyl-tetrahydromethanopterin and the energy-conserving reduction of heterodisulfide by the $F_{420}H_2$: heterodisulfide oxidoreductase (for a review of methanogenesis see (Deppenmeier *et al.*, 1999)). The regeneration of the reduced form of F_{420} is performed by the F_{420}-reducing hydrogenases. Wu and Mandrand (Wu and Mandrand, 1993) have grouped these hydrogenases with the F_{420}-non-reducing hydrogenases and the NAD-linked hydrogenases due to the observed high similarity between them.

The small subunits of F_{420}-reducing hydrogenases carry three [4Fe-4S] clusters. As in the other hydrogenases, the proximal cluster is ligated by the common CxxC C C pattern (Cys 15, 18, 89 and, 128 in the *M. jannaschii* sequence). Surprisingly, the sequence from *M. thermoautotrophicum* contains an aspartate residue in place of the second Cys, suggesting that in this organism the proximal cluster will be $(Cys)_3Asp$ ligated.

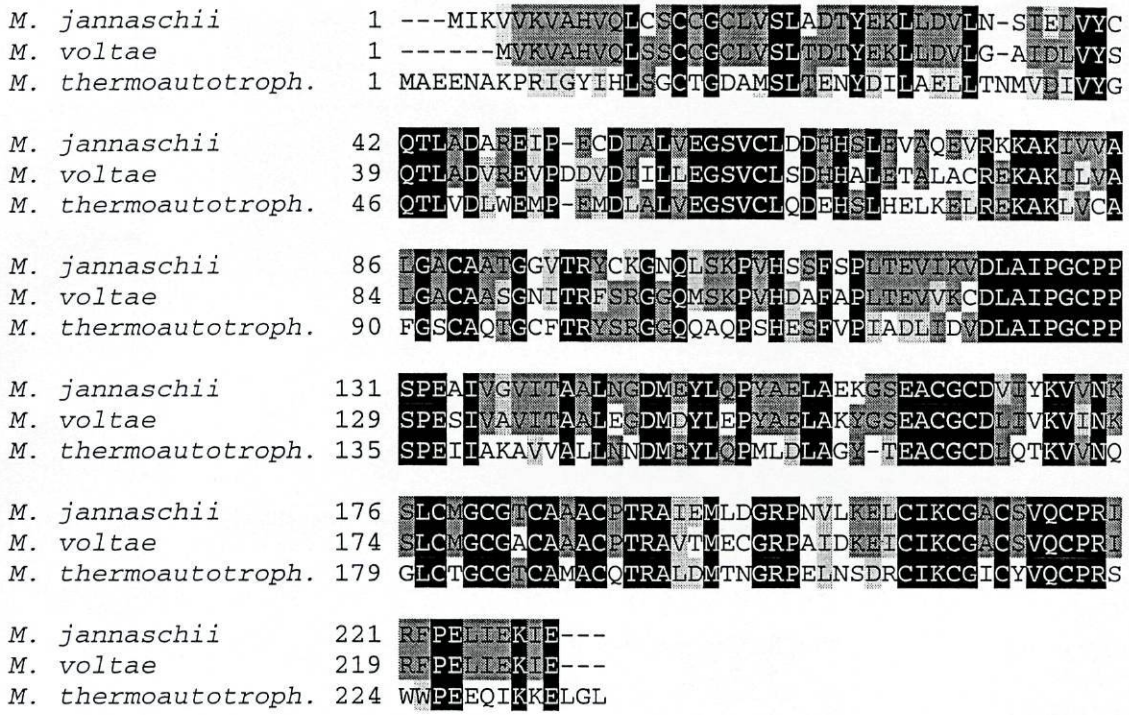

Figure 7.9 Multiple alignment of small subunits of F_{420}-reducing hydrogenases. Strictly conserved amino acids are shaded black; amino acids conserved in most sequences are shaded dark grey; similar amino acids are shaded light grey.

The intermediate and distal iron-clusters are each ligated by four Cys arranged in the traditional "ferredoxin-like" pattern (**C**xx**C**GxxxC**C**x**C**), which sets them apart from the clusters found in the small subunits of other hydrogenases, usually ligated by novel motifs (see above). Despite their high conservation, the cluster-binding regions cannot be used as specific signatures for these hydrogenases due to their very high similarity to the cluster-binding regions in ferredoxins and polyferredoxins. However, two strictly conserved motifs — LxEGSVCLxDxHxL (at position 57 in the *M. jannaschii* sequence) and EACGCDxxxKV (at position 162 in the *M. jannaschii* sequence) — are only found in the small subunits of these hydrogenases. In particular, the first of these motifs allows the specific detection of every F_{420}-reducing hydrogenase sequence present in the relevant databases.

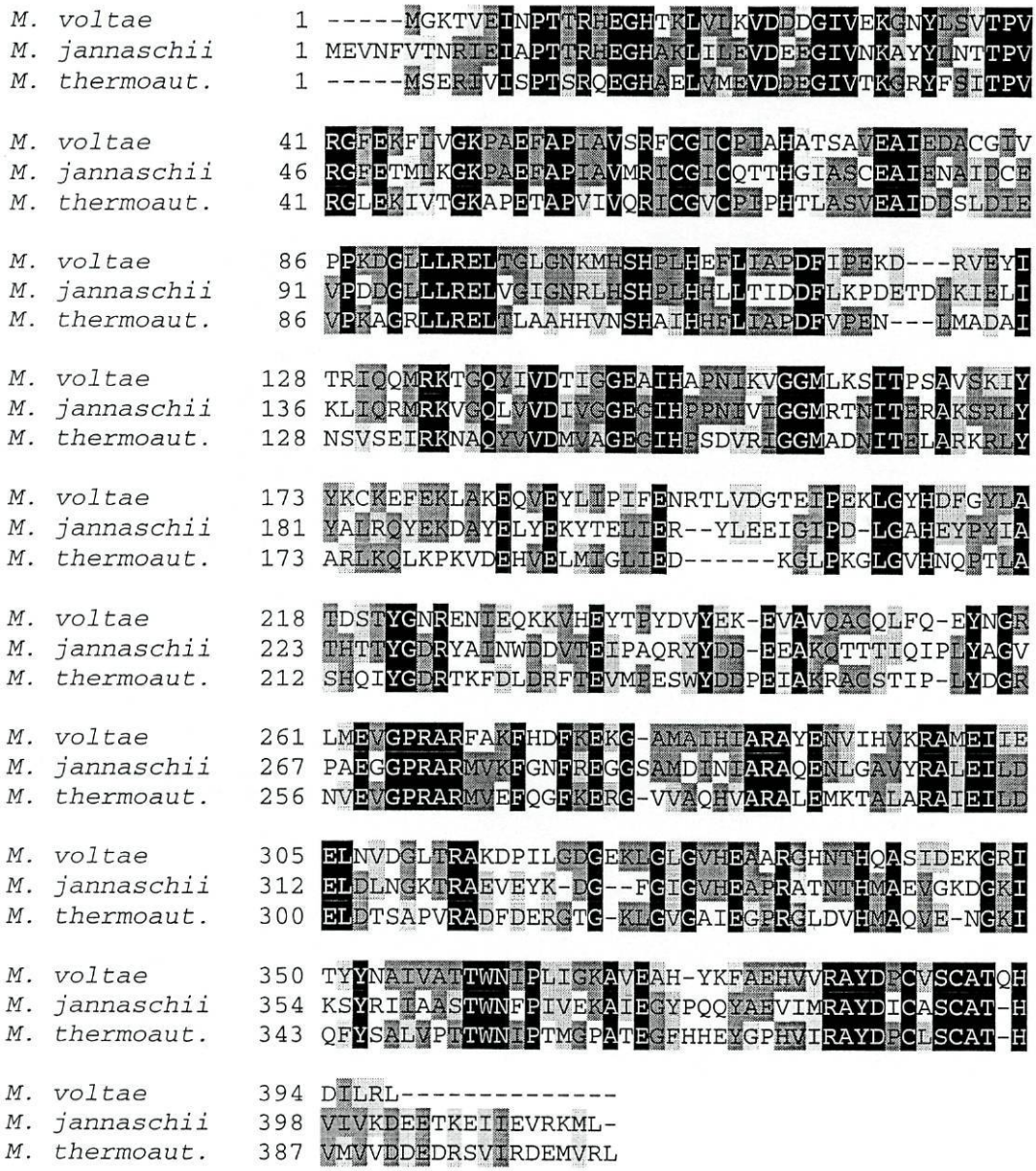

Figure 7.10 Multiple alignment of large subunits of F_{420}-reducing hydrogenases. Strictly conserved amino acids are shaded black; amino acids conserved in most sequences are shaded dark grey; similar amino acids are shaded light grey.

The large subunits of F_{420}-reducing hydrogenases show very high similarity to the corresponding subunits of NAD-linked and F_{420}-non-reducing hydrogenases. It is therefore very difficult to find specific signatures able to discriminate between them. The only specific signature found in the large subunits of F_{420}-reducing hydrogenases was YxGxxxExGPRAR (at position 263 in the *M. jannaschii* sequence).

7.7 COMPLEX MEMBRANE-BOUND HYDROGENASES

Multi-subunit membrane-hydrogenases are built up by at least six subunits which are all homologous to complex I subunits. These hydrogenases seem to couple proton reduction to the generation of a proton motive force (chapter 6, Fox *et al.*, 1996b and Künkel *et al.*, 1998). In *Methanobacterium thermoautotrophicum*, the energy accumulated in this proton gradient has been proposed to drive the reduction of very-low-potential electron carriers. These would function as efficient electron donors to

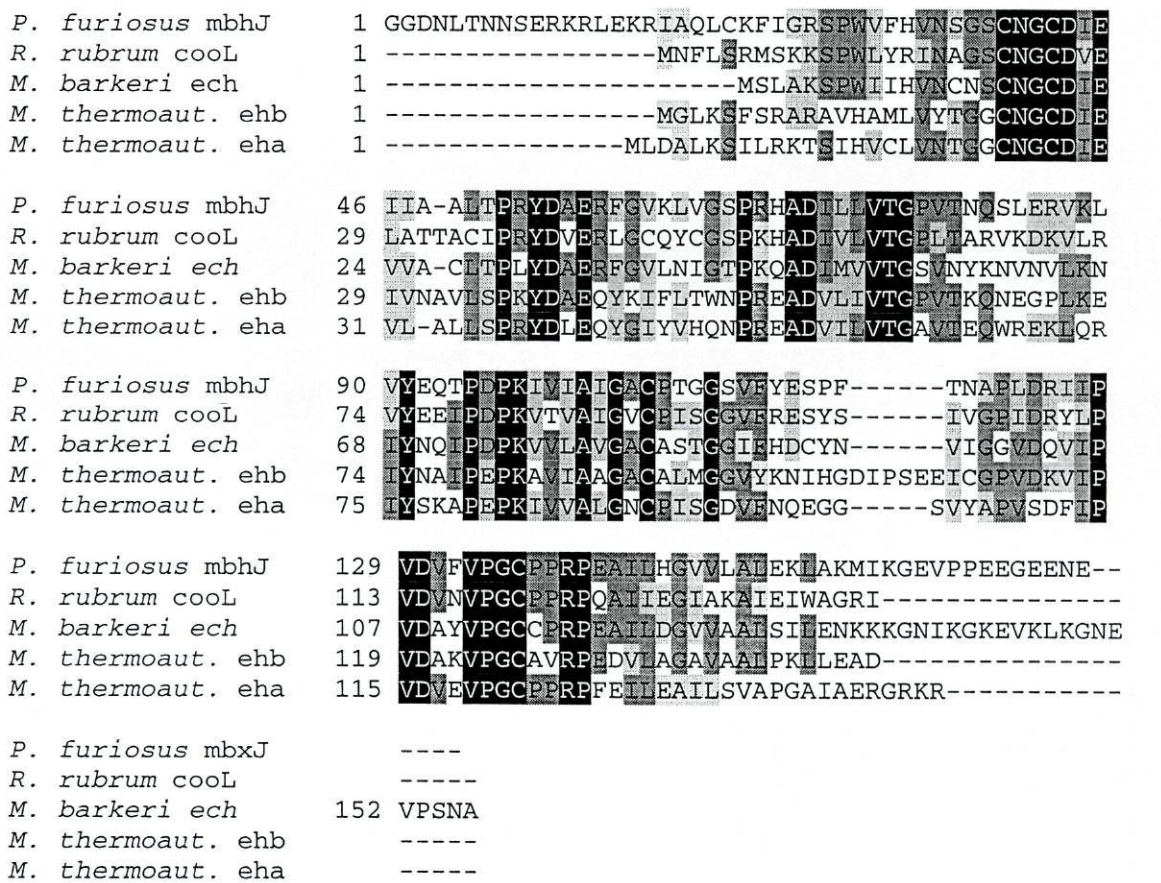

Figure 7.11 Multiple alignment of small subunits of complex membrane-bound hydrogenases. Strictly conserved amino acids are shaded black; amino acids conserved in most sequences are shaded dark grey; similar amino acids are shaded light grey.

reactions with a redox potential lower than the H^+/H_2 couple. (Tersteegen and Hedderich, 1999).

The small and large subunits of these hydrogenases show a higher degree of sequence identity to the corresponding complex I subunits than to other [NiFe] hydrogenases (Friedrich and Weiss, 1997). The identification of specific signatures that allow the unambiguous assignment of these proteins thus assumes special relevance.

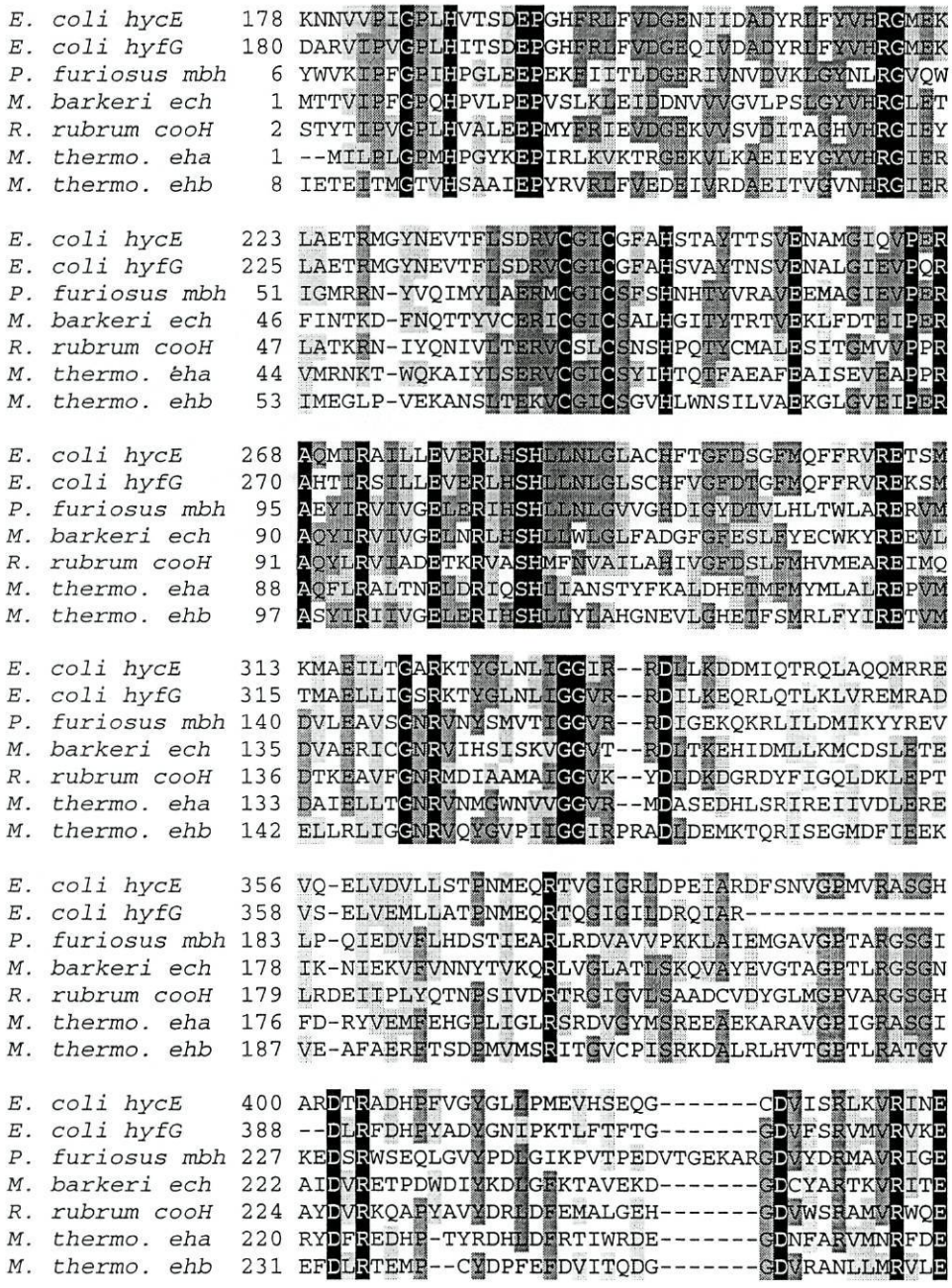

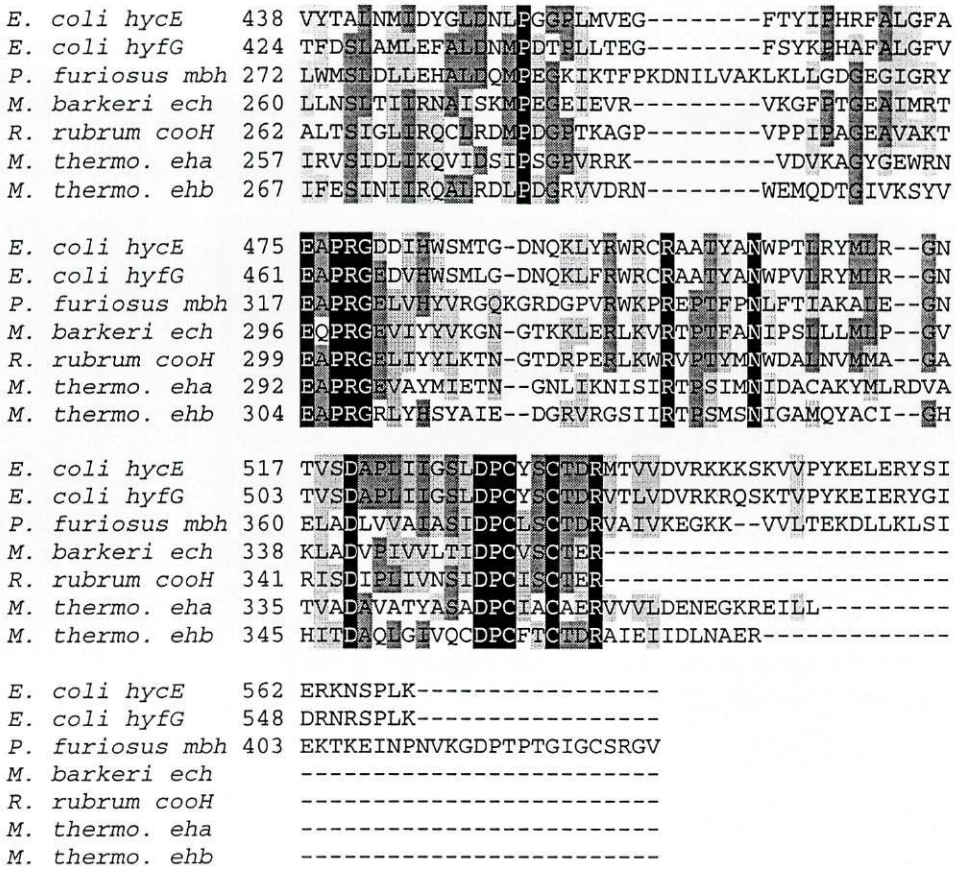

Figure 7.12 Multiple alignment of "large" subunits of complex membrane-bound hydrogenases. Strictly conserved amino acids are shaded black; amino acids conserved in most sequences are shaded dark grey; similar amino acids are shaded light grey. The E. coli proteins posses a very long N-terminal absent from the other hydrogenases. Therefore the alignment is shown only from the point where similarity between all sequences exist.

The "small" subunits of complex membrane-bound hydrogenases are even shorter than the small subunits of the NAD-linked hydrogenases (Figure 7.11). These subunits are very similar to NADH-ubiquinone oxidoreductase "20 kDa" (nuoB) subunits, and only marginally similar to the small subunits of other hydrogenases. However, all four Cys residues involved in the coordination of the proximal cluster in regular hydrogenases are present in these proteins (Cys 37, 41, 106 and 136 in *P. furiosus* MbhJ). Two signatures that enable the distinction of these small subunits from their NADH-ubiquinone oxidoreductase homologs have been found. These are

P (R/K) x AD***VTGpvt (where * stands for a hydrophobic residue) and P (D/E) PKiv*AiGaC. The Cys in the second signature is Cys106, a ligand to the [4Fe-4S] cluster.

The large subunits of the complex membrane-bound hydrogenases are a quite diverse group (Figure 7.12). Phylogenetic analysis of the alignment shows that this group further separates into two subclusters (Figure 7.2). The two "energy-conserving" hydrogenases from *M. thermoautotrophicum* (Tersteegen and Hedderich, 1999) cluster together, apart from the cluster that includes the other hydrogenases. The two hydrogenases from *E. coli* seem to form yet another subdivision inside this cluster. They are also considerably longer than the other large subunits. Two specific signatures for the large subunits of these diverse group have been found: E l e R l h S H l l (from amino acid 95 in the *P. furiosus* large subunit) and D P C l s C t - R (the C-terminal Ni-binding motif). This last signature affords however one single misidentification: mesothelin or CAK1 antigen precursor from humans bears the sequence D P C W S C G D R close to the N-terminal. Because of the paucity of sequences in the subclusters no reliable fingerprints to assign a protein to one of them could be found.

7.8 ATYPICAL HYDROGENASES (MBXJ FROM *P. FURIOSUS* AND HOMOLOGUES)

The genome of *P. furiosus* contains an operon that has been proposed to code for an atypical complex membrane-bound hydrogenase. Homologs of this atypical hydrogenase have been found in the genomes of other *Pyrococcus* species and of the hyperthermophilic Bacterium *Thermotoga maritima*. The small subunits of these hydrogenases are very similar to each other. Like the "small" subunits of the regular complex-membrane-bound hydrogenases, they are very short and contain the four conserved Cys proposed to bind the proximal [4Fe-4S] cluster. Five conserved motifs

that are absent in all other proteins (including the closely related NADH: ubiquinone oxidoreductase components and membrane-bound hydrogenases) have been found. These are (from the N-terminal to the C-terminal of the sequences): CTGCG**E*PP, which includes two Cys involved in the binding of the Fe-S cluster, KTLkRiI, LDkYIPVDV, GEADGWkRY and ENYEWYrkNQ. Only this very limited set of sequences is available, and it is likely that some of the observed motifs will not be present in more divergent members of this class. This also applies to the first motif described, for which a function is known: the first half of the motif (**CTGCG**) is

The small subunits

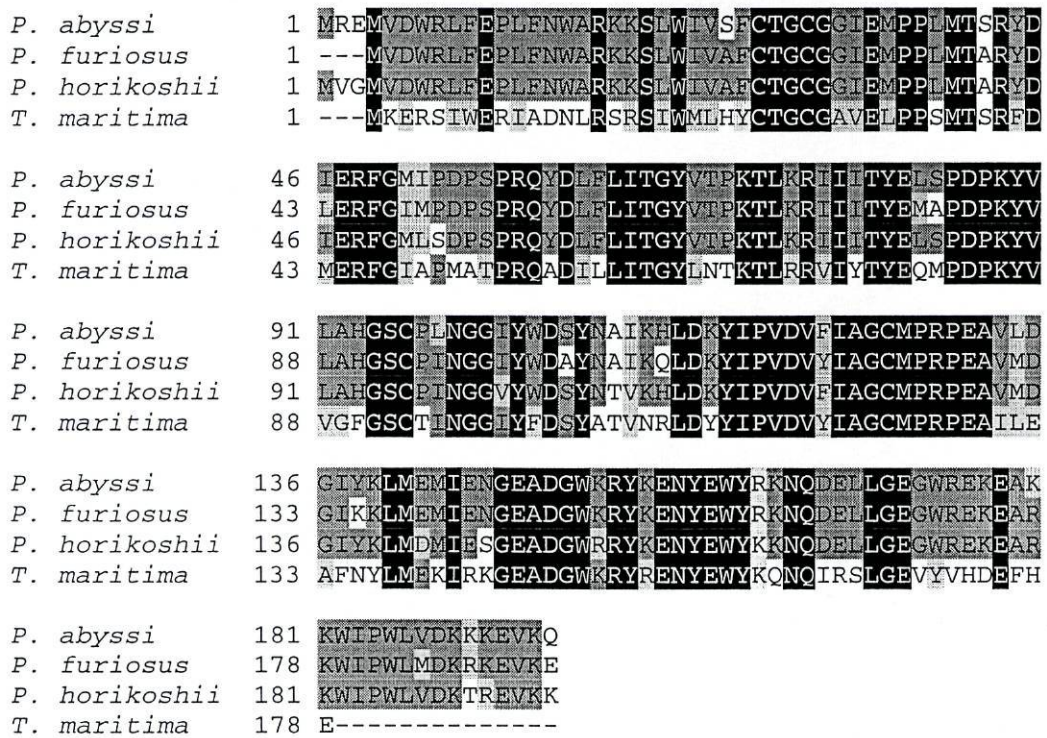

Figure 7.13 Multiple alignment of "small" subunits of atypical membrane-bound hydrogenases. Strictly conserved amino acids are shaded black; amino acids conserved in most sequences are shaded dark grey; similar amino acids are shaded light grey.

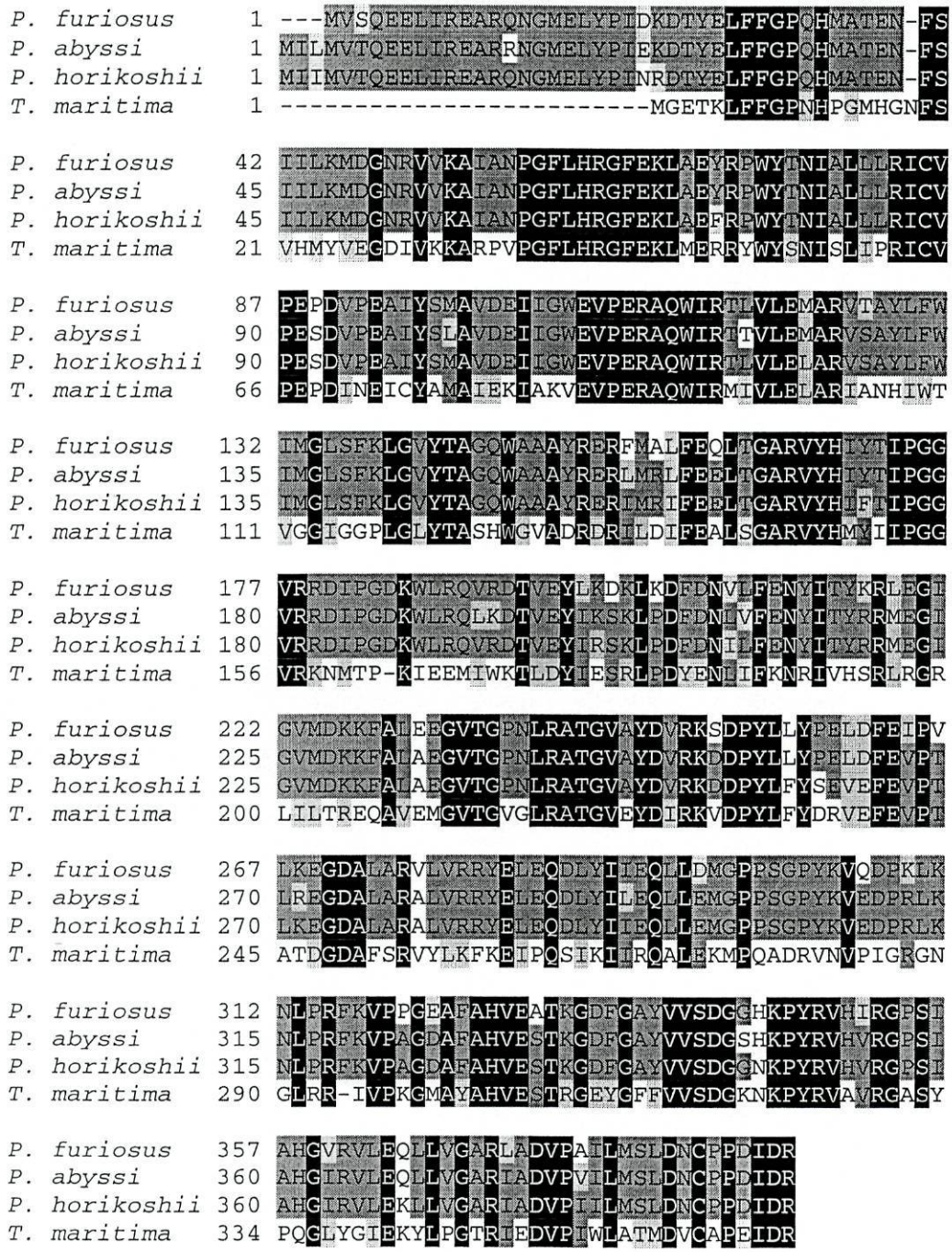

Figure 7.14 Multiple alignment of "large" subunits of atypical membrane-bound hydrogenases. Strictly conserved amino acids are shaded black; amino acids conserved in most sequences are shaded dark grey; similar amino acids are shaded light grey.

present in a wide range of proteins, and more divergent members of this class may not conserve the second half (**E*PP). It seems therefore wiser to use the signatures of the "large" subunit (see below) to look for atypical hydrogenases. "Small" subunits might be found by comparing neighboring genes to the known sequences of these "small" subunits.

As with the "small" subunit, most of the sequences of the homologs of the "large" subunit of the putative fourth hydrogenase from *P. furiosus* are also from members of the genus *Pyrococcus*. They are all very similar to each other, and this complicates the task of finding reliable signatures, since most of the sequences are very conserved. The slight divergence of the sequence from *Thermotoga maritima* allows the detection of a somewhat stricter consensus. The putative Ni-coordinating motifs are atypical, since they do not contain four Cys as usual. In each of these motifs, the second Cys (which bridges the two metals (Fe and Ni) present in the active site) is replaced by an acidic residue, which suggests that the binuclear cluster in these hydrogenases will be μ-oxo-bridged. These two motifs (L * * R I **C** V P **E** * D — at position 84 on the *P. furiosus* sequence — and D x **C** p P (**D/E**) I D R — on the C-terminal) are very conserved, and a search with those motifs identifies no proteins outside this class. Although many of the other conserved regions are also present totally or partially in NADH: ubiquinone oxidoreductase subunits, some other putative conserved motifs were found to be very specific: ExRxWYxNI, FEeLtGARVYH, GxAfAHVEsT(R/K) and LvGaRiaDVP. However, since the sequences used are not very diverse and no function for these motifs can readily be ascertained by the analysis, there is a possibility that these will not be conserved in more divergent (yet undiscovered) members of this class.

7.9 DISCUSSION

Several of the classes of hydrogenases proposed by Wu and Mandrand (Wu and Mandrand, 1993) were not fully characterized at the time due to the small number of relevant sequences available. The recent availability of many new hydrogenase sequences has provided a means to refine the proposed classification of hydrogenases.

The study described in the preceding pages has afforded some new insights into the phylogeny and molecular diversity of these hydrogenases. In particular. sulfhydrogenases appear to be approximately equally distant from F_{420}-non-reducing, F_{420}-reducing and NAD-linked hydrogenases, forming a fourth subclass in Wu and Mandrand's class IV. The discovery of several specific fingerprints characteristic of each class of these hydrogenase may assist in the rapid assignment of a newly discovered sequence into one of these classes. Analysis of the cluster-binding regions raises the possibility that in sulfhydrogenases and F_{420}-non-reducing hydrogenases at least one of the clusters will have a pH-dependent redox potential, which may be yet another way of fine-tuning the enzymatic activity of these hydrogenases.

The study of complex and atypical membrane-bound hydrogenases revealed several highly specific signatures able to efficiently discriminate these hydrogenases from very similar NADH: ubiquinone oxidoreductases, with which they have so far been confused. It has further confirmed the specificity of the novel binding-motif suggested to bind the [NiFe] cluster in the atypical hydrogenases. However, the identification of the physiological role of these atypical hydrogenases cannot be deduced solely from the molecular analysis and must wait the purification and characterization of at least one member of this class. Due to the unprecedented nature of the cluster-binding motifs, some unusual chemistry may nonetheless be expected.

8

CONCLUSIONS

The pathway proposed to be involved in the disposal of reducing equivalents through H_2 production (1) (Ma *et al.*, 1994) was studied. This included the individual investigation of the involved enzymes (SuDH and sulfhydrogenase), as well as of the physiological activities in cell extracts.

(1) fermentation → ferredoxin → FNOR(SuDH) → NADPH → sulfhydrogenase → H^+

8.1 SULFHYDROGENASE

Sulfhydrogenase revealed a very rich and intricate temperature-dependent redox chemistry. Although the enzyme has measurable H_2-uptake activity at 45 °C, analysis of the temperature-dependence of this activity suggests that the kinetic properties of the enzyme change markedly at 64 °C (section 4.3 – Catalytic properties). This may reflect a change of conformation of the protein or of the active site, e. g., the transition of the [NiFe] center from the "unready" to the "ready" state or a change of the redox potentials of the metal centers involved. Upon incubation of the oxidized sulfhydrogenase in the presence of H_2 a remarkable increase in activity occurs. After activation the H_2-evolution / H_2-uptake ratio was observed to be less than unity, suggesting that the role of sulfhydrogenase in H_2 evolution will not be as important as assumed in the model of Ma *et al.*.

Incubation of anaerobically-oxidized sulfhydrogenase at 80 °C revealed a complex process of temperature-induced self-reduction. The identity of the internal reductant responsible for this process is not clear. Dithiothreitol seems to inhibit this process, suggesting the involvement of disulfide bridges in the process. This process has provided a very convenient way to generate different states of the [NiFe] active center for spectroscopic study. Most of these states are heterogeneous, showing signals attributed to "ready" and "unready" hydrogenase. Their EPR spectra are also

significantly more rhombic than the ones observed in mesophilic hydrogenases. Several other interesting differences were also found. The Ni-C signal of *P. furiosus* sulfhydrogenase saturates much easier than the corresponding signals from *Desulfovibrio* hydrogenases and, though the Ni-C signal disappears upon illumination at low temperature as observed in regular hydrogenases (section 4.4 – EPR measurements), no new paramagnetic species (corresponding to Ni-L) were detected.

All of these data point to the existence of subtle differences in the electronic environment of the [NiFe] center of the *P. furiosus* enzyme. It is possible that some of these differences reflect an adaptation of the active site to the thermodynamic conditions under which it must operate.

The role of the detected [Fe-S] clusters is still not clear. Sequence analysis has indicated that probably more [Fe-S] clusters are present in the enzyme than have so far been examined by EPR. Whether these clusters are not detected due to very low redox potentials or to other unusual properties remains to be determined. The results of a redox titration at high temperature suggest that under some conditions one of the clusters cannot be reduced by dithionite, even though the solution potential is much lower than the redox potential of this cluster. The undetected clusters may have a similar behavior, e. g. kinetically hampered reduction due to inaccessibility from the solvent.

8.2 SULFIDE DEHYDROGENASE

Sulfide dehydrogenase is a versatile flavo-iron-sulfur protein that catalyzes both the reduction of polysulfide by NADPH and of $NADP^+$ by ferredoxin (Ma and Adams, 1994; Ma *et al.*, 1994). Reduction of $NADP^+$ has been proposed to be a necessary step in the disposal of reducing equivalents as H_2 (scheme 1). The physiological role of sulfur reduction, however, is not clear (Schicho *et al.*, 1993).

A detailed study of the prosthetic groups of the sulfide dehydrogenase through sequence analysis and EPR-monitored redox titrations has provided a clearer picture of the composition of sulfide dehydrogenases. The protein was shown to carry three [Fe-S] clusters, each of them atypical in some way: a putative [2Fe-2S] cluster with novel $Asp(Cys)_3$ coordination and with the combination of physico-chemical properties hitherto exclusively ascribed to Rieske-type clusters; an apparently regular [3Fe-4S] cluster with an unusually high reduction potential; and a [4Fe-4S] cluster with unusual relaxation properties and reduction properties. The redox potential of the flavin is consistent with the proposed functions as S^0-reductase and ferredoxin: $NADP^+$ oxidoreductase, but the role of the high potential [2Fe-2S] and [3Fe-4S] in these reactions is not obvious.

Each of the subunits of SuDH appears to be a member of a different class of iron-sulfur flavoproteins. The SudB subunit is very similar to the reductase+ferredoxin systems from plants and algae. The SudA subunit carries the basic pattern found in a small class of iron-sulfur flavoproteins with iron-sulfur clusters of unusual properties, and for which crystallographic data are not yet available. It is likely that structural and functional studies of these homologous proteins may shed light on the mechanism of action and physiological functions of sulfide dehydrogenase.

8.3 THE PATHWAY OF HYDROGEN EVOLUTION FROM REDUCED FERREDOXIN

The actual hydrogen production by cell extracts of *P. furiosus* is much higher than accounted for by the activities of the enzymes involved in the pathway proposed by Ma et al. (Ma *et al.*, 1994). Most of the ferredoxin-dependent H_2-evolution is associated with the membrane.

The membrane-bound hydrogenase has been partially purified and characterized. It is a hydrogen-evolving hydrogenase (H_2-evolution *ca.* 250 times greater than H_2 uptake) virtually insensitive to CO. It can be inactivated by incubation with DCCD, which suggests the presence of proton-translocating segments in the protein. The membrane-bound hydrogenase may thus couple H_2 evolution to the formation of an electrochemical Na^+ or H^+ gradient, as proposed for similar hydrogenases from *M. barkeri* (Meuer *et al.*, 1999) and *R. rubrum* (Fox *et al.*, 1996b).

The protein is predicted to harbor three [Fe-S] clusters. EPR measurements show a signal originating from at least two interacting clusters with a redox potential *ca.* – 0.33 V (at room temperature). No EPR signals originating from the [NiFe] active site could be found. Even at room temperature the membrane-bound hydrogenase is quite active, and redox titrations are hampered by the diversion of reducing equivalents to proton reduction. In order to circumvent this problem it might be worthwhile to inhibit the enzyme with DCCD prior to a redox titration, since in principle DCCD will not interfere with the active site, but only with the MbhM subunit.

The thermodynamics of the process are also not fully understood. It is known that the redox potential of ferredoxin at high (i.e physiological) temperature is approximately equal to that of the proton/H_2 couple (Hagedoorn *et al.*, 1998), but this value is probably less relevant for the bioenergetics because ferredoxin is an electron-transfer intermediate. Presumably more important values (presently not available) will be the steady-state concentrations of the ultimate electron donors, glyceraldehyde-3-phosphate and pyruvate and their oxidation products. This knowledge would allow the estimation of the magnitude of the electrochemical gradient that might be generated by the membrane-bound hydrogenase.

The results obtained nonetheless allow the formulation of a novel model of the hydrogen metabolism in *P. furiosus*. Reduced ferredoxin produced by the catabolism transfers its electrons to the membrane-bound hydrogenase, which reduces protons to

H_2. If the ΔG of the process is favorable, concomitant H^+ or Na^+ translocation through the membrane will occur, allowing the formation of a gradient to be used in ATP synthesis or active transport. When the flow of reducing equivalents from ferredoxin is greater than can be handled efficiently by the membrane-bound hydrogenase, the pathway proposed by *Ma et al.* will become very relevant to the cell, allowing the disposal of the extra electrons. The H_2 formed can be used by the soluble hydrogenase to reduce $NADP^+$, thus providing an extra source of NADPH for anabolic processes.

8.4 INSIGHTS FROM SEQUENCE COMPARISONS

The recently available genome information shows the presence of another operon in *P. furiosus* that may code for a membrane-bound hydrogenase. The operon contains fourteen genes, each of them preceded by a ribosome-binding site. This suggests that this operon is effectively transcribed under at least some conditions. This putative hydrogenase contains an unusual binding motif for the [NiFe] cluster, which appears to be μ-oxo instead of μ-sulfo-bridged. Its electronic properties can thus be expected to deviate from those observed in the other hydrogenases.

Sequence comparisons between several hydrogenases have allowed the description of specific signatures that can be used to selectively distinguish these membrane-bound hydrogenases from each other and from the very similar NADH: ubiquinone oxidoreductases. Similar comparisons between sulfhydrogenases, F_{420}-reducing-, F_{420}-non-reducing- and NAD-linked hydrogenases have suggested the possibility that some of the clusters in the small subunits of sulfhydrogenases and F_{420}-non-reducing-hydrogenases may have pH-dependent potentials, allowing a more precise regulation of activity according to the physiological conditions. The validity of this proposal should be tested by redox titrations performed at different pHs.

9

REFERENCES

ADAMS, M. W. W. (1990) The structure and mechanism of iron-hydrogenases. *Biochim. Biophys. Acta* **1020**: 115-145.

ADAMS, M. W. W. (1992) Novel iron-sulfur centers in metalloenzymes from extremely thermophilic bacteria. *Adv. Inorg. Chem.* **38**: 341-396.

ADAMS, M. W. W. (1993) Enzymes and proteins from organisms that grow near and above 100 °C. *Annu. Rev. Microbiol.* **47**: 627-658.

ALBRACHT, S. P. (1994) Nickel hydrogenases: in search of the active site. *Biochim. Biophys. Acta* **1188**: 167-204.

ALBRACHT, S. P., GRAF, E. G. AND THAUER, R. K. (1982) The EPR properties of nickel in hydrogenase from *Methanobacterium thermoautotrophicum*. *FEBS Lett.* **140**: 311-313.

ALEX, L. A., REEVE, J. N., ORME-JOHNSON, W. H. AND WALSH, C. T. (1990) Cloning, sequence determination, and expression of the genes encoding the subunits of the nickel-containing 8-hydroxy-5-deazaflavin reducing hydrogenase from *Methanobacterium thermoautotrophicum* ΔH. *Biochemistry* **29**: 7237-7244.

ALTSCHUL, S. F., MADDEN, T. L., SCHAFFER, A. A., ZHANG, J., ZHANG, Z., MILLER, W. AND LIPMAN, D. J. (1997) Gapped BLAST and PSI-BLAST: a new generation of protein database search programs. *Nucleic Acids Res.* **25**: 3389-3402.

ANDREWS, S. C., BERKS, B. C., MCCLAY, J., AMBLER, A., QUAIL, M. A., GOLBY, P. AND GUEST, J. R. (1997) A 12-cistron *Escherichia coli* operon (hyf) encoding a putative proton-translocating formate hydrogenlyase system. *Microbiology* **143**: 3633-3647.

APPEL, J. AND SCHULZ, R. (1996) Sequence analysis of an operon of a NAD(P)-reducing nickel hydrogenase from the cyanobacterium *Synechocystis* sp. PCC 6803 gives additional evidence for direct coupling of the enzyme to NAD(P)H-dehydrogenase (complex I). *Biochim. Biophys. Acta* **1298**: 141-147.

APPEL, J., PHUNPRUCH, S., STEINMULLER, K. AND SCHULZ, R. (2000) The bidirectional hydrogenase of *Synechocystis* sp. PCC 6803 works as an electron valve during photosynthesis. *Arch. Microbiol.* **173**: 333-338.

ARENDSEN, A. F., VEENHUIZEN, P. T. AND HAGEN, W. R. (1995) Redox properties of the sulfhydrogenase from *Pyrococcus furiosus*. *FEBS Lett.* **368**: 117-121.

BAGLEY, K. A., VAN GARDEREN, C. J., CHEN, M., DUIN, E. C., ALBRACHT, S. P. AND WOODRUFF, W. H. (1994) Infrared studies on the interaction of carbon monoxide with divalent nickel in hydrogenase from *Chromatium vinosum*. *Biochemistry* **33**: 9229-9236.

BAGLEY, K. A., DUIN, E. C., ROSEBOOM, W., ALBRACHT, S. P. AND WOODRUFF, W. H. (1995) Infrared-detectable groups sense changes in charge density on the nickel center in hydrogenase from *Chromatium vinosum*. *Biochemistry* **34**: 5527-5535.

BAGYINKA, C., WHITEHEAD, J. P. AND MARONEY, M. J. (1993) An X-ray absorption spectroscopic study of nickel redox chemistry in hydrogenase. *J. Am. Chem. Soc.* **115**: 3576-3585.

BÉLAICH, J.-P., BRUSCHI, M. AND GARCIA, J.-L. (1990) MICROBIOLOGY AND BIOCHEMISTRY OF STRICT ANAEROBES INVOLVED IN INTERSPECIES HYDROGEN TRANSFER, Plenum Press, New York and London.

BENEMANN, J. (1996) Hydrogen biotechnology: progress and prospects. *Nature Biotechnology* **14**: 1101-1103.

BENSADOUN, A. AND WEINSTEIN, D. (1976) Assays of proteins in the presence of interfering materials. *Anal. Biochem.* **70**: 241-250.

BERENDT, U., HAVERKAMP, T., PRIOR, A. AND SCHWENN, J. D. (1995) Reaction mechanism of thioredoxin: 3'-phospho-adenylylsulfate reductase investigated by site-directed mutagenesis. *Eur. J. Biochem.* **233**: 347-356.

BERTRAND, P., DOLE, F., ASSO, M. AND GUIGLIARELLI, B. (2000) Is there a rate-limiting step in the catalytic cycle of [NiFe] hydrogenases? *J. Biol. Inorg. Chem.* **5**: 682-690.

BINGEMANN, R. AND KLEIN, A. (2000) Conversion of the central [4Fe-4S] cluster into a [3Fe-4S] cluster leads to reduced hydrogen-uptake activity of the F_{420}-reducing hydrogenase of *Methanococcus voltae*. *Eur. J. Biochem.* **267**: 6612-6618.

BJELLQVIST, B., HUGHES, G. J., PASQUALI, C., PAQUET, N., RAVIER, F., SANCHEZ, J. C., FRUTIGER, S. AND HOCHSTRASSER, D. F. (1993) The focussing positions of polypeptides in immobilized pH gradients can be predicted from their amino acid sequences. *Electrophoresis* **14**: 1023-1031.

BLAMEY, J. M. AND ADAMS, M. W. (1993) Purification and characterization of pyruvate ferredoxin oxidoreductase from the hyperthermophilic archaeon *Pyrococcus furiosus*. *Biochim. Biophys. Acta* **1161**: 19-27.

BLUMENTALS, I. I., ITOH, M., OLSON, G. J. AND KELLY, R. M. (1990) Role of polysulfides in reduction of elemental sulfur by the hyperthermophilic archaebacterium *Pyrococcus furiosus*. *Appl. Environ. Microbiol.* **56**: 1255-1262.

BÖHM, R., SAUTER, M. AND BOCK, A. (1990) Nucleotide sequence and expression of an operon *in Escherichia coli* coding for formate hydrogenlyase components. *Mol. Microbiol.* **4**: 231-243.

BORGES, K. M., BRUUET, S. R., BOGERT, A., DAVIS, M. C., HUJER, K. M., DOMKE, S. T., SZASZ, J., RAVEL, J., DIRUGGIERO, J., FULLER, C., CHASE, J. W. AND ROBB, F. T. (1996) A survey of the genome of the hyperthermophilic archaeon *Pyrococcus furiosus*. *Genome Sci. Technol.* **1**: 37-46.

BREDT, D. S., HWANG, P. M., GLATT, C. E., LOWENSTEIN, C., REED, R. R. AND SNYDER, S. H. (1991) Cloned and expressed nitric oxide synthase structurally resembles cytochrome P-450 reductase. *Nature* **351**: 714-718.

BRUNS, C. M. AND KARPLUS, P. A. (1995) Refined crystal structure of spinach ferredoxin reductase at 1.7 Å resolution: oxidized, reduced and 2'-phospho-5'-AMP bound states. *J. Mol. Biol.* **247**: 125-145.

BRYANT, F. O. AND ADAMS, M. W. (1989) Characterization of hydrogenase from the hyperthermophilic archaebacterium, *Pyrococcus furiosus*. *J. Biol. Chem.* **264**: 5070-5079.

BULT, C. J., WHITE, O., OLSEN, G. J., ZHOU, L., FLEISCHMANN, R. D., SUTTON, G. G., BLAKE, J. A., FITZGERALD, L. M., CLAYTON, R. A., GOCAYNE, J. D., KERLAVAGE, A. R., DOUGHERTY, B. A., TOMB, J. F., ADAMS, M. D., REICH, C. I., OVERBEEK, R., KIRKNESS,

E. F., WEINSTOCK, K. G., MERRICK, J. M., GLODEK, A., SCOTT, J. L., GEOGHAGEN, N. S. M., WEIDMAN, J. F., FUHRMANN, J. L., NGUYEN, D., UTTERBACK, T. R., KELLEY, J. M., PETERSON, J. D., SADOW, P. W., HANNA, M. C., COTTON, M. D., ROBERTS, K. M., HURST, M. A., KAINE, B. P., BORODOVSKY, M., KLENK, H. P., FRASER, C. M., SMITH, H. O., WOESE, C. R. AND VENTER, J. C. (1996) Complete genome sequence of the methanogenic archaeon *Methanococcus jannaschii*. *Science* **273**: 1058-1073.

BURNS, R. C. AND BULEN, W. A. (1965) ATP-dependent hydrogen evolution by cell-free preparations of *Azotobacter vinelandii*. *Biochim. Biophys. Acta* **105**: 437-445.

CAMMACK, R. (1992) Iron-sulfur clusters in enzymes: themes and variations. *Adv. Inorg. Chem.* **38**: 281-322.

CAMMACK, R., PATIL, D. S., HATCHIKIAN, E. C. AND FERNANDEZ, V. M. (1987) Nickel and iron-sulphur centres in *Desulfovibrio gigas* hydrogenase: ESR spectra, redox properties and interactions. *Biochim. Biophys. Acta* **912**: 98-109.

CAMMACK, R., BAGYINKA, C. AND KOVACS, K. L. (1989) Spectroscopic characterization of the nickel and iron-sulphur clusters of hydrogenase from the purple photosynthetic bacterium *Thiocapsa roseopersicina*. 1. Electron spin resonance spectroscopy. *Eur. J. Biochem.* **182**: 357-362.

CAVICCHIOLI, R., KALESNIKOW, T., CHIANG, R. C. AND GUNSALUS, R. P. (1996) Characterization of the aegA locus of *Escherichia coli*: control of gene expression in response to anaerobiosis and nitrate. *J. Bacteriol.* **178**: 6968-6974.

CHAN, M. K., MUKUND, S., KLETZIN, A., ADAMS, M. W. W. AND REES, D. C. (1995) Structure of a hyperthermophilic tungstopterin enzyme, aldehyde ferredoxin oxidoreductase. *Science* **267**: 1463-1469.

CLARK, W. M. (1960) ***THE OXIDATION-REDUCTION POTENTIALS OF ORGANIC SYSTEMS***, Williams and Wilkins, Baltimore.

CONOVER, R. C., KOWAL, A. T., FU, W. G., PARK, J. B., AONO, S., ADAMS, M. W. AND JOHNSON, M. K. (1990) Spectroscopic characterization of the novel iron-sulfur cluster in *Pyrococcus furiosus* ferredoxin. *J. Biol. Chem.* **265**: 8533-8541.

CONSALVI, V., CHIARALUCE, R., POLITI, L., VACCARO, R., DE ROSA, M. AND SCANDURRA, R. (1991) Extremely thermostable glutamate dehydrogenase from the hyperthermophilic archaebacterium *Pyrococcus furiosus. Eur. J. Biochem.* **202**: 1189–1196.

COREMANS, J. M., VAN DER ZWAAN, J. W. AND ALBRACHT, S. P. (1992) Distinct redox behaviour of prosthetic groups in ready and unready hydrogenase from *Chromatium vinosum. Biochim. Biophys. Acta* **1119**: 157-168.

DAVIDSON, G., CHOUDHURY, S. B., GU, Z., BOSE, K., ROSEBOOM, W., ALBRACHT, S. P. J. AND MARONEY, M. J. (2000) Structural examination of the nickel site in *Chromatium vinosum* hydrogenase: redox state oscillations and structural changes accompanying reductive activation and CO binding. *Biochemistry* **39**: 7468-7479.

DE GIOIA, L., FANTUCCI, P., GUIGLIARELLI, B. AND BERTRAND, P. (1999a) Ni-Fe hydrogenases: A density functional theory study of active site models. *Inorg. Chem.* **38**: 2658-2662.

DE GIOIA, L., FANTUCCI, P., GUIGLIARELLI, B. AND BERTRAND, P. (1999b) *Ab initio* investigation of the structural and electronic differences between active-site models of [NiFe] and [NiFeSe] hydrogenases. *Int. J. Quantum Chem.* **73**: 187-195.

DE LACEY, A. L., HATCHIKIAN, E. C., VOLBEDA, A., FREY, M., FONTECILLA-CAMPS, J. C. AND FERNANDEZ, V. M. (1997) Infrared-spectroelectrochemical characterization of the [NiFe] hydrogenase of *Desulfovibrio gigas. J. Am. Chem. Soc.* **119**: 7181-7189.

DECKERS, H. M., WILSON, F. R. AND VOORDOUW, G. (1990) Cloning and sequencing of a [NiFe] hydrogenase operon from *Desulfovibrio vulgaris* Miyazaki F. *J. Gen. Microbiol.* **136**: 2021-2028.

DEPPENMEIER, U., LIENARD, T. AND GOTTSCHALK, G. (1999) Novel reactions involved in energy conservation by methanogenic archaea. *FEBS Lett.* **457**: 291-297.

DIRMEIER, R., KELLER, M., FREY, G., HUBER, H. AND STETTER, K. O. (1998) Purification and properties of an extremely thermostable membrane-bound sulfur-reducing complex from the hyperthermophilic *Pyrodictium abyssi. Eur. J. Biochem.* **252**: 486-491.

DOLE, F., MEDINA, M., MORE, C., CAMMACK, R., BERTRAND, P. AND GUIGLIARELLI, B. (1996) Spin-spin interactions between the Ni site and the [4Fe-4S] centers as a probe of light-induced structural changes in active *Desulfovibrio gigas* hydrogenase. *Biochemistry* **35**: 16399-16406.

DOLE, F., FOURNEL, A., MAGRO, V., HATCHIKIAN, E. C., BERTRAND, P. AND GUIGLIARELLI, B. (1997) Nature and electronic structure of the Ni-X dinuclear center of *Desulfovibrio gigas* hydrogenase. Implications for the enzymatic mechanism. *Biochemistry* **36**: 7847-7854.

EGGINK, G., ENGEL, H., VRIEND, G., TERPSTRA, P. AND WITHOLT, B. (1990) Rubredoxin reductase of *Pseudomonas olevorans*. Structural relationship to other flavoprotein oxidoreductases based on one NAD and two FAD fingerprints. *J. Mol. Biol.* **212**: 135-142.

ERKENS, A., SCHNEIDER, K. AND MÜLLER, A. (1996) The NAD-linked soluble hydrogenase from *Alcaligenes eutrophus* H16: detection and characterization of EPR signals from nickel and flavin. *J. Biol. Inorg. Chem.* **1**: 99-110.

FAN, C., TEIXEIRA, M., MOURA, J., MOURA, I., HUYNH, B. H., LE GALL, J., PECK, H. D. J. AND HOFFMAN, B. M. (1991) Detection and characterization of exchangeable protons bound to the hydrogen-activation nickel site of *Desulfovibrio gigas* hydrogenase: a proton and deuteron Q-band ENDOR study. *J. Am. Chem. Soc.* **113**: 20-24.

FARKAS, A. (1936) ***ORTOHYDROGEN, PARAHYDROGEN AND HEAVY HYDROGEN***, Cambridge Univ. Press, London.

FAUQUE, G., PECK, H. D. J., MOURA, J. J., HUYNH, B. H., BERLIER, Y., DERVARTANIAN, D. V., TEIXEIRA, M., PRZYBYLA, A. E., LESPINAT, P. A., MOURA, I. AND LE GALL, J. (1988) The three classes of hydrogenases from sulfate-reducing bacteria of the genus *Desulfovibrio*. *FEMS Microbiol. Rev.* **4**: 299-344.

FELSENSTEIN, J. (1985) Confidence limits on phylogenies: an approach using the bootstrap. *Evolution* **39**: 783-791.

FERNANDEZ, V. M., HATCHIKIAN, E. C. AND CAMMACK, R. (1985) Properties and reactivation of two different deactivated forms of *Desulfovibrio gigas* hydrogenase. *Biochim. Biophys. Acta* **832**: 69-79.

FIALA, G. AND STETTER, K. O. (1986) *Pyrococcus furiosus* sp. nov. represents a novel genus of marine heterotrophic archaebacteria growing optimally at 100° C. *Arch. Microbiol.* **145**: 56-61.

FONTECILLA-CAMPS, J. C. (1996) The active site of Ni-Fe hydrogenases: model chemistry and crystallographic results. *J. Biol. Inorg. Chem.* **1**: 91-98.

FOX, J. D., KERBY, R. L., ROBERTS, G. P. AND LUDDEN, P. W. (1996a) Characterization of the CO-induced CO-tolerant hydrogenase from *Rhodospirillum rubrum* and the gene encoding the large subunit of the enzyme. *J. Bacteriol.* **178**: 1515-1524.

FOX, J. D., HE, Y., SHELVER, D., ROBERTS, G. P. AND LUDDEN, P. W. (1996b) Characterization of the region encoding the CO-induced hydrogenase of *Rhodospirillum rubrum*. *J. Bacteriol.* **178**: 6200-6206.

FRIEDRICH, T. AND WEISS, H. (1997) Modular evolution of the respiratory NADH: ubiquinone oxidoreductase and the origin of its modules. *J. Theor. Biol.* **187**: 529-541.

GARCIN, E., VERNEDE, X., HATCHIKIAN, E. C., VOLBEDA, A., FREY, M. AND FONTECILLA-CAMPS, J. C. (1999) The crystal structure of a reduced [NiFeSe] hydrogenase provides an image of the activated catalytic center. *Structure Fold Des* **7**: 557-566.

GENOSCOPE (2000) COMPLETE GENOME SEQUENCING OF *PYROCOCCUS ABYSSI*. Available online at http://www.genoscope.cns.fr/cgi-bin/Pab.cgi

GLASSTONE, W. S., LAIDLER, K. J. AND EYRING, H. (1941) ***THE THEORY OF RATE PROCESSES***, McGraw Hill Book Company, New York and London.

GONNET, G. H., COHEN, M. A. AND BENNER, S. A. (1992) Exhaustive matching of the entire protein sequence database. *Science* **256**: 1443-1445.

GRAF, E. G. AND THAUER, R. K. (1981) Hydrogenase from *Methanobacterium thermoautotrophicum*, a nickel containing enzyme. *FEBS Lett.* **136**: 165-169.

GU, Z. J., DONG, J., ALLAN, C. B., CHOUDHURY, S. B., FRANCO, R., MOURA, J. J. G., LEGALL, J., PRZYBYLA, A. E., ROSEBOOM, W., ALBRACHT, S. P. J., AXLEY, M. J., SCOTT, R. A. AND MARONEY, M. J. (1996) Structure of the Ni sites in hydrogenases by X-ray absorption spectroscopy. Species variation and the effects of redox poise. *J. Am. Chem. Soc.* **118**: 11155-11165.

HAGEDOORN, P.-L., DRIESSEN, M. C. P. F., VAN DEN BOSCH, M., LANDA, I. AND HAGEN, W. R. (1998) Hyperthermophilic redox chemistry: a re-evaluation. *FEBS Lett.* **440**: 311-314.

HAGEDOORN, P. L., FREIJE, J. R. AND HAGEN, W. R. (1999) *Pyrococcus furiosus* glyceraldehyde 3-phosphate oxidoreductase has comparable W6+/5+ and W5+/4+ reduction potentials and unusual [4Fe-4S] EPR properties. *FEBS Lett.*. **462**: 66-70.

HAGEN, W. R. (1989) in ***ADVANCED EPR: APPLICATIONS IN BIOLOGY AND BIOCHEMISTRY.*** (Hoff, A. J., Ed.) pp 785-812, Elsevier, Amsterdam.

HAGEN, W. R., DUNHAM, W. R., JOHNSON, M. K. AND FEE, J. A. (1985) Quarter field resonance and integer-spin/half-spin interaction in the EPR of *Thermus thermophilus* ferredoxin. Possible new fingerprints for three iron clusters. *Biochim. Biophys. Acta* **828**: 369-374.

HAGEN, W. R., VANONI, M. A., ROSENBAUM, K. AND SCHNACKERZ K. D. (2000) On the iron-sulfur clusters in the complex redox enzyme dihydropyrimidine dehydrogenase. *Eur. J. Biochem.* **267**: 3640-3646.

HÄGERHÄLL, C. (1997) Succinate: quinone oxidoreductases. Variations on a conserved theme. *Biochim. Biophys. Acta* **1320**: 107-141.

HALBOTH, S. AND KLEIN, A. (1992) *Methanococcus voltae* harbors four gene clusters potentially encoding two [NiFe] and two [NiFeSe] hydrogenases each of the cofactor F_{420}-reducing or F_{420}-non-reducing types. *Mol. Gen. Genet.* **233**: 217-224.

HE, S.-H., TEIXEIRA, M., LEGALL, J., PATIL, D. S., MOURA, I., MOURA, J. J. G., DERVARTANIAN, D. V., HUYNH, B.-H. AND PECK, H. D. J. (1989) EPR studies with 77Se-enriched [NiFeSe] hydrogenase of *Desulfovibrio baculatus*. *J. Biol. Chem.* **264**: 2678-2682.

HEDDERICH, R., KLIMMEK, O., KRÖGER, A., DIRMEIER, R., KELLER, M. AND STETTER, K. O. (1999) Anaerobic respiration with elemental sulfur and with disulfides. *FEMS Microbiol. Rev.* **22**: 351-381.

HEIDER, J., MAI, X. AND ADAMS, M. W. (1996) Characterization of 2-ketoisovalerate ferredoxin oxidoreductase, a new and reversible coenzyme A-dependent enzyme involved in peptide fermentation by hyperthermophilic archaea. *J. Bacteriol.* **178**: 780-787.

HEMMINGSEN, T. (1992) The electrochemical reaction of sulphur-oxygen compounds - part I. A review of literature on the electrochemical properties of sulphur/sulphur-oxygen compounds. *Electrochim. Acta* **37**: 2275-2284.

HIGUCHI, Y., YAGI, T. AND YASUOKA, N. (1997) Unusual ligand structure in Ni-Fe active center and an additional Mg site in hydrogenase revealed by high resolution X-ray structure analysis. *Structure* **5**: 1671-1680.

HIGUCHI, Y. AND YAGI, T. (1999a) Liberation of hydrogen sulfide during the catalytic action of *Desulfovibrio* hydrogenase under the atmosphere of hydrogen. *Biochem. Biophys. Res. Commun.* **255**: 295-299.

HIGUCHI, Y., OGATA, H., MIKI, K., YASUOKA, N. AND YAGI, T. (1999b) Removal of the Bridging Ligand Atom at the Ni-Fe Active Site of [NiFe] Hydrogenase Upon Reduction with H_2, as Revealed by X-Ray Structure Analysis at 1.4 Å Resolution. *Structure Fold Des* **7**: 549-556

HORNHARDT, S., SCHNEIDER, K. AND SCHLEGEL, H. G. (1986) Characterization of a native subunit of the NAD-linked hydrogenase isolated from a mutant of *Alcaligenes eutrophus* H16. *Biochimie* **68**: 15-24.

HU, Y., FAHAM, S., ROY, R., ADAMS, M. W. W. AND REES, D. C. (1998) Formaldehyde ferredoxin oxidoreductase from *Pyrococcus furiosus*: the 1.85 Å resolution crystal structure and its mechanistic implications. *J. Mol. Biol.* **286**: 899-914.

HUANG, C. J. AND BARRETT, E. L. (1991) Sequence analysis and expression of the *Salmonella typhimurium asr* operon encoding production of hydrogen sulfide from sulfite. *J. Bacteriol.* **173**: 1544-1553.

HUYETT, J. E., CAREPO, M., PAMPLONA, A., FRANCO, R., MOURA, I., MOURA, J. J. G. AND HOFFMAN, B. M. (1997) ^{57}Fe Q-band pulsed ENDOR of the hetero-dinuclear site of the nickel hydrogenase: Comparison of the NiA, NiB, and NiC states. *J. Am. Chem. Soc.* **119**: 9291-9292.

JOHNSON, M. K., DUDERSTADT, R. E. AND DUIN, E. C. (1999) Biological and synthetic [Fe_3S_4] clusters. *Adv. Inorg. Chem.* **47**: 1-82.

JONGSAREEJIT, B., RAHMAN, R. N. Z. A., FUJIWARA, S. AND IMANAKA, T. (1997) Gene cloning, sequencing and enzymatic properties of glutamate synthase from the hyperthermophilic archaeon *Pyrococcus* sp. KOD1. *Mol. Gen. Genet.* **254**: 635-642.

KARPLUS, P. A. AND BRUNS, C. M. (1994) Structure-function relations for ferredoxin reductase. *J. Bioenerg. Biomembr.* **26**: 89-99.

KAWARABAYASI, Y., SAWADA, M., HORIKAWA, H., HAIKAWA, Y., HINO, Y., YAMAMOTO, S., SEKINE, M., BABA, S., KOSUGI, H., HOSOYAMA, A., NAGAI, Y., SAKAI, M., OGURA, K., OTUKA, R., NAKAZAWA, H., TAKAMIYA, M., OHFUKU, Y., FUNAHASHI, T., TANAKA, T., KUDOH, Y., YAMAZAKI, J., KUSHIDA, N., OGUCHI, A., AOKI, K., NAKAMURA, Y., ROBB, T. F., HORIKOSHI, K., MASUCHI, Y., SHIZUYA, H. AND KIKUCHI, H. (1998) Complete sequence and gene organization of the genome of a hyper-thermophilic archaebacterium, *Pyrococcus horikoshii* OT3. *DNA Res.* **5**: 55-76.

KENGEN, S. W. M. AND STAMS, A. J. M. (1994) Formation of L-alanine as a reduced end product in carbohydrate fermentation by the hyperthermophilic archaeon *Pyrococcus furiosus*. *Arch. Microbiol.* **161**: 168-175.

KENGEN, S. W., DE BOK, F. A., VAN LOO, N. D., DIJKEMA, C., STAMS, A. J. AND DE VOS, W. M. (1994) Evidence for the operation of a novel Embden-Meyerhof pathway that involves ADP-dependent kinases during sugar fermentation by *Pyrococcus furiosus*. *J. Biol. Chem.* **269**: 17537-17541.

KENGEN, S. W. M., STAMS, A. J. M. AND DE VOS, W. M. (1996) Sugar metabolism of extremophiles. *FEMS Microbiol. Rev.* **18**: 119-138.

KIM, C., WOODWARD, C. A., KAUFMAN, E. N. AND ADAMS, M. W. W. (1999) Stability and sulfur-reduction activity in non-aqueous phase liquids of the hydrogenase from the hyperthermophile *Pyrococcus furiosus*. *Biotechnol. Bioeng.* **65**: 108-113.

KRAFT, T., BOKRANZ, M., KLIMMEK, O., SCHRÖDER, I., FAHRENHOLZ, F., KOJRO, E. AND KRÖGER, A. (1992) Cloning and nucleotide sequence of the *psrA* gene of *Wolinella succinogenes* polysulfide reductase. *Eur. J. Biochem.* **206**: 503-510.

KRASNA, A. I. AND RITTENBERG, D. (1954) The mechanism of action of the enzyme hydrogenase. *J. Am. Chem. Soc.* **76**: 3015-3020.

KÜNKEL, A., VORHOLT, J. A., THAUER, R. K. AND HEDDERICH, R. (1998) An *Escherichia coli* hydrogenase-3-type hydrogenase in methanogenic archaea. *Eur. J. Biochem.* **252**: 467-476.

LAEMMLI, U. K. (1970) Cleavage of structural proteins during the assembly of the head of bacteriophage T4. *Nature* **227**: 680-685.

LEIF, H., SLED, V. D., OHNISHI, T., WIESS, H. AND FRIEDRICH, T. (1995) Isolation and characterization of the proton-translocating NADH: ubiquinone oxidoreductase from *Escherichia coli*. *Eur. J. Biochem.* **230**.

LINK, T. A. (1999) The structure of Rieske and Rieske-type proteins. *Adv. Inorg. Chem.* **47**: 83-157.

MA, K., SCHICHO, R. N., KELLY, R. M. AND ADAMS, M. W. (1993) Hydrogenase of the hyperthermophile *Pyrococcus furiosus* is an elemental sulfur reductase or sulfhydrogenase: evidence for a sulfur-reducing hydrogenase ancestor. *Proc. Natl. Acad. Sci. USA* **90**: 5341-5344.

MA, K., ZHOU, Z. H. AND ADAMS, M. W. W. (1994) Hydrogen production from pyruvate by enzymes purified from the hyperthermophilic archaeon, *Pyrococcus furiosus*: A key role for NADPH. *FEMS Microbiol. Lett.* **122**: 245-250.

MA, K. AND ADAMS, M. W. (1994) Sulfide dehydrogenase from the hyperthermophilic archaeon *Pyrococcus furiosus*: a new multifunctional enzyme involved in the reduction of elemental sulfur. *J. Bacteriol.* **176**: 6509-6517.

MA, K., HUTCHINS, A., SUNG, S. J. S. AND ADAMS, M. W. (1997) Pyruvate ferredoxin oxidoreductase from the hyperthermophilic archaeon, *Pyrococcus furiosus*, functions as a CoA-dependent pyruvate decarboxylase. *Proc. Natl. Acad. Sci. USA* **94**: 9608-9613.

MA, K., WEISS, R. AND ADAMS, M. W. W. (2000) Characterization of hydrogenase II from the hyperthermophilic archaeon *Pyrococcus furiosus* and assessment of its role in sulfur reduction. *J. Bacteriol.* **182**: 1864-1871.

MAI, X. AND ADAMS, M. W. (1994) Indolepyruvate ferredoxin oxidoreductase from the hyperthermophilic archaeon *Pyrococcus furiosus*. A new enzyme involved in peptide fermentation. *J. Biol. Chem.* **269**: 16726-16732.

MAI, X. AND ADAMS, M. W. (1996a) Characterization of a fourth type of 2-keto acid-oxidizing enzyme from a hyperthermophilic archaeon: 2-ketoglutarate ferredoxin oxidoreductase from *Thermococcus litoralis*. *J. Bacteriol.* **178**: 5890-5896.

MAI, X. AND ADAMS, M. W. W. (1996b) Purification and Characterization of Two Reversible and ADP-Dependent Acetyl Coenzyme A Synthetases from the Hyperthermophilic Archaeon *Pyrococcus furiosus*. *J. Bacteriol.* **178**: 5897-5903.

MASSEY, V. AND HEMMERICH, P. (1978) Photoreduction of flavoproteins and other biological compounds catalyzed by deazaflavins. *Biochemistry* **17**: 9-16.

MATHEWS, R., CHARLTON, S., SANDS, R. H. AND PALMER, G. (1974) On the nature of the spin coupling between the iron-sulfur clusters in the eight-iron ferredoxins. *J. Biol. Chem.* **249**: 4326-4328.

MENON, S. AND RAGSDALE, S. W. (1996) Unleashing hydrogenase activity in Carbon Monoxide Dehydrogenase/Acetyl-CoA Synthase and Pyruvate: Ferredoxin Oxidoreductase. *Biochemistry* **35**: 15814-15821.

MEUER, J., BAROSCHEK, S., KOCH, J., KÜNKEL, A. AND HEDDERICH, R. (1999) Purification and catalytic properties of Ech hydrogenase from *Methanosarcina barkeri*. *Eur. J. Biochem.* **265**: 325-335.

MONTET, Y., AMARA, P., VOLBEDA, A., VERNEDE, X., HATCHIKIAN, E. C., FIELD, M. J., FREY, M. AND FONTECILLA-CAMPS, J. C. (1997) Gas access to the active site of Ni-Fe

hydrogenases probed by X-ray crystallography and molecular dynamics. *Nat. Struct. Biol.* **4**: 523-526.

MUKUND, S. AND ADAMS, M. W. (1991) The novel tungsten-iron-sulfur protein of the hyperthermophilic archaebacterium, *Pyrococcus furiosus*, is an aldehyde ferredoxin oxidoreductase. Evidence for its participation in a unique glycolytic pathway. *J. Biol. Chem.* **266**: 14208-14216.

MUKUND, S. AND ADAMS, M. W. (1993) Characterization of a novel tungsten-containing formaldehyde ferredoxin oxidoreductase from the hyperthermophilic archaeon, *Thermococcus litoralis*. A role for tungsten in peptide catabolism. *J. Biol. Chem.* **268**: 13592-13600.

MUKUND, S. AND ADAMS, M. W. (1995) Glyceraldehyde-3-phosphate ferredoxin oxidoreductase, a novel tungsten-containing enzyme with a potential glycolytic role in the hyperthermophilic archaeon *Pyrococcus furiosus*. *J. Biol. Chem.* **270**: 8389-8392.

MURA, G. M., PEDRONI, P., PRATESI, C., GALLI, G., SERBOLISCA, L. AND GRANDI, G. (1996) The [Ni-Fe] hydrogenase from the thermophilic bacterium *Acetomicrobium flavidum*. *Microbiology* **142**: 829-836.

NELSON, K. E., CLAYTON, R. A., GILL, S. R., GWINN, M. L., DODSON, R. J., HAFT, D. H., HICKEY, E. K., PETERSON, J. D., NELSON, W. C., KETCHUM, K. A., MCDONALD, L., UTTERBACK, T. R., MALEK, J. A., LINHER, K. D., GARRETT, M. M., STEWART, A. M., COTTON, M. D., PRATT, M. S., PHILLIPS, C. A., RICHARDSON, D., HEIDELBERG, J., SUTTON, G. G., FLEISCHMANN, R. D., EISEN, J. A., WHITE, O., SALZBERG, S. L., O., S. H., VENTER, J. C. AND FRASER, C. M. (1999) Evidence for lateral gene transfer between Archaea and bacteria from genome sequence of *Thermotoga maritima*. *Nature* **399**: 323-329.

NICOLET, Y., PIRAS, C., LEGRAND, P., HATCHIKIAN, C. E. AND FONTECILLA-CAMPOS, J. C. (1999) *Desulfovibrio desulfuricans* iron hydrogenase: the structure shows unusual coordination to an active site Fe binuclear center. *Structure Fold. Des.* **7**: 13-23.

NISHIHARA, H., MIYASHITA, Y., AOYAMA, K., KODAMA, T., IGARASHI, Y. AND TAKAMURA, Y. (1997) Characterization of an extremely thermophilic and oxygen-stable

membrane-bound hydrogenase from a marine hydrogen-oxidizing bacterium *Hydrogenovibrio marinus*. *Biochem. Biophys. Res. Commun.* **232**: 766-770.

NIU, S. Q., THOMSON, L. M. AND HALL, M. B. (1999) Theoretical characterization of the reaction intermediates in a model of the nickel-iron hydrogenase of *Desulfovibrio gigas*. *J. Am. Chem. Soc.* **121**: 4000-4007.

PAGE, R. D. M. (1996) TREEVIEW: An application to display phylogenetic trees on personal computers. *Computer Applications in the Biosciences* **12**: 357-358.

PAVLOV, M., SIEGBAHN, P. E. M., BLOMBERG, M. R. A. AND CRABTREE, R. H. (1998) Mechanism of H-H activation by nickel-iron hydrogenase. *J. Am. Chem. Soc.* **120**: 548-555.

PAVLOV, M., BLOMBERG, M. R. A. AND SIEGBAHN, P. E. M. (1999) New aspects of H_2 activation by nickel-iron hydrogenase. *Int. J. Quantum Chem.* **73**: 197-207.

PEDRONI, P., DELLA VOLPE, A., GALLI, G., MURA, G. M., PRATESI, C. AND GRANDI, G. (1995) Characterization of the locus encoding the [Ni-Fe] sulfhydrogenase from the archaeon *Pyrococcus furiosus*: evidence for a relationship to bacterial sulfite reductases. *Microbiology* **141**: 449-458.

PERRIERE, G. AND GOUY, M. (1996) WWW-query: an on-line retrieval system for biological sequence banks. *Biochimie* **78**: 364-369.

PERSHAD, H. R., DUFF, J. L. C., HEERING, H. A., DUIN, E. C., ALBRACHT, S. P. J. AND ARMSTRONG, F. A. (1999) Catalytic electron transport in *Chromatium vinosum* [NiFe]-hydrogenase: application of voltammetry in detecting redox-active centers and establishing that hydrogen oxidation is very fast even at potentials close to the reversible H^+/H_2 value. *Biochemistry* **38**.

PETERS, J. W. (1999) Structure and mechanism of iron-only hydrogenases. *Curr. Opin. Struct. Biol.* **9**: 670-676.

PETERS, J. W., LANZILOTTA, W. N., LEMON, B. J. AND SEEFELDT, L. C. (1998) X-ray crystal structure of the Fe-only hydrogenase (CpI) from *Clostridium pasteurianum* to 1.8 angstrom resolution. *Science* **282**: 1853-1858.

PETERS, J. W. AND LEMON, B. J. (1999) Binding of exogenously added carbon monoxide at the active site of the iron-only hydrogenase CpI from *Clostridium pasteurianum. Biochemistry* **38**: 12969-12973.

PIERIK, A. J. AND HAGEN, W. R. (1991) S = 9/2 EPR signals are evidence against coupling between the siroheme and the Fe/S cluster prosthetic groups in *Desulfovibrio vulgaris* (Hildenborough) dissimilatory sulfite reductase. *Eur. J. Biochem.* **195**: 505-516.

PIERIK, A. J., HAGEN, W. R., REDEKER, J. S., WOLBERT, R. B., BOERSMA, M., VERHAGEN, M. F., GRANDE, H. J., VEEGER, C., MUTSAERS, P. H., SANDS, R. H. AND DUNHAM, W. R. (1992) Redox properties of the iron-sulfur clusters in activated Fe-hydrogenase from *Desulfovibrio vulgaris* (Hildenborough). *Eur. J. Biochem.* **209**: 63-72.

PIERIK, A. J., HULSTEIN, M., HAGEN, W. R. AND ALBRACHT, S. P. (1998) A low-spin iron with CN and CO as intrinsic ligands forms the core of the active site in [Fe]-hydrogenases. *Eur. J. Biochem.* **258**: 572-578.

PIERIK, A. J., ROSEBOOM, W., HAPPE, R. P., BAGLEY, K. A. AND ALBRACHT, S. P. (1999) Carbon monoxide and cyanide as intrinsic ligands to iron in the active site of [NiFe]-hydrogenases. $NiFe(CN)_2CO$. Biology's way to activate H_2. *J. Biol. Chem.* **274**: 3331-3337.

PIHL, T. AND MAIER, R. J. (1991) Purification and characterization of the hydrogen uptake hydrogenase from the hyperthermophilic Archaebacterium *Pyrodictium brockii. J. Bacteriol.* **273**: 1839-1844.

PIHL, T. D., BLACK, L. K., SCHULMAN, B. A. AND MAIER, R. J. (1992) Hydrogen-oxidizing electron transport components in the hyperthermophilic archaebacterium *Pyrodictium brockii. J. Bacteriol.* **174**: 137-143.

PRZYBYLA, A. E., ROBBINS, J., MENON, N. AND PECK, H. D., JR. (1992) Structure-function relationships among the nickel-containing hydrogenases. *FEMS Microbiol. Rev.* **88**: 109-135.

RÁKHELY, G., ZHOU, Z. H., ADAMS, M. W. W. AND KOVÁCS, K. L. (1999) Biochemical and molecular characterization of the [NiFe] hydrogenase from the hyperthermophilic archaeon, *Thermococcus litoralis. Eur. J. Biochem.* **266**: 1158-1165.

REEVE, J. N., BECKLER, G. S., CRAM, D. S., HAMILTON, P. T., BROWN, J. W., KRZYCKI, J. A., KOLODZIEJ, A. F., ALEX, L., ORME-JOHNSON, W. H. AND WALSH, C. T. (1989) A hydrogenase-linked gene in *Methanobacterium thermoautotrophicum* strain ΔH encodes a polyferredoxin. *Proc. Natl. Acad. Sci. U.S.A.* **86**: 3031-3035.

ROBB, F. T., PARK, J. B. AND ADAMS, M. W. W. (1992) Characterization of an extremely thermostable glutamate dehydrogenase: a key enzyme in the primary metabolism of the hyperthermophilic archaebacterium, *Pyrococcus furiosus*. *Biochim. Biophys. Acta* **1120**: 267-272.

ROBERTS, L. M. AND LINDAHL, P. A. (1994) Analysis of oxidative titrations of *Desulfovibrio gigas* hydrogenase; implications for the catalytic mechanism. *Biochemistry* **33**: 14339-14350.

ROSENBAUM, K., JAHNKE, K., CURTI, B., HAGEN, W. R., SCHNACKERZ, K. D. AND VANONI, M. A. (1998) Porcine recombinant dihydropyrimidine dehydrogenase: comparison of the spectroscopic and catalytic properties of the wild-type and C671A mutant enzymes. *Biochemistry* **37**: 17598-17609.

ROUSSET, M., MONTET, Y., GUIGLIARELLI, B., FORGET, N., ASSO, M., BERTRAND, P., FONTECILLA-CAMPS, J. C. AND HATCHIKIAN, E. C. (1998) [3Fe-4S] to [4Fe-4S] cluster conversion in *Desulfovibrio fructosovorans* [NiFe] hydrogenase by site-directed mutagenesis. *Proc. Natl. Acad. Sci. U.S.A.* **95**: 11625-11630.

SAPRA, R., VERHAGEN, M. F. J. M. AND ADAMS, M. W. W. (2000) Purification and characterization of a membrane-bound hydrogenase from the hyperthermophilic archaeon *Pyrococcus furiosus*. *J. Bacteriol.* **182**: 3423-3428.

SCHÄFFER, T. AND SCHÖNHEIT, P. (1991) Pyruvate metabolism of the hyperthermophilic archaebacterium *Pyrococcus furiosus*. *Arch. Microbiol.* **155**: 366-377.

SCHÄFFER, T. AND SCHÖNHEIT, P. (1992) Maltose fermentation to acetate, carbon dioxide and hydrogen in the anaerobic hyperthermophilic archaeon *Pyrococcus furiosus*: Evidence for the operation of a novel sugar fermentation pathway. *Arch. Microbiol.* **158**: 188-202.

SCHÄFFER, T. AND SCHÖNHEIT, P. (1993) Gluconeogenesis from pyruvate in the hyperthermophilic archaeon *Pyrococcus furiosus*: involvement of reactions of the Embden-Meyerhof pathway. *Arch. Microbiol.* **159**: 354-363.

SCHÄFFER, T., XAVIER, K. B., SANTOS, H. AND SCHÖNHEIT, P. (1994) Glucose fermentation to acetate and alanine in resting cell suspensions of *Pyrococcus furiosus*: Proposal of a novel glycolytic pathway based on ^{13}C labelling data and enzyme activities. *FEMS Microbiol. Lett.* **121**: 107-114.

SCHICHO, R. N., MA, K., ADAMS, M. W. AND KELLY, R. M. (1993) Bioenergetics of sulfur reduction in the hyperthermophilic archaeon *Pyrococcus furiosus*. *J. Bacteriol.* **175**: 1823-1830.

SCHINK, B. (1997) Energetics of syntrophic cooperation in methanogenic degradation. *Microbiol. Mol. Biol. Rev.* **61**: 262-280.

SCHMITZ, O., BOISON, G., HILSCHER, R., HUNDESHAGEN, B., ZIMMER, W., LOTTSPEICH, F. AND BOTHE, H. (1995) Molecular biological analysis of a bidirectional hydrogenase from cyanobacteria. *Eur. J. Biochem.* **233**: 266-276.

SCHNEIDER, K., CAMMACK, R., SCHLEGEL, H. G. AND HALL, D. O. (1979) The iron-sulphur centres of soluble hydrogenase from *Alcaligenes eutrophus*. *Biochim. Biophys. Acta* **578**: 445-461.

SELIG, M., XAVIER, K. B., SANTOS, H. AND SCHÖNHEIT, P. (1997) Comparative analysis of Embden-Meyerhof and Entner-Doudoroff glycolytic pathways in hyperthermophilic archaea and the bacterium *Thermotoga*. *Arch. Microbiol.* **167**: 217-232.

SERRE, L., VELLIEUX, F. M., MEDINA, M., GOMEZ-MORENO, C., FONTECILLA-CAMPS, J. C. AND FREY, M. (1996) X-ray structure of the ferredoxin: $NADP^+$ reductase from the cyanobacterium Anabaena PCC 7119 at 1.8 Å resolution, and crystallographic studies of $NADP^+$ binding at 2.25 Å resolution. *J. Mol. Biol.* **263**: 20-39.

SETZKE, E., HEDDERICH, R., HEIDEN, S. AND THAUER, R. K. (1994) H_2: heterodisulfide oxidoreductase complex from *Methanobacterium thermoautotrophicum*. Composition and properties. *Eur. J. Biochem.* **220**: 139-148.

SIMPSON, F. J. AND BURRIS, R. H. (1984) A nitrogen pressure of 50 atmospheres does not prevent evolution of hydrogen by nitrogenase. *Science* **224**: 1095-1097.

SMITH, F. E., HERBERT, J., GAUDIN, J., HENNESSEY, D. J. AND REID, G. R. (1984) Serum iron determination using ferene triazine. *Clin. Biochem.* **17**: 306-310.

SOLIOZ, M. (1984) Dicyclohexylcarbodiimide as a probe for proton-translocating enzymes. *Trends Biochem. Sci.* **9**: 309-312.

SORGENFREI, O., LINDER, D., KARAS, M. AND KLEIN, A. (1993) A novel very small subunit of selenium-containing [NiFe] hydrogenase of *Methanococcus voltae* is post-translationally processed by cleavage at a defined position. *Eur. J. Biochem.* **213**: 1355-1358.

STAMS, A. J. M. (1994) Metabolic interactions between anaerobic bacteria in methanogenic environments. *Antonie van Leeuwenhoek* **66**: 271-294.

STEIGERWALD, V. J., BECKLER, G. S. AND REEVE, J. N. (1990) Conservation of hydrogenase and polyferredoxin structures in the hyperthermophilic archaebacterium *Methanothermus fervidus*. *J. Bacteriol.* **172**: 4715-4718.

SURERUS, K. K., CHEN, M., VAN DER ZWAAN, J. W., RUSNAK, F. M., KOLK, M., DUIN, E. C., ALBRACHT, S. P. AND MUNCK, E. (1994) Further characterization of the spin coupling observed in oxidized hydrogenase from *Chromatium vinosum*. A Mössbauer and multifrequency EPR study. *Biochemistry* **33**: 4980-4993.

SYMONS, M. C. R., ALY, M. M. AND WEST, D. X. (1979) Electron spin resonance data for the hydrogen-transition metal bond in the complex $[HNi(CN)_4]^{2-}$. *J. Chem. Soc., Chem. Commun.*: 51-52.

TEIXEIRA, M., MOURA, I., XAVIER, A. V., DERVARTANIAN, D. V., LEGALL, J., PECK, H. D. J. H. B. H. AND MOURA, J. J. (1983) *Desulfovibrio gigas* hydrogenase: redox properties of the nickel and iron-sulfur centers. *Eur. J. Biochem.* **130**: 481-484.

TEIXEIRA, M., MOURA, I., XAVIER, A. V., HUYNH, B. H., DERVARTANIAN, D. V., PECK, H. D. J., LEGALL, J. AND MOURA, J. J. (1985) Electron paramagnetic resonance studies on the mechanism of activation and the catalytic cycle of the nickel-containing hydrogenase from *Desulfovibrio gigas*. *J. Biol. Chem.* **260**: 8942-8950.

TEIXEIRA, M., MOURA, I., FAUQUE, G., CZECHOWSKI, M., BERLIER, Y., LESPINAT, P. A., LE GALL, J., XAVIER, A. V. AND MOURA, J. J. (1986) Redox properties and activity studies on a nickel-containing hydrogenase isolated from a halophilic sulfate reducer *Desulfovibrio salexigens*. *Biochimie* **68**: 75-84.

TEIXEIRA, M., FAUQUE, G., MOURA, I., LESPINAT, P. A., BERLIER, Y., PRICKRIL, B., PECK, H. D. J., XAVIER, A. V., LE GALL, J. AND MOURA, J. J. (1987) Nickel-[iron-sulfur]-selenium-containing hydrogenases from *Desulfovibrio baculatus* (DSM 1743). Redox centers and catalytic properties. *Eur. J. Biochem.* **167**: 47-58.

TEIXEIRA, M., MOURA, I., XAVIER, A. V., MOURA, J. J., LEGALL, J., DERVARTANIAN, D. V. AND PECK, H. D. J. H. B. H. (1989) Redox intermediates of *Desulfovibrio gigas* [NiFe] hydrogenase generated under hydrogen. Mössbauer and EPR characterization of the metal centers. *J. Biol. Chem.* **264**: 16435-16450.

TERSTEEGEN, A. AND HEDDERICH, R. (1999) *Methanobacterium thermoautotrophicum* encodes two multisubunit membrane-bound [NiFe] hydrogenases. Transcription of the operons and sequence analysis of the deduced proteins. *Eur. J. Biochem.* **264**: 930-943.

THAUER, R. K., KÄUFER, B., ZÄHRINGER, M. AND JUNGERMANN, K. (1974) The reaction of the iron-sulfur protein hydrogenase with carbon monoxide. *Eur. J. Biochem. 1974, 42, 447.* **42**: 447-452.

THOMPSON, J. D., GIBSON, T. J., PLEWNIAK, F., JEANMOUGIN, F. AND HIGGINS, D. G. (1997) The CLUSTAL X windows interface: flexible strategies for multiple sequence alignment aided by quality analysis tools. *Nucleic Acids Res.* **25**: 4876-4882.

TRAN-BETCKE, A., WARNECKE, U., BOCKER, C., ZABOROSCH, C. AND FRIEDRICH, B. (1990) Cloning and nucleotide sequences of the genes for the subunits of NAD-reducing hydrogenase of *Alcaligenes eutrophus* H16. *J. Bacteriol.* **172**: 2920-2929.

TUSNÁDY, G. E. AND SIMON, I. (1998) Principles governing amino acid composition of integral membrane proteins: application to topology prediction. *J. Mol. Biol.* **283**: 489-506.

VAN DER SPEK, T. M., ARENDSEN, A. F., HAPPE, R. P., YUN, S., BAGLEY, K. A., STUFKENS, D. J., HAGEN, W. R. AND ALBRACHT, S. P. (1996) Similarities in the architecture of the active

sites of Ni-hydrogenases and Fe-hydrogenases detected by means of infrared spectroscopy. *Eur. J. Biochem.* **237**: 629-634.

VAN DER ZWAAN, J. W., ALBRACHT, S. P. J., FONTIJN, R. D. AND SLATER, E. C. (1985) Monovalent nickel in hydrogenase from *Chromatium vinosum*. Light sensitivity and evidence for direct interaction with hydrogen. *FEBS Lett.* **179**: 271-277.

VAN DIJK, C., MAYHEW, S. G., GRANDE, H. AND VEEGER, C. (1979) Purification and characterization of hydrogenase from *Megasphaera elsdenii*. *Eur. J. Biochem.* **102**: 317-330.

VANONI, M. A. AND CURTI, B. (1999) Modular architecture of glutamate synthase: a complex iron-sulfur flavoprotein. *Cell. Mol. Life Sci.* **55**: 617-638.

VANONI, M. A., EDMONDSON, D. E., ZANETTI, G. AND CURTI, B. (1992) Characterization of the flavins and the iron-sulfur centers of glutamate synthase from *Azospirillum brasilense* by absorption, circular dichroism, and electron paramagnetic resonance spectroscopies. *Biochemistry* **31**: 4613-4623.

VANONI, M. A., RESCIGNO, M., NUZZI, L., ZANETTI, G. AND CURTI, B. (1991) The kinetic mechanism of the reactions catalyzed by the glutamate synthase from *Azospirillum brasilense*. *Eur. J. Biochem.* **202**: 181-189.

VOET, D. AND VOET, J. G. (1990) ***BIOCHEMISTRY***, 3rd ed., John Wiley & Sons, Inc.

VOLBEDA, A., CHARON, M. H., PIRAS, C., HATCHIKIAN, E. C., FREY, M. AND FONTECILLA-CAMPS, J. C. (1995) Crystal structure of the nickel-iron hydrogenase from *Desulfovibrio gigas*. *Nature* **373**: 580-587.

VOLBEDA, A., GARCIN, E., PIRAS, C., DE LACEY, A. L., FERNANDEZ, V. M., HATCHIKIAN, E. C., FREY, M. AND FONTECILLA-CAMPS, J. C. (1996) Structure of the [NiFe] hydrogenase active site: evidence for biologically uncommon Fe ligands. *J. Am. Chem. Soc.* **118**: 12989-12996.

VOORDOUW, G. (1992) Evolution of hydrogenase genes. *Adv. Inorg. Chem.* **38**: 397-422.

VOORDOUW, G., MENON, N. K., LEGALL, J., CHOI, E. S., PECK, H. D. J. AND PRZYBYLA, A. E. (1989) Analysis and comparison of nucleotide sequences encoding the genes for [NiFe]

and [NiFeSe] hydrogenases from *Desulfovibrio gigas* and *Desulfovibrio baculatus*. *J. Bacteriol.* **171**: 2894-2899.

WARD, D. E., KENGEN, S. W. M., VAN DER OOST, J. AND DE VOS, W. M. (2000) Purification and Characterization of the Alanine Aminotransferase from the Hyperthermophilic Archaeon *Pyrococcus furiosus* and Its Role in Alanine Production. *J. Bacteriol* **182**: 2559–2566.

WASSINK, J. H. AND MAYHEW, S. G. (1975) Fluorescence titration with apoflavodoxin: a sensitive assay for riboflavin 5'-phosphate and flavin adenine dinucleotide in mixtures. *Anal. Biochem.* **68**: 609-616.

WEIDNER, U., GEIER, S., PROCK, A., FRIEDRICH, T., LEIF, H. AND WEISS, H. (1993) The gene locus of the proton-translocating NADH: ubiquinone oxidoreductase in *Escherichia coli.* Organization of the 14 genes and relationship between the derived proteins and subunits of mitochondrial complex I. *J. Mol. Biol.* **233**: 109-122.

WHITEHEAD, J. P., GURBIEL, R. J., BAGYINKA, C., HOFFMAN, B. M. AND MARONEY, M. J. (1993) The hydrogen binding site in hydrogenase:35-GHz ENDOR and XAS studies of the nickel-C active form and the nickel-L photoproduct. *J. Am. Chem. Soc.* **115**: 5629-5635.

WU, L. F. AND MANDRAND, M. A. (1993) Microbial hydrogenases: primary structure, classification, signatures and phylogeny. *FEMS Microbiol. Rev.* **10**: 243-269.

YAGI, T. (1987) Inhibition of NADH-ubiquinone reductase activity by N, N'-dicyclohexylcarbodiimide and correlation of this inhibition with the occurrence of energy-coupling site 1 in various organisms. *Biochemistry* **26**: 2822-2828.

YAGI, T. AND HATEFI, Y. (1988) Identification of the dicyclohexylcarbodiimide-binding subunit of NADH-ubiquinone oxidoreductase (Complex I). *J. Biol. Chem.* **263**: 16150-16155.

ZORIN, N. A., DIMON, B., GAGNON, J., GAILLARD, J., CARRIER, P. AND VIGNAIS, P. M. (1996) Inhibition by iodoacetamide and acetylene of the H-D-exchange reaction catalyzed by *Thiocapsa roseopersicina* hydrogenase. *Eur. J. Biochem.* **241**: 675-681.

Appendix

A SHORT PRIMER ON SEQUENCE COMPARISONS

The simultaneous alignment of many nucleotide or amino acid sequences is now an essential tool in molecular biology. Multiple alignments are used to find diagnostic patterns to characterize protein families; to detect or demonstrate homology between new sequences and existing families of sequences; to help predict the secondary and tertiary structures of new sequences; to suggest oligonucleotide primers for PCR; as an essential prelude to molecular evolutionary analysis. The rate of appearance of new sequence data is steadily increasing and the development of efficient and accurate automatic methods for multiple alignment is, therefore, of major importance.

In order to align just two sequences, it is standard practice to use dynamic programming (2).

The dynamic programming paradigm

Dynamic programming is a very general technique. It is applicable when a large search space can be structured into a succession of stages such that the initial stage contains trivial solutions to sub-problems and each partial solution in a later stage can be calculated by recurring on only a fixed number of partial solutions from an earlier stage.

Let us take two sequences, s and t, with lengths m and n, respectively. We can write them as s_m and t_n (In this notation s_i denotes the portion of the sequence composed of the first i characters of s). The calculation of the optimal alignment can be performed using the dynamic programming paradigm. To do this we first need to find a way to quantify the similarity of two full sequences (or truncated sequences). As a first approximation we can model the similarity of two sequences by considering the simple one-step operations that turn s into t. It is useful at this stage to introduce a new notation. We introduce a gap character "-" and make the following definitions:

(a,a) denotes a match (no change from s to t)

(a,-) denotes the deletion of character a from sequence s

(a,b) denotes the replacement of a (in s) by b(in t)

(-,a) denotes the insertion of character a in s

Since the problem is symmetric, an insertion in s is equivalent to a deletion in t, and vice-versa. For example, an s sequence "AGGCACTA" can aligned with the t sequence "AGCGCACA", stepwise in several ways:

```
s:    A-GGCACTA       AG-GCACTA
t:    AGCGCACA-       AGCGCAC-A
```

If the alignment is read column-wise, we have a protocol of one-step changes that turn s into t:

Left alignment	Right alignment
Match (A,A)	Match (A,A)
Insert (-,G)	Match (G,G)
Replace (G,C)	Insert (-,C)
Match (G,G)	Match (G,G)
Match (C,C)	Match (C,C)
Match (A,A)	Match (A,A)
Match (C,C)	Match (C,C)
Replace (T,A)	Delete (T,-)
Delete (A,-)	Match (A,A)

The left-hand alignment shows an insertion, a deletion and two replacements. The right-hand alignment shows an insertion and a deletion. The transformation protocol can be turned into a measure of distance between the sequences by assigning a "cost" to each operation. For instance, we may define the cost of every operation other

than a match as 1 and define a cost of 0 for a match. The cost of an alignment will be the sum of the individual costs of every operation needed to transform s into t. An optimal alignment of s and t will be the alignment with the lower cost among all possible alignments. In the preceding example, the cost of the left-hand alignment would be 4, and that of the right-hand alignment would be 2.

The number of possible alignments between two sequences is very large, and unless the cost function is very simple it may seem to be very difficult to find an optimal alignment. However, this can be easily done by the dynamic programming algorithm.

Let us assume we already know optimal alignments between all shorter truncations of s and t, in particular those of:

- s_{i-1} and t_j
- s_i and t_{j-1}
- s_{i-1} and t_{j-1}

The optimal alignment of s_i and t_j must be an extension of one of the above by:

- A replacement (s_i,t_j) or a match (s_i,t_j), depending on whether the character at the ith position of s is different or equal to the jth character of t.
- A deletion
- An insertion

We simply have to choose the minimum from the following values:

- cost of the (s_{i-1}, t_{j-1}) alignment + cost of the replacement (s_i,t_j) or match (s_i,t_j)
- cost of the (s_i,t_{j-1}) alignment + cost of the insertion $(-,t_j)$
- cost of the (s_{i-1},t_j) alignment + cost of the deletion $(s_j,-)$

There is no choice when one of the segments is empty. Therefore:

- cost of $(s_0,t_0) = 0$
- cost of (s_i,t_0) = cost of (s_{i-1},t_0) + cost $(s_i,-)$
- cost of (s_0,t_j) = cost of (s_0,t_{j-1}) + cost $(-,t_j)$

According to this scheme, and for a given cost, the costs of the alignments of every truncation of the sequences s and t define a $(m+1) \times (n+1)$ cost matrix. The three-way choice in the minimization formula for the cost of (s_i,t_j) leads to the following pattern of dependencies between matrix elements

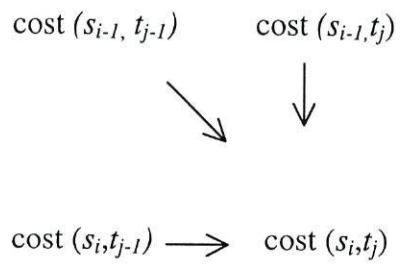

The bottom right corner of the cost matrix contains the desired result.

This is the distance matrix for the previous example:

			t							
		A	**G**	**C**	**G**	**C**	**A**	**C**	**A**
	0	**1**	**2**	**3**	**4**	**5**	**6**	**7**	**8**
A	**1**	0	1	2	3	4	5	6	7
G	**2**	1	0	1	2	3	4	5	6
G	**3**	2	1	1	1	2	3	4	5
C	**4**	3	2	1	2	1	2	3	4
A	**5**	4	3	2	2	2	1	2	3
C	**6**	5	4	3	3	2	2	1	2
T	**7**	6	5	4	4	3	3	2	2
A	**8**	7	6	5	5	4	3	3	2

s

In order to find the optimal alignment one only has to draw a path though the distance matrix indicating which case was chosen when taking the minimum (as shown below). A Diagonal line means an Replacement or Match, vertical line means Deletion and a horizontal line means Insertion. Note that in some cases the minimal choice is not unique, and different paths may be drawn with alternative optimal alignments.

		A	G	C	G	C	A	C	A
	0	1	2	3	4	5	6	7	8
A	1	0							
G	2		0	1					
G	3				1				
C	4					1			
A	5						1		
C	6							1	
T	7							2	2
A	8								2

s

In this case the optimal alignments would be:

```
s:    AG-GCACTA        AG-GCACTA
t:    AGCGCACA-        AGCGCAC-A
```

This technique guarantees a mathematically optimal alignment, given a table of scores for matches and mismatches between all amino acids or nucleotides and penalties for insertions or deletions of different lengths. Several cost matrices have been especially produces for aligning aminoacid or nucleotide sequences. In these matrices, the costs of replacing an aminoacid (or a nucleotide) by another can be very different, according to the greater or lesser similarity in the physical and chemical properties of the residues.

Unfortunately, the technique cannot be used to perform multiple alignments of *n* different sequences. Since the search space increases exponentially with *n* the problem soon becomes intractable with present computing power. Therefore, all of the methods capable of handling larger problems in practical timescales, make use of heuristics. Currently, the most widely used approach is to exploit the fact that homologous sequences are evolutionarily related. One can build up a multiple alignment progressively by a series of pairwise alignments, following the branching order in a phylogenetic tree (1). One first aligns the most closely related sequences, gradually adding in the more distant ones. This approach is sufficiently fast to allow alignments of virtually any size. Further, in simple cases, the quality of the alignments is excellent, as judged by the ability to correctly align corresponding domains from sequences of known secondary or tertiary structure (5). In more difficult cases, the alignments give good starting points for further automatic or manual refinement.

References

1.Feng, D.-F. and Doolittle, R.F. (1987). J. Mol. Evol. 25, 351-360.

2.Needleman, S.B. and Wunsch, C.D. (1970). J. Mol. Biol. 48, 443-453.

3.Dayhoff, M.O., Schwartz, R.M. and Orcutt, B.C. (1978) in *Atlas of Protein Sequence and Structure*, vol. 5, suppl. 3 (Dayhoff, M.O., ed.), pp 345-352, NBRF, Washington.

4.Henikoff, S. and Henikoff, J.G. (1992). Proc. Natl. Acad. Sci. USA 89, 10915- 10919.

5.Barton, G.J. and Sternberg, M.J.E. (1987). J. Mol. Biol. 198, 327-337.